Two-fluid models of turbulence for axi-symmetrical jets and sprays

by

Norberto Fueyo.

Thesis submitted for the degree of
Doctor of Philosophy
in the Faculty of Engineering,
University of London,
and for the Diploma of Membership
of Imperial College.

Computational Fluid Dynamics Unit,
Room 319, Chem Engg Bdg,
Imperial College of Science, Technology and Medicine,
Exhibition Road,
London SW7 2BX.

June 1989.

Abstract

The two-fluid model of turbulence of Spalding is applied in this work to the simulation of single-phase, round jets and of sprays.

The **round-jet model** proposed represents turbulence as the outcome of the interaction of two miscible fluids, which share the space. The fluids are assumed to be organised in fragments, and the interaction between them takes the form of the exchange of mass, momentum and other properties through the fragment boundaries. The fluid-fragment size is computed in the present model from differential equations which take into account fragment growth by entrainment and agglomeration, and fragment break-up by shear.

The results provided by the model are compared with existing experimental data, and the agreement is satisfactory. The centreline values of the fragment size are found to be proportional, after a region of jet development, to the Prandtl mixing-length. A parametric analysis is also carried out, showing the influence on the results of the several model constants, and the roles in the model of their associated terms.

In the **spray model**, a droplet size-distribution is incorporated into each fluid by the use of a no-slip technique, which breaks the size range into a number of size groups. A differential equation is used for the mass fraction occupied by each size group in each fluid. Droplet vaporisation is represented by the transfer of mass fraction from larger-size groups into smaller-size groups. The assessment

of the spray model is accomplished by comparison of the results with published data for both cold (ie non-evaporating) and evaporating sprays. It is shown that the accuracy of the two-fluid-model predictions is closer to the experimental evidence than that provided by locally-homogeneous-flow models, and comparable to that of stochastically-separated-flow models.

A **combustion case** is also presented, which uses an extension of the Simple Chemically-Reacting System (or Shvab-Zeldovich formulation) for flows in which two miscible phases are present. In these circumstances, the "passive scalar" of the single-phase formulation is no longer a conserved property, since its equation has a source term arising from the interphase exchange. The notion of passive scalar has been therefore redefined, and the conditions in which the proposed extension of the formulation is applicable have been established. Although of a purely demonstrative purpose, the model results show how the two-fluid model can represent the hot-cold fragmentariness of turbulent combustion.

Preface and acknowledgements

The present thesis is the outcome of my work on spray modelling at the Computational Fluid Dynamics Unit (CFDU, Imperial College), which I joined as a Research Assistant in December 1986.

My research at the CFDU started with a familiarisation period of approximately six months, in which I got acquainted with the CFD techniques and software employed in the Unit. These were applied, during this period, to a number of different problems, such as the simulation of a catalytic converter for cars, several kinds of two-phase flow and a tentative (and unsuccessful!) multiphase technique.

The direction the research would take became soon apparent as consisting in the development of a two-fluid model of turbulence (then being investigated in the CFDU) for sprays.

Subsequent months were spent in the study of early two-fluid models for single-phase flows, which are reviewed in the second chapter of this thesis. The study led eventually to the model for single-phase jets proposed in this work. During 1988, the model was extended to allow the representation of sprays, and tested using published experimental data for both cold and evaporating sprays.

Finally, the combustion model was developed and applied during the first semester of 1989. This task was carried out, to a great extent, in parallel with the writing up of this thesis, which was completed in June 1989.

The work reported here was carried out under the supervision of Prof DB Spalding. The research compiled in the thesis is mainly based upon his ideas on two-fluid models of turbulence, the essence of which he skilfully taught me. However, the benefits of Prof Spalding's supervision permeates the mere scientific layer: he influences one's patterns of work, and also the way in which the results of such work are conveyed to others. Working with him has been both fruitful and enjoyable.

I am also grateful to Prof GF Hewitt, who undertook my supervision upon Prof Spalding's retirement in September 1988.

I cannot either fail to acknowledge the role in this work of Prof César Dopazo (University of Zaragoza, Spain). It was through him that I knew about Prof Spalding's offer of a Research Assistanship; and he also willingly backed my application for the position. Furthermore, his contribution to my Fluid Mechanics background and his continual support during my stay in the CFDU have been essential factors in the successful completion of this work.

Thanks are also due to the staff and colleagues of the CFDU, too numerous to be named here without unwantedly leaving someone out. They not only provided high-quality administrative and technical help, but also managed to maintain, in the Unit, the kind of friendly atmosphere that invites to work.

On the financial side, my thanks go to the SERC, which was the main source of funding, and to CHAM Ltd (London), which funded the late part of the research. The Research Council (CONAI) of the Regional Government of Aragón (Spain) provided complementary (but crucial) support. CHAM Ltd is also thanked for granting the free use of PHOENICS, the flow-simulation package in which the mathematical model proposed in this thesis was built.

Finally, I would also like to thank my family and friends for their continual support during these years.

22 June 1989,
South Kensington,
London.

Table of contents

Preliminaries

Abstract 2
Preface 4
Table of contents 7
List of figures 15
List of tables 19

Chapter 1: Introduction

1.1 Opening remarks 21
1.1.1 The problem addressed and its practical relevance 21
1.1.2 The remainder of this chapter 22
1.2 Spray modelling: a literature survey 23
1.2.1 Introduction 23
1.2.2 Spray equation (Eulerian) 23
1.2.3 LHF – Locally-homogeneous-flow models (Eulerian) 26
1.2.4 NSC – No-slip-cloud model (Eulerian) 27
1.2.5 SIC – Several-interpenetrating-continua models (Eulerian) 28
1.2.6 Early Eulerian-Lagrangian methods 30
1.2.7 Recent Eulerian-Lagrangian models 32
1.3 The present contribution 34
1.3.1 Nature and extent 34
1.3.2 Layout of the thesis 35

Chapter 2: Two-fluid models of turbulence

2.1 Introduction 37
2.1.1 The purpose of this chapter 37
2.1.2 Layout of this chapter 37
2.2 Conventional and two-fluid models of turbulence 38
2.3 Two-fluid models: some ancestors 41
2.3.1 Reynolds' and Prandtl's ideas 41
2.3.2 Intermittency models 42
2.4 Two-fluid models 44
2.4.1 The concept 44
2.4.2 The equations 45
2.5 The early two-fluid models 47
2.5.1 The first proposal: Spalding (1982a) 47
2.5.2 Xi's (1986) and Malin's (1987) turbulent/non-turbulent models 48
2.6 The current thinking 49
2.6.1 Symmetric mass transfer 50
2.6.2 Viscosity formula 51
2.6.3 The shear-related source of momentum in the cross-stream-velocity equation 51
2.7 Other applications 52
2.8 Closure 54

Chapter 3: Numerical-integration method

3.1 Introduction 55
3.1.1 The problem to be tackled 55
3.1.2 The method chosen 56
3.1.3 The extent of the present description 57
3.1.4 Outline of the chapter 57
3.2 The finite-difference grid 58
3.2.1 The idea 58

	3.2.2	The storage of the variables	58
	3.2.3	Notation	59
	3.2.4	Grid fineness: accuracy versus economy	60
3.3		Finite-volume (algebraic) equations	61
	3.3.1	From differential equations to algebraic equations	61
	3.3.2	Transient term	61
	3.3.3	Convective term	62
	3.3.4	Diffusion term	63
	3.3.5	Interfluid-transfer term	65
	3.3.6	Other source terms	65
	3.3.7	The final finite-volume equation	66
	3.3.8	The velocity-components equations	66
	3.3.9	Boundary conditions	67
3.4		Solution procedure	67
	3.4.1	Step 1: Solution of the volume-fraction equations and correction	69
	3.4.2	Step 2: Solution of PEA-treated equations for scalar-variables	70
	3.4.3	Step 3: Solution of the momentum equations	71
	3.4.4	Step 4: Solution of the pressure-correction equation	71
	3.4.5	The linear-equation solver	73
3.5		Convergence promotion and control	74
	3.5.1	Introduction	74
	3.5.2	Convergence monitoring	76
	3.5.3	Convergence promotion	76
3.6		The computer program	77
3.7		Closure	78

Chapter 4: The single-phase, axi-symmetrical, turbulent jet

4.1		Introduction	79
	4.1.1	The purpose of this chapter	79
	4.1.2	The models discussed	79
	4.1.3	The layout of the chapter	80

4.2 The flow considered 80
4.3 Mathematical model 81
4.3.1 Equations 81
4.3.2 Auxiliary relations 83
4.3.3 Boundary conditions 84
4.4 Fragment-size models 85
4.4.1 Model a: algebraic 85
4.4.2 Model b: differential equations 85
4.4.3 Boundary conditions for l 86
4.5 Model constants 87
4.6 Results 88
4.6.1 Presentation 88
4.6.2 Further analysis 90
(a) Volume fractions 91
(b) Shear source 93
(c) Viscosity profile 93
(d) Cross-stream velocity 93
(e) Fragment size 93
4.6.3 Confidence tests 96
4.6.4 Parametric study 103
4.6.5 Some numerical details 112
4.7 Closure 114

Chapter 5: A two-fluid model for sprays

5.1 Introduction 116
5.1.1 The purpose of this chapter 116
5.1.2 Layout of the chapter 116
5.2 The situation studied 116
5.3 Mathematical model: differential equations 118
5.3.1 Background 118
5.3.2 Droplet-concentration equations 119
(a) Change of size variable. 120
(b) Transport equation for the number of droplets 120
(c) Change of dependent variable 121

(d) New equation in m_i 121

(e) Discretisation of the s interval 122

(f) Integration of the equation for m_i 123

5.3.3 Vapour mass-fraction equations 124

5.3.4 Modified w-momentum equations 125

5.4 Auxiliary relations 125

5.4.1 Density and liquid mass-fraction 126

(a) The liquid mass-fraction, y_i^l 126

(b) The vapour mass-fraction, y_i^v 126

(c) The air mass-fraction, y_i^g 126

5.4.2 Droplet vaporisation-rate 127

5.5 Model constants 128

5.6 Boundary conditions 128

5.7 Closure 130

Chapter 6: Spray-model assessment

6.1 Introduction 133

6.1.1 The purpose of this chapter 133

6.1.2 Layout of the chapter 133

6.2 Experimental data 133

6.2.1 The source of experimental data 133

6.2.2 Non-evaporating spray 134

6.2.3 Evaporating spray 135

6.3 Non-evaporating spray: results 138

6.4 Evaporating spray: results 142

6.5 Grid independence and numerical details 149

6.5.1 Numerical details 149

6.5.2 Grid-independence studies 149

6.6 Further analysis 150

6.6.1 The fragment length *l* 150

6.6.2 Evolution of the Sauter Mean Diameter 154

6.6.3 Effect of droplet diffusion 154

	6.6.4	Effect of the vaporisation rate, s'	156
	6.6.5	Increase in the number of droplet groups	160
	6.6.6	Density differences between both fluids	162
	6.6.7	Effect of the interphase-transfer constants	162
6.7		Closure	165

Chapter 7: Further studies: combustion

7.1		Introduction	167
	7.1.1	The purpose of this chapter	167
	7.1.2	Layout of this chapter	167
7.2		The Simple Chemically-Reacting System (SCRS)	168
	7.2.1	The SCRS for single-phase flows	168
	7.2.2	An SCRS for two-fluid models (SCRS2)	171
7.3		The mathematical model	175
	7.3.1	Droplets, vapour and total fuel	176
	7.3.2	The quasi-conserved-scalar equation	177
	7.3.3	Mass fractions of oxidant and product	177
	7.3.4	Gas and droplet temperature, and droplet-vaporisation rate	177
	7.3.5	Reaction rate	178
	7.3.6	Boundary conditions and other data	179
7.4		Checking the SCRS2 formulation	180
7.5		Results: presentation and discussion	183
7.6		Closure	191

Chapter 8: Summary

8.1		Purpose and layout of this chapter	192
8.2		Summary of achievements	192
	8.2.1	The two-fluid model	192
	8.2.2	Application to the single-phase, axi-symmetrical jet	193
	8.2.3	Application to cold and evaporating sprays	194

	8.2.4	Combustion studies	195
8.3		Suggestions for future work	196
	8.3.1	Immediate development	196
	8.3.2	Long-term development	198
8.4		Closure	199

Appendix A: The size-distribution equations

a.1		Introduction	200
a.2		The transport equation for m_i^k, $k \neq 1$	201
a.3		Transport equation for m_i^1	204
	a.3.1	The problem	204
	a.3.2	The solution	205

Appendix B: The complete equations

b.1		Single-phase jet	207
b.2		Non-evaporating spray	208
b.3		Evaporating spray	209
b.4		Combusting spray	210

Appendix C: Q1 files

c.1		Introduction	213
c.2		Single-phase jet	214
c.3		Non-evaporating spray	219
c.4		Evaporating spray	225
c.5		Combusting spray	231

Appendix D: FORTRAN coding

d.1 Introduction 238
d.2 GROUND subroutine 239

Nomenclature

Nomenclature 266

References

References 272

List of figures

Chapter 1: Introduction

F1.1 Spray-modelling techniques 24

Chapter 3: Numerical-integration method

F3.1 Finite-volume grids 58
F3.2 Scalar and velocity locations 59
F3.3 Control volumes for scalars and velocity components 61
F3.4 Control volume -- East face 63
F3.5 Slabwise storage-arrangements for parabolic problems 68
F3.6 The IPSA solution-cycle 69
F3.7 u_e and its driving pressures 72
F3.8 Values introduced by the substitutions for ϕ_P, ϕ_S, and ϕ_W 74
F3.9 Solution-procedure integration-levels 75

Chapter 4: The single-phase, axi-symmetrical, turbulent jet

F4.1 The problem considered 81
F4.2 Boundaries of the computational domain 84
F4.3 Axial-velocity profile 89
F4.4 Axial-velocity decay 89
F4.5 Fluid-2 volume-fraction 92
F4.6 Shear-source profile 92
F4.7 Viscosity profile 94
F4.8 Cross-stream-velocity profile 94

F4.9 Fragment sizes 95
F4.10 Axial evolution of fragment size 95
F4.11 Self-similarity test 97
F4.12 Grid independence: w 97
F4.13 Grid independence: decay rate 99
F4.14 Grid independence: jet spread 99
F4.15 Grid independence: fragment size 100
F4.16 Axial velocity for several Reynolds numbers 100
F4.17 Jet spread for several Reynolds numbers 101
F4.18 Fragement size for several Reynolds numbers 101
F4.19 Parametric analysis - axial-velocity profile 102
F4.20 C_f - Axial-velocity decay 104
F4.21 C_f - Jet spread 104
F4.22 C_f - Fragment size 105
F4.23 Exchange of w-momentum through $|v_1-v_2|$ 105
F4.24 C_m - Axial-velocity decay 107
F4.25 C_m - Fragment size 107
F4.26 C_μ - Jet spread 108
F4.27 C_μ - Fragment size 108
F4.28 C_v - Jet spread 109
F4.29 C_v - Axial evolution of fragment size 109
F4.30 Ca - Fragment size 111
F4.31 C_a - Decay 111
F4.32 C_b - Fragment size 113
F4.33 C_b - Decay 113

Chapter 5: A two-fluid model for sprays

F5.1 The situation considered 117
F5.2 Typical size-distribution 119
F5.3 Average m_i in group k 122
F5.4 m_i for group 1 (m_i^1) 124

Chapter 6: Spray-model assessment

F6.1 Inlet size-distribution for the non-evaporating spray 136
F6.2 Inlet size-distribution for the evaporating spray 136
F6.3 Radial profile of axial velocity at z/D=100 (non-evaporating).....139
F6.4 Radial profile of axial velocity at z/D=250 (non-evaporating).....139
F6.5 Radial profile of axial velocity at z/D=500 (non-evaporating).....140
F6.6 Radial profile of axial liqiud-flux at z/D=100 (non-evaporating) .140
F6.7 Radial profile of axial liquid-flux at z/D=250 (non-evaporating) .141
F6.8 Radial profile of axial liquid-flux at z/D=500 (non-evaporating) .141
F6.9 Centreline evolution of the axial velocity (non-evaporating) 143
F6.10 Centreline evolution of the axial liquid-flux (non-evaporating).....143
F6.11 Radial profile of axial velocity at z/D=100 (evaporating).....145
F6.12 Radial profile of axial velocity at z/D=250 (evaporating).....145
F6.13 Radial profile of axial velocity at z/D=500 (evaporating).....146
F6.14 Radial profile of freon concentration at z/D=100 (evaporating).....146
F6.15 Radial profile of freon concentration at z/D=250 (evaporating).....147
F6.16 Radial profile of freon concentration at z/D=500 (evaporating).....147
F6.17 Centreline evolution of the axial velocity (evaporating) 148
F6.18 Centreline evolution of the freon concentration (evaporating).....148
F6.19 Grid independence: axial velocity at z/D=250 151
F6.20 Grid independence: freon concentration at z/D=250 151
F6.21 Grid independence: axial evolution of axial velocity 152
F6.22 Grid independence: axial evolution of freon concentration.....152
F6.23 Axial evolution of l/l_p 153
F6.24 Computed and experimental axial evolution of SMD.....153
F6.25 Radial profiles of droplet concentration.....155
F6.26 Effect of droplet diffusion on droplet concentration.....155
F6.27 Effect of size-dependent diffusion-coefficients on SMD 157
F6.28 Effect of s' on SMD 157
F6.29 Size distribution for s'=0.....158
F6.30 Size distribution for s'=2.48e-9.....158
F6.31 Size distribution for s'=5.0e-9.....159

F6.32 Size distribution for s'=1.0e-8 159
F6.33 Inlet size-distribution with 8 size-groups (evaporating spray) 161
F6.34 SMD evolution with 5 and 8 size-groups (evaporating spray) 161
F6.35 Radial profile of liquid volume-fraction in each fluid (normalised with the axial value for fluid 2) 163
F6.36 Radial profile of density difference (in % of the local average density) 163
F6.37 Effect of Cf on density difference 164
F6.38 Effect of Cm on density difference 164
F6.39 Qualitative representation of results 166

Chapter 7: Further studies: combustion

F7.1 Two-stream system 173
F7.2 SCRS2 check -- Radial profiles 181
F7.3 SCRS2 check -- Axial profiles 181
F7.4 Axial evolution of temperatures 182
F7.5 Radial profiles of temperature (T_2) 182
F7.6 Radial profiles of temperature (z/D=10.05) 185
F7.7 Radial profiles of temperature (z/D=10.55) 185
F7.8 Radial profiles of temperature (z/D=17.40) 186
F7.9 Radial profiles of average mixture-fraction (z/D=10.05) 186
F7.10 Radial profiles of average mixture-fraction (z/D=17.40) 187
F7.11 Radial profiles of fuel mass-fraction (z/D=10.05) 187
F7.12 Radial profiles of oxidant mass-fraction (z/D=10.55) 189
F7.13 Radial profiles of product mass-fraction (z/D=10.55) 189
F7.14 Radial profiles of product mass-fraction (z/D=17.40) 190

Appendix A: The size-distribution equations

Fa.1 The interval $[s_-^k, s_+^k]$ 201
Fa.2 Top-hat and linear profiles for the first interval 205

List of tables

Chapter 4: The single-phase, axi-symmetrical, turbulent jet

T4.1 Auxilary relations for the single-phase jet 83
T4.2 Boundary conditions for the single-phase jet 84
T4.3 Model constants 87
T4.4 Spread rate 90
T4.5 Scaling factors 91
T4.6 Runs with several Reynolds numbers 98
T4.7 Run-time for several machines 114

Chapter 5: A two-fluid model for sprays

T5.1 Additional constants for the spray model 128
T5.2 Additional boundary conditions 129

Chapter 6: Spray-model assessment

T6.1 Non-evaporating-spray data 135
T6.2 Evaporating-spray data 137
T6.3 Additional Freon-11 properties 137
T6.4 Grid-independence test-cases 150
T6.5 Size-dependent diffusion-coefficients 156

Chapter 7: Further studies: combustion

T7.1 Additional boundary conditions for the combusting spray 179
T7.2 Additional numerical data 180

Chapter 1

Introduction

1.1 Opening remarks

1.1.1 The problem addressed and its practical relevance

The present investigation is concerned with the mathematical modelling and numerical (computer) simulation of sprays.

A spray is a dispersion of liquid droplets in a gas, normally formed through the high-speed injection of the liquid into the gas. Sprays are therefore flows in which two different phases co-exist: the gaseous phase (also referred to as the **continuous** or **carrier** phase) and the liquid phase (also called the **disperse** or **particulate** phase).

In practice, spray flows are especially interesting in processes which require the evaporation of a liquid phase; for the large surface-to-volume ratio afforded by the droplets enhances the transfer of heat from the gas to the liquid. Thus, sprays are of common occurrence in:-

(a) **The food and the biochemical industries**, which use spray drying to remove the water from certain substances (milk, coffee, medicines), thus reducing their weight and also increasing their storage life.

(b) **Energy production.** Liquid fuels are widely available; and, furthermore, the liquid state is particularly convenient for their storage and handling. However, nearly all liquid fuel which is to be used as a source of energy must go through an atomisation process. The increased surface-to-volume ratio promotes a rapid vaporisation, and therefore an efficient, economical combustion. This has led to the use of spray-combustion systems in liquid rockets, diesel engines and industrial furnaces.

Sprays are also used in processes which require the liquid to be thinly and evenly distributed over a surface. This is the case, for instance, in:-

(a) Surface treatment, such as spray painting and particle coating;

(b) Industrial cleaning, eg of electronic components;

(c) Agricultural spraying of insecticides and fertilizers.

The present thesis will propose and assess a new model for the mathematical representation and computer simulation of spray flows. The precise nature of the proposal and the objectives of the work will be stated towards the end of the chapter.

1.1.2 The remainder of this chapter

Following this introductory section that is now closing, Section 1.2 below is a literature survey of the spray-modelling techniques most frequently used. Section 1.3 follows with an outline of the purpose, nature and extent of the contribution, and a description of the layout of this thesis.

1.2 Spray modelling: a literature survey

1.2.1 Introduction

This section reviews the modelling techniques most commonly used for the numerical simulation of sprays, in preparation for the new model proposed later in this work.

The present section is structured as shown in figure F1.1 The modelling schemes are classified into Eulerian and Lagrangian according to the treatment given to the disperse phase. Specifically, Eulerian models describe the droplet motion by using transport equations which yield, at each point and at any time, the average properties of the disperse phase at the point. Lagrangian models, on the other hand, track the droplets as they move through the continuous phase using equations which give their position, velocity, size, temperature and other properties as a function of time.

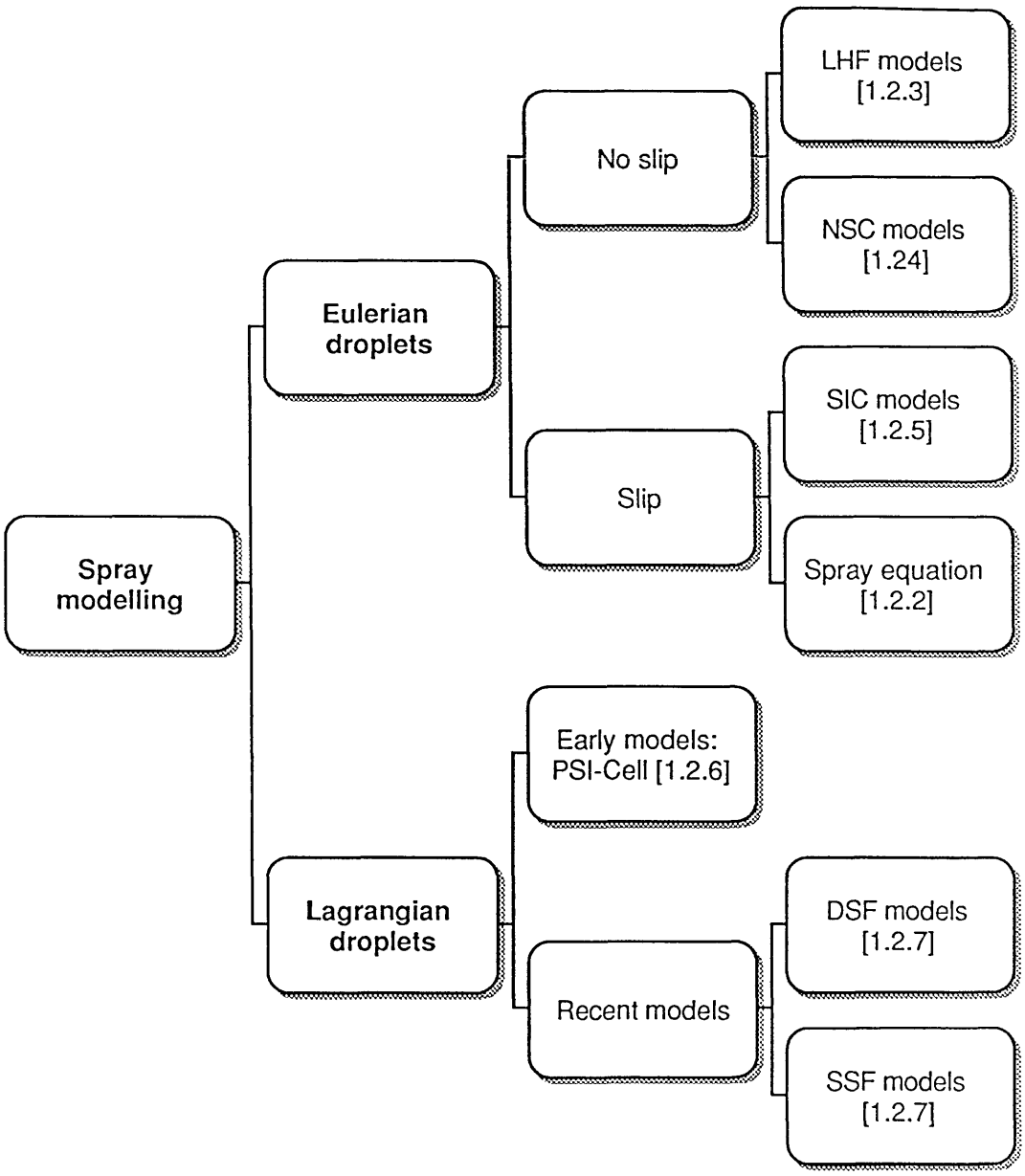
Eulerian schemes are further classified, in this survey, into two categories: those which allow for the velocities for gas and droplets to differ at each point, and those which do not. One of the former is discussed in the next sub-section.

1.2.2 Spray-equation model (Eulerian)

Williams (1965, 1985) points out that, owing to the presence of many particles with different characteristics, the only practical approach to the full modelling of spray behaviour is a **statistical** one. A full description of the spray should therefore be given by a distribution-density function f=func(**x**, t, **V**, R), such that

$$f(\mathbf{x}, t, \mathbf{V}, R)\, d\mathbf{x}\, d\mathbf{V}\, dR$$

is the number of droplets with radii between R and R+dR, velocities between **V** and **V**+d**V**, and position between **x** and **x**+d**x**. (Bold type indicates vector.)



• *Figure F1.1: Spray-modelling techniques* •

(In square brackets, the section in this chapter in which the model is reviewed)

A differential equation for f is derived by Williams (1965), following the analysis employed in the kinetic theory of gases. The equation is:

$$\frac{\partial f}{\partial t} + \nabla(\mathbf{v}f) + \nabla_{\mathbf{v}}(\mathbf{F}f) + \frac{\partial(R'f)}{\partial R} = S \qquad \text{[E1.1]}.$$

In this equation,

- **v** is the particle-velocity vector;
- **F** is the rate of change of **v** (ie, **F** is force per unit mass);
- R' is the rate of change of R, the droplet radius;
- S is a source term accounting for droplet break-up, collision and coalescence.

The inclusion of droplet velocity and droplet radius as **independent** variables in the equation allows for the existence, at any point in space, of droplets having different sizes and velocities, and also the **same** size but **different** velocities; and the analysis can be extended to other properties, such as temperature or chemical composition (the latter originally included in Williams' formulation).

Whilst providing a complete description of the spray, equation E1.1 poses the major hindrance of its large dimensionality. For it must be integrated, together with those for the continuous phase, in an eight-dimensional space (t, x, y, z, u, v, w, R); and this is not considered feasible for most practical purposes (Faeth, 1983).

Practicability is achieved, in most spray-modelling methods, by compromising in the detail of the description, namely by considering, at each point, only property **averages** (ie average droplet-size, average droplet-velocity, etc). A review of these simplified Eulerian models follows below.

(However, it must be pointed out that an alternative Lagrangian solution-procedure for the spray equation, amounting to a Monte Carlo technique, has been proposed by O'Rourke and Bracco (1980), and will be reviewed in Section 1.2.7 below.)

1.2.3 LHF – Locally-homogeneous-flow models (Eulerian)

LHF models are the most simplified Eulerian approach to spray modelling; for they presume that all droplets have, at each point, the same velocity, size, temperature etc; and further, that the droplet velocity is the same as the gas velocity. As a consequence, the flow is, for modelling purposes, **a single-phase one**, the only phase being the mixture of gas and no-slip droplets. (Droplets can be regarded, in these conditions, as a "chemical species" for which a concentration equation suffices.)

LHF models also rest upon simplifying assumptions which render the mixture fraction **f** (defined as the ratio of injected fluid to total amount of fluid at a point) a conserved property of the flow, and the state relationship only a function of f (Shearer *et al*, 1979).

Any property ζ related to f by a state relationship is calculated from

$$\overline{\zeta} = \int_0^1 \zeta(f)\ P(f)\ df \qquad \text{[E1.2]},$$

where P(f) is the probability-density function (pfd) of the mixture fraction f.

In LHF models, the pdf is normally specified by two parameters. These are:-

- The mixture fraction f, obtainable from its differential equation;

- and its variance g, defined as

$$g = \int_0^1 (f - \overline{f})^2 \, P(f) \, df \qquad \text{[E1.3]},$$

for which a differential equation (Spalding, 1971) is also postulated. LHF models which use the equation for g in conjuction with the k-ε turbulence model are referred to as k-ε-g models.

LHF models have been applied in the past to:-

- particle-laden jets (Shuen *et al*, 1983; Shuen *et al*, 1985);
- non-evaporating sprays (Solomon *et al*, 1985b);
- evaporating sprays (Shearer *et al*, 1979; Solomon *et al*, 1985a);
- and combusting sprays (Khalil and Whitelaw, 1976; Mao *et al*, 1981).

1.2.4 NSC – No-slip-cloud model (Eulerian)

An extension of the LHF idea was proposed by Spalding (1980a, 1985). This approach, christened "no-slip cloud" by Spalding, removes the single-size limitation of LHF models. Droplets are therefore allowed to differ in size, but all the droplets must still have the same velocity at each point, and their velocity must still be equal to that of the gas.

In Spalding's approach, the size range is broken into a number of discrete intervals, and a transport equation is written for the mass fraction occupied by the droplets in each group. The total liquid mass-fraction is computed by adding these, and it is thereafter used in the state relationships. Droplet vaporisation is represented by transactions between droplet size-groups; and droplet coalescence and breakup could be dealt with similarly.

This no-slip technique has been employed in this work for the incorporation of the spray droplets into the single-phase, two-fluid model. Full details will be accordingly provided in subsequent chapters (notably Chapter 5).

1.2.5 SIC – Several-interpenetrating-continua models (Eulerian)

SIC models regard both the continuous and the disperse phase as interpenetrating continua, sharing the space and a common pressure. Therefore, and unlike preceding models, SIC models allow for each phase to have a different velocity at each point. Conservation equations can be derived, as for single-phase flows, for the product $r_i\phi_i$, where i is the phase index; r_i is the phase volume-fraction; and ϕ_i is a property. These equations have the general form:

$$\frac{\partial(\rho_i r_i \phi_i)}{\partial t} + \nabla(\rho_i r_i \mathbf{V}_i \phi_i) + \nabla(r_i \mathbf{J}_{\phi i}) = I_{ji}(\phi_j - \phi_i) + S_{\phi i} \qquad \text{[E1.4]},$$

where

$\mathbf{J}_{\phi i}$ is a diffusion flux;

I_{ji} is the interphase transfer-rate;

$S_{\phi i}$ represents other sources (such as pressure gradients).

In these SIC models, the pressure field drives two or more velocity fields; and the resulting volume fractions have to satisfy an overall continuity equation (namely, $\Sigma r_i=1$). Therefore, equations such as E1.4 could not be integrated numerically using existing single-phase procedures, such as SIMPLE (Patankar and Spalding, 1972).

The need for a new numerical scheme was met independently by two different groups, one at Los Alamos (Harlow and Amsdem, 1975a and 1975b), and the other at Imperial College (Spalding, 1976c, 1980b). The former group's method

(originally developed for nuclear-reactor safety-studies) uses the momentum equations to obtain mass fluxes which are subsequently inserted into the phase volume-fraction equations to yield a mass residue for each phase. From these, a pressure correction is computed for each phase, and the phase volume-fractions are corrected to bring all the phase pressures into local equilibrium. Spalding's method is slightly different, and will be described in some detail in Chapter 3 of the present work.

SIC models are usually two-phase: one phase represents the gas and the other represents the disperse phase (see, eg, Spalding, 1982d; Rizk and Elgobashi, 1989). The solution of the Eulerian equations for the disperse phase is, in these circumstances, a single (average) value for droplet size, velocity, temperature, etc, at each cell. In reality, droplets of different sizes, or even droplets of the same size and different velocity or temperature, may be present at each cell.

This limitation can be avoided by the use of multiphase models, in which one phase represents the gas but several phases are used to describe the particulate phase (Mostafa and Elgobashi, 1985; Mostafa and Mongia, 1987). Each phase is assigned to a size-group, thus allowing the existence, at the same point in space, of droplets having different sizes. By including also droplet veloctiy as a phase-defining property, droplets with the **same** size would be allowed to have **different** velocities.

Needless to say, the inclusion of additional phases increases the computational expense; for Eulerian schemes solve the phase equations everywhere in the computational domain, even where the phase is not present at all. Eulerian-Lagrangian models, reviewed in the next subsection, provide an alternative formulation that circumvents this drawback.

1.2.6 Early Eulerian-Lagrangian methods

Unlike Eulerian-Eulerian (SIC) models, Eulerian-Lagrangian models do not use Eulerian equations for the disperse phase; instead, the particles are tracked as they move through the continuous-phase field by integrating **Lagrangian** equations.

In a simplified approach, the influence of the disperse phase on the continuous phase is neglected, and the particle trajectory is then integrated over a fixed continuous field (which could be the outcome of either an experiment or a computation). This scheme, sometimes called "droplet-history model", has been used in the past, among others, by Gauvin *et al* (1975), Boyson and Swithenbank (1979), Mao *et al* (1981) and Chin *et al* (1985).

However, in most practical situations the coupling between the continuous and disperse phases is a two-way one, and both sets of equations have to be solved simultaneously. The credit for the first interactive combination of the Lagrangian technique for droplets and Eulerian technique for the gas phase lies with Crowe and co-workers at the Washington State University (Crowe and Pratt, 1972; Crowe *et al*, 1977). Their scheme, christened PSI-Cell (**P**article-**S**ource-**I**n **Cell**), regards the disperse phase as a source of mass and momentum in the continuous-phase equations. The interaction between the two sets of equations (Eulerian for gas and Lagrangian for droplets) is dealt with by iterating, in the solution procedure, between them as follows:-

1. The Eulerian equations are solved by means of single-phase techniques, similar to those that, for two-phase flows, are described in Chapter 3 of this work. For the purpose of the description of Crowe's method, it must be stated here that these techniques divide the domain into a (large) number of

computational cells, and integrate the Eulerian transport equations over each cell.

2. The Lagrangian equations for the droplets (or particles) are then integrated, by means of the computed gas-field, to obtain droplet trajectories, sizes, velocities, temperatures, etc. Each particle is tracked, during the integration, as it crosses each cell. The crossing entails the exchange of mass, momentum and other properties between both phases; and this exchange is computed for each cell.

3. The continuous-phase equations are solved again, with the exchange terms computed in (2) now taken into account by way of sources for each cell (hence the name Particle-Source-In Cell).

4. The process 2-3 is repeated until a sufficiently-converged solution is achieved.

In the pioneering work of Crowe *et al*, the mathematical model was kept to the bare essentials. Thus, both phases were uncoupled as far as turbulence was concerned: although a k-ε model was used within the gas phase (Crowe *et al*, 1977), the effect of the presence of particles was not considered; and neither was the effect of gas turbulence on particle trajectory.

The modelling of particle-turbulence interaction is, in fact, the subject addressed by later versions of the Eulerian-Lagrangian approach. These recent models are reviewed in the next sub-section.

1.2.7 Recent Eulerian-Lagrangian models

The name discrete-droplet models (DDM - Gosman and Jones, 1980; Faeth, 1983) was coined in the early 80's for models built around the PSI-Cell idea. Later, the treatment of particle-turbulence interaction added (Faeth, 1987) a further differentiation of DDMs models into deterministically-separated-flow models (DSF) and stochastically-separated-flow models (SSF).

The name DSF is given to those models models which continue to ignore the effects of turbulence on particles, and sometimes even the modification of the continuous-phase turbulence owing to the presence of a disperse phase (see, eg, Beshay, 1985). Mean continuous-phase variables are therefore used in the Lagrangian equations for the particles.

SSFs, on the other hand, **do** account for:-

1. The effect on the continuous-phase turbulence of the presence of particles (the "turbulence modulation" of Al Tawel and Landau, 1977);

2. The dispersion (diffusion) of particles caused by the random, turbulent fluctuations of the velocity field;

3. The effect of turbulent fluctuations in the interphase exchange of properties.

One of the first SSF treatments for sprays was that of Dukowicz (1980). He introduced, in the gas-phase equation, a void fraction (the volume fraction of Eulerian schemes) that accounts for the volume occupied by particles and therefore unavailable to the continuous phase. Turbulent diffusion of droplets was modelled by introducing, in the drag-force term, an extra gas-velocity sampled

from a Gaussian distribution, the variance of which was related to the local turbulence kinetic-energy. This *turbulent velocity-component* was assumed to act during a time equal to the turbulence time-scale. Unlike the PSI-Cell method, Dukowicz's scheme treated the droplet-gas linkage explicitly, which meant that no iteration was needed between both sets of equations. (His method, however, considered only momentum transfer, and neither mass nor heat transfer.)

O'Rourke (1981), and O'Rourke and Bracco (1980), report a (probably) pioneering attempt to model thick sprays with SSF models. Although a spray equation (Williams, 1965, 1985) is employed to characterise the spray at each point (including space, time, size, velocity and temperature as **independent** variables), the equation is not solved directly. They used, instead, "parcels" of droplets tracked by a Lagrangian procedure, in what amounts to a stochastic (Monte-Carlo-like) solution of the spray equation. All droplets in a parcel have the same properties (ie droplet size, velocity and temperature); these properties are stochastically sampled from the inlet distribution. As a major contribution, droplet collision and coalescence are also modelled through a source term on the RHS of the spray equation, representing the transactions of droplets between size, velocity and temperature levels. The turbulent dispersion of droplets was modelled along the lines of Dukowicz's (1980) proposal, but the interaction time was now taken as the time needed for the particle to cross the eddy (found from the eddy size and the relative velocity). This meant, in fact, the retrieval, for spray modelling, of the idea of particle-eddy interaction of Hutchinson *et al* (1971): particles in turbulent flows are randomly displaced by the drag forces exerted by eddies that have captured the particles.

The droplet-diffusion model was afterwards further refined by choosing the particle-eddy interaction-time as the minimum of the crossing time and the eddy life. The new approach, first put forward by Brown and Hutchinson (1979), was

subsequently incorporated into SSF models by Gosman and Ioannides (1981), and then by many others (eg Shuen *et al*, 1983; Solomon *et al*, 1985a and 1985b; Watkins and Khaleghi, 1987; Mostafa and Mongia, 1987; Shirikawa *et al*, 1987; Mostafa et al 1989; Dodge and Schwalb, 1989).

1.3 The present contribution

1.3.1 Nature and extent

The aim of this thesis is the development and testing, for axi-symmetrical jets and sprays, of a relatively new kind of turbulence model. The new model focuses on some classical (but frequently ignored) concepts in turbulence modelling, such as fragmentariness, intermittency and the role of shear.

In the model proposed, turbulence is represented, **even for single-phase flows**, as the result of the interaction of two fluids, and hence the name of "two-fluid models". The mathematical representation of both fluids will be of the kind referred to, in Section 1.2.5, as SIC (Several Interpenetrating Continua). Thus, and unlike the SIC multiphase models of the preceding section, the fluids in two-fluid models are not, therefore, two different thermodynamic phases.

The model is first developed for and applied to single-phase jets, and then extended to sprays by the incorporation of a disperse phase. Since the single-phase model requires by itself two-phase techniques, the inclusion of the droplets in the model will be, for this reason, carried out using an extension of the no-slip-cloud method described in Section 1.2.4.

The resulting system of differential equations which constitute the model is solved using numerical (finite-difference) methods for two-phase flows. The performance of the model is assessed in the following situations:-

(a) Single-phase, round jet;
(b) Cold spray;
(c) Evaporating spray;
(d) Combusting spray (demonstrative case).

Comparison of the model results with available experimental data is provided for cases (a), (b) and (c).

1.3.2 Layout of the thesis

The purpose of the present chapter was to provide an introduction to spray modelling and to the present work. It is followed by **Chapter 2**, with an introduction to two-fluid models, in which due account is given of their origins, evolution and present formulation. **Chapter 3** describes the numerical-integration method, which is used in subsequent chapters for model testing. **Chapter 4** proposes and assesses a two-fluid model for single-phase, round jets. **Chapter 5** extends the single-phase model for two-phase, disperse flows (such as sprays), and **Chapter 6** applies this extension to the simulation of both cold and evaporating sprays. In **Chapter 7**, the study considers the case in which a fuel is the liquid injected, which subsequently evaporates and ignites. A combustion model is proposed, and the corresponding results are analysed. Finally, **Chapter 8** closes the work with a summary of successes and failures, and with some suggestions for further development of the model.

Four appendixes are then provided: **Appendix A** complements the theory presented in Chapter 5; **Appendix B** is a compilation of the whole set of equations

which constitute each model; and **Appendixes C** and **D** include listings of the data-input files and FORTRAN modules used in this work. The **Nomenclature** and **References** sections can be found, in this order, following Appendix D.

Chapter 2

Two-fluid models of turbulence

2.1 Introduction

2.1.1 The purpose of this chapter

Two-fluid models, which are the subject of the present work, constitute a relatively new approach to turbulence modelling. For that reason, a detailed description of the ideas behind them is desirable.

This is the purpose of this chapter, in which the introduction takes the form of a historical review, depicting how they appeared and developed to their current version. The review concerns only the application of **two**-fluid models to **single**-phase flows, since the introduction of two-phase flows into the two-fluid-model suite, which is the main purpose of this study, will be dealt with in Chapter 4.

2.1.2 Layout of this chapter

The next section (2.2) points out some circumstances in which the two-fluid character of turbulence renders conventional models inadequate, and explains why two-fluid models should be developed.

In Section 2.3, the origins of the ideas are traced back to Reynolds and Prandtl; and an account is also made of the more recent "intermittency models". Then, in Section 2.4, two-fluid models are introduced, first conceptually and then through the general differential equations.

Sections 2.5 and 2.6 are devoted to the evolution of the model, from the first proposal to the form employed in the present work. Some other applications not covered in these two sections are reviewed in Section 2.7. Finally, Section 2.8 closes the chapter with a summary.

2.2 Conventional and two-fluid models of turbulence

Turbulence is characterised by the presence of small-scale variations of properties both in space and time. The direct solution of the transport equations by numerical means requires the use of very fine computational grids and small time steps. Although this expensive approach to turbulence modelling is currently being investigated (see Hunt, 1988 and Gertz *et al* 1989 for recent examples), it is considered impractical for most engineering purposes. For these, such a detailed account of the instantaneous flow field is unnecessary, and only mean values are the sought-for outcome of a model.

Conventional turbulence models substitute the detailed description of the flow field by some account of the local statistics of the turbulence. This account entails, normally, the definition of turbulence-related quantities, such as the turbulent kinetic energy $\mathbf{k}$, its dissipation rate ε, the vorticity fluctuations $\mathbf{W}$ or a turbulence mixing-length l. These quantities are usually found from transport (differential) equations, for which an "exact" time-average form is derived from the instantaneous Navier-Stokes equations. However, unknown correlations appear in the process, and these have to be expressed in terms of knowable quantities by

the use of modelling assumptions (Launder and Spalding, 1972). The turbulence quantities obtained from the resulting differential equations are then combined into algebraic equations (eg the Prandtl-Kolmogorov formula) to account for increased diffusion caused by turbulence.

Conventional turbulence models pay little attention to the "fragmentariness" or "spottiness" of turbulence: the turbulent flow appears to be arranged in intermingling fragments (like lakes and islands) which have different properties.

The fragmentariness of turbulent flow can be observed in many practical situations. Thus, in shear flows, turbulent patches intermingle with irrotational ones. (This can be observed, for example, in a car-exhaust jet, in the plume emerging from a chimney or in a fast-flowing river). High speed photography of sprays shows regions of high droplet concentration interspersed with regions of low droplet concentration. And similar remarks can be made about turbulent flames, in which burned and unburned fragments can be distinctively spotted at the flame front.

The fragmentariness of turbulence has sometimes important consequences for the hydrodynamics of the flow. For instance, in the combustion cases just mentioned, the "hot" (burned) and "cold" (unburned) fragments respond in a different manner to the prevailing pressure gradient: the less dense (hotter) fragments tend to accelerate more rapidly than the denser (colder) ones, and are therefore "pushed" through them. (Experimental evidence of this has been provided, among others, by Shepherd and Moss, 1981). Only a "multiphase" model for turbulent flows can reproduce these effects.

A particular realisation of this phenomenon is the so-called "counter-gradient diffusion". It is brought about when the pressure gradient is such that the hot

fragments are pushed towards hotter regions, therefore yielding a counter-gradient flux of heat. This effect has been shown experimentally by several authors (eg, LaRue and Libby, 1977; Moss, 1980). Conventional turbulence models, which assume co-gradient diffusion, cannot reproduce this situation. (Libby and Bray (1981) had to resort to the use of an "intermittency model" with conditional velocities for the unburned and burned matter.)

More recently, counter-gradient diffusion has been shown to appear in direct numerical simulation of shear flows with temperature gradients, but without combustion (Gertz *et al*, 1989). The existence of intermingling patches of hotter and colder fluid was also detected, in a fine example of what is called, in preceding paragraphs, fragmentariness.

The presence of non-gradient diffusion has been identified by Spalding (1984a) in many practical instances in which the interaction of density differences, pressure gradients and body forces results in relative velocity between different fragments of the fluid. The term "turbulent sifting" has been used by Spalding (1984a) to refer generally to these phenomena, which cannot be adequately represented by conventional models.

The two-fluid-like behaviour of Nature described in this section has suggested the development of two-fluid models, which are introduced in the remainder of the chapter. The next section starts by identifying some ancestors of the type of model proposed later in the chapter.

2.3 Two-fluid models: some ancestors.

2.3.1 Reynolds' and Prandtl's ideas

The effect of the large-scale fragmentariness was indeed in the minds of the pioneering authors in turbulence research. Reynolds (1874), when analysing the transfer of heat between a surface and a fluid, includes in his study the role of "the eddies caused by visible motion which mixes the fluid up and continually brings fresh particles into contact with the surface".

The original idea of treating the turbulent flow as an addition of fluid "fragments" was, probably, first formulated by Prandtl, in his work "Report on the investigation into developed turbulence" (Prandtl, 1925). The following paragraphs, taken from the translation of this work by Spalding (1982b), show how these ideas were, in fact, the very essence of his (so well-known) mixing-length theory.

> "In the Boussinesq formula, $\tau = \rho\,\varepsilon\,\frac{du}{dy}$, ε is a measure of the turbulent "mixing"; according to its dimensions, which are the same of those of ν, ε **can be regarded as the product of a length and a velocity**, which will be now given mechanistic significances. The velocity will be taken as **the transverse velocity**, w, with which the **fluid "parcels"** travel, from either side, across the surface in which the mean velocity of the flow is u.
>
> The fluid "parcels" which come from the side in which the flow velocity is greater bring with them higher values of u than do those from the other side, so that more momentum is always transported in the one direction than in the other (except in the vicinity of a maximum in the u≈y curve). The sought-for length, l, is now defined as being equal to the distance from the considered surface at which the time-averaged velocities of the fluid parcels are: $u + l\frac{du}{dy}$ and $u - l\frac{du}{dy}$. **The magnitude of l must be of the same order as the diameter of the fluid parcels** themselves, or rather it is the "braking length" of the parcels in the surrounding fluid, which is however proportional to the parcel diameter. What can be also said about l is that it must fall to zero as the wall is

> approached, in order that the parcels, which must be smaller in size than the distance from the wall, can move at all in the manner which has been described. Further, l should vary in a smooth manner.
>
> [...] It is now necessary to make a usable hypothesis for the mixing velocity, w. The transverse momentum associated with this velocity must be constantly and abruptly destroyed by braking, and as constantly re-established. We therefore suppose that it is established by **the collision of two parcels of different u-velocity, and is therefore proportional to the quantity** $l \frac{du}{dy}$."
>
> (Present author's bold type.)

The Prandtl-mixing-length theory enjoys nowadays a considerable popularity; but the original idea of fragmentariness has been (to a great extent) lost. Two-fluid models of turbulence do not only recover this notion, but also stress, as it will be shown, the essential role of the cross-stream velocity, outlined in the first paragraph of the previous quotation. Furthermore, a formal connection between two-fluid models and Prandtl's theory has been established by Spalding (1984b).

2.3.2 Intermittency models

Many of the ideas thus far exposed about the two-fluid character of turbulence were already present in the intermittency models of the 70's. Spiegel (1972), one of the first proposers, considered turbulence as a "fluid of excitation moving through the actual (or laminar) fluid". Although his model was highly qualitative in nature, Spiegel's ideas included the interaction of both fluids; furthermore, the turbulent fluid was thought of as "composed of quasiparticles", in a clear reference to the fragmentariness of the flow. Terms such as "two-fluid system" and "two-fluid model" were used throughout.

Libby (1975, 1976) proposed a transport equation for an intermittency indicator (the "conditioning function"), of value 1 for the turbulent fluid and 0 for the non-turbulent one. The equation included a postulated source-term to account for the

creation of turbulent fluid. His approach, suggested by the experimental conditional-sampling technique, provided equations for the conditioned velocities (ie the turbulent and non-turbulent velocities), and for the intermittency factor (which is the average of the conditioning function described above). These equations were obtained from the postulated equation for the conditioning function, from the unconditioned velocity field (therefore assumed known) and from several modelling assumptions which were needed to close the intervening correlations. The theory was thereafter employed to investigate a number of self-similar flows (2D mixing-layer, wake of a heated cylinder).

Libby's ideas were later revised by Dopazo (1977), who derived the exact conditioned equations, thus avoiding the need of postulating a transport equation for the conditioning function. The unknown, surface-integral terms appearing as a consequence of the process in the conditioned equations were claimed to be physically meaningful, and therefore easier to close. Dopazo's formalism was further re-stated by Dopazo and O'Brien (1980), and then applied to self-similar flows.

Kollmann (1984) and Pope (1984) have proposed the use of pdf methods for the prediction of the intermittency factor and conditioned velocities. Kollmann uses standard finite-difference methods to solve the transport equation for the pdf of a single scalar taking intermittency into account. Pope derives the joint pdf for the velocity and a conserved scalar; the larger dimensionality of the problem requires the use of Monte Carlo techniques (Pope, 1985) for the solution of the transport equations.

The simulation of intermittent flows was, in fact, the aim of the early two-fluid models, which are dealt with in the Section 2.5.

2.4 Two-fluid models

2.4.1 The concept

Two-fluid models assume that a **single-phase** flow can be described, both conceptually and mathematically, as the outcome of the interaction of two different (but miscible) fluids which share the physical space. The intermingling fluids are thought of as being separated by a sharp (although flexible and permeable) interface, which allows the exchange of mass and properties between the fluids.

The share of the unit volume occupied by each fluid is called the volume fraction, $r_i(x,y,z,t)$ (i is the phase index, i=1,2). r_i can also be interpreted as the probability of the existence of fluid **i** at (x,y,z,t). In either case, it follows from the definition that r_1 and r_2 satisfy $0 \leq r_i \leq 1$; and, further,

$$r_1 (x,y,z,t) + r_2 (x,y,z,t) = 1.0 \qquad \text{[E2.1].}$$

E2.1 means that both fluids together occupy the whole of the space; or, under the second interpretation of r_i, that at any location (x,y,z) at time t there is either fluid 1 or fluid 2.

The properties of both fluids (velocity, density, temperature, chemical composition) are, in general, different. On the assumption that each property ϕ_i of fluid i has a counterpart ϕ_j in fluid j, the average of this property ϕ for the flow is defined as

$$\phi = \frac{r_1 \rho_1 \phi_1 + r_2 \rho_2 \phi_2}{r_1 \rho_1 + r_2 \rho_2} \qquad \text{[E2.2a].}$$

(For flows in which both fluids have the same density, E2.2a is reduced to

$$\phi = r_1 \phi_1 + r_2 \phi_2 \qquad \text{[E2.2b].)}$$

One of the properties is normally chosen to distinguish the fluids from one another. This "christening" property varies from a type of flow to another, since a global, all-encompassing theory is yet to be formulated. For instance, the choice of the "christening" property has given rise, in the past, to:-

- o hot/cold models, in which the fluids are distinguished by their temperature;
- o turbulent/non-turbulent or intermittency models, in which the fluids are distinguished by their vorticity;
- o up/down models, in which the fluids are distinguished by their cross-stream velocity.

A literature survey of the models mentioned above will be provided later in the Chapter. First, the subject of how r_i and ϕ_i are calculated is addressed in the next section.

2.4.2 The equations

With the considerations made in the preceding section, the flow can be described by the conventional two-phase, Eulerian transport equations. For the volume fractions r_i, these have the form:

$$\frac{\partial(\rho_i r_i)}{\partial t} + \nabla(\rho_i r_i \mathbf{V}_i) - \nabla(\Gamma_{ri}\, r_i\, \nabla r_i) = m_{ji} \qquad \text{[E2.3]},$$

where m_{ji} is the rate of mass transfer from fluid j to fluid i, fulfilling $m_{ij}=-m_{ji}$. The meaning of the rest of the symbols in E2.3 is detailed in the nomenclature section.

For any other variable ϕ_i:

$$\frac{\partial(\rho_i r_i \phi_i)}{\partial t} + \nabla(\rho_i r_i \mathbf{V}_i \phi_i) - \nabla(r_i \Gamma_{\phi i} \nabla \phi_i) - \nabla(\Gamma_{ri} \phi_i r_i \nabla r_i) =$$

$$([\![m_{ji}]\!] + f_{ji})(\phi_j - \phi_i) + S_{\phi i} \qquad \text{[E2.4]},$$

where $[\![x]\!]$ is x if x>0, and 0 otherwise; f_{ji} is the interphase diffusion of ϕ (eg, a drag force if ϕ is a velocity); and $S_{\phi i}$ represents other intra-fluid sources of ϕ_i.

It is when the exchange terms m_{ji} and f_{ji} are formulated that another main feature of two-fluid models appears: **fragmentariness.** Both fluids are assumed to be arranged in fragments, and to behave as such during the exchange processes. Since these take place across the fragment boundaries, the surface area of the fragment (or, equivalently, its characteristic length) is a local property of the fluid which can be expected to intervene in the inter-fluid exchange-terms of the transport equations (E2.3 and E2.4). Sections 2.5 and 2.6 will propose a formulation for these terms.

It can be therefore summarised here that two-fluid models of turbulence hinge upon:-

- The "christening" property which is chosen to distinguish the fluids;
- The relations between both fluids, materialised in the exchange of mass, momentum and other properties;
- The "patchiness" or "fragmentariness" of the flow, which intervenes in the exchange formulae (and probably in other properties) through the fragment size.

The next section is a review of how these items were implemented in the models used in the past.

2.5 The early two-fluid models

2.5.1 The first proposal: Spalding (1982a)

The first example of the kind of model proposed in this work is to be found in a paper by Spalding (1982a), in which it appears as the natural evolution of the ESCIMO theory of turbulent combustion (Spalding, 1976a, 1976b). ESCIMO was aimed at the description of the creation and destruction of the fine structure of turbulence (the "folds" of ESCIMO), but failed to account for the large-structure effects: the large-scale fragmentariness.

In this first paper on the subject by Spalding (1982a), the two-fluid idea was sketched using a typical round-jet configuration. The roles assigned to each fluid were turbulent (the injected fluid) and non-turbulent (the surrounding fluid). The volume fraction of the turbulent fluid (say r_2) is then the probability of having turbulent fluid, and it can be therefore regarded as an intermittency factor.

The interphase mass-transfer is assumed to be from fluid 1 (non-turbulent) to fluid 2 (turbulent), and proportional to:-

- The relative velocity, $|\mathbf{V}_1-\mathbf{V}_2|$; and
- The surface area of the fragment of phase 2.

If **n** is the number of fragments of fluid 2 per unit volume and l is the local fragment size, then $n=r_2/l^3$, and the surface area per unit volume is $nl^2=r_2/l$. Therefore, the interphase mass-transfer should be

$$m_{21}=C_m\, r_2\, \rho\, |\mathbf{V}_1-\mathbf{V}_2| / l.$$

However, in order to cut out the transfer of mass when there is no phase one present, C_m is substituted by $C_m r_1$, thus resulting in:

$$m_{21}=C_m\, r_1\, r_2\, \rho\, |V_1-V_2| / l \qquad \text{[E2.5]}.$$

Similarly, a source/sink of momentum arising from interphase friction was suggested for the momentum equations, having the form:

$$f_{ji}\,(\phi_j-\phi_i) = C_f\, \rho\, r_1\, r_2\, |V_1-V_2|\,(\phi_j-\phi_i) / l \qquad \text{[E2.6]},$$

where ϕ is a velocity component.

A Prandtl mixing-length law was selected to represent the effect of turbulent diffusion of mass and momentum, in the form:

$$\mu = C\mu\, \rho_i\, s\, l^2,$$

where s is a "stretch rate", eg $s = \left|\frac{\partial w}{\partial y}\right|$ if **z** is the axial dimension, and **y** the cross-stream one.

Although no computations were yet presented in this preliminary work, it can be considered to have laid the foundations on which current versions have been built.

2.5.2 Xi's (1986) and Malin's (1987) turbulent/non-turbulent models

Xi's PhD Thesis (Xi, 1986) applies the above ideas to single-phase and two-phase jets, the latter of both miscible and immiscible types. Two important simplifications were however made in his work: the fragment size was prescribed by a simple algebraic law (namely, the mixing-length law for a turbulent round jet, l=0.01584 z); and further, the modelling of the turbulent diffusion of mass and momentum was confined to a constant-effective-viscosity model, in the form $\mu_{eff} = C_\mu\, \rho\, w_{inlet}\, D_{inlet}$.

The results obtained by Xi were nevertheless encouraging: the conditional axial velocities for the turbulent and non-turbulent fluids were fairly well predicted, as were the evolution of the mean axial velocity along the centreline and the radial profile of the intermittency factor. The rate of spread ($\frac{dy_{0.5}}{dz}$) was, however, underpredicted by 7%.

Malin's work meant a step forward in the simulation of intermittency phenomena in jets, wakes and plumes. In addition to the features listed above, Malin's model uses a two-equation, k-ε model **within the turbulent phase.** The turbulent viscosity is thereafter computed from k (turbulent kinetic energy) and ε (rate of dissipation of k) as

$$\mu_t = C_1 \rho k^2 / \varepsilon .$$

The length scale, which still intervenes in the interphase exchange terms of E2.3 and E2.4, is also obtained from k and ε via the equation

$$l = C_2 k^{3/2} / \varepsilon .$$

Malin's model did perform satisfactorily in predicting the streamwise-velocity profile, both conditional (ie, turbulent and non-turbulent components) and mean. The intermittency factor was however **over**predicted; and a value of 0.082 was produced for the decay rate, with 0.086 being the experimental reference.

2.6 *The current thinking*

Two-fluid models underwent a major refurbishment from 1984 to 1986 (Spalding, 1984b; Wu, 1987), which brought the model into conformity with Prandtl's thinking, abandoning the initial idea of the simulation of turbulent/non-turbulent intermittency. The main conceptual modification was the

acknowledgement, in the model, of the role of shear in the production of turbulence. Thus, the cross-stream velocities were given the relevance first attributed by Prandtl (Section 2.4.1 above); the turbulent viscosity was re-formulated as a function of the cross-stream velocity-difference, $|v_1-v_2|$; and a shear-related source of lateral momentum was introduced as driving force of this difference.

The main model modifications will now be described, since they constitute the essence of the model employed in the present work.

2.6.1 Symmetric mass transfer

Previous two-fluid models assumed that the inter-phase mass transfer takes place in one direction only, namely from fluid 2 to fluid 1, regardless of the volume fraction of each fluid. Although this might be an appropriate choice for the turbulent jet under the intermittency model (where turbulent fluid "swallows" non-turbulent one), it is hard to support in many other instances.

An additional factor $(0.5-r_2)$ is therefore included which reverses the sign of the mass-transfer rate when one of the phases becomes dominant. The resulting mass-transfer source-term in the r_i equation (E2.3) is then:

$$m_{ji} = (-1)^i C_m \rho r_1 r_2 (0.5-r_2) |V_1-V_2| / l \qquad [E2.7].$$

(Since this symmetric law brings the volume fractions r_1 and r_2 close to 0.5, the phase-diffusion term in the equations E2.3 and E2.4, which is proportional to ∇r_i, will be neglected from now on.)

2.6.2 Viscosity formula

Spalding (1984b) revived Prandtl's interpretation of μ_t[§] as the product of a length (l) and a "transverse" mixing-velocity (v_t), so that $\mu_t \approx l\, v_t$. Prandtl assumed that v_t was proportional to $l\,|\frac{dw}{dy}|$, and, therefore, $\mu_t \approx l^2|\frac{dw}{dy}|$, which is his well-known mixing-length law. Spalding (1984b) establishes a formal connection between two-fluid and Prandtl's theory, and concludes that this transverse velocity v_t is, in fact, the difference of the cross-stream velocities: $|v_1-v_2|$. Therefore:

$$\mu_t \approx l\ |v_1-v_2| \qquad \text{[E2.8]}.$$

2.6.3 The shear-related source of momentum in the cross-stream-velocity equation

Thus far, the general form of the model equations has been provided in Section 2.3.2 (equations E2.3 and E2.4), together with the formulae for the interphase friction (E2.6), interphase mass-transfer (E2.7) and viscosity (E2.8).

However, and in the absence of density differences, pressure gradients, buoyancy effects, and Coriolis and centrifugal forces (all absent in many instances, such as a single-phase jet in the open), the equations yield $\phi_1=\phi_2$ for all the variables. Particularly, and since $|v_1-v_2|=0$, there is no turbulent flux of momentum. This has led Spalding (1984b) to postulate the existence of a shear-related source of cross-stream momentum for the v-equations. This term, derived by assuming that the shear source is equilibrated by the inter-phase friction, has the form:

$$S_v = \pm C_v \frac{l_p}{l} \rho\, |v_1-v_2|\, |\frac{\partial w}{\partial y}| \qquad \text{[E2.9]},$$

---

§ Note that Prandtl's nomenclature in the quotation above has been changed here to make it compatible with the rest of this work.

where

y	is the cross-stream direction;
z	is the axial direction;
Cv	is a constant;
l_p	is the Prandtl mixing-length, l_p=constant*z
l	is the fragment length;
w	is the average axial-velocity, $w= r_1 w_1 + r_2 w_2$.

The plus sign is used in the v-equation for one of the fluids (arbitrarily chosen as fluid 2 in this work), and the minus sign is used for the other.

The physical meaning of such a term in the v-momentum equations is clear: whenever we have a shear layer with v_1 and v_2 equal to zero but with finite $\partial w/\partial y$ and $|V_1-V_2|$, the source term introduces a cross-stream component which expresses the tendency of the layer to break into a series of vortices. These vortices, as they are convected downstream by the mean flow, are seen by a fixed observer as trains of up-moving fluid ($v>0$) and down-moving fluid ($v<0$) in rapid succession.

Two-fluid models incorporating this source term are, for the reasons outlined in the preceding paragraph, referred to as **in-and-out** (or up-and-down) models.

2.7 *Other applications*

The ability of two-fluid model to represent turbulent flows with variable density has been explained in Section 2.2 above. This potential was recognised since the very early stages of model development. Spalding (1983) discussed the adequacy of two-fluid models to convey the essence of turbulent combustion by defining the fluids as burned and unburned. A first computational assessment of Spalding's ideas

can be found in the work of Wu (1984), in which a two-fluid model was applied to the computation of premixed flames. This was an idealised, one-dimensional problem contrived to bring forward the consequences of two-fluid thinking. Thus, a relative slip between both fluids was shown to be the effect of the interaction between pressure gradient and density differences. The role of this interaction in flame propagation was also studied by Spalding (1984a), again for an idealised situation.

The more recent version of the model (as discussed in Section 2.6) has been applied by Spalding (1984b) to a Couette flow with heat transfer, in which the shear-induced source of cross-stream momentum (Section 2.6.2) drives one of the fluids upwards while the other moves downwards. Further applications have been also reported which explore the use of two-fluid models for the simulation of flat-plate boundary-layers (Ilegbusi and Spalding, 1987a), pipe and channel flows and plane and round jets (Ilegbusi and Spalding, 1987b).

The same new version was further used by Wu (1987) for the prediction of premixed flames in the wake of a flame holder. Comparisons with existing experimental data were provided, showing a promising agreement.

Two-fluid models constitute an attractive option for the representation of reciprocating-engine combustion. Spalding (1987, 1988) shows how the piston-induced acceleration interacts with density differences, resulting in the development of a Rayleigh-Taylor instability. Despite some simplifying assumptions (entrainment is one-directional, combustion is represented by entrainment itself and thermodynamics are kept to the bare essentials), it is clearly shown how combustion is enhanced by burned, hot products being entrained by unburned fuel as a consequence of the instability.

The Rayleigh-Taylor instability is, in itself, the focus of Andrews' experimental and theoretical study (Andrews, 1986). In the experimental part of his work, the instability is brought about by situating a heavier fluid (brine) on top of a lighter one (clear water) in the gravitational field. In the theorical part, a two-fluid model is proposed for the phenomenon, and then integrated numerically. The computed volume-fraction field is compared with photographs of the experimental run showing the evolutions of both fluids as the instability develops. Satisfactory qualitative agreement was found.

More recently, Youngs (1988) has proposed a multifluid model for the study of the Rayleigh-Taylor instability, in which a density range is assigned to each fluid.

2.8 Closure

A [relatively] new kind of turbulence model has been introduced in this chapter. These models propose the treatment of turbulence in a single-phase flow as the outcome of the interaction of two different (but miscible), intermingling fluids.

The origins of the idea have been traced back to the early days of turbulence modelling, and a similar scheme has been reported to be present in "intermittency" models of the 70's and 80's. The evolution of two-fluid models to their current state has been traced with a survey of the relevant works.

It may be concluded that two-fluid models bring to the forefront of turbulence modelling ideas such as fragmentariness, intermittency and the interaction of larger structures. It is hoped that they can, at least, bring an alternative view to that of conventional models.

Chapter 3

Numerical-integration method

3.1 Introduction

3.1.1 The problem to be tackled

As stated in preceding chapters, the aim of the present work is the formulation and assessment of a mathematical model for the simulation of single-phase jets and of sprays.

Although the actual equations which constitute the model have not been formally stated yet, they were introduced in Chapter 2 as having the general form:

$$\underbrace{\frac{\partial(\rho_i r_i \phi_i)}{\partial t}}_{\text{Transient}} + \underbrace{\nabla(\rho_i r_i \mathbf{V}_i \phi_i)}_{\text{Convection}} - \underbrace{\nabla(r_i \Gamma_{\phi i} \nabla \phi_i)}_{\text{Diffusion}} = \underbrace{([\![m_{ji}]\!] + f_{ji})(\phi_j - \phi_i)}_{\text{Interfluid}} + \underbrace{S_{\phi i}}_{\text{Source}} \quad \text{[E3.1]},$$

where r_1 and r_2 (the volume fractions) verify:

$$r_1 (x, y, z, t) + r_2 (x, y, z, t) = 1 \quad \text{[E3.2]}.$$

Several equations like E3.1 (one for each flow variable) are needed to describe a problem, and the resulting system of partial differential equations is not only highly non-linear but also strongly interconnected. As a consequence, an **analytical** solution of such a set of equations is not feasible except in a very limited number of simple cases. However, solution methods do exist which, with the aid of digital computers, yield an approximate solution in a finite number of

space/time points of the set of equations, if adequate thermophysical properties and boundary and initial conditions are supplied. One of such methods will be used in this work to integrate numerically the differential equations which govern the problem under study. This method is described in the remainder of this third chapter.

3.1.2 The method chosen

A number of numerical methods have been developed over the last twenty-five years for the numerical solution of fluid-flow problems described by equations similar to E3.1. While some of these methods were devised for specific problems (and are, therefore, of little use for the present purposes), others were created with the aim of generality; and one of the latter will be selected for this work. This is the finite-difference-like method known as the "finite-volume method" (Patankar and Spalding, 1972; Patankar, 1980; Spalding, 1980a). This will be supplemented with the technique contrived by Spalding (1981) to extend the method to flows in which two or more phases co-exist.

The finite-volume method can be thought of as having three well-defined stages:-

1. The flow domain is broken up into a finite number of small elements (cells), conforming the so-called **computational grid.**

2. The transport equations E3.1 are integrated over each cell, thus resulting in a system of **algebraic equations** with the values of the variables at each cell as unknowns.

3. This set of interconnected, non-linear equations is **solved** in an **iterative** fashion, using specially-designed algorithms to ensure [hopefully swift] convergence to the solution.

The finite-volume method poses a major advantage over finite-element and other finite-difference methods: if the solution is adequately converged, the conservation laws are fulfilled for each individual cell, and therefore for the whole of the domain. No mass or property is therefore "created" by inaccuracies brought about by the use of a coarse grid.

3.1.3 The extent of the present description

The two-phase finite-volume method employed in this work is based upon a corresponding one for single-phase flows; and as such, it has been used, with constant improvements, over the last 20 years. A detailed account of it would be, for this reason, inappropriate in the context of this thesis.

Consequently, only the main features of the solution procedure are provided with entries in this chapter. Particular attention is paid to those aspects which are specific of the two-phase solution-algorithm; and references which give full details are provided where appropriate.

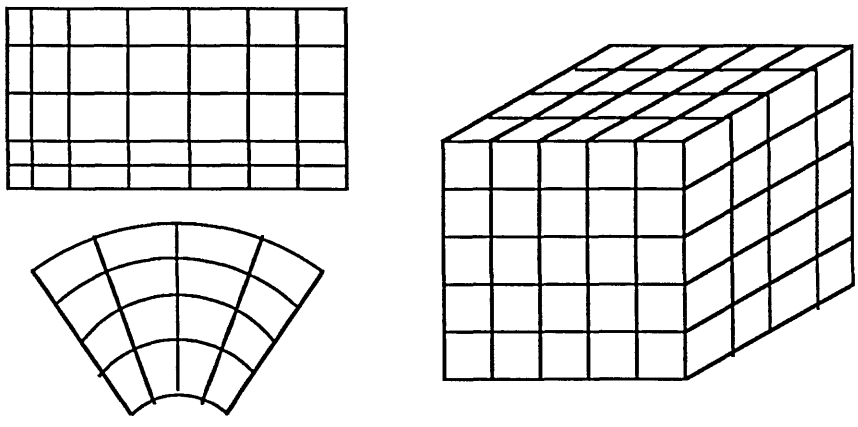
3.1.4 Outline of the chapter

The three steps of the finite-volume procedure, as described in Section 3.1.2 above, are dealt with in Sections 3.2 (computational grid), 3.3 (derivation of algebraic equations) and 3.4 (solution of the equations). Section 3.5 refers to **control** of the solution procedure, and Section 3.6 to the computer program used. Section 3.7 closes the chapter.

3.2 The finite-difference grid

3.2.1 The idea

The finite-volume method starts by breaking up the fluid-flow domain into a number of orthogonal, contiguous cells forming a cartesian or cylindrical-polar grid, such as those represented in figure F3.1. (Extensions of the method to more general and non-orthogonal grids do exist, but they will not be considered in this work.)



• ***Figure F3.1: Finite-volume grids*** •

In time-dependent problems, the time must also be discretised into a number of intervals, much as a spatial coordinate in which events occur only in one "direction" (from "old" times to "new" times).

3.2.2 The storage of the variables

Each of these cells is assigned a value for each of the intervening dependent variables. (Working out these values is, of course, the purpose of the numerical method). The location to which the value is attached depends on the variable considered: whilst the so-called "scalar" variables (pressure, enthalpy, volume fractions, concentrations) are stored at the **cell centre**, the velocity components

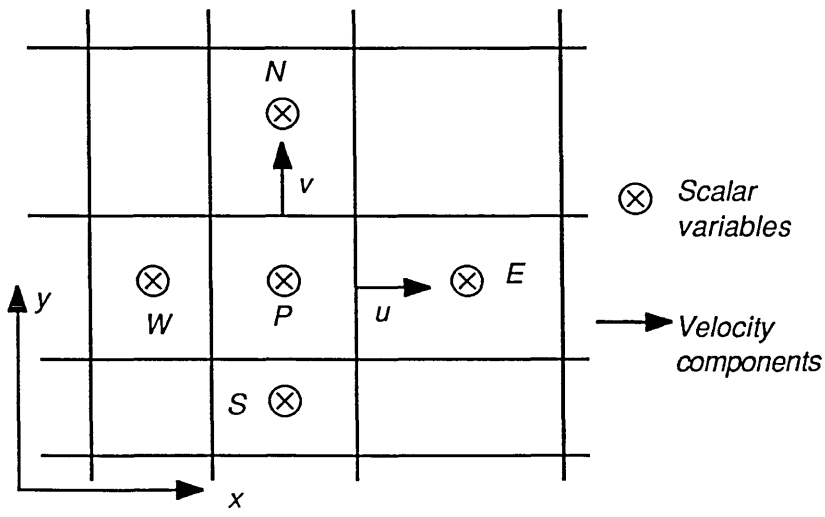
are stored at the **cell faces.** This scheme, known as the "staggered-grid arrangement", is shown in figure F3.2 for **u** and **v** and. It was first used by Harlow and Welch (1965), and has two major advantages:-

(a) The velocities are stored between two adjacent pressure-locations, and this is coherent with the role of pressure differences as driving forces for the velocities (the terms $\partial p/\partial x$, $\partial p/\partial y$, $\partial p/\partial z$ in the momentum equations).

(b) It provides the value of the velocity at the cell face without the need of interpolation between node values. It will be seen in subsequent sections that this value is needed during the solution procedure.

3.2.3 Notation

Figure F3.2 shows also the notation employed in this chapter for the grid points. The cells next to P are referred to as W(est), E(ast), N(orth) and S(outh), plus H(igh) for the higher-z cell and L(ow) for the lower-z cell (not shown in F3.2). The cell P at the previous time-step is referred to as cell T.



• ***Figure F3.2: Scalar and velocity locations*** •

The P-cell faces are named with the same criterion, but using small letters instead (thus: w, e, n, s, h, l).

3.2.4 Grid fineness: accuracy versus economy

Whether the solution of the resulting set of algebraic equations represents to a suitable degree of accuracy the physical phenomenon is a central issue which depends on:-

a. The adequacy of the mathematical model (embodied in the differential equations) chosen to represent the phenomenom;

b. The adequacy of the numerical method chosen to solve the set of differential equations.

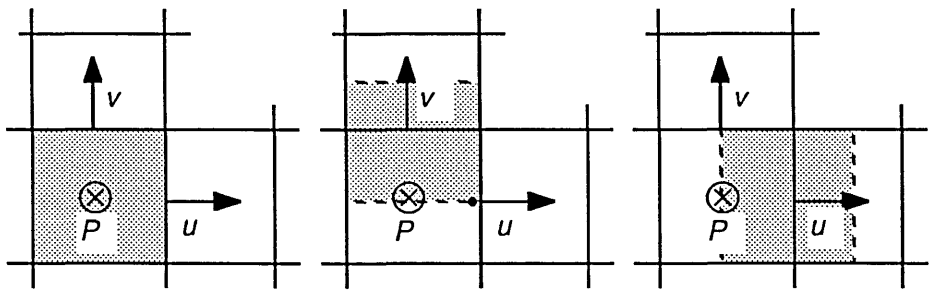
c. The adequacy of the parameters of the numerical method (eg number of grid points, number of time-steps, number of iterations, tolerance).

Proving the adequacy of the mathematical model (point **a** above) is indeed the aim of this thesis. The numerical method (point **b**), on the contrary, will be deemed dependable in the light of the experience accumulated over the past 25 years. As for the fineness of the computational grid and the sufficiency of other numerical parameters (point **c**), the issue here is one of a trade-off between accuracy and economy: more cells, for instance, mean more algebraic equations to be solved, and therefore more computer time to be spent. In this work, the independence of the solution from the numerical parameters will be nevertheless proved where appropriate.

3.3 Finite-volume (algebraic) equations

3.3.1 From differential equations to algebraic equations

The differential equation E3.1 is transformed into an algebraic equation by integrating it over each cell P. (For the velocity components, staggered cells are built around the storage point, as shown in figure F3.3).



• ***Figure F3.3: Control volumes for scalars and velocity components*** •

This process is now outlined for each of the terms of equation E3.1.

3.3.2 Transient term

The integration of the transient term over the control volume yields (phase-index i dropped for simplicity):

$$\mathfrak{T} = \iiint_{V_P} \frac{\partial(\rho\, r\, \phi)}{\partial t} dv = \frac{V_P}{\Delta t} (r_P \rho_P \phi_P - r_T \rho_T \phi_T) \qquad [E3.3],$$

where

V_P is the cell volume;

Δt is the current time step;

P refers to the values of the variables at P and at the end of the time step;

T refers to the values of the variables at p at the previous time step.

In E3.3, the variables have been assumed to be constant throughout the control volume, and equal to their value at P.

3.3.3 Convective term

The volume-integral of the convective-term is transformed into an integral over the cell surface using the divergence theorem of Gauss:

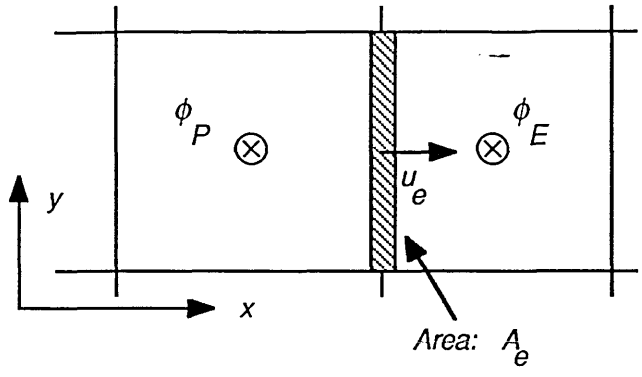
$$\mathbb{C} = \iiint_{V_p} \nabla (\rho\, r\, \mathbf{V}\, \phi)\, dv = \iint_{Ap} \rho\, r\, \mathbf{V}\, \phi \; d\mathbf{A} = \sum_{\text{all faces}} \rho\, r \mathbf{V}\, \phi \; \mathbf{A} \qquad \text{[E3.4]},$$

where **A** is the area vector for the face in question, and the phase-index **i** has again been dropped for brevity.

E3.4 will now be illustrated for **one** of the cell faces, namely the **east** one (figure F3.4). The term to compute is, therefore:

$$\mathbb{C}_e = [\rho r \mathbf{V} \phi\, \mathbf{A}]_e = [\rho r \phi]_e\, u_e\, A_e \qquad \text{[E3.5]}$$

While, owing to staggering, u is stored at e (figure F3.4), ρ, r and ϕ are **not**, and some kind of interpolation is needed. (NB ρ is not a dependent variable; but it is nevertheless a property which is computed as a function of variables which **are** stored at P: pressure, temperatures, ...)



• ***Figure F3.4: Control volume -- East face*** •

The so-called "upwind" practice (Patankar 1980, Spalding 1980a) is employed to compute the values of ρ_e, r_e and ϕ_e . Under this scheme, the sign of u_e determines which values are used for the contribution of the cell east-face:-

- o if $u_e>0$, and therefore the matter at e has been convected from P, the values at P are used: ρ_P, r_P and ϕ_P.

- o But if $u_e<0$, then the values at E are selected: ρ_E, r_E and ϕ_E.

The contribution of the east face to the convection of property through the cell limits is, therefore:

$$\mathbb{C}_e = \rho_P r_P \phi_P \, A_e \, [\![u_e]\!] - \rho_E r_E \phi_E \, A_e \, [\![-u_e]\!] \qquad \text{[E3.6].}$$

3.3.4 Diffusion term

The integral over the cell volume of the diffusion term in E3.1 is also transformed into a surface integral. Therefore:

$$\mathbb{D} = -\iiint_{V_p} \nabla (r \, \Gamma \, \nabla\phi) \, dv = -\iint_{Ap} (r \, \Gamma \, \nabla\phi) \; d\mathbf{A} =$$

$$= -\sum_{\text{all faces}} r \, \Gamma \, \nabla\phi \, \mathbf{A} \qquad \text{[E3.7].}$$

For the **east** face (F3.4), the term to compute is:

$$\mathfrak{D}_e = - [r\,\Gamma\,(\nabla\phi)\,\mathbf{A}]_e = - [r\,\Gamma]_e\,(\nabla\phi)_e\,A_e \qquad \text{[E3.8].}$$

The volume fraction r and the diffusion coefficient Γ are stored at P and E, but not at e (figure F3.4). The value $[r\,\Gamma]_e$ is therefore taken as the average of $[r\,\Gamma]$ at P and E. Then:

$$[r\,\Gamma]_e = \frac{r_P\,\Gamma_P + r_E\,\Gamma_E}{2} \qquad \text{[E3.9].}$$

The gradient term is computed as

$$(\nabla\phi)_e = \frac{\phi_E - \phi_P}{|PE|} \qquad \text{[E3.10],}$$

with |PE| being the distance between P and E.

The resulting diffusion term is, therefore, for the east face:

$$\mathfrak{D}_e = - D_e\,(\phi_E - \phi_P) \quad \text{with } D_e = \frac{r_P\,\Gamma_P + r_E\,\Gamma_E}{2}\,\frac{A_e}{|PE|} \qquad \text{[E3.11].}$$

In the present work, [E3.11] is further multiplied by the factor $[\![1.0-\zeta\,|F_e/D_e|]\!]$, with ζ being a constant coefficient of value 0.0 or 0.5, and F_e being the convective flux through the face in question: $F_e = \rho_P r_P\,A_e\,[\![u_e]\!] - \rho_E r_E\,A_e\,[\![-u_e]\!]$.

The resulting diffusion contribution is therefore:

$$\mathfrak{D}_e = - [\![1.0 - \zeta\,|F_e/D_e|]\!]\,D_e\,(\phi_E - \phi_P) \qquad \text{[E3.12].}$$

- When ζ=0.0, the diffusion term is

$$\mathfrak{D}_e = - D_e\,(\phi_E - \phi_P) \qquad \text{[E3.13],}$$

which together with the convection contribution of E3.6 constitute the **upwind scheme.**

- When ζ=0.5, the contribution is

$$\mathfrak{D}_e = - [\![1.0 - 0.5\ |F_e/D_e|]\!]\ D_e\ (\phi_E - \phi_P) \qquad \text{[E3.14]},$$

which is cut out when the Pecklet number $|F_e/D_e|$ is greater than 2. This, together with the convection contribution (E3.6) constitute the **hybrid scheme** (Spalding, 1972). This is the option employed in the present work.

3.3.5 Interfluid-transfer term

Integration of the interfluid-transfer term yields:

$$\mathfrak{I} = \iiint_{V_P} ([\![m]\!] + f)\ (\phi_j - \phi)\ dv \approx ([\![m_P]\!] + f_P)\ (\phi_{jP} - \phi_P)\ V_P \qquad \text{[E3.15]},$$

where

- the subindices ji and i in equation E3.1 have now been dropped;
- m_P and f_P are the values of the interphase-transfer rates in the cell, presumed constant over the cell volume V_P;

3.3.6 Other source terms

The within-fluid source $S_{\phi i}$ is also integrated over the volume V_P; and the integrated value is further assumed to be linearised, so that it may be written as

$$\mathfrak{S} = \iiint_{V_P} S_\phi\ dv \approx V_P\ C_{\phi P}\ (V_{\phi P} - \phi_P) \qquad \text{[E3.16]},$$

with $C_{\phi P}$ and $V_{\phi P}$ being the coefficients in the linear form.

3.3.7 The final finite-volume equation

The results of preceding subsections can now be gathered in the finite-volume counterpart of the partial differential equation E3.1:

$$a_P \phi_P = \sum_{F=W,E,S,N,H,L} a_F \phi_F + a_T \phi_T + V_P C_{\phi P} V_{\phi P} + ([\![m_P]\!] + f_P) V_P \phi_{jP} \quad [E3.17],$$

the coefficients of which are given by:

- $$a_T = \frac{V_P}{\Delta t} r_T \rho_T \quad [E3.18];$$

- $$a_E = \rho_E r_E A_e [\![-u_e]\!] + D_e \quad \text{(and similarly for other RHS a's)} \quad [E3.19];$$

- $$a_P = \frac{V_P}{\Delta t} r_p \rho_p + \sum_{F=W,E,S,N,H,L} (\rho_F r_F A_f [\![u_f]\!] + D_f) + V_P C_{\phi P}$$

  $$+ ([\![m_P]\!] + f_P) V_P \quad [E3.20].$$

In the parabolic cases considered in this work, there is no influence on ϕ_P from the downstream-direction value ϕ_H, and therefore a_H=0 in E3.17.

3.3.8 The velocity-components equations

The velocity components, as pointed out in Section 3.3.1, are stored at staggered locations, and their equations are integrated over staggered control volumes. Their finite-volume equation can be derived following the procedure outlined above, the result being a linear equation similar to E3.17.

3.3.9 Boundary conditions

The boundary conditions are inserted in the finite-volume equation via source terms affecting the cells involved. These sources have the linear form of E3.16:

$$S_{\phi P} = C_{\phi P}(V_{\phi P} - \phi_P) \qquad [E3.21].$$

It can be easily shown (Patankar, 1980) that this practice caters for two kind of boundary conditions:-

(a) **Fixed-value (Dirichlet) boundary-conditions**: A value (say, $V_{\phi P}$) can be imposed at the cell if $C_{\phi P}$ is large enough to reduce the finite-volume equation E3.17 to

$C_{\phi P}(V_{\phi P} - \phi_P) \approx 0 \Rightarrow C_{\phi P}\phi_P = C_{\phi P}V_{\phi P} \Rightarrow \phi_P = V_{\phi P}$.

(b) **Fixed-flux (Von Newman) boundary-conditions**, procured by making the coefficient $C_{\phi P}$ very small, and setting $V_{\phi P}$ to the desired flux divided by $C_{\phi P}$.

3.4 Solution procedure

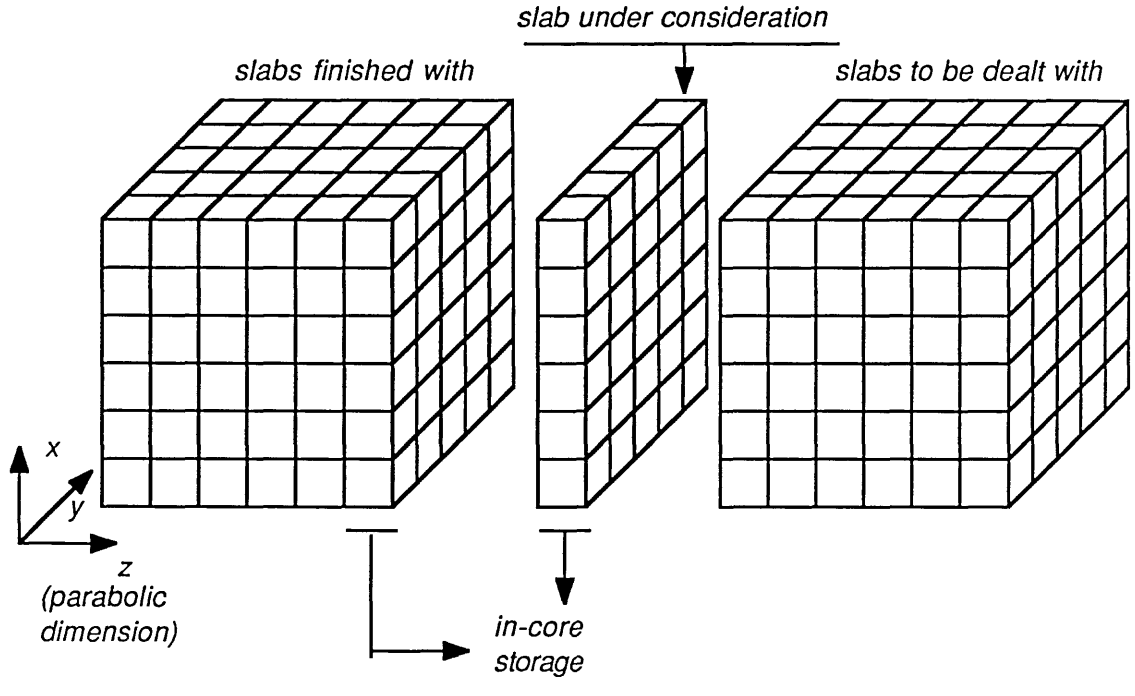
The sets of finite-volume equations having the form of E3.17 are solved using the IPSA algorithm of Spalding (1976c, 1981). IPSA is an acronym for **I**nter**p**hase **S**lip **A**lgorithm, and is the two-phase counterpart of the well-know SIMPLE series for single-phase flows (Spalding, 1980a; Patankar, 1981).

The version of the solution cycle selected for this work proceeds in a slab-by-slab fashion. When a slab (xy array of cells) has been dealt with, the solver moves on to the next one. Several sweeps of the domain are, in the general case, needed, since

the off-slab values are treated temporarily as known. But, for a parabolic flow in which z is the parabolic dimension, the absence of upstream influences means that:

(a) Only one sweep of the domain is needed, since the upstream slab of unknown values does not intervene in the equations for the current slab;

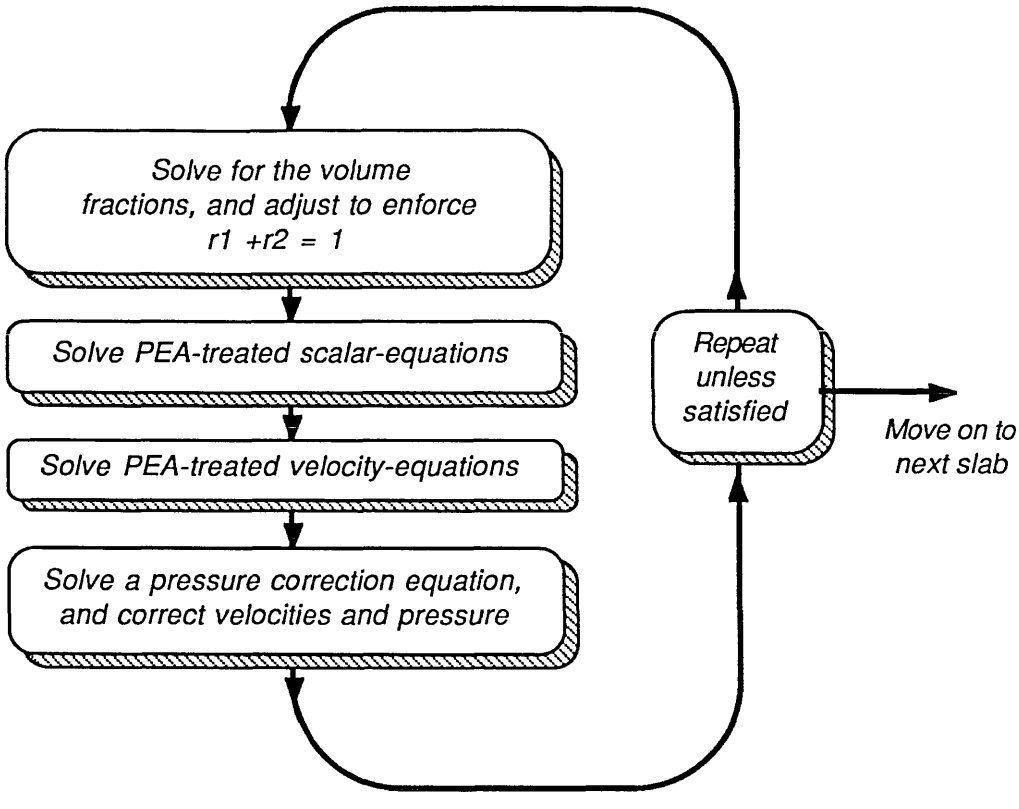
(b) Only the current and the previous slab need to be stored in memory (figure F3.5).



• ***Figure F3.5: Slabwise storage-arrangements*** •

for parabolic problems

The IPSA solution-cycle (sketched in figure F3.6) proceeds by solving the equations using a "guessed" or "initial" pressure field, and then correcting the pressure and velocities via a "pressure-correction equation", which enforces the fulfilment of the joint-continuity equation. The key steps of IPSA are commented below.



• ***Figure F3.6: The IPSA solution-cycle*** •

3.4.1 Step 1: Solution of the volume-fraction equations and correction

The finite-volume equations for r_1 and r_2 (obtainable from the general equation E3.1 by setting ϕ_i=1 and putting a unique source term m_{ji}) are solved using a linear solver (Section 3.4.5 below). The volume fractions thus obtained (say r_1^* and r_2^*) are unlikely to verify $r_1^*+r_2^*=1$, since the velocity field used is not the correct (converged) one. Therefore, the r_i^*'s are corrected, before proceeding, by dividing them by $r_1^*+r_2^*$. Thus:

$$r_i = \frac{r_i^*}{r_1^* + r_2^*} \qquad \text{[E3.22].}$$

(Note that there is no correction in the converged solution, in which $r_1^*+r_2^*=1$.)

3.4.2 Step 2: Solution of PEA-treated equations for scalar-variables

The finite-volume equations for a scalar variable ϕ can be rewritten so as to stress the interphase dependence brought about by the interphase-friction term on the RHS of the equation. Thus (subindex P omitted):

$$p_1 \phi_1 = q (\phi_2 - \phi_1) + t_1 \qquad \text{[E3.23a];}$$

$$p_2 \phi_2 = q (\phi_1 - \phi_2) + t_2 \qquad \text{[E3.23b],}$$

with p, q and t being coefficients, the form of which can be obtained by matching E3.23 and E3.17.

From E3.23a, it follows that

$$\phi_1 = (q \phi_2 + t_1)/(p_1 + q) \qquad \text{[E3.24a];}$$

and, similarly, from E3.23b:

$$\phi_2 = (q \phi_1 + t_2)/(p_2 + q) \qquad \text{[E3.24b].}$$

If q is large (ie, if there is a strong interphase coupling), E3.24a and E3.24b are respectively reduced to $\phi_1 \approx \phi_2$ and $\phi_2 \approx \phi_1$. This means that each variable is given the other's previous value, and therefore successive substitution during the iteration procedure leaves the values unchanged. The **P**artial-**E**limination **A**lgorithm (PEA, Spalding 1976c, 1981) was devised to speed up convergence in these circumstances.

Under the PEA scheme, the value of ϕ_2 in E3.24a is substituted by that given by E3.24b. A similar operation is carried out in E3.24b, giving:-

$$\phi_1 = \frac{p_2 t_1 + (t_1 + t_2)\, q}{p_1 p_2 + (p_1 + p_2)\, q} \qquad \text{[E3.25a];}$$

$$\phi_2 = \frac{p_1 t_2 + (t_1 + t_2)\, q}{p_1 p_2 + (p_1 + p_2)\, q} \qquad \text{[E3.25b].}$$

For large values of q, both ϕ_1 and ϕ_2 tend now to $\phi_1 = \phi_2 = \frac{t_1 + t_2}{p_1 + p_2}$ but not to each other's **previous** value.

(NB ϕ_2 is still present in E3.25a through the coefficients p_2 and t_2, and similarly for ϕ_1 in E3.25b; the elimination is, therefore, only **partial**, and hence the name of the algorithm.)

3.4.3 Step 3: Solution of the momentum equations

The momentum equations are solved using, initially, a guessed pressure field. Since there is an interphase linkage via the friction term (drag), the equations are previously treated with the PEA algorithm.

3.4.4 Step 4: Solution of the pressure-correction equation

The solution procedure, as outlined so far, cannot secure the overall conservation of mass. Mass conservation is enforced in IPSA by the **pressure-correction equation**. The procedure to obtain this equation has been reported in detail in several papers by Spalding (1980b, 1982c). The essentials are described below.

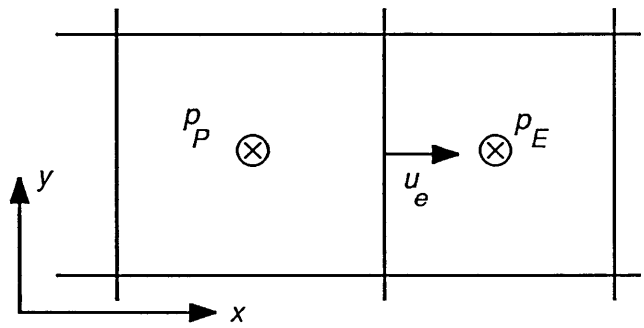
1. IPSA builds a "joint continuity equation" by adding the two volume-fraction equations, which have been previously multiplied by weighting factors (the local phase-specific-volume, $1/\rho_i$).

2. The existing velocity and volume-fraction fields do not satisfy, in general, this equation, yielding instead a "continuity error" ε_p.

3. The joint equation is differentiated with respect to pressure, and equated to ε_p. Thus, for example, the variable u_e yields the terms (figure F3.7):

$$u_e \longrightarrow \frac{\partial u_e}{\partial p_P}(p_P - p_P^*) + \frac{\partial u_e}{\partial p_E}(p_E - p_E^*) \qquad \text{[E3.26].}$$

(Volume fractions are temporarily treated as independent from pressure.)



• ***Figure F3.7: u_e and its driving pressures*** •

This operation gives, at each cell, an equation for the pressure correction $p_P' = p_P - p_P^*$ needed to satisfy continuity.

4. The terms $\frac{\partial u_e}{\partial p_P}$, $\frac{\partial u_e}{\partial p_E}$, etc, are found from the momentum equations. If these are written (eg for u_e) as:

$$u_e = \frac{a + b\,(p_P - p_E)}{d} \qquad \text{[E3.27].}$$

Then:

$$\frac{\partial u_e}{\partial p_P} \approx -\frac{\partial u_e}{\partial p_E} \approx -\frac{b}{d} \qquad \text{[E3.28].}$$

5. The resulting equations

$$L(p_P', p_W', p_E', p_S', p_N', p_L', p_H') - \varepsilon_p = 0,$$

of which there is one at each cell, are then solved using the linear solver.

6. The pressure and velocity components are corrected.

When steps 1 to 6 are completed, IPSA proceeds to restart the solution cycle by solving the volume-fraction equations (Section 3.4.1 above), unless the results are considered to be adequately converged.

3.4.5 The linear-equation solver

At each slab (or xy array of cells) the system of linear equations is solved by a generalised (two-dimensional) version of the TDMA (**T**ri-**d**iagonal-**M**atrix **A**lgorithm). The off-slab values (ϕ_L and ϕ_H) of the variable in question are temporarily treated as known, and the equation is reduced to:

$$a_P \phi_P = a_W \phi_W + a_E \phi_E + a_S \phi_S + a_N \phi_N + B \qquad \text{[E3.29]},$$

where B includes the off-slab terms.

(Note: For parabolic flows in which z is the parabolic direction, the off-slab values **are** known: ϕ_L is the result of the previous slab, and ϕ_H has no influence on ϕ_P. This is the reason why the solver can proceed in a single "sweep" of the computational domain, as stated in Section 3.4.)

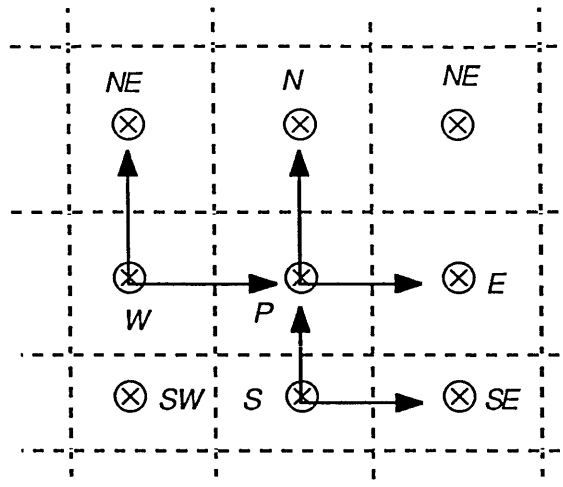
Then, the algorithm postulates the existence of a relationship in the form:

$$\phi_P = N_P \phi_N + E_P \phi_E + F_P \qquad \text{[E3.30]}.$$

By substituting E3.30 in E3.29 for ϕ_P, ϕ_S, and ϕ_W, the values of N_P, E_P and F_P are found as functions of:-

(a) N_S, N_W, E_S, E_W, F_S, F_W;

(b) ϕ_{SE} and ϕ_{NW}, introduced by the substitution E3.30 (see fig F3.8).



• ***Figure F3.8: Values introduced by the substitutions •***

for ϕ_P, ϕ_S, and ϕ_W

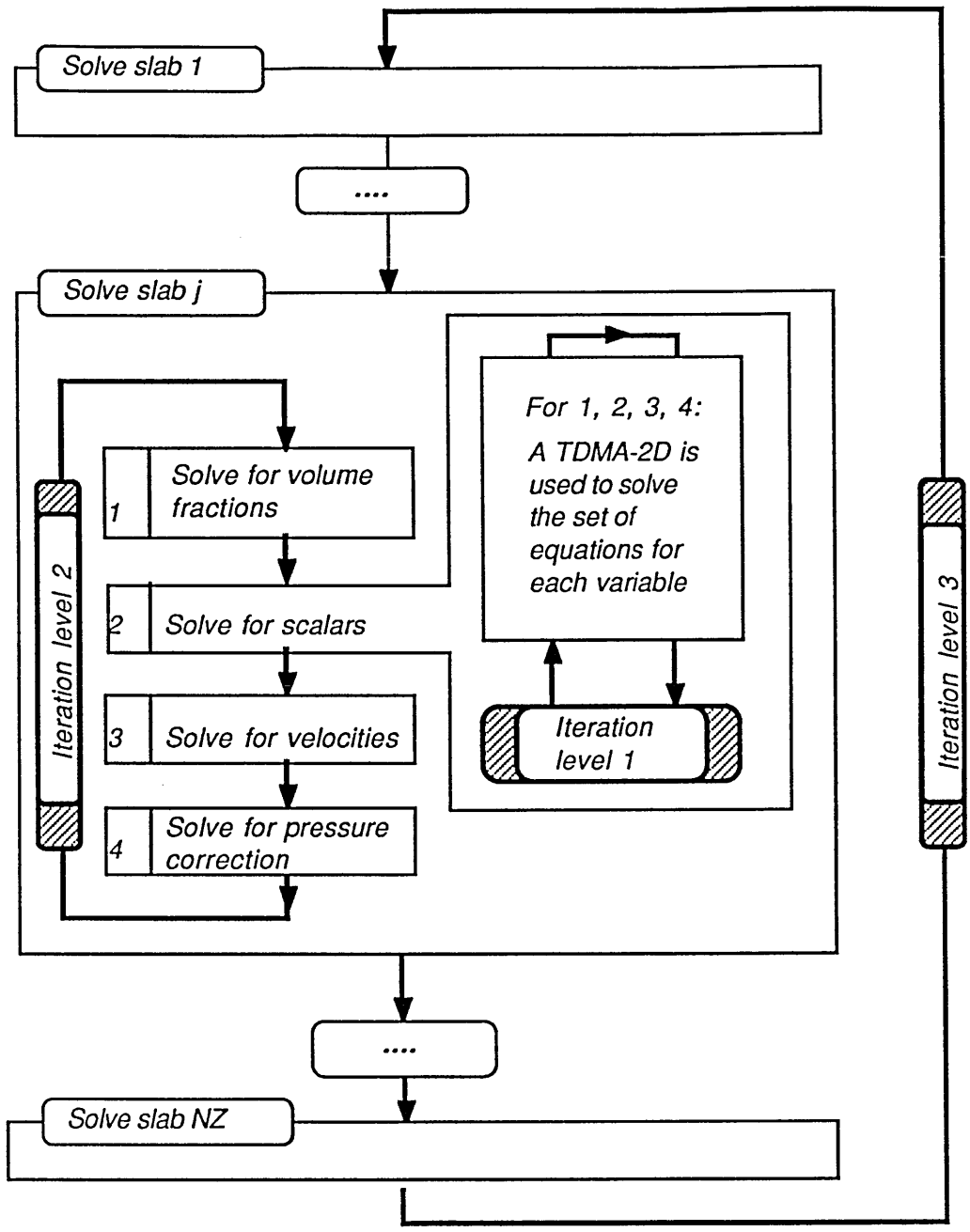
The slab is then swept once from the SW corner to the NE, finding the coefficients N, E and F for each cell; and then it is swept "backwards" from the NE corner to compute the ϕ's using E3.30. Additionally, iteration is required because of the presence of ϕ_{SE} and ϕ_{NW} (with guessed values) in the equations for E, N and/or F. (For one-dimensional slabs the algorithm is reduced to the ordinary TDMA, in which no values are guessed and no iteration needed.)

3.5 Convergence promotion and control

3.5.1 Introduction

The idea of **iteration** has been used in several occasions throughout this chapter, making of it the core of the numerical-solution mechanism.

However, it must be summarised that there are **three** distinctive levels of iteration in the solution method selected. These have been sketched in figure F3.9, and are:-



• ***Figure F3.9: Solution-procedure iteration-levels*** •

i. The **inner level** (level 1), which solves, at each slab, the interconnected set of linear equations for each ϕ. This is the TDMA iteration.

ii. The **hydrodynamic level** (level 2), which deals with the coupling of the equations for different ϕ's at each slab. This is the IPSA iteration-cycle, which, by making the necessary adjustments, "blends together" the results to enforce the overall conservation of mass and properties on that slab.

iii. The **outer level** (level 3), which sweeps the domain to propagate the slab changes to neighbouring slabs. In the parabolic cases of this work, this level is not necessary, as discussed in Section 3.4.5.

The next two sections refer to the mechanisms employed to monitor this iterative process, and to foster the convergence to the solution.

3.5.2 Convergence monitoring

Convergence is monitored in the present work through the residuals ε, defined as the difference between the RHS and the LHS of equation E3.17:

$$\varepsilon_P = a_P \phi_P - \sum_{F=W,E,S,N,H,L} a_F \phi_F + a_T \phi_T + V_P C_{\phi P} V_{\phi P} + (\llbracket m_P \rrbracket + f_P) V_P \phi_{jP} \qquad [E3.31].$$

The quantity monitored is $\Sigma|\varepsilon_P|$, where the sum is extended to the current slab.

3.5.3 Convergence promotion

Convergence is fostered by means of two different devices:

(a) The prescription of the range in which some variables and properties are allowed to take values, thus avoiding the overshooting of physically realistic limits during the iteration process.

(b) Relaxation, which limits the change of the variable in each iteration.

Both linear and inertial relaxation are used. Linear relaxation sets the value of ϕ to

$$\phi = \alpha \phi_{new} + (1-\alpha) \phi_{old} \qquad [E3.32],$$

where α is the relaxation coefficient ($0<\alpha\leq 1$).

Inertial relaxation amounts to the use of a false time-step Δt_f. A source term of the form:

$$S_\phi = \frac{\rho r V_p}{\Delta t_f} (\phi_{old} - \phi) \qquad [E3.33]$$

is added to the finite-volume equation E3.17.

3.6 *The computer program*

The solution procedure so far described is embodied, together with other alternatives not selected for the present work, in the PHOENICS computer code of Spalding (Spalding, 1982c; Rosten and Spalding, 1987).

PHOENICS (an acronym for **P**arabolic, **H**yperbolic **O**r **E**lliptic **N**umerical **I**ntegration **C**ode **S**eries) is a general-purpose computer-code which caters for fluid-flow problems which are:

- o one or two phase;
- o transient or steady;
- o zero, one, two or three dimensional;
- o parabolic, hyperbolic or elliptic;
- o turbulent or laminar.

PHOENICS provides a flexible framework with both

- o Built-in features (such as a choice of grid generators, solvers, property formulae, print-out provisions) selectable by use of a special CFD language (the **P**HOENICS **I**nput **L**anguage, PIL).

- o The possibility of supplementing (or, indeed, replacing) these features with one's own coding, to cater, for instance, for complex boundary conditions, special sources or new property formulae.

3.7 Closure

A numerical-solution method has been outlined which allows the numerical integration of two-phase, Eulerian equations having the general form of E3.1. The method is a finite-difference one which uses the IPSA algorithm to solve the pressure-velocity coupling.

The method is available as a collection of switch-on features in a commercially-available software-package PHOENICS, which supplemented by purpose-written offshootings where necessary, will be employed for this work.

Chapter 4

The single-phase, axi-symmetrical, turbulent jet

4.1 Introduction

4.1.1 The purpose of this chapter

The numerical simulation of single-phase jets by means of two-fluid models of turbulence was mentioned in Chapter 1 as one of the aims of this work. In this chapter, two alternatives are proposed and investigated, always within the framework of the two-fluid models described in Chapter 2. Both alternatives differ, essentialy, in the method used to model the fragment size. The performance of each of them is assessed by comparison of the results with available experimental data.

4.1.2 The models discussed

The fragment size has already been singled out in Sections 2.4 and 2.5 as a major component of the two-fluid theory. In the differential equations of Chapter 2, it intervenes in the viscosity formulae (E2.8), and in the source terms representing the exchange of both mass and properties between both phases (E2.6 and E2.7).

This chapter will formulate, apply and analyse two different options for fragment-size modelling, namely:-

a. The fragment size is computed, similarly to the Prandtl mixing-length theory, from an algebraic formula;

b. The fragment is computed through differential equations which account for the physical processes that the fragment undergoes. (These processes will be postulated below.)

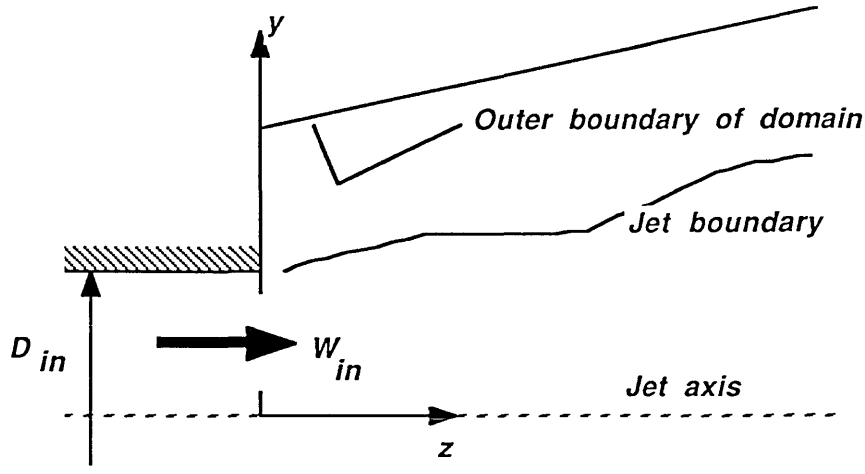
4.1.3 The layout of the chapter

The chapter has been set out in a conventional manner. The problem to be modelled is introduced in Section 4.2; Sections 4.3 to 4.5 establish the mathematical model; Section 4.6 presents the results, and the relevant conclusions are gathered in Section 4.7.

4.2 The flow considered

A steady, single-phase, turbulent, round jet is considered, as sketched in figure F4.1. Air is injected into quiescent surroundings at 30 m/s, through a nozzle of 2.5 cm diameter. The densities and viscosities of both the injected and the surrounding fluids are considered to be constant and equal, respectively, to 1 kg/m^3 and 10^{-5} m^2/s respectively. The resulting Reynolds number is 75000, although inlet diameter and velocity will be subsequently changed to cover a wide range of Reynolds numbers.

A cylindrical-polar coordinate-system will be used, in which **z** is taken as the axial direction, **y** is the radial direction and **x** is the circumferential direction. Since axial symmetry is considered, the problem is solved on the **yz** plane.



• *Figure F4.1: The problem considered* •

4.3 Mathematical model

The mathematical model employed for the numerical simulation is set out in this section. This is, as expected, a two-fluid model along the lines of those described in Section 2.5, in which two fluids (labelled 1 and 2) share the space. The source of cross-stream momentum introduced in Section 2.5.2 is positive for fluid 2, thereby termed "up-moving fluid".

4.3.1 Equations

Although the **general** form of the equations has been already established in Chapter 2, the actual equations employed to model the flow will be stated here for sake of completeness. (Appendix B compiles, as well, the whole set of equations for all the models proposed in this work.)

The independent variables which intervene in the equations are **y** (the radial direction) and **z** (the axial direction); the dependent variables are: r_1 and r_2 (the volume fractions), $v_1/v_2/w_1/w_2$ (the velocity components), p (the common pressure), and, in model b, l_1 and l_2 (the fragment sizes). The corresponding equations are listed below.

(a) Volume-fraction equations

$$\nabla(\rho_i r_i \mathbf{V}_i) = m_{ji} \qquad \text{[E4.1]},$$

where

m_{ji} is the interphase mass-transfer rate, to be given below;

ρ_i is the fluid density ($\rho_1=\rho_2=1$ for the single-phase jet).

(b) y-momentum equation

$$\nabla(\rho_i r_i \mathbf{V}_i v_i) - \nabla(r_i \mu \nabla v_i) = [\![m_{ji}]\!](v_j - v_i) + f_{ji}(v_j - v_i) -$$

$$- r_i \frac{\partial p}{\partial y} + (-1)^i S_v \qquad \text{[E4.2]},$$

where

- $\mu = \mu_l + \mu_t$;
- The first term on the RHS accounts for the increase/decrease of momentum owing to entrainment (the meaning of $[\![\bullet]\!]$ was explained in Chapter 2 as being $[\![x]\!]=x$ if $x>0$ and $[\![x]\!]=0$ otherwise);
- The second term is the interphase friction, with f_{ji} to be supplied below;
- And the last term on the RHS is the source of lateral (v) momentum, positive for fluid 2, to be specified below.

(c) z-momentum equation

$$\nabla(\rho_i r_i V_i w_i) - \nabla(r_i \mu \nabla w_i) = [\![m_{ji}]\!](w_j - w_i) + f_{ji}(w_j - w_i) - r_i \frac{\partial p}{\partial z} \qquad \text{[E4.3].}$$

The meaning of the terms on the RHS is similar to those for the v-momentum equation (E4.2).

(d) Closure equation

$$r_1 + r_2 = 1 \qquad \text{[E4.4],}$$

which states that both fluids fill the whole of the space.

4.3.2 Auxiliary relations

A number of auxiliary relations must be used in conjunction with the equations introduced in 4.3.1. These are defined in table T4.1 below.

• Table T4.1: Auxiliary relations for the single-phase jet •

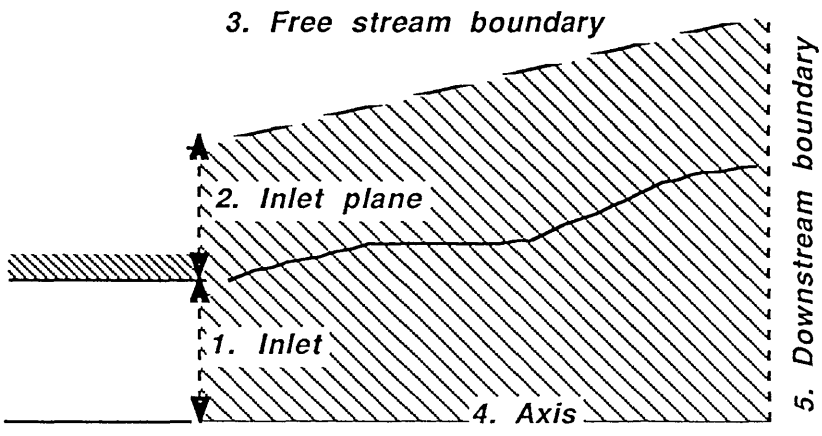
Viscosity	$\mu_t = C_\mu \rho r_1 r_2 \lvert v_1 - v_2 \rvert l$	[E4.5]
Interphase mass-transfer	$m_{ji} = C_m \rho r_1 r_2 (0.5 - r_i) \lvert V_1 - V_2 \rvert / l$	[E4.6]
Interphase friction	$f_{ji} = C_f \rho r_1 r_2 \lvert V_1 - V_2 \rvert / l$	[E4.7]
Source of v momentum	$S_v = C_v \frac{l_p}{l} \rho \lvert V_1 - V_2 \rvert \lvert \frac{\partial w}{\partial y} \rvert$	[E4.8]
Fragment length, l	To be supplied in Section 4.4	

4.3.3 Boundary conditions

Boundary conditions are required for the entry plane, the free-stream boundary and the symmetry axis; since the flow is (and is computed as) a parabolic one, no boundary condition is needed for the down-stream limit of the computational domain. The boundary conditions applied are listed in table T4.2, which refers to figure F4.2.

• ***Table T4.2: Boundary conditions for the single-phase jet*** •

Boundary	r_1	r_2	v_1	v_2	w_1	w_2	Pres-sure	Mass flux
Inlet	0.0	1		0.0		Win		ρ Win
Inlet plane	0.5	0.5	0.0	0.0	0.0	0.0	0.0	
Free stream	0.5	0.5	0.0	0.0	0.0	0.0	0.0	
Axis	no flux							0.0
Downstream	Not required since parabolic							



• ***Figure F4.2: Boundaries of the computational domain*** •

4.4 Fragment-size models

Section 4.1.2 announced the study of two different fragment-size models as one of the aims of this chapter; these models are now introduced.

4.4.1 Model a: algebraic

Model **a** explores the algebraic option for the fragment length, in which l is computed as $l=C_l z$. This option, much favoured in the past (Ilegbusi and Spalding 1987b, Xi 1986, Malin 1986), is therefore akin to a Prandtl-mixing-length assumption for l. In the present work, C_l will be taken as $C_l=0.01794$ (Ilegbusi and Spalding, 1987b).

4.4.2 Model b: differential equations

Model **b** studies the use of differential equations for the phase fragment-size, as exemplified by Spalding for a different type of flow (namely a Couette one, Spalding 1984b). These equations must bring into the mathematical model some postulated "rules" of fragment behaviour. These rules are:-

(a) That fragment growth is caused by two different mechanisms:

(i) **Entrainment**, by which a fragment of one of the fluids "swallows" or "engulfs" matter from the *other* fluid;

(ii) **Agglomeration**, by which two fragments of the *same* fluid coalesce to form a fragment.

(b) That size diminution is caused by shear, which distorts the fragment (eg by stretching) until it breaks into several fragments of smaller size.

The rate of-growth by entrainment will be here considered proportional to the velocity difference $|V_1-V_2|$. A further assumption is that growth by agglomeration is also proportional to that difference. Finally, the rate of size diminution (fragment break-up) will be taken as proportional to the rate of shear distortion, S_i.

The equations for the fragment size have therefore the form:

$$\frac{D l_i}{Dt} = C_a |V_1-V_2| - C_b l_i S_i \qquad [E4.9],$$

where S_i is a measure of the rate of shear distortion. (In this work, S_i is taken as $S_i = |\frac{\partial w_i}{\partial y}|$). The l_i factor multiplying S_i, which is also necessary on dimensional grounds, indicates that the break-up of a larger fragment is more likely to occur than that of a smaller fragment.

The fragment size for the auxiliary relations (formulae in table T4.1) is taken as the minimum of l_1 and l_2, thus assuming that the fluid whose fragments offer less surface for the exchange processes is actually controlling them.

4.4.3 Boundary conditions for l

The second model, as presented in the previous section, introduces two differential equations for the fragment-size (an equation for each fluid), and requires therefore the provision of two additional sets of boundary conditions. These are (see figure F4.2 above for nomenclature):-

- **At the inlet:** l_1 and l_2 should be given the value 0.0; but, as a measure to promote convergence, they are instead given a small value in the first slab. It will be shown that this has little effect on the solution, apart from the desired improvement to the speed of convergence in the first slabs.

- **At the inlet plane and free-stream boundary:** l_1 and l_2 are taken as 0.0, therefore proposing that the fragment-size must be zero where there is no velocity difference (ie, where, so to speak, "nothing happens").

4.5 *Model constants*

The model, as proposed, requires the provision of values for a total of 6 constants, which are listed in Table T4.3. The values of some of them have been chosen on "historical" grounds (ie, based on the experience of previous researchers); and other have been, in the present work, "tuned up" to optimise the model results.

• Table T4.3: Model constants •

Constant	Affecting term/property	Value	Reference
C_f	Inter-fluid friction	0.0375	Ilegbusi and Spalding, 1987b
C_m	Inter-fluid mass-transfer	10.0	Spalding, 1984b
C_μ	Viscosity	15.0	Ilegbusi and Spalding, 1987b
C_v	Shear source S_v	0.250 C_f 0.175 C_f	(this work, model **a**) (this work, model **b**)
C_a	Fragment growth	0.03	(this work)
C_b	Fragment break-up	0.01	(this work)

The effect of changing the constant values will be explored in Section 4.6.

4.6 Results

4.6.1 Presentation

The results provided by both models **a** (algebraic law for l) and **b** (differential equations for l_1 and l_2) are here compared with the experimental data of Rodi (1972) for the single-phase, round, turbulent jet.

Figure F4.3 represents the radial evolution of the average axial velocity w. It is computed as the average of w_1 and w_2 through the expression $w = r_1 w_1 + r_2 w_2$; in figure F4.3, this quantity has been represented in the well-known non-dimensional form: w/w_{ax} against $y/y_{0.5}$ (where $y_{0.5}$ is the y value for which $w=1/2\ w_{ax}$).

The graph shows how both models perform adequately in the region $0.0 \leq y/y_{0.5} \leq 1.25$. From $y/y_{0.5} \geq 1.25$, the algebraic model tends to underpredict the values of the axial velocity, whereas the predictions of the model which uses differential equations for l are much closer to the experimental reference.

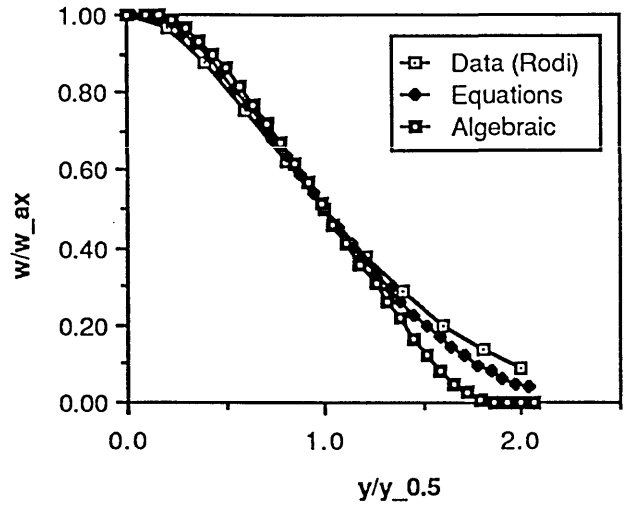
The axial-velocity decay-rate (**d**), defined as

$$d = \frac{d(w_{in}/w_{ax})}{d(z/D)} ,$$

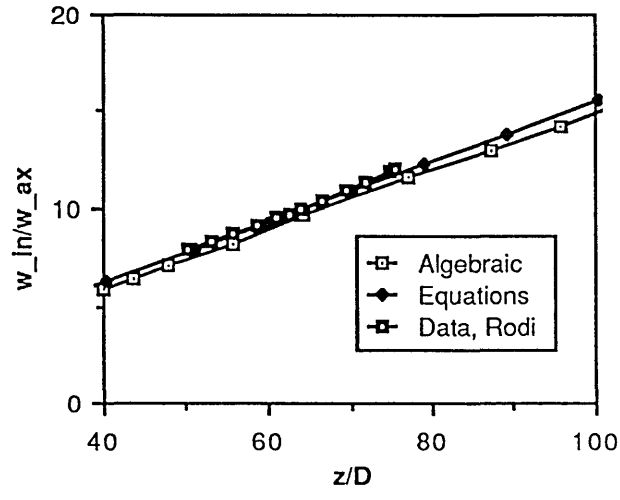
is represented in figure F4.4, together with Rodi's data. Both models provide suitable predictions, but the model using differential equations outperforms the algebraic one.

Finally, table T4.4 presents the values of the jet-spread rate (**s**), defined as

$$s = \frac{dy_{0.5}}{dz} .$$



• *Figure F4.3: Axial-velocity profile* •



• *Figure F4.4: Axial-velocity decay* •

• ***Table T4.4: Spread rate*** •

Model	s
a-Algebraic	0.0866
b-Differential Equations	0.0877
Experimental (Rodi)	0.086

Both models yield values for **s** within a 2% of the experimental data. However, it must be pointed out that **s** can be accurately matched by tuning up the model constants (particularly C_V), whereas the w profile is not as sensitive to the variation of these.

4.6.2 Further analysis

This section aims to gaining further understanding of the processes involved in the two-fluid idea by analysing some aspects of the flow for which a direct comparison with experimental data is not feasible.

In this section, some quantities have been made non-dimensional to allow a comparison of the results of both models. Therefore, a quantity in brackets means that the quantity has been made non-dimensional by multiplying by suitable scaling factors. Table T4.5 contains a list of the scaling factors used for this purpose.

• ***Table T4.5: Scaling factors*** •

Quantity	Factor
l, l_p	z
y	$y_{0.5}$
v, w, V	w_{ax}
μ	$z\ w_{ax}$
shso*	$\rho\ w_{ax}^2/y_{0.5}$

* Shear source of momentum

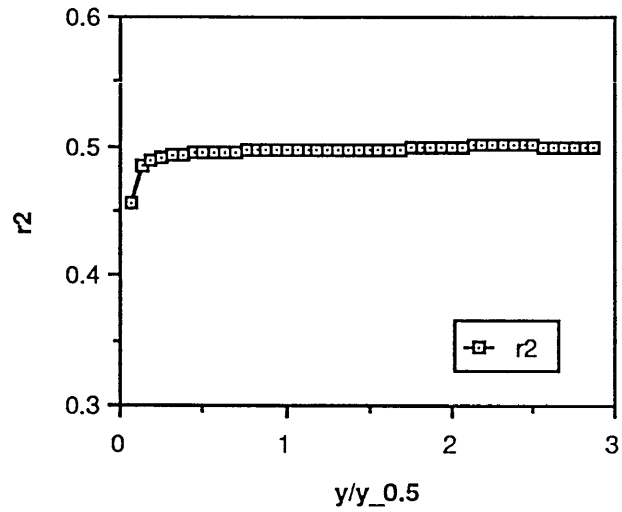
(a) Volume fractions

Figure F4.5 represents the radial profile of fluid-2 volume-fraction, r_2. (r_1 is, from E4.4, $1-r_2$). The volume fraction is close to 0.5 throughout, at it should be expected from the symmetric mass-transfer law (E4.6); but the small departures from that quantity have a paramount significance in two-fluid models.

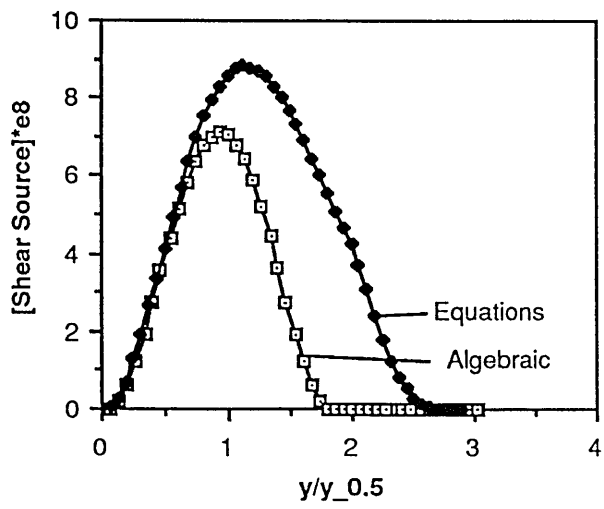
Thus, close to the axis r_2 is **less** than 0.5, a fact that complies with several aspects of the theory:-

i Since no fluid can cross the jet axis, the in-moving fluid (ie fluid 1) must be converted into fluid 2; and mass transfer occurs from fluid 1 to fluid 2 only when $r_2<0.5$ (equation E4.6).

ii Also, fluid 2 is being shifted away by the shear-related source of momentum, whilst fluid 1 is being brought in.



• *Figure F4.5: Fluid-2 volume-fraction* •



• *Figure F4.6: Dimensionless shear-source profile* •

(b) Shear source

The shear-related source of cross-stream momentum (which appears on the RHS of E4.2) was mentioned in Chapter 2 as being one of the major novelties of the new kind of two-fluid models. The non-dimensional, self-similar radial-profile of shear source has been represented in figure F4.6. The figure shows how the model using differential equations gives a higher shear source in the region $y/y_{0.5} \geq 1$; and this may in fact explain why this model provides a better w-profile in that region.

(c) Viscosity profile

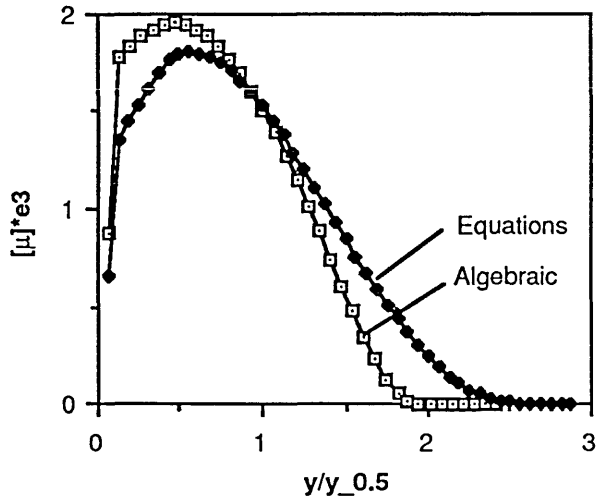
The viscosity profile is, however, very similar for both models, as figure F4.7 reveals. (Viscosity is shown here in a non-dimensional form.)

(d) Cross-stream velocity

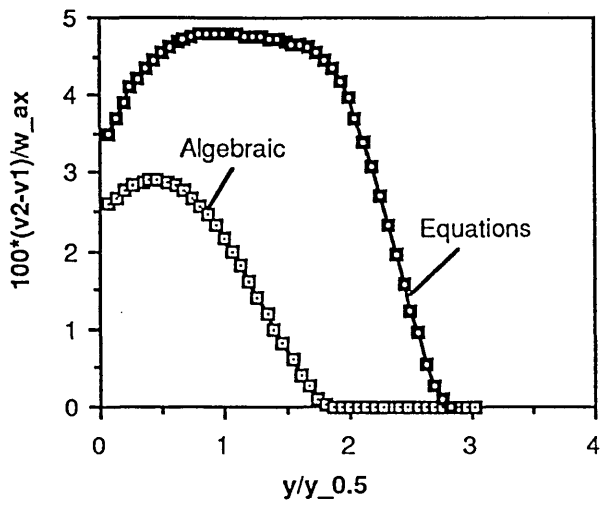
Figure F4.8 is a cross-stream profile of the cross-stream-velocity difference, $|v_1 - v_2|$. The level is higher for model **b** (equations) than for model **a** (algebraic), undoubtedly a consequence of the higher values of the shear-source term as shown in figure F4.6.

(e) Fragment size

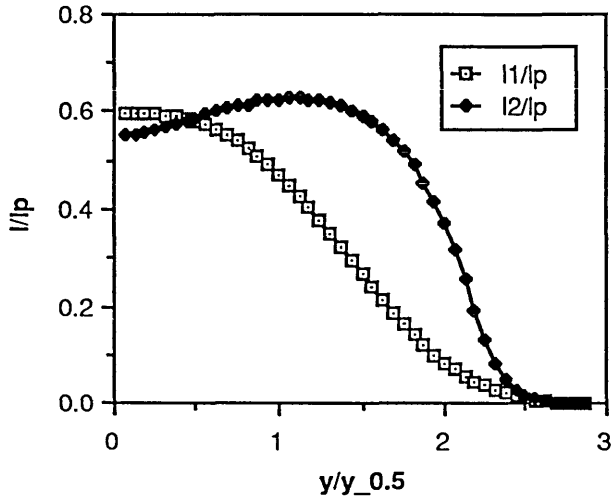
The fragment sizes yielded by each model are represented in figure F4.9. For model **b** (equations), the fragment size is taken, as discussed in Section 4.4.2, as the minimum of the sizes for each fluid. The figure shows that the maximum size under model **b** is about one half of the Prandtl mixing-length, which is the fragment size in model **a**. This explains why both models give similar levels of viscosity



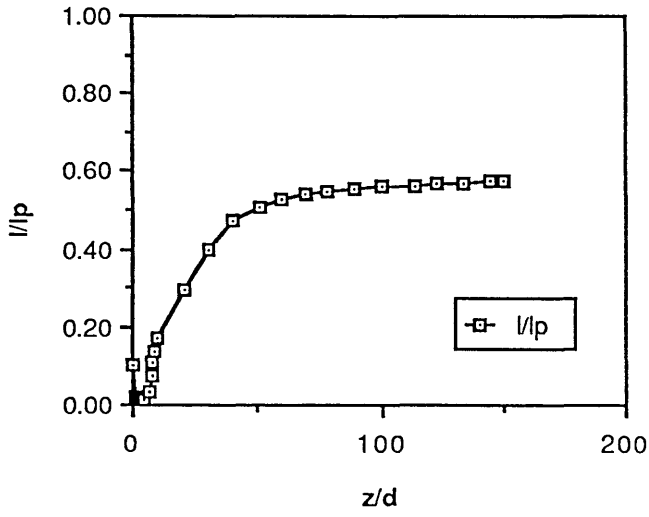
• ***Figure F4.7: Dimensionless viscosity profile*** •



• ***Figure F4.8: Cross-stream-velocity profile*** •



• *Figure F4.9: Fragment sizes* •



• *Figure F4.10: Axial evolution of fragment size* •

(proportional to $r_1\ r_2\ |V_1-V_2|\ l$ and represented in figure F4.7): although $|V_1-V_2|$ is higher for model **b** (figure F4.8), l in model **a** is nearly twice as large.

Figure F4.10 represents the axial evolution of the axial value of the fragment size for model **b** (equations). After an initial region of development, the size reaches approximately one half of the Prandtl-mixing-length value, and remains fairly constant thereafter.

4.6.3 Confidence tests

Although the results have been presented and analysed in preceding sections, nothing has yet been done to assess the reliability of the model. This is the purpose of this section, in which the reliability will be tested in three different respects:-

a The attainment of self-similarity;

b Grid independence;

c Validity over a range of inlet conditions.

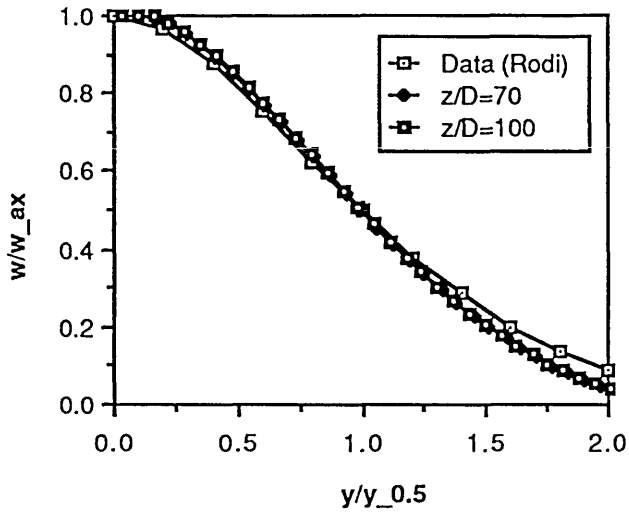
For economy of space, only the results of these tests for model **b** (differential equations) will be presented here.

(a) Self-similarity

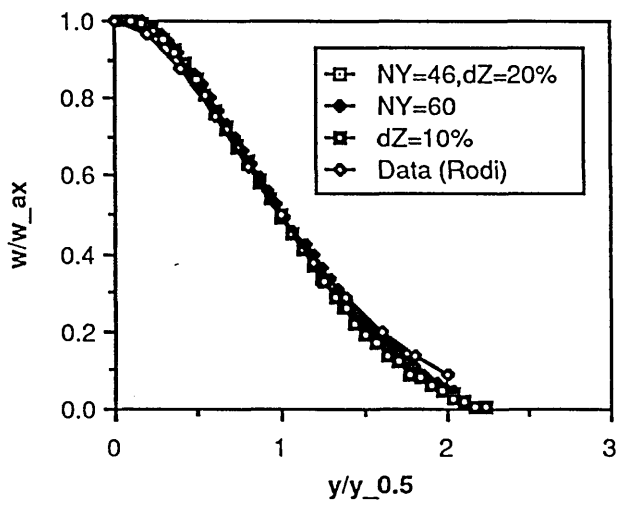
Figure F4.11 shows the similarity profile of w at two different axial positions: 70 and 100 diameters from inlet. The graph confirms that:-

i The model correctly yields self-similar results;

ii Self-similarity has been attained at z/D=70, where the cross-stream graphs of preceding sections were obtained.



• ***Figure F4.11: Self-similarity test*** •



• ***Figure F4.12: Grid independence: w*** •

(b) Grid independence

The standard run, discussed above, was computed using 46 grid-cells in the y-direction, and a forward step in the z-direction equal to a 20% of the jet width ($y_{1\%}$). Two grid-independence tests were therefore devised, one increasing the number of cells to 60 and the other reducing the forward step to a 10% of $y_{1\%}$. The results for the standard run and the two test runs are shown in figure F4.12 (w profile), F4.13 (decay rate), F4.14 (jet spread based on $y_{1\%}$), and F4.15 (axial evolution of fragment-size l). None of these figures shows any discrepancy advising the use of a finer grid.

(c) Validity for a range of Reynolds numbers

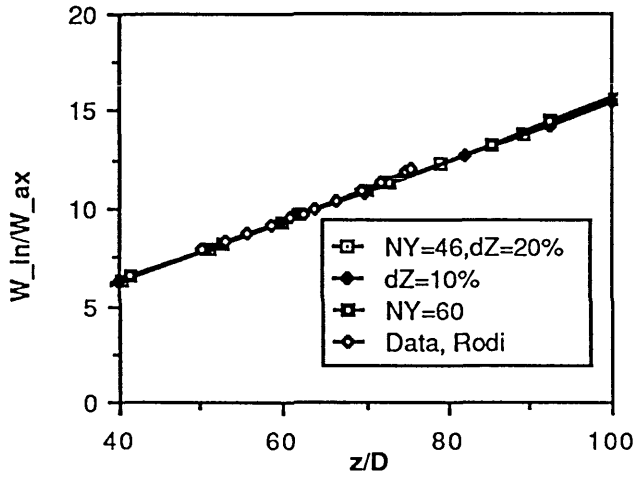
Several runs were also performed to test the consistency of the results under different inlet conditions (diameter and velocity). These runs are summarised in table T4.6.

• ***Table T4.6: Runs with several Reynolds numbers*** •

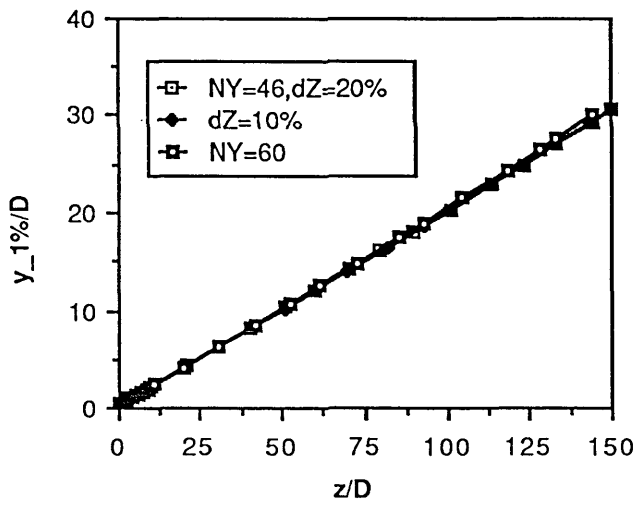
Case	Inlet diameter (m)	Inlet velocity (m/s)	Re number
1	0.002	30	6,000
2	0.025	15	37,500
3§	0.025	30	75,000
4	1.0	5	500,000

§Base run

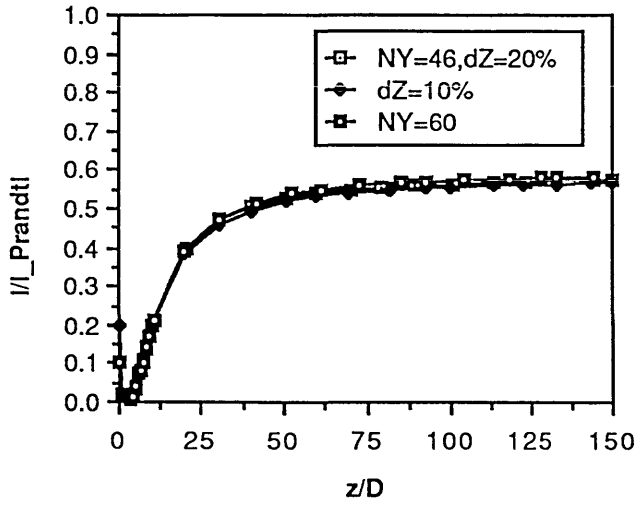
Figures F4.16 to F4.19 represent the main quantities for all four cases. The figures confirm the independency from the Reynolds number in the range of conditions tested.



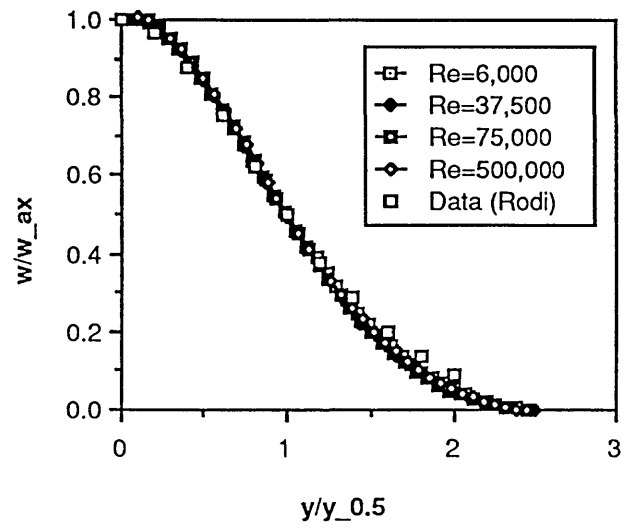
• *Figure F4.13: Grid independence: decay rate* •



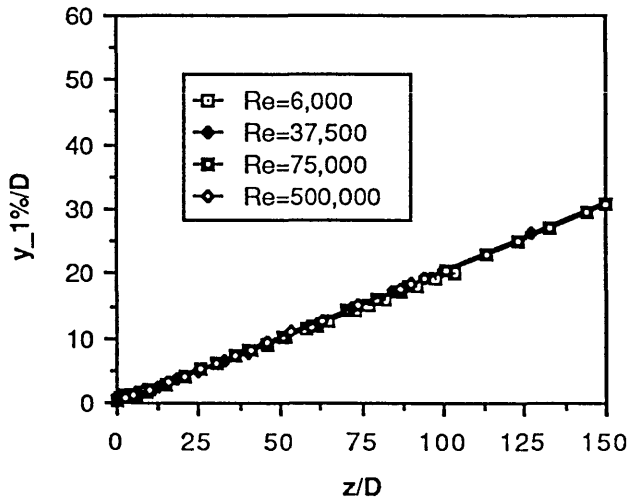
• *Figure F4.14: Grid independence: jet spread* •



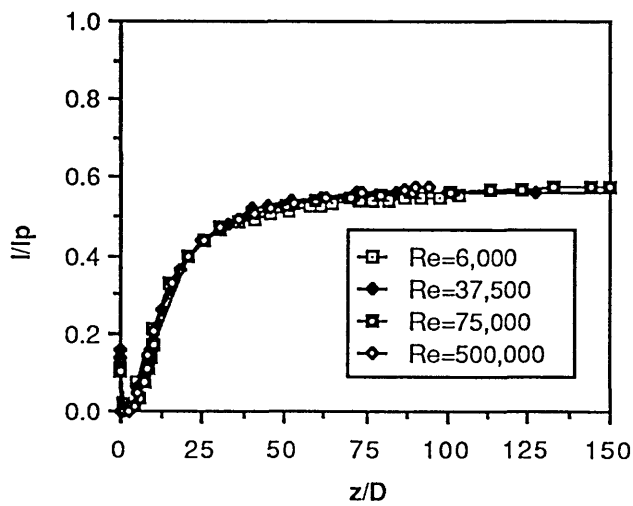
• *Figure F4.15: Grid independence: fragment size* •



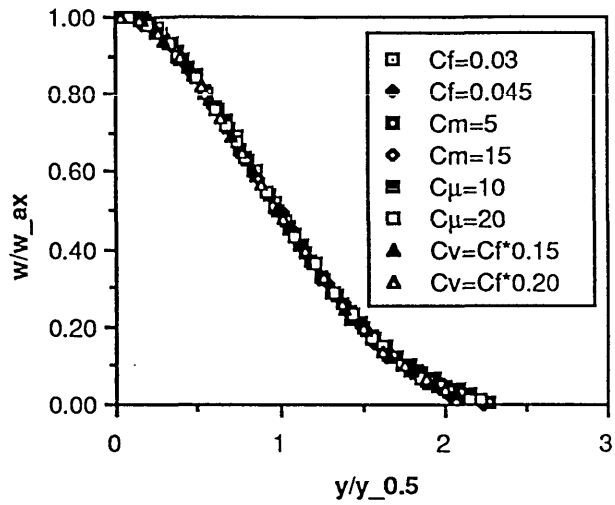
• *Figure F4.16: Axial velocity for several Reynolds numbers* •



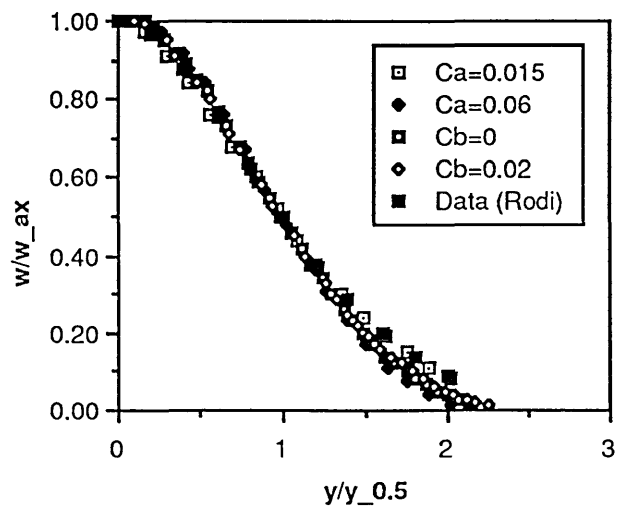
• *Figure F4.17: Jet spread for several Reynolds numbers* •



• *Figure F4.18: Fragment size for several Reynolds numbers* •



• *Figure F4.19a: Parametric analysis - axial-velocity profile* •



• *Figure F4.19b: Parametric analysis - axial-velocity profile* •

4.6.4 Parametric study

Further analysis of the mechanisms involved in the two-fluid idea follows in this Section, in which the effect of varying the model constants (and, therefore, the role played by the corresponding terms) is assessed. A list of the constants and their default values has been presented in table T4.3.

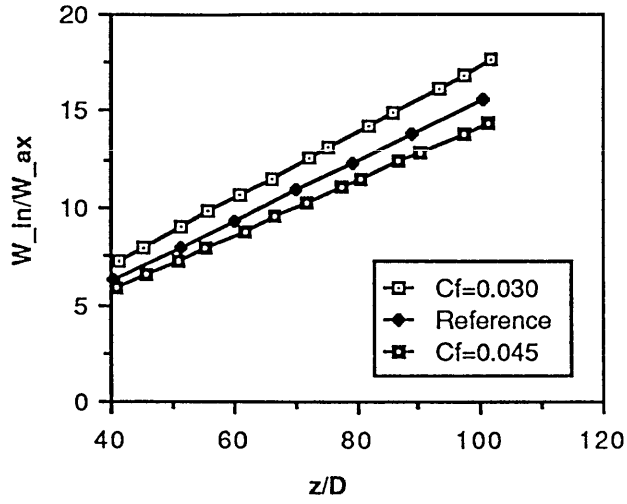
(a) Effect of C_f

- Related figures: F4.19a shows the axial-velocity profile;
  F4.20 shows the axial-velocity decay;
  F4.21 shows the jet spread;
  F4.22 shows the axial evolution of fragment size.

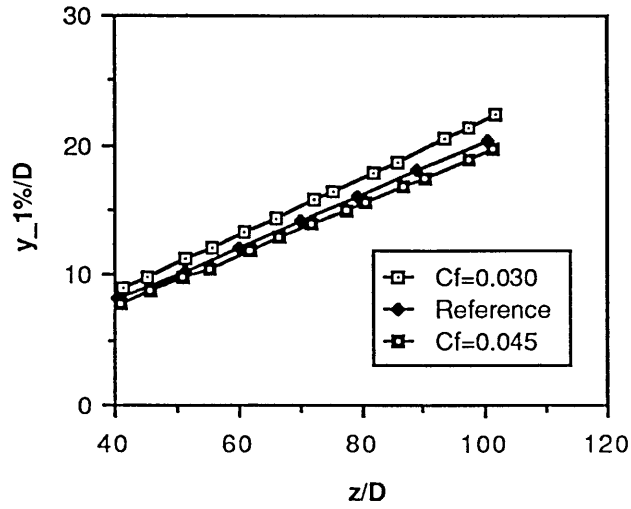
- Remarks: Figures F4.20 and F4.21 reveal how the decay and spread rates decrease when C_f is increased. This is so because a larger inter-phase friction means a smaller velocity difference between both phases, and particularly a smaller cross-stream-velocity difference. And the cross-stream velocity (v_i) is partly responsible for the exchange of co-stream momentum between "external" and "internal" layers, by shifting away out-moving fluid (with high w-momentum) and bringing in in-moving fluid, with low w-momentum. This process has been sketched in figure F4.23.

  (It should be pointed out that this is one of the two mechanisms which account, in this model, for the radial exchange of w-momentum, the other being the conventional co-gradient diffusion controlled by C_μ.)

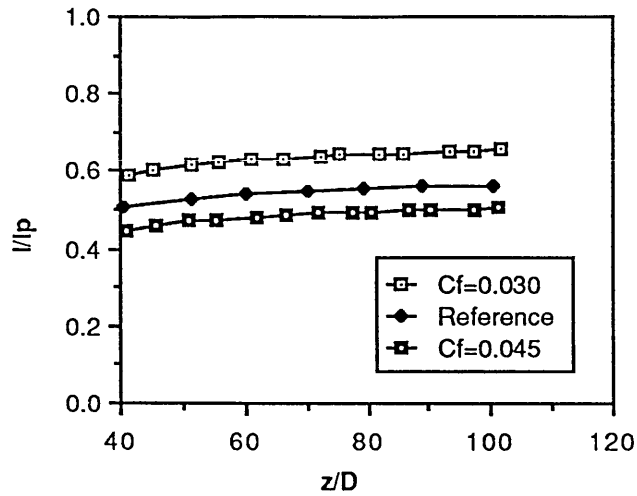
  The decrease of $|V_1-V_2|$ should also lead to a decrease of the fragment size, since the relative velocity is the driving force for fragment growth (E4.9). Figure F4.22 confirms this side effect.



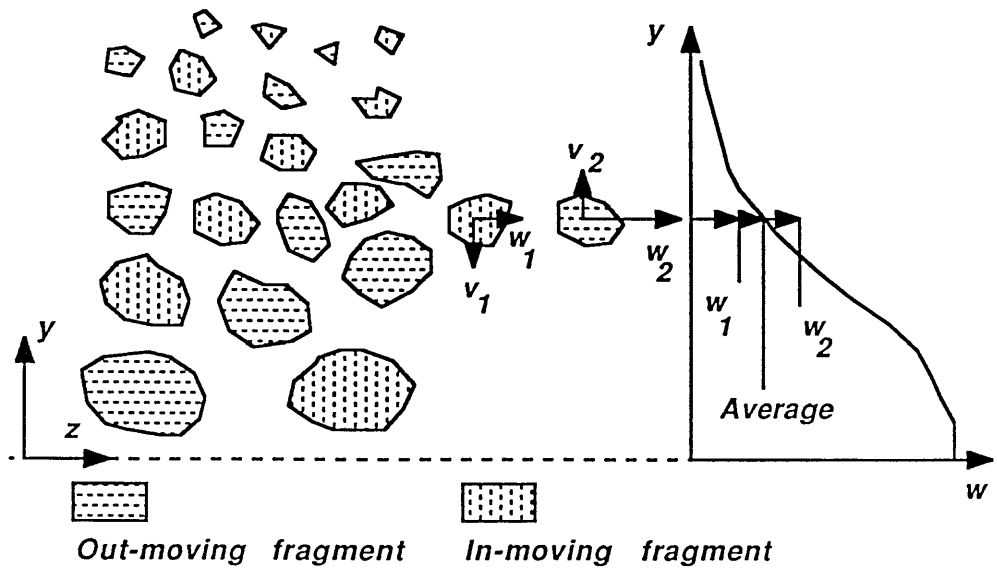
• ***Figure F4.20: C_f - Axial-velocity decay*** •



• ***Figure F4.21: C_f - Jet spread*** •



• *Figure F4.22: C_f - Fragment size* •



• *Figure F4.23: Exchange of w-momentum through $|v_1-v_2|$* •

(b) Effect of C_m

- Related figures: F4.19a shows the axial-velocity profile;
  F4.24 shows the axial-velocity decay;
  F4.25 shows the axial evolution of the fragment size.

- Remarks: An increase or decrease of C_m by a 50% does not have a substantial effect on the results, because C_m=10 (the standard value) is high enough to keep the volume fractions close to the equilibrium value of 0.5

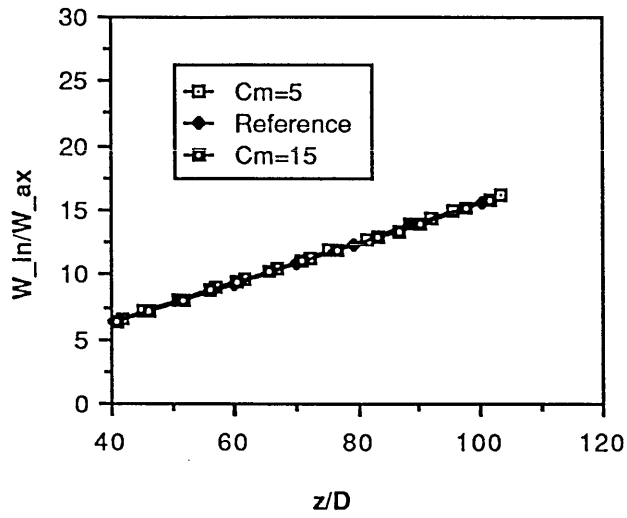
(c) Effect of C_μ

- Related figures: F4.19a with the radial profile of w;
  F4.26 with the jet spread;
  F4.27 with the axial evolution of the fragment size.

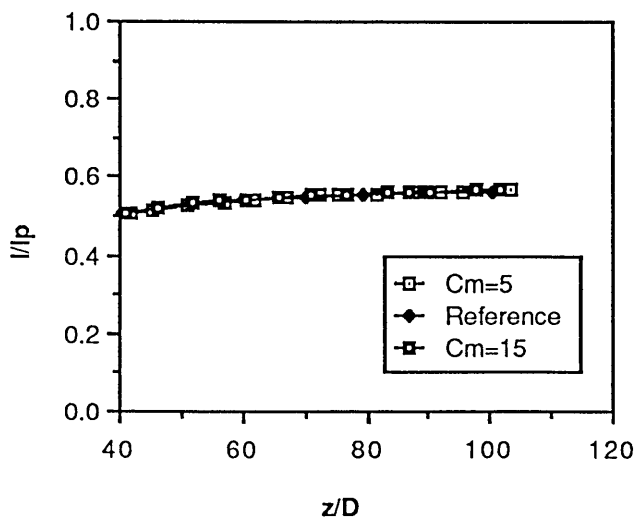
- Remarks: C_μ is the constant affecting the within-phase, turbulent diffusion of momentum. An increase of the spread rate should therefore be expected to be the consequence of an increase of C_μ; and since the relative velocity $|V_1-V_2|$ is not affected by a variation in C_μ, the fragment-size evolution should not be substantially different. Both results are confirmed by figures F4.26 and F4.27 respectively.

(d) Effect of C_v

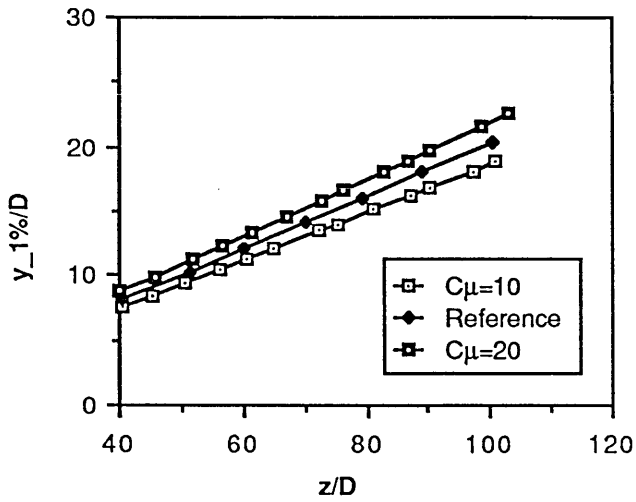
- Related figures: F4.19a with the radial profile of w;
  F4.28 showing the jet spread;
  F4.29 showing the axial evolution of fragment size.



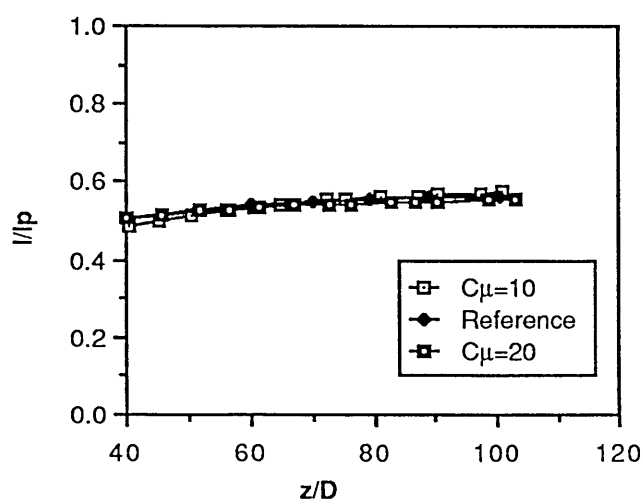
• *Figure F4.24: C_m - Axial-velocity decay* •



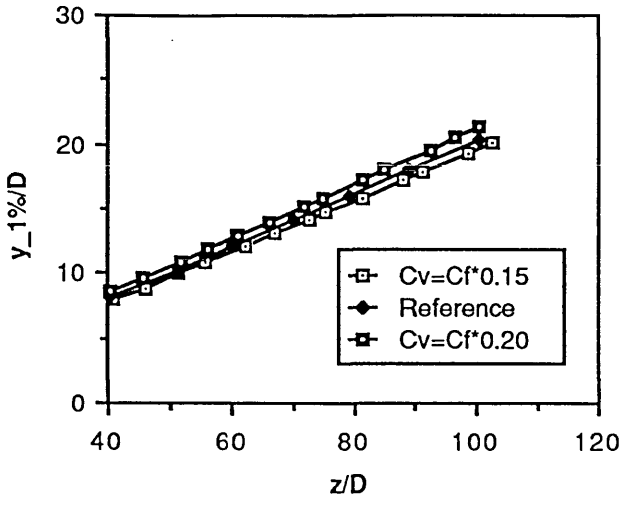
• *Figure F4.25: C_m - Fragment size* •



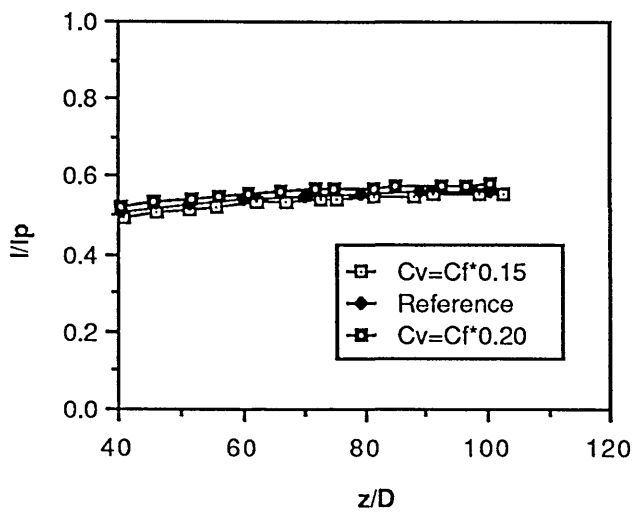
• ***Figure F4.26: C_μ - Jet spread*** •



• ***Figure F4.27: C_μ - Fragment size*** •



• *Figure F4.28: C_V - Jet spread* •



• *Figure F4.29: C_V - Axial evolution of fragment size* •

- Remarks: C_v is the constant affecting the source of lateral (v) momentum induced by gradients of the w velocity in the mean flow, as defined by E4.8 in table T4.1. An increase of C_v leads, therefore, to an increase of the relative cross-stream velocity $|v_1-v_2|$. The effect of this difference in the present model has been discussed in (a) above; and the increase of C_v should have a similar effect to the decrease of C_f, since both entail an increase of $|v_1-v_2|$. This is confirmed by figures F4.28 and F4.29.

(e) Effect of C_a

- Related figures: F4.19b shows the radial profile of w;
  F4.30 with the fragment-size evolution;
  F4.31 with the jet spread.

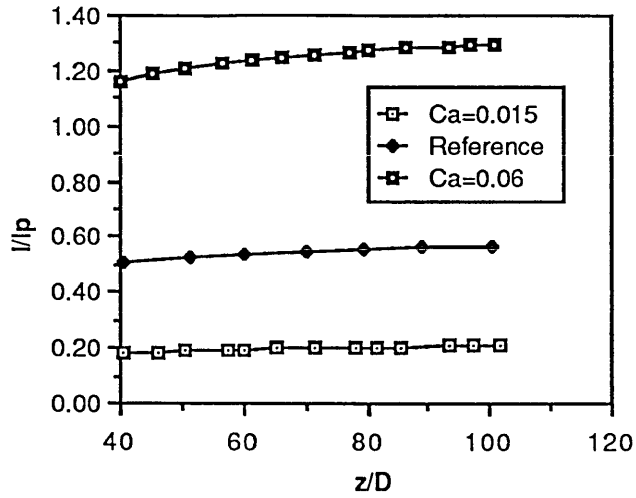
- Remarks: C_a is the constant affecting the fragment growth by entrainment and agglomeration; the fragment size can therefore be expected to be sensitive to variations of C_a.

F4.30 shows how the fragment size increases when C_a increases, and decreases when C_a does. The jet spread (F4.31) is higher for smaller values of C_a, which is a consequence of:

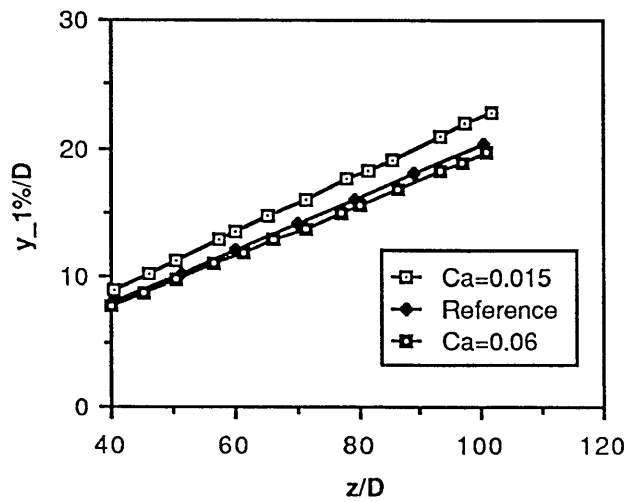
(i) The higher shear-source, since this is proportional to l_p/l (E4.8);

(ii) The larger interphase friction, since this is proportional to $1/l$ (E4.7).

(The smaller viscosity, which is proportional to l, tends to compensate these effects.)



• *Figure F4.30: C_a - Fragment size* •



• *Figure F4.31: C_a - Jet spread* •

(e) Effect of C_b

- Related figures: Figure F4.19b with the radial profile of w;
  Figure F4.32 with the axial evolution of the fragment size;
  Figure F4.33 with the velocity decay.

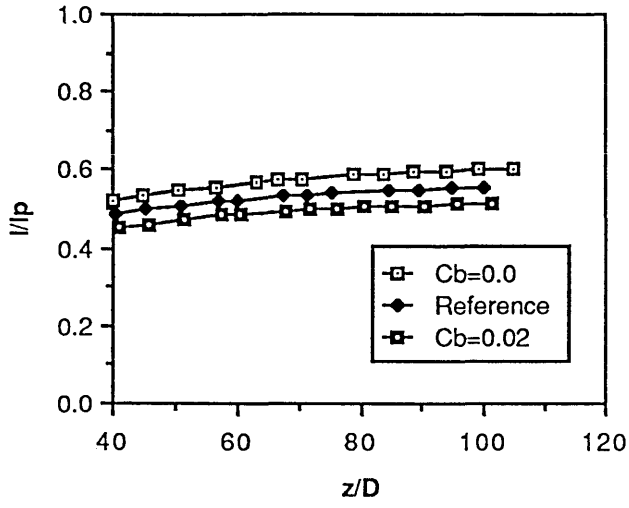
- Remarks: The increase of C_b, the constant affecting fragment break-up by shear, has the expected effect of decreasing the fragment size, as F4.32 shows. Comparison of F4.30 (C_a doubled) and F4.32 (C_b doubled) reveals that the model is more sensitive to changes in C_a than it is to changes in C_b.

4.6.5 Some numerical details

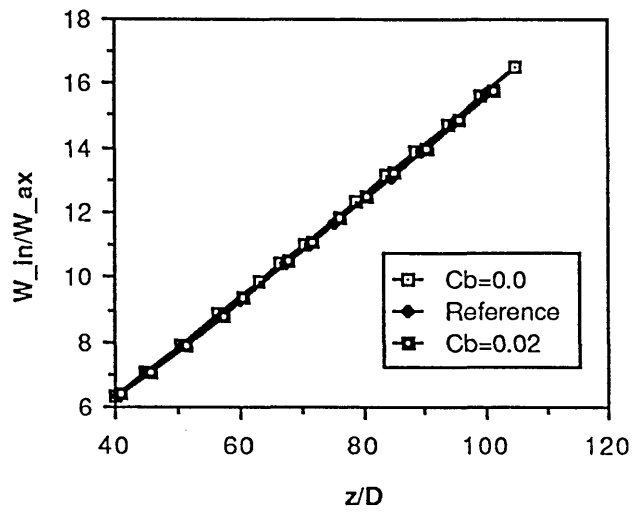
As pointed out in Section 4.6.3, 46 cells are employed in the **y** (cross-stream) direction, together with a forward step in the **z** (axial) direction equal to a 20% of the jet width ($y_{1\%}$).

A typical run performs 40 iterations over each slab (**y** array of computational cells). Some 90 slabs (forward steps) are needed to reach z/D=70, where the self-similar cross-stream profiles of preceding sections have been taken.

The computer employed was as 32-bit Acorn Cambridge Workstation, running the PANOS operating system. A run as described above takes 50 minutes on this machine, which is equivalent to 33 seconds per slab. Table T4.7 details the estimated times for a mainframe (VAX 8600) and a supercomputer (CRAY X-MP).



• *Figure F4.32: C_b - Fragment size* •



• *Figure F4.33: C_b - Decay* •

• ***Table T4.7: Run-time for several machines*** •

Machine	Time
Acorn	50 m
VAX 8600	6 m (estimated)
CRAY X-MP	0.8 m (estimated)

4.7 Closure

A two-fluid model of turbulence, along the lines of those introduced in Chapter 2, has been proposed, in this chapter, for the single-phase, axi-symmetrical jet. The proposal includes two different submodels for the fluid fragment-size, namely:-

(a) An algebraic one, akin to the Prandtl mixing-length.

(b) A submodel using differential equations to account for the growth of the fragment owing to entrainment and agglomeration, and also for the fragment break-up caused by shear.

In the subsequent process of model assessment, the results provided by submodel (b) were found to be closer to the experimental evidence than those provided by (a).

Values have also been recommended for the model constants (table T4.3). Some of these values have been taken from previous works and left unchanged (C_f, C_m, C_μ). Others have been adjusted in this work to give the best possible results (C_v, C_a, C_b).

The model results appear to be, as they should, self-similar, grid-independent and consistent over a wide variety of inlet conditions yielding a broad range of Reynolds numbers.

The most interesting finding concerns, probably, the fragment size (l) when differential equations are employed for its calculation: the axial values of l are proportional to the Prandtl mixing-length (l_p) after a region of jet development. Two other interesting observations can further be made concerning this same finding:-

(a) The constant to which the ratio l/l_p tends does not depend on the inlet conditions (inlet velocity, inlet diameter), and shows little dependence on the value of the model constants other than the size-equation ones.

(b) The region in which the ratio develops to a constant coincides, roughly, with the jet development region (z/D<50); and this, again, regardless of inlet conditions and model constants.

In the following chapters, the model introduced in this one is extended to cater for disperse two-phase flows, and then is applied to the simulation of sprays.

Chapter 5

A two-fluid model for sprays

5.1 Introduction

5.1.1 The purpose of this chapter

The development of a two-fluid model of turbulence for sprays and the testing of such a model under a number of conditions (namely cold and evaporating sprays) were mentioned in the first chapter as two of the objectives of the present work.

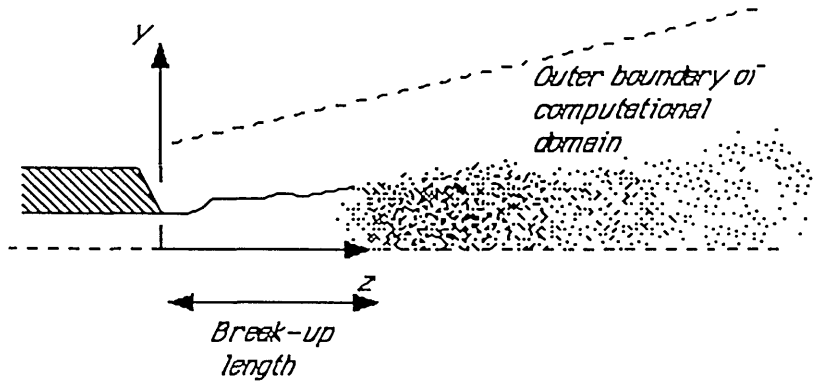
This chapter addresses the first task (development of the mathematical model), while the assessment of the model performance is tackled in Chapter 6.

5.1.2 Layout of the chapter

After this introductory section, the situation considered is detailed in Section 5.2. Subsequent sections record the mathematical model, with Section 5.3 dealing with the differential equations; 5.4 with the properties and auxiliary relationships; 5.5 with the model constants; and 5.6 boundary conditions. Finally, Section 5.7 closes the chapter with the relevant conclusions.

5.2 The situation studied

An air-atomising nozzle is considered, which delivers a full-cone, non-swirling spray as sketched in figure F5.1.



• ***Figure F5.1: The situation considered*** •

Soon after injection, the liquid column breaks up into a droplet distribution. The unbroken portion of the spray is known as the break-up length (Hiroyasu, 1987), and is not considered in the present model. Instead, a droplet distribution will be assumed at the inlet of the computational domain.

Droplet break-up and coalescence are relevant phenomena in the early stages of spray development (O'Rourke,1981), and could be easily accommodated within the model proposed; they will not be however considered at the present stage, in which the downstream distribution will be taken as the inlet one, therefore minimising the effect of ignoring droplet-to-droplet interaction.

The problem is considered to be axi-symmetrical, and therefore two dimensional; and a cylindrical-polar coordinate-system is used, with **z** being the axial direction and **y** being the radial direction (figure F5.1). Furthermore, the flow is regarded (and computed) as parabolic.

5.3 Mathematical model: differential equations

5.3.1 Background

A two-fluid model of the kind described in previous chapters is employed, in which fluid 1 is again thought to be the down-moving fluid, and fluid 2 the up-moving one. In the light of the results presented in the preceding chapter, two differential equations will be used to compute the fluid fragment-size, l_i.

The spray droplets are represented within each fluid by using the no-slip technique devised by Spalding (1985). The incorporation of this technique into turbulence models of the two-fluid kind is accomplished in this section.

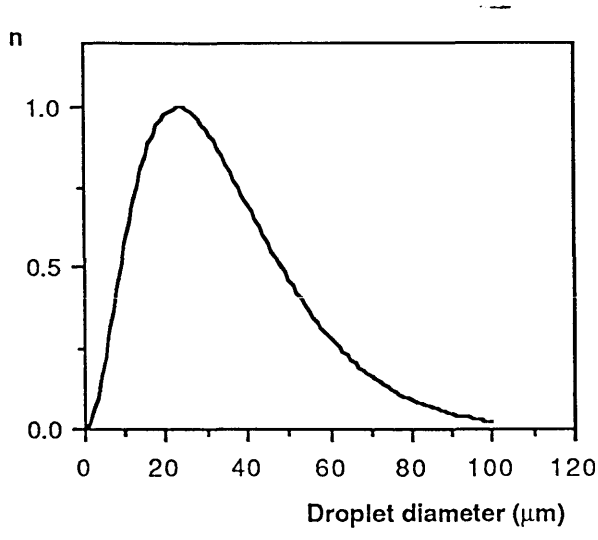
In a spray, the droplet size-distribution can be represented at each point by a function n(D), with

D	standing for droplet diameter; and
n(D) dD	being the number of droplets with diameters between D and D+dD per unit volume.

A typical n(D) function has been represented in figure F5.2.

In the approach presented here, the droplet size-range is broken up into a finite number of intervals, and a differential equation is written for the number of droplets in each group (or, in fact, for any other related magnitude).

The volume fraction of liquid at each point can be worked out by summing up the number of droplets in each group. Once the liquid volume-fraction (or, equivalently, the mass fraction) has been computed, the contribution of the droplets to the local density can be easily taken into account.



• *Figure F5.2: Typical size-distribution* •

The dependent variables are, therefore, those for the single-phase jet (p, r_1, r_2, v_1, v_2, w_1, w_2, l_1, l_2), plus the droplet-concentration variables (discussed in Section 5.3.2 below) and, for the evaporating-spray model, the vapour mass-fraction in each fluid (presented in Section 5.3.3). Furthermore, the w-momentum equations of the single-phase jet (E4.3) are amended to include the effect of gravity (details in section 5.3.4).

5.3.2 Droplet-concentration equations

In addition to the equations listed for the single-phase jet, transport equations must now be provided for the number of droplets in each size-group. Since the whole derivation of the equations cannot be included here without diverting the attention from the essence of the model, the details of such a derivation have been included in this work as Appendix A. The basic steps are nevertheless revised here.

(a) Change of size variable.

The droplet-number distribution n=func(D) is rewritten using $s=D^2$ as size variable, rather that D. (The advantages of this change are stated in Appendix A.)

(b) Transport equation for the number of droplets

A transport equation for n(s) can be written as (Spalding, 1980a):-

$$\frac{\partial(r_i n_i)}{\partial t} + \nabla(r_i n_i V_i) + \nabla(\mathbf{j}_{ni}) = -\frac{\partial(r_i n_i s')}{\partial s} +$$

$$+ \ (f_{ji}^{*} + [\![m_{ji}^{*}]\!]) \ (n_j - n_i) \qquad \text{[E5.1]},$$

where

- The index **i** indicates phase;
- The vector $\mathbf{j}_{n_i}$ is a diffusion flux (eg, turbulent diffusion);
- s' is the rate of change of s;
- n_i is, in general, a function of space, time and size (s);
- f_{ji}^{*} and m_{ji}^{*} are the interphase-transfer rates, similar to those employed for other variables (E4.6, E4.7) but without the average density;
- The transient term has been included only to add generality to the derivation, since only steady sprays will be considered.

The appearance of a new **independent** variable (namely s) in E5.1 should be noted.

(c) Change of dependent variable

The droplet-number distribution n=n(s) is transformed into a mass-fraction distribution by the following change of variable:

$$m_i(s) = \frac{n_i(s)M(s)}{\rho_i} \qquad \text{[E5.2]},$$

where

$n_i(s)$ ds is the number of particles with sizes between s and s+ds per unit volume and per unit s;

$M(s)$ is the mass of a particle of size s;

ρ_i is the local-mixture density.

The meaning of m_i is clear: $m_i$ds is the mass fraction of the droplets with sizes between s and s+ds. (Note that both n_i and m_i are not only a function of the size s, but also of space and time.)

(d) New equation in m_i

As a result of the change, the equation for n_i (E5.1) can be rewritten as:-

$$\frac{1}{M(s)}\left[\frac{\partial(r_i\rho_i m_i)}{\partial t} + \nabla(r_i\rho_i m_i V_i) - \nabla(r_i\Gamma_{m_i}\nabla m_i)\right] = -\frac{\partial}{\partial s}\left(\frac{r_i\rho_i m_i s'}{M(s)}\right) +$$

$$+ (f_{ji}^{*} + [\![m_{ji}^{*}]\!])\frac{1}{M(s)}(\rho_j m_j - \rho_i m_i) \qquad \text{[E5.3]}.$$

Concerning E5.3, the following notes must be made:-

- j_{n_i} has been replaced by a gradient-diffusion assumption, $j_{n_i} = -r_i\Gamma_{m_i}\nabla m_i$;

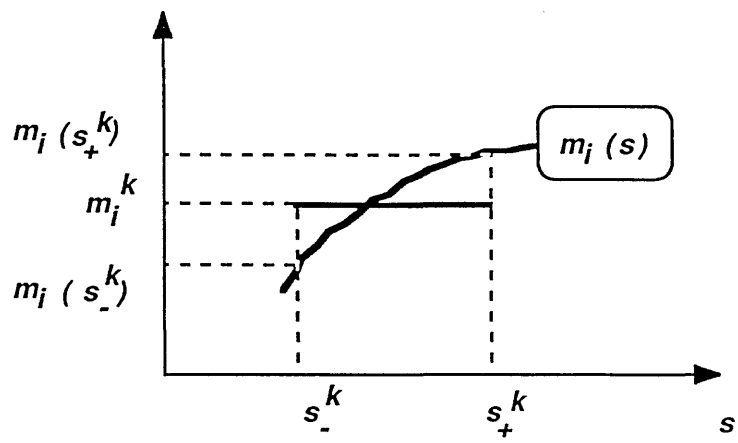
- As a consequence of the change of variable E5.2, the phase density now appears in the equation, which has therefore the form of the general ϕ equation;
- However, **s** is still present in E5.3 as an independent variable.

(e) Discretisation of the s interval

In order to remove s as an independent variable in E5.3, the s range (and, therefore, the m_i function) is broken up into a finite number of intervals, and a **mean** m_i is defined for each group k as :-

$$m_i^k = \frac{1}{s_+^k - s_-^k} \int_{s_-^k}^{s_+^k} m_i \, ds \quad , \qquad \text{[E5.4]},$$

where s_+^k and s_-^k are the interval limits (figure F5.3).



• *Figure F5.3: Average m_i in group k, m_i^k* •

(f) Integration of the equation for m_i

E5.3 is then integrated over each s-interval. Only the final form of the equation is shown here, but the whole process has been included in Appendix A:-

$$\frac{\partial(r_i\rho_i m_i^k)}{\partial t} + \nabla(r_i\rho_i m_i^k \mathbf{V}_i) - \nabla(r_i \Gamma_{m_{ik}} \nabla m_i^k) = \Pi_i^k +$$

$$+ (f_{ji} + [\![m_{ji}]\!])\ (m_j^k - m_i^k) \qquad \text{[E5.5]},$$

with

$$\Pi_i^k = \begin{cases} r_i\ \rho_i\ |s'|\ \frac{1}{s_2}\ [m_i^2 - \xi\ m_i^1] & \text{if } k = 1 \\ r_i\ \rho_i\ |s'|\ \frac{1}{s_+ - s_-}\ \{m_i^{k+1} - [1 + \xi\ \ln(\frac{s_+}{s_-})]\ m_i^k\} & \text{if } k > 1 \end{cases}$$

In E5.5,

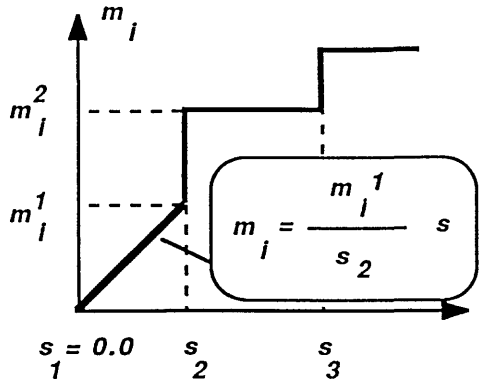
ξ is a geometrical factor, relating s to droplet volume. (Namely, volume=$4\pi s^{\xi}/3$, and therefore ξ=3/2 if $s=D^2$.)

s', the rate of change of droplet size, has been assumed to be negative (vaporisation), and **independent from s.** This is frequently admitted if $s=D^2$ (see, eg, Chigier, 1976; Law, 1982; Aggarwal *et al*, 1984).

s_+, s_- are the interval limits, the k index having been dropped for brevity. For the first interval, a linear profile is assumed for m_i^k (figure F5.4), and m_i^1 is the maximum of m in that interval.

$\Gamma_{m_{ik}}$ is the turbulent-diffusion coefficient, for which the form of other coefficients is proposed:

$$\Gamma_{m_{ik}} = C_{m_{ik}}\ \rho\ r_1\ r_2\ |v_1 - v_1|\ l \qquad \text{[E5.6]}.$$



• ***Figure F5.4: m_l for group 1 (m_l^1)*** •

E5.5 is the final form of the equation to be solved along with those for r_i, v_i, w_i, l_i and the closure equation $r_1+r_2=1$.

5.3.3 Vapour mass-fraction equations.

For the evaporating spray, the following equations are used for the mixture fraction of vapour y_i^v:

$$\nabla(\rho_i r_i V_i y_i^v) - \nabla(r_i \Gamma_{y_{iv}} \nabla y_i^v) = r_i M_{vi} + [\![m_{ji}]\!](y_j^v - y_i^v) +$$

$$+ f_{ji} (y_j^v - y_i^v) \qquad [E5.7],$$

where

$\Gamma_{y_{iv}}$, the effective-diffusion coefficient, has the form

$$\Gamma_{y_{iv}} = C_{y_{iv}} \rho r_1 r_2 |v_1 - v_2| l \qquad [E5.8].$$

M_{vi} is the source of vapour mass-fraction owing to droplet vaporisation, given by

$$M_v = \int n(R) 4\pi R^2 |R'| dR =$$

$$= \frac{3}{2}\rho_i \, |s'|[\, m_i^1 + \sum_{k=2} m_i^k \, \ln\left(\frac{s_+}{s_-}\right) \,] \qquad \text{[E5.9]}.$$

5.3.4 Modified w-momentum equations

As stated in Section 5.3.1, a source of momentum is added to the w-velocity equations (E4.3) to take into account the effect of gravity. This source has the form

$$r_i \, g \, (\rho_i - \rho_g) \qquad \text{[E5.10]},$$

where

- g is the gravitational acceleration; and
- ρ_g is the density of the surrounding gas (air).

The final equation is, therefore,

$$\nabla(\rho_i r_i V_i w_i) - \nabla(r_i \mu \nabla w_i) = [\![m_{ji}]\!](w_j - w_i) + f_{ji}(w_j - w_i) -$$

$$- r_i \frac{\partial p}{\partial z} + r_i \, g \, (\rho_i - \rho_g) \qquad \text{[E5.11]}.$$

5.4 Auxiliary relations

Since the mathematical model is, in fact, an extension of the single-phase one (Chapter 4), the same auxiliary relations are used for μ_t, m_{ji}, f_{ji} and l. These were listed in table T4.1.

New expressions are, on the other hand, required for

- the fluid density;
- s', the droplet vaporisation rate.

5.4.1 Density and liquid mass-fraction

The contribution of the liquid phase to the local density must now be taken into account. It is clear that ρ_i depends on m_i^k (the larger the number of droplets, the larger the density; but m_i^k depends, in turn, on ρ_i as a matter of definition (E5.1). This subsection deals with this coupling.

The fluid density is computed from the mass-fractions and density of each of the three mixture-components (liquid, vapour and gas) as

$$\frac{1}{\rho_i} = \frac{y_i^l}{\rho_l} + \frac{y_i^v}{\rho_v} + \frac{y_i^g}{\rho_g} \qquad \text{[E5.12].}$$

Paragraphs (a), (b) and (c) below detail how the mass fractions are obtained.

(a) The liquid mass-fraction, y_i^l

y_i^l is calculated by integrating the size-group mass-fraction m_i^k. Thus:

$$y_i^l = \int m_i(s)\, ds = \frac{s_2\, m_i^1}{2} + \sum_{k=2} m_i^k\, (s_+ - s_-) \qquad \text{[E5.13].}$$

(b) The vapour mass-fraction, y_i^v

y_i^v is zero for the cold spray, whereas for the evaporating spray it is computed from the differential equation E5.7.

(c) The air mass-fraction, y_i^g

y_i^g is the mass fraction of the surrounding gas (air). Since all mass fractions must satisfy

$$y_i^l + y_i^v + y_i^g = 1,$$

y_i^g is taken as

$$y_i^g = 1 - y_i^l + y_i^v \qquad \text{[E5.14]}.$$

5.4.2 Droplet vaporisation-rate

The droplet vaporisation-rate, s', appears on the right-hand side of the equations for m_i^k (E5.5) and y_i^v (E5.7).

For the purpose of model validation against experimental data, the following three assumptions will be made:-

(1) The vaporisation rate proceeds following the equilibrium-vaporisation rules (Spalding, 1979). This means that the latent heat of vaporisation is compensated by heat conduction from the gas to the droplet, and therefore that the droplet temperature remains constant.

(2) Further, the droplet vaporisation-rate obeys the law (Spalding, 1979)

$$s' = \frac{\lambda_v}{C_v \rho_l} \ln \left(1 + \frac{C_v (T_g - T_{bp})}{L}\right) \qquad \text{[E5.15]},$$

which complies with the requirement (stated in equation E5.5) of being independent from s. (The notation corresponding to E5.15 can be found in the nomenclature section.)

(3) Finally, it is assumed that the vaporisation process does not change the gas temperature T_g. This simplifying hypothesis is not a model constraint, and will be removed in the combusting-spray model (Chapter 7). (Estimations carried out with that model indicate that the maximum drop in gas

temperature is, in the conditions employed for model testing, a 6%. This would mean a decrease in s' of a 5%).

5.5 Model constants

The addition of two new sets of equations (those for the droplet-group mass-fraction and for the vapour mass-fraction) has brought two additional sets of constants into the mathematical model, namely those intervening in the effective-diffusion laws (E5.6 and E5.8).

The values initially proposed for these constants are listed in table T5.1; the effect of some exploratory variations will be looked into in Chapter 6.

• ***Table T5.1: Additional constants for the spray model*** •

Constant	Value proposed
C_{yvi}	$2 \cdot C\mu = 30.0$
C_{mik}	$2 \cdot C\mu = 30.0$

All other constants retain the value used in the single-phase-jet model, as listed in table T4.3.

5.6 Boundary conditions

In addition to the boundary conditions provided for the single-phase problem (Table T4.2), new conditions must now be supplied for the droplet mass-fractions (m_i^k, E5.5) and the vapour mass-fraction (y_i^v, E5.7). These are given in table T5.2.

• ***Table T5.2: Additional boundary conditions*** •

	m_i^k	y_i^v
Inlet	See below	0.0
Free stream	0.0	0.0
Axis	no flux	no flux

The inlet size-distribution (ie, the values prescribed for the m_i^k 's at the inlet) is worked out from the nozzle type and the experimentally-measured Sauter mean-diameter assuming a distribution function of the kind proposed by Rosin and Rammler (1933) and Nukizama and Tanasawa (1940), namely:

$$\frac{dn}{dD} = a\, D^{\alpha}\, e^{-bD^{\beta}} \qquad \text{[E5.16].}$$

E5.16 has four parameters (a, b, α, β), the values of which are determined as follows:

- α and β depend on the type of nozzle. According to Tanasawa and Tesima (1958), the values α=2 and β=1 provide a size distribution which is adequate for the single-hole nozzle, which is the type considered in this work.

- **b** is computed so that the resulting SMD of the theoretical distribution matches the experimental SMD. The SMD yielded by E5.16 is

$$D_{32} = \frac{\int_0^{\infty} D^3\, dn}{\int_0^{\infty} D^2\, dn} = b^{-1/\beta}\, \frac{\Gamma\left(\frac{\alpha+4}{\beta}\right)}{\Gamma\left(\frac{\alpha+3}{\beta}\right)} \qquad \text{[E5.17]}$$

And therefore, for the hole nozzle (α=2 and ß=1):

$$D_{32} = \frac{5}{b} \quad \Rightarrow \quad b = \frac{5}{D_{32}} \quad .$$

- **a** is a multiplicative coefficient, which is tuned so as to match the overall amount of injected liquid.

The continuous distribution thus built is then discretised into the m_i^k groups following the practices introduced in Section 5.3.2 and Appendix A. Typical continuous distributions arising from E5.16, together with the discrete m_i^k's, will be shown in the next chapter.

5.7 *Closure*

In the previous chapter (Chapter 4), a two-fluid model of turbulence for the single-phase jet was proposed and assessed. In the present chapter, that model has been further enhanced to simulate cold and evaporating sprays having a droplet-size distribution.

Thus, in addition to the transport equations employed for the single-phase jet, new/modified equations have been proposed for:-

m_i^k, the mass fraction of the droplets in size-group k of phase i.

y_i^v, the vapour mass-fraction in the evaporating spray

w_i, the axial velocity, in which a source term has been added to account for buoyancy effects.

The density calculation has also been amended to account for the different mixture components (air, vapour, droplets), and an expression for the vaporisation rate (s') has been provided.

All other features of the model have remained unchanged through the upgrade from single- to two-phase. These features include:

- the interphase transport rates, m_{ji} and f_{ji};
- the diffusion-transport coefficients, Γ;
- The fragment-size model (fragment-size computed from differential equations); and
- the model constants.

A number of simplifications have also been introduced in the version of the model presented in this chapter. These include:-

(a) The use of the same diffusion constant for all the droplet groups, regardless of the droplet size. Droplet response to turbulent fluctuations of the velocity field might not be the same for large and small droplets: where the former tend to be carried by the local fluctuations, the latter can be expected to follow more independent paths. The use of different diffusion coefficients for different groups may therefore be justified.

(b) The enthalpy is not modelled, since the droplet temperature is constant, and the influence of droplet vaporisation on gas temperature is neglected.

(c) A vaporisation law of the type D•D'=constant is considered.

These simplifications are not, it should be noted, limitations of the model. They are introduced so as to allow focusing on other aspects of the flow, and will be removed in exemplary cases to be shown in subsequent chapters.

There are also two immediate areas in which model development can proceed further:-

(a) The modelling of droplet break-up and coalescence, which can be easily accounted for by means of source and sink terms in the equations for m_i^k. These terms would represent the transactions between the size groups brought in by these phenomena. Since the tracking of individual droplets cannot be efficiently managed under an Eulerian scheme (short of using a superimposed lagrangian one), the approach to droplet collision should be a statistical one.

(b) Two-dimensional droplet-distributions can be contrived, in which drops belonging to different groups differ in two properties (eg size and temperature). The computational expense of such an arrangement is not, however, negligible: with five size intervals for each property, one ends up with 25 variables per fluid to represent the droplet groups only.

Chapter 6

Spray-model assessment

6.1 Introduction

6.1.1 The purpose of this chapter

The two-fluid model for sprays developed in Chapter 5 is, in this chapter, assessed by comparing the results with existing experimental data.

6.1.2 Layout of the chapter

Following this introductory section, Section 6.2 below describes the experimental situation to be simulated and provides details on the source of experimental data; Sections 6.3 and 6.4 present and analyse the results for, respectively, the non-evaporating and the evaporating sprays; Section 5.5 addresses the issue of grid independence; Section 6.6 conveys further analysis of the results, beyond the formal comparison with experimental data of preceding sections; and Section 6.7 closes the chapter with the relevant conclusions.

6.2 Experimental data

6.2.1 The source of experimental data

The experiments of Solomon *et al* (1985a and 1985b) are chosen for the purpose of model validation, since:-

- They use real spray nozzles, and realistic (high) loading ratios.

- A complete set of measurements is provided, including radial profiles at several stations, and also axial distributions.

- The quantities reported are suitable for comparison with the output of the present model.

- And, furthermore, Stochastically-Separated-Flow (SSF) models and Locally-Homogeneous-Flow (LHF) models have been applied to the same problem by Solomon *et al*, and this will allow a comparison of the performance of the different models.

6.2.2 Non-evaporating spray

The problem to be analysed is that detailed in Solomon *et al* (1985a), where an air-atomising injector is considered, its nozzle being 1.194 mm diameter. This atomiser delivers a full-cone, non-swirling, downward-directed spray. The injected fluid is vacuum pump oil, the density of which is given in table T6.1 along with other relevant inlet conditions. The temperature and liquid properties are such as to prevent the vaporisation of droplets.

Some additional assumptions must be made here for some of the properties and inlet conditions appearing in the mathematical model as proposed in the preceding chapter. These are:-

(a) The gas density is constant, and equal to 1 kg/m^3.

(b) The inlet distribution of droplets, which is the same at any location of the inlet boundary, is calculated as set out in Section 5.6, with the

experimentally-obtained Sauter Mean Diameter (SMD) of 87μm. The resulting continuous and discretised distributions are represented in figure F6.1

• ***Table T6.1: Non-evaporating-spray data • (from Solomon et al, 1985a)***

Nozzle diameter	1.194 mm
Gas flow-rate	216 mg/s
Liquid flow-rate	1400 mg/s
Sauter Mean Diameter, SMD	87 μm
Inlet velocity (assuming LHF *)	43.3 m/s
Ambient temperature	300 K
Ambient pressure	97 kPa
Liquid density	878 kg/m^3

* LHF - Locally Homogeneous Flow.

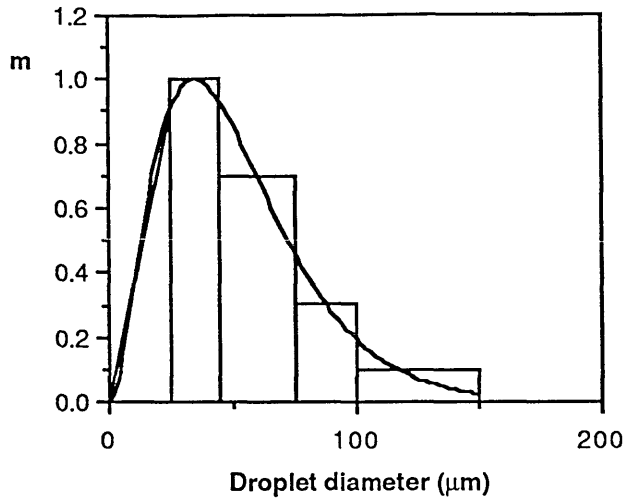
6.2.3 Evaporating spray

The experimental set-up considered for the evaporating spray (Solomon *et al*, 1985b) is similar to that for the cold spray. The injected liquid is now Freon-11, which provides an adequate volatility at ambient temperature. Further details on the experimental conditions, as supplied by Solomon *et al* (1985b) are given in table T6.2.

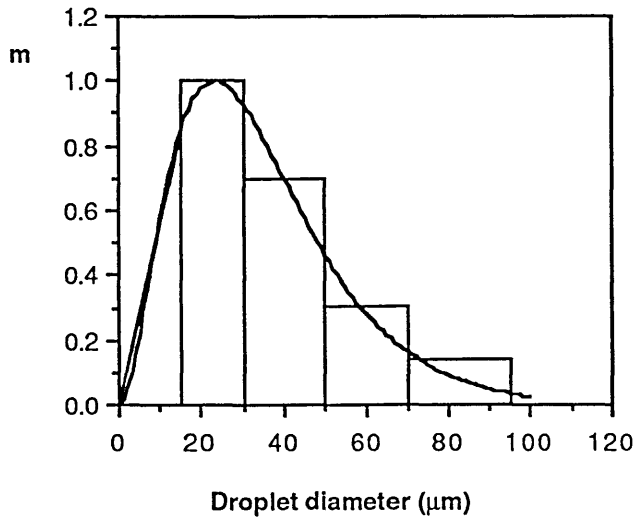
These conditions must be complemented, as for the non-evaporating spray, with some additional properties and inlet-condition data:

(a) The air density is again taken as 1 kg/m^3.

(b) Some other properties of the Freon-11 are listed in table T6.3.



• ***Figure F6.1: Inlet size-distribution (non-evaporating spray)*** •



• ***Figure F6.2: Inlet size-distribution (evaporating spray)*** •

• *Table T6.2: Evaporating-spray data • (from Solomon et al, 1985b)*

Nozzle diameter	1.194 mm
Gas flow-rate	120 mg/s
Liquid flow-rate	1894 mg/s
Sauter Mean Diameter, SMD	51.8 μm
Inlet velocity (assuming LHF *)	29.64 m/s
Ambient temperature	300 K
Ambient pressure	97 kPa

* LHF - Locally Homogeneous Flow.

• *Table T6.3: Additional Freon-11 properties* •

Symbol	Property	Value
ρ_l	Liquid density	1494.0 kg/m^3
ρ_v	Vapour density	5.86 kg/m^3
C_v	Vapour specific heat	$0.594 \cdot 10^3$ J/kg
λ_v	Vapour thermal conductivity	$2.585 \cdot 10^{-3}$ J/s m C
L	Latent heat of vaporisation	$1.804 \cdot 10^5$ J/kg
T_{bp}	Boiling point of liquid	23.82 ° C

The vaporisation rate resulting from these data is, from E5.15:

$$s' = 2DD' = 2.48 \cdot 10^{-9} \text{ m}^2/\text{s}.$$

(c) As for the non-evaporating spray, the inlet distribution of droplets is built from the experimental Sauter Mean Diameter using the procedure of Section 5.6. The continuous and discrete size-distributions are represented in figure F6.2.

6.3 Non-evaporating spray: results

The results provided by the model for the cold spray are now compared with the experimental results of Solomon *et al* (1985a). Further analysis of these results will follow in Section 6.5.

Figure F6.3 to F6.5 represent the radial profile of axial velocity at several axial locations (z/D=100, 250 and 500 respectively). Four different quantities are displayed in the same graph, in an arrangement which will be repeated in subsequent plots. These quantities are:-

(a) The experimental data (labelled **data** in the graph legend).

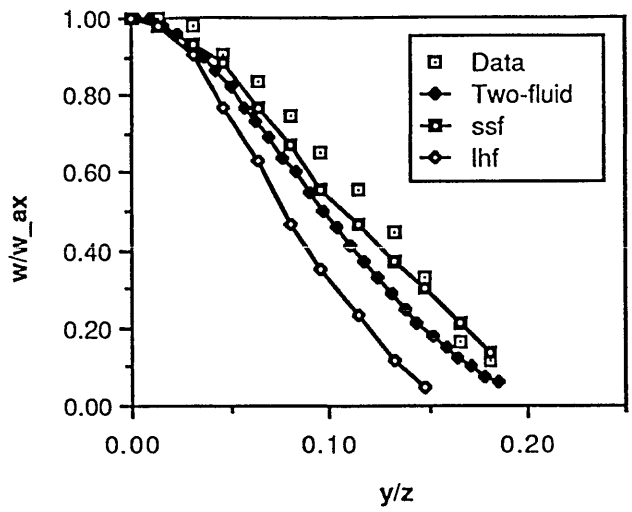
(b) The value predicted by the present model, marked **two-fluid.** This value is the computed as the average of the values for the out- and in-moving fluids, ie $w=(r_1\rho_1 w_1+r_1\rho_1 w_2)/\rho$.

(d) The values predicted by a locally-homogeneous-flow model (Eulerian), marked **lhf.** LHF models were revised in Section 1.2 of the introductory chapter. The LHF results shown here are those provided by Solomon *et al* (1985a).

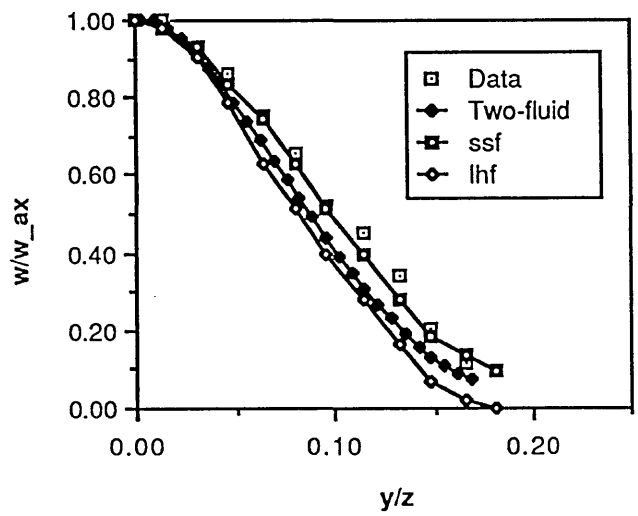
(d) The values predicted by the (Lagrangian) stochastically-separated-flow model of Solomon *et al* (1985a), labelled **ssf.** SSF models have also been revised in the first chapter of this thesis (Section 1.2).

Figures F6.6 to F6.8 present a similar arrangement for the liquid flux, which in the present model is computed as the average of $y_i^l w_i$, where y_i^l is the mass fraction of liquid. Thus:

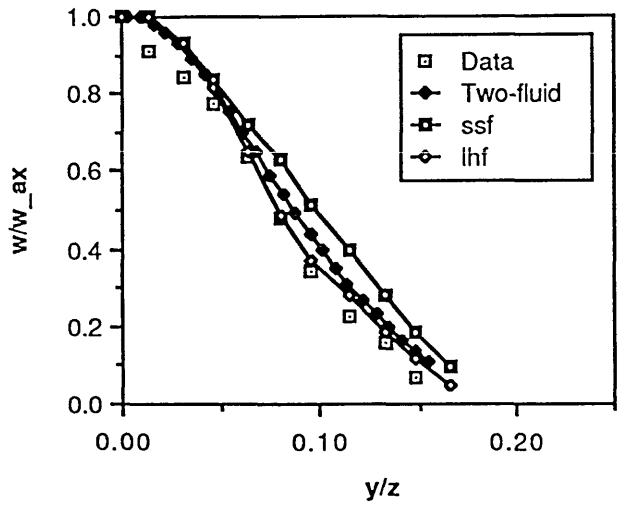
$$lf=(r_1\rho_1 y_1^l w_1+ r_2\rho_2 y_2^l w_2)/\rho \qquad [E6.1].$$



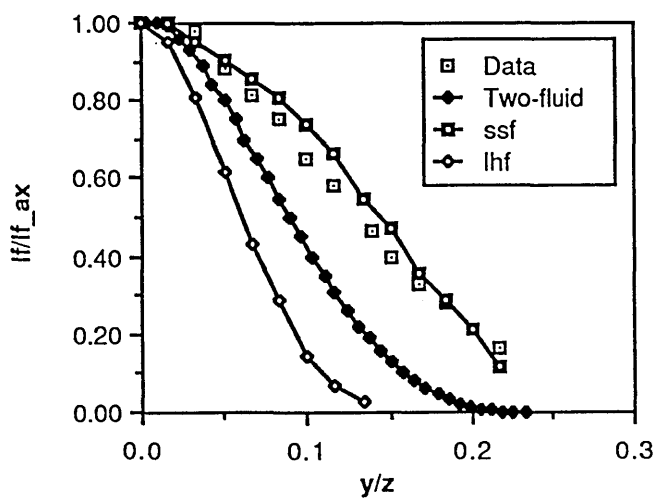
• *Figure F6.3: Radial profile of axial velocity at z/D=100 • (non-evaporating)*



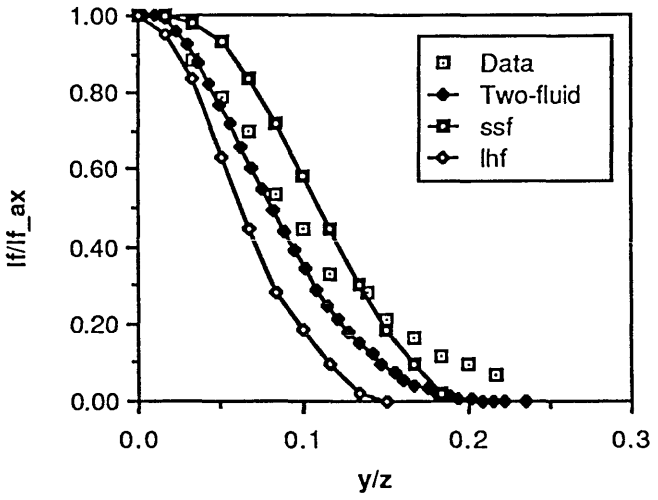
• *Figure F6.4: Radial profile of axial velocity at z/D=250 • (non-evaporating)*



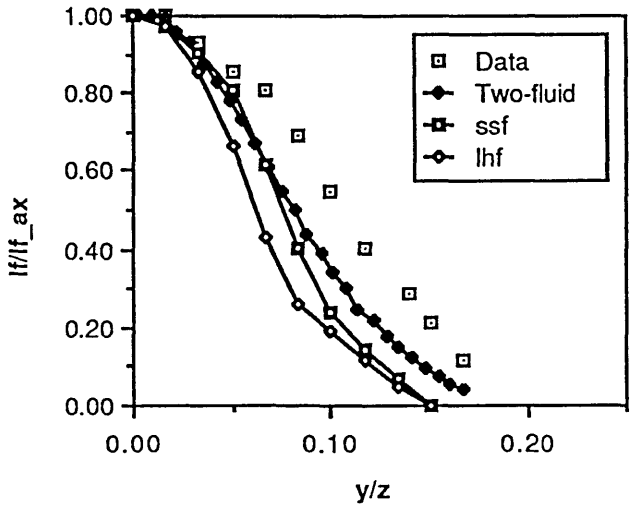
• *Figure F6.5: Radial profile of axial velocity at z/D=500 • (non-evaporating)*



• *Figure F6.6: Radial profile of axial liquid-flux at z/D=100 • (non-evaporating)*



• *Figure F6.7: Radial profile of axial liquid-flux at z/D=250 • (non-evaporating)*



• *Figure F6.8: Radial profile of axial liquid-flux at z/D=500 • (non-evaporating)*

Both sets of figures (axial velocity and axial liquid-flux) show the two-fluid-model predictions midway between LHF and SSF in the early stages of spray development (z/D=100). At z/D=250, the results provided by the two-fluid model are comparable, in accuracy, to those from the SSF model; and at z/D=500, they are even slightly better.

(It must be pointed out at this stage that the SSF model employed by Solomon *et al* (1985a) starts the computation at z/D=50, using experimental measurements at that station as inlet conditions. However, both the LHF model and the two-fluid model start from the injector nozzle. This might, in fact, explain the superiority of the SSF results at z/D=100.)

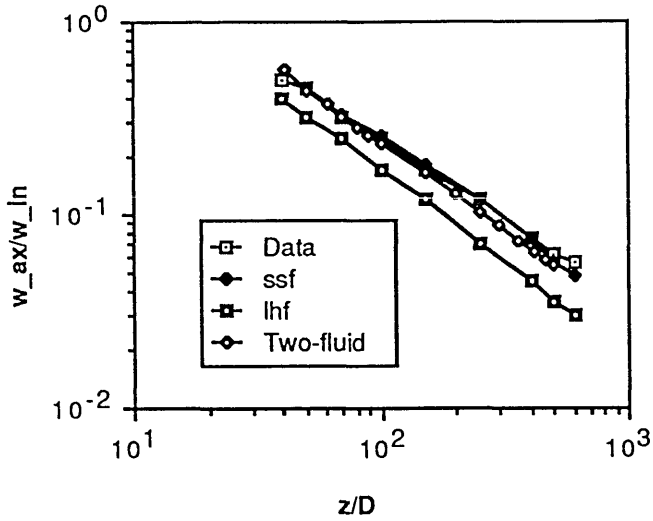
Figures F6.9 and F6.10 represent the axial evolution of the centreline values of (respectively):

- axial velocity;
- axial liquid-flux.

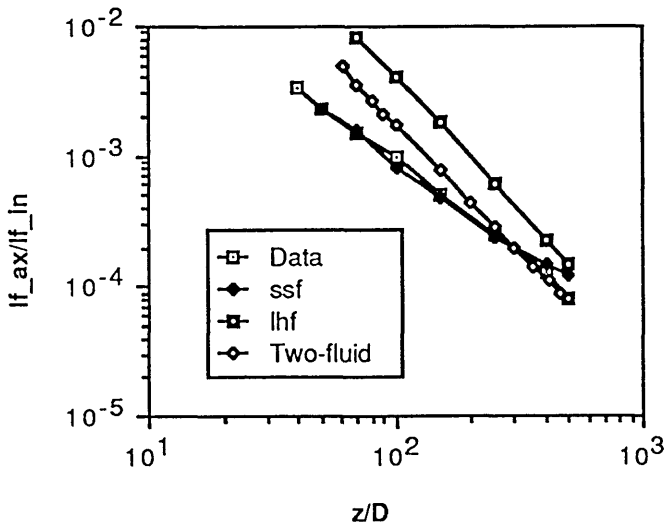
As for the radial profiles of preceding figures, the agreement between experimental and computed results is better for the velocity than it is for the liquid flux; and the results for the latter quantity also improve as the computation proceeds downstream. Again, the different starting locations for the computation should be borne in mind when these graphs are analysed, for experimental and SSF profiles coincide at z/D=50 because this is a boundary condition for the SSF model.

6.4 *Evaporating spray: results*

The results provided by the model for the evaporating spray are, in this section, compared with the experimental data of Solomon *et al* (1985b). As for the non-evaporating spray, this comparison will take the form of radial and axial profiles



• ***Figure F6.9: Centreline evolution of axial velocity (non-evaporating)*** •



• ***Figure F6.10: Centreline evolution of axial liquid-flux (non-evaporating)*** •

of the model results, the experimental data and the results provided by other models (LHF, SSF).

Figures F6.11 to F6.13 represent the radial evolution of the axial velocity at different locations (namely z/D=100, 250 and 500). At z/D=100, the two-fluid model and the SSF model yield a similar profile, even though the SSF computation starts at z/D=50 using experimental data as boundary conditions. The predictions given by all three models are also very similar for z/D=250 and z/D=500, a fact which is probably due to the decreasing presence of droplets as they evaporate.

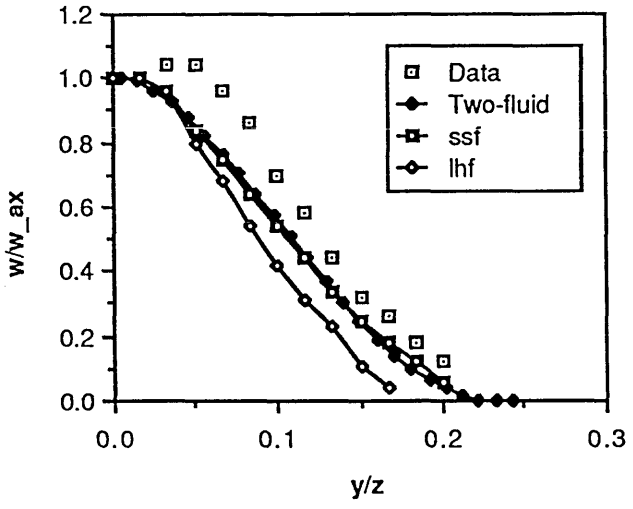
Figures F6.14 to F6.16 represent the radial evolution of total Freon-concentration (liquid and vapour). For the present two-fluid model, this is found, using the nomenclature of Chapter 5, as:-

$$fc=[r_1\rho_1(y_1^{l}+y_1^{v}) + r_2\rho_2(y_2^{l}+y_2^{v})]/\rho \qquad [E6.2].$$

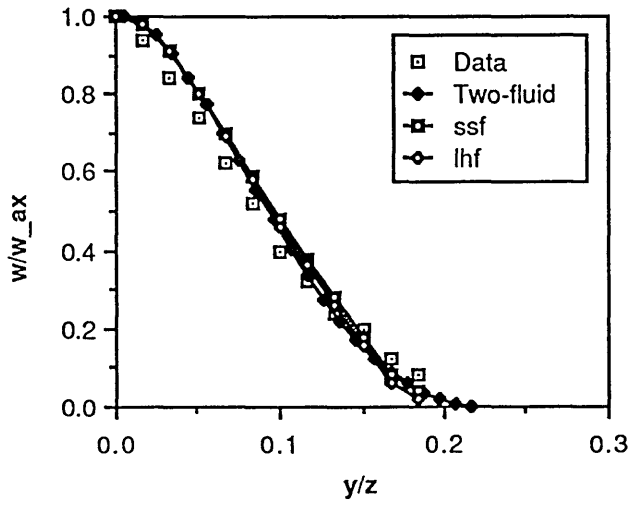
AT z/D=100, the Freon-concentration profile is slightly over-predicted by the two-fluid model in the central region of the spray, and it is more accurately matched at the spray edge. A similar pattern can be found in figure F6.15 at z/D=250, while at z/D=500 the present model performs similarly to the SSF model.

Figures F6.17 and F6.18 convey the axial evolution of the above quantities (gas velocity and Freon concentration) at the centreline. Both figures evince the superiority of two-fluid models and SSF models over LHF models, which grossly over-predict the rate of decay.

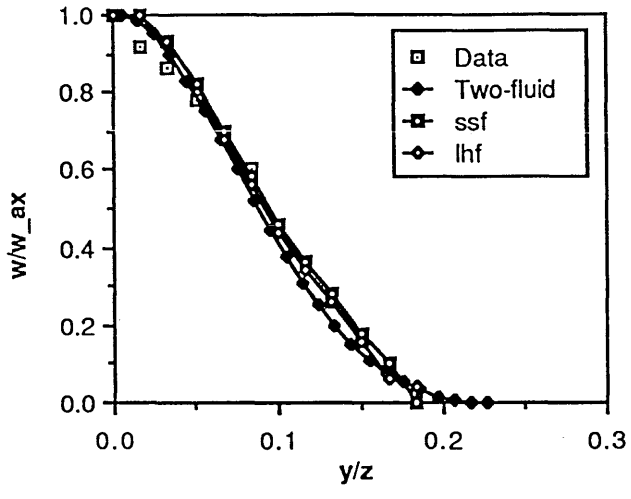
The accuracy of the predictions is strikingly higher for the evaporating spray than for the cold spray. This has been attributed by Solomon *el al* (1985b) to the decreasing presence of particles, as they evaporate. In the view of the present



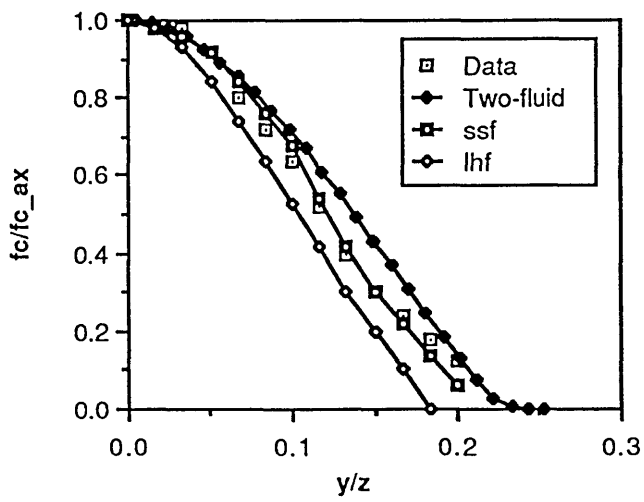
• *Figure F6.11: Radial profile of axial velocity at z/D=100 • (evaporating)*



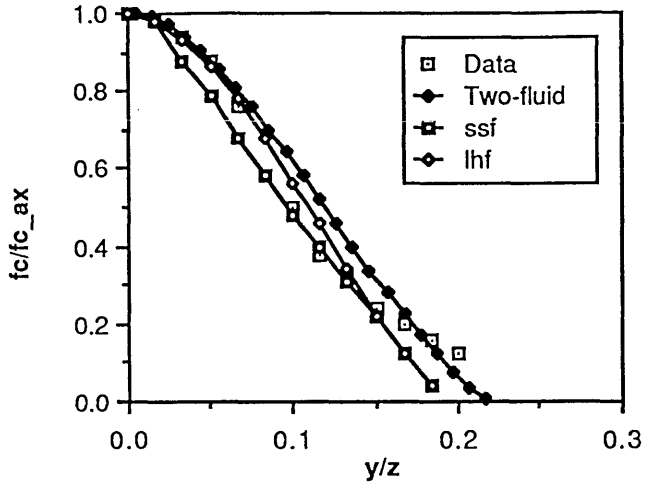
• *Figure F6.12: Radial profile of axial velocity at z/D=250 • (evaporating)*



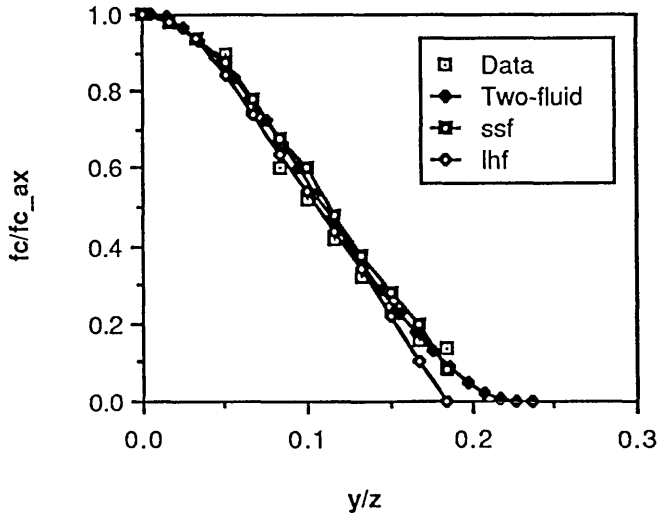
• *Figure F6.13: Radial profile of axial velocity at z/D=500 • (evaporating)*



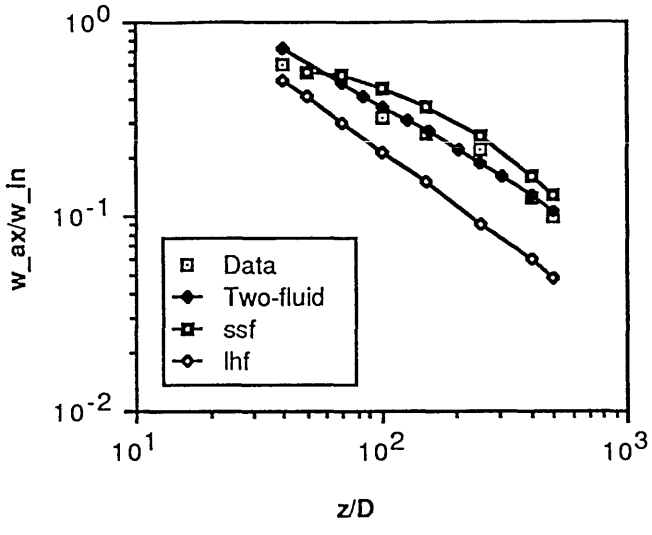
• *Figure F6.14: Radial profile of freon concentration at z/D=100 • (evaporating)*



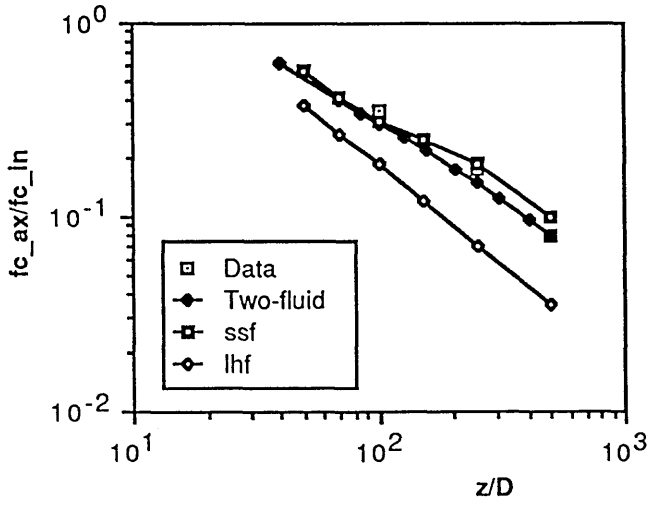
• *Figure F6.15: Radial profile of freon concentration at z/D=250 • (evaporating)*



• *Figure F6.16: Radial profile of freon concentration at z/D=500 • (evaporating)*



• *Figure F6.17: Centreline evolution of axial velocity (evaporating)* •



• *Figure F6.18: Centreline evolution of freon concentration (evaporating)* •

author, a further reason is the magnitude chosen to represent the liquid: whereas **concentration** is used for the evaporating spray, **liquid flux** is used for the cold one. And LHF and two-fluid models cannot predict, as a separate quantity, liquid velocity, which intervenes in the flux but not in the concentration.

6.5 Grid independence and numerical details

6.5.1 Numerical details

The numerical-integration method employed a 30-cell grid in the y-direction for the cases presented in preceding sections. The forward step in the z-direction was taken as a 20% of the spray width $y_{1\%}$. Around 130 of these steps were needed to reach the last axial station (z/D=500).

The computer used was, as for the single-phase jet, an Acorn Cambridge Workstation. A typical run as described above needed, for the evaporating spray, 2h17m to be completed.

6.5.2 Grid-independence studies

Four additional runs were performed to assess the independency of the results from the fineness of numerical mesh employed. Since the cold-spray model can be regarded as a simplified version of the evaporating-spray one, only this second case is tested here.

The values of the number of cells in the cross-stream direction (NY) and the forward step (DZ) for the test cases are listed in table T6.4, together with the labels used in the graphs that will follow.

• *Table T6.4: Grid-independence test-cases* •

NY	DZ	Label in graphs
30	20%	30/20% (standard)
60	20%	60/20%
20	20%	20/20%
30	10%	30/10%
30	30%	30/30%

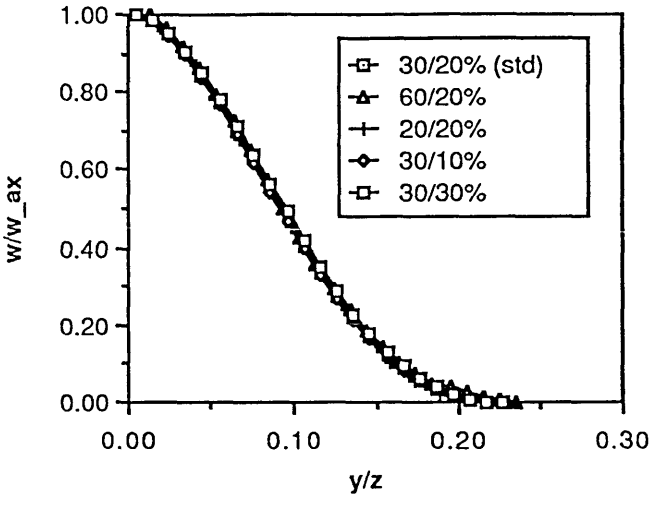
Radial and axial profiles of axial velocity and Freon mass-fraction are provided in figures F6.19 to F6.22. These reveal that the 30/20% grid employed is enough to guarantee grid independence, and that coarser grids could indeed have been used.

6.6 *Further analysis*

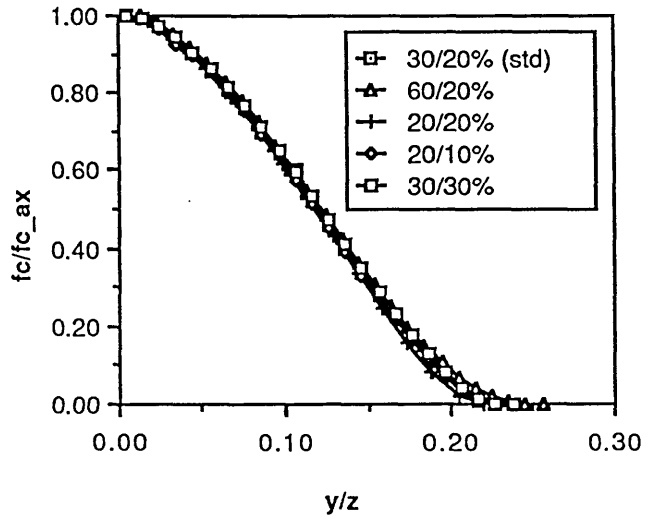
The performance of the proposed model is, in this section, explored beyond the formal comparison with experimental data of preceding sections. Some implications of the two-fluid idea will be brought out in the process.

6.6.1 The fragment length l

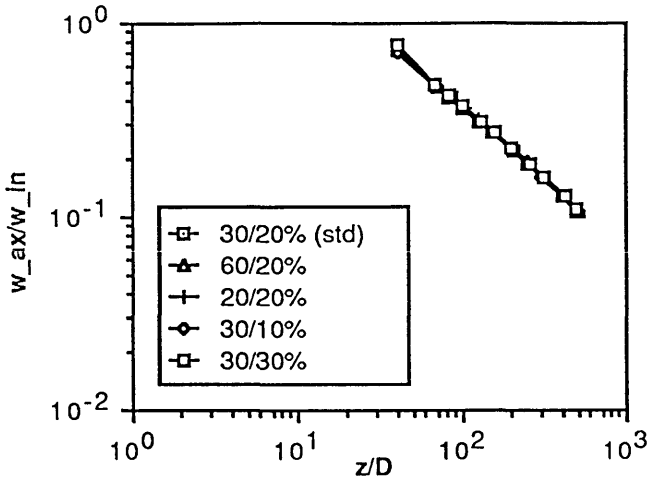
The fragment length l is computed, in the present model, from partial differential equations, as set out in Section 4.4.2. Figure F6.23 (corresponding to the evaporating-spray run) confirms the result achieved for single-phase jets: after a region of jet development, the ratio l/l_p tends to a constant value.



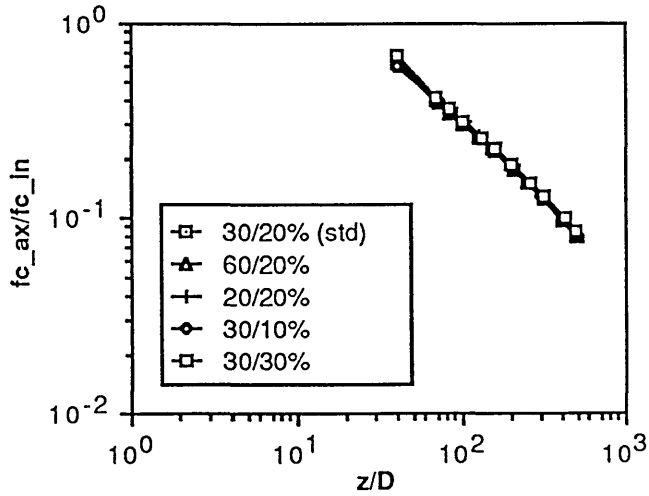
• ***Figure F6.19: Grid independence • axial velocity at z/D=250***



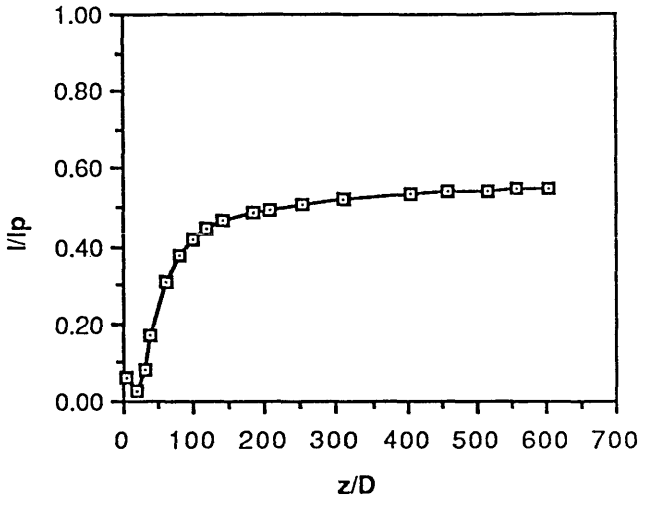
• ***Figure F6.20 Grid independence • freon concentration at z/D=250***



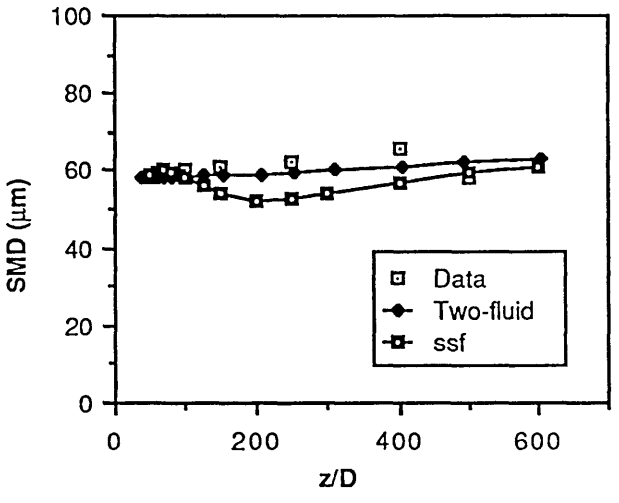
• ***Figure F6.21: Grid independence • axial evolution of axial velocity***



• ***Figure F6.22: Grid independence • axial evolution of freon concentration***



• ***Figure F6.23: Axial evolution of l/l_p*** •



• ***Figure F6.24: Computed and experimental evolution of SMD*** •

6.6.2 Evolution of the Sauter Mean Diameter

The local Sauter Mean Diameter (SMD) may be obtained, for each phase, from the m_i^k-distribution (obtained from E5.5) as:

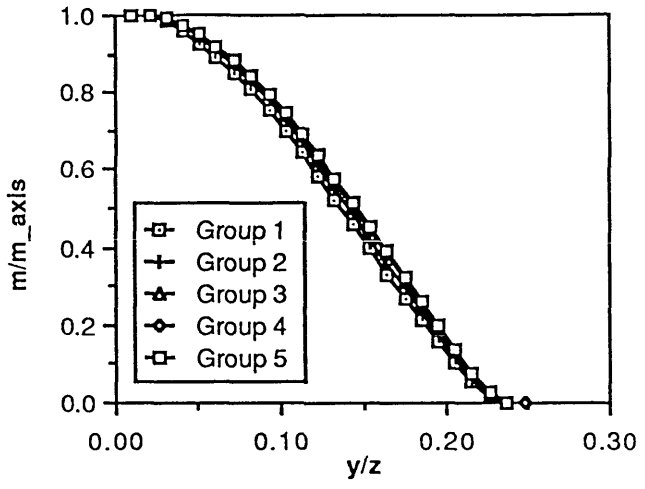
$$D_{32_i} = \frac{\int_0^\infty D^3 F(D)\, dD}{\int_0^\infty D^2 F(D)\, dD} = \frac{\frac{m_i^1 s_2^{(2)}}{6} + \sum \frac{m_i^k (s_{k+1}^{(2)} - s_k^{(2)})}{4}}{\frac{m_i^1 s_2^{(3/2)}}{5} + \sum \frac{m_i^k (s_{k+1}^{(3/2)} - s_k^{(3/2)})}{3}} \qquad \text{[E6.3].}$$

(On the RHS, superscripts in brackets indicate ordinary power.)

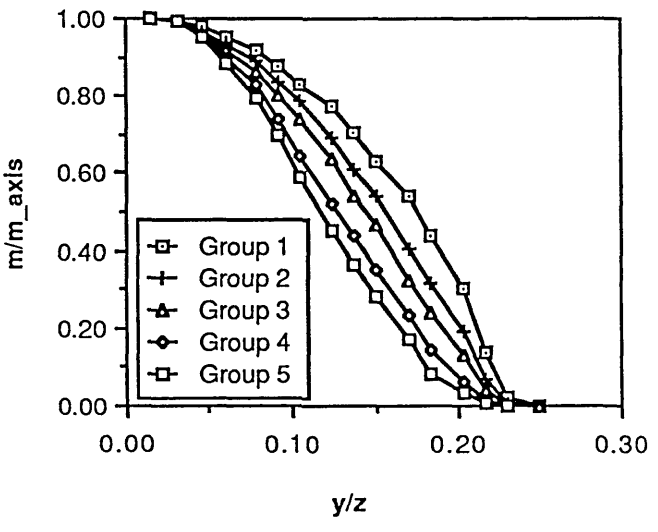
The axial evolution of the computed SMD for the evaporating spray is shown in figure F6.24, along with the experimental evolution and that provided by the SSF model of Solomon *et al* (1985b). The increase of the SMD is justified by Solomon *et al* (1985b) as being the consequence of turbulent droplet-diffusion: the smaller droplets tend to be carried away from the axis, whereas the larger droplets remain close to the axis. The two-fluid model employed uses, however, the same diffusion law for all sizes (E5.6 and T5.1), and yet the SMD increases. A plausible explanation of this phenomenon will be proposed in Section 6.6.4. And the effect of droplet diffusion on the SMD will be assessed in the next section.

6.6.3 Effect of droplet diffusion

As pointed out in the preceding section, the models employed use droplet-diffusion laws which do not depend on the droplet size. The radial distribution of droplet concentration arising from these laws is nearly the same for all droplet groups, as shown in figure F6.25.



• *Figure F6.25: Radial profiles of droplet concentration* •



• *Figure F6.26: Effect of droplet diffusion on droplet concentration* •

This section explores the consequences of considering size-dependent laws. This is achieved by assigning a different diffusion-constant $C_{m_{ik}}$ (E5.6) to each size group, fostering the diffusion of smaller droplets and limiting it for the larger ones. The set of constants employed is detailed in table T6.5, and the resulting radial profiles of droplet concentration are shown in figure F6.26 (non-evaporating spray, only fluid-2 size-groups shown).

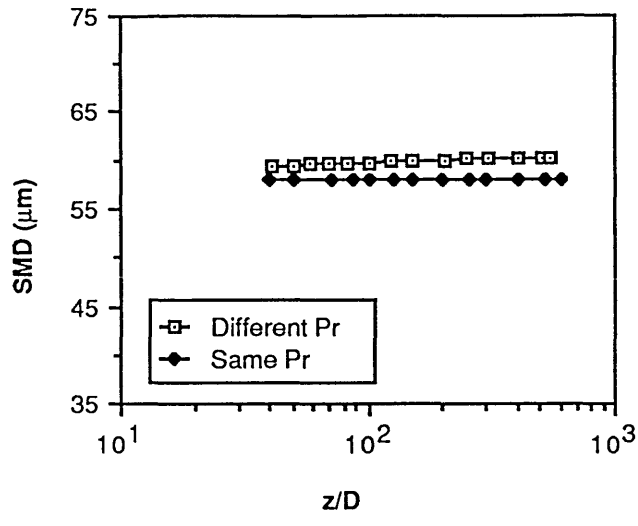
- ***Table T6.5: Size-dependent diffusion-coefficients*** $C_{m_{ik}}$.

Size group	Standard run (F6.25)	This run (F6.26)
1 (smallest)	$2 \cdot C_\mu$	$4 \cdot C_\mu$
2	$2 \cdot C_\mu$	$8 \cdot C_\mu / 3$
3	$2 \cdot C_\mu$	$2 \cdot C_\mu$
4	$2 \cdot C_\mu$	$4 \cdot C_\mu / 3$
5 (largest)	$2 \cdot C_\mu$	$1 \cdot C_\mu$

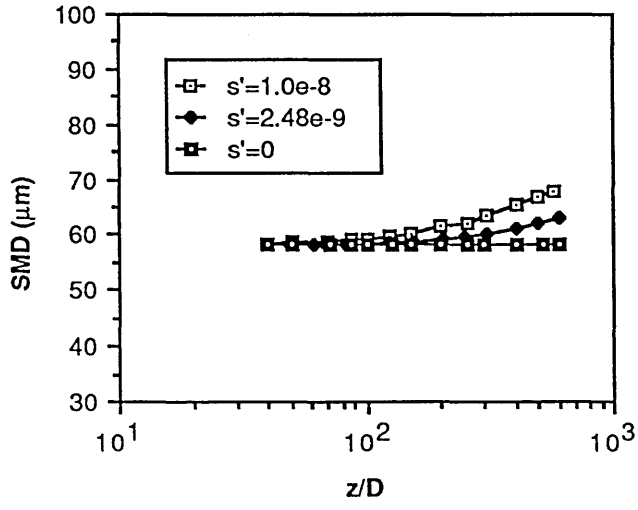
The effect of these settings on the SMD, which can be seen in figure F6.27, is, as expected, the increase of SMD with reference to the standard run for the non-evaporating spray, also shown in this figure.

6.6.4 Effect of the vaporisation rate, s'

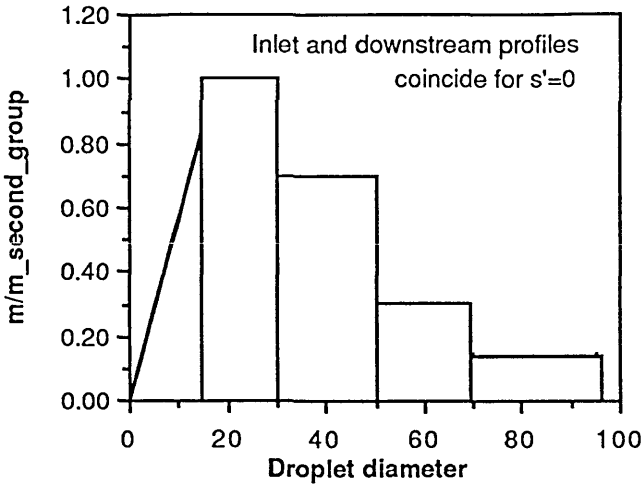
Figure F6.28, with the axial evolution of the SMD for several vaporisation rates, shows how a larger vaporisation rate s' means an increased SMD. An explanation for this behaviour can be gathered from figures F6.29 to F6.32. These represent the droplet distribution at a centreline station for the different vaporisation rates. The inlet distribution is also shown in each figure, and, to allow the comparison of the distribution **shapes**, each distribution has been normalised with the



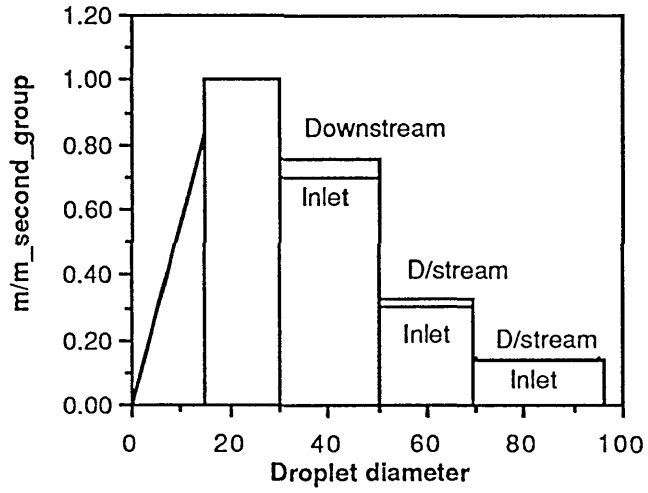
• *Figure F6.27: Effect of size-dependent diffusion-coefficients* •



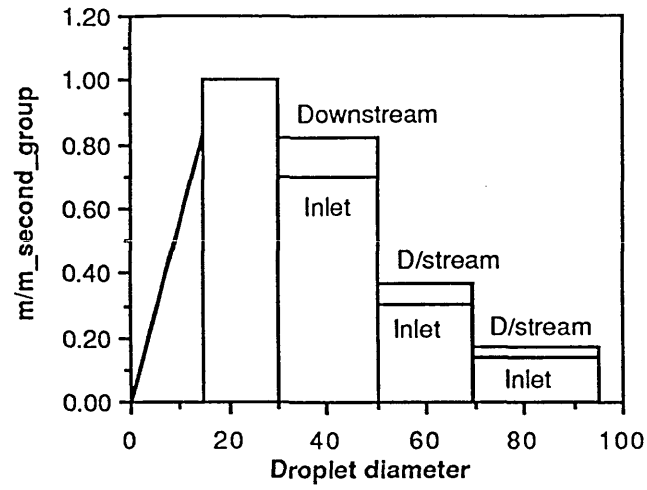
• *Figure F6.28: Effect of vaporisation rate on SMD* •



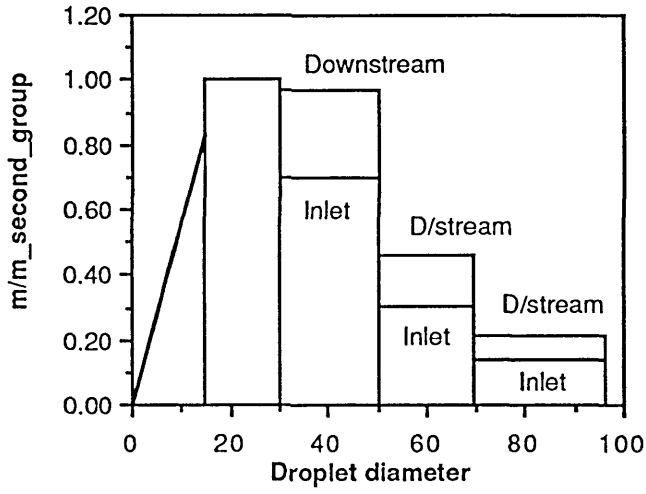
• *Figure F6.29: Size distribution at the axis for s'=0* •
(fluid 2 only; normalised with the value for group 2)



• *Figure F6.30: Size distribution at the axis for s'=2.48e-9* •
(fluid 2 only; normalised with the value for group 2)



• *Figure F6.31: Size distribution at the axis for s'=5.0e-9 • (fluid 2 only; normalised with the value for group 2)*



• *Figure F6.32: Size distribution at the axis for s'=1.0e-8 • (fluid 2 only; normalised with the value for group 2)*

respective maximum (which happens to be, in all cases, the mass fraction of droplets in the second group).

In figure F6.29, for s'=0, the downstream shape coincides with the inlet one¶. This is the expected result, since there is no vaporisation and the diffusion coefficient is the same for all size groups; and this is the reason why the SMD remains constant (case s'=0 in F6.28).

Figures F6.30 to F6.32 show how the droplet-vaporisation law implies a re-shaping of the initial distribution: the difference between the concentration of droplets in the smaller groups (first and second) and the larger groups diminishes, and this implies an increase of the SMD as evinced by figure F6.28. The re-shaping of the droplet distribution is not surprising; for the vaporisation law (s'=constant) implies that the smaller droplets evaporate more rapidly, since D'=constant/D.

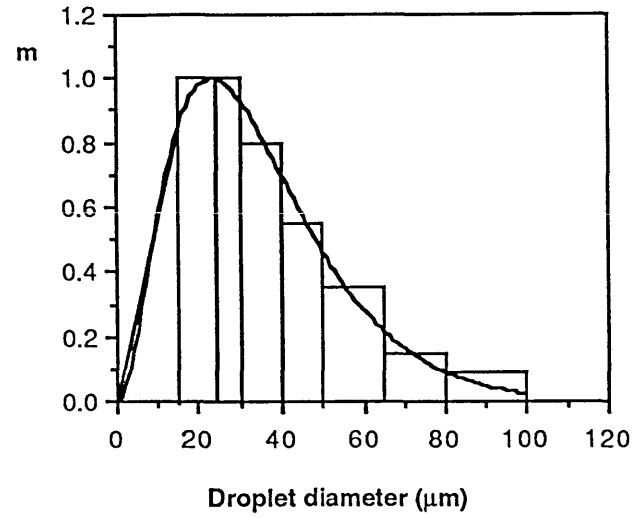
It may be therefore concluded that a large vaporisation rate has probably a stronger effect on the initial increase of the SMD than droplet diffusion (provided, of course, that the **real** vaporisation law is sensibly similar to a D^2-law and that the inlet distribution is similar to that postulated).

6.6.5 Increase in the number of droplet groups

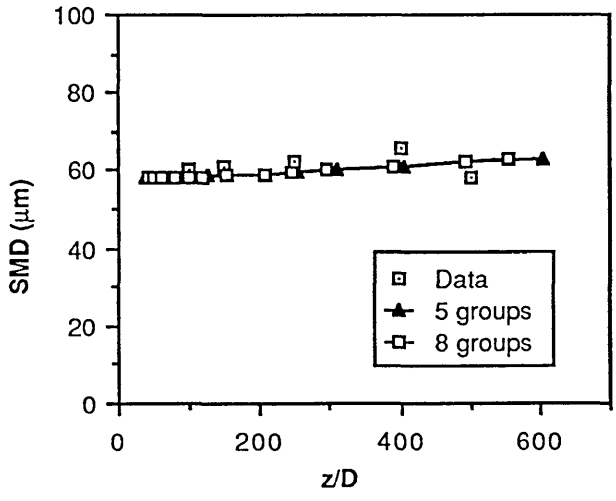
In the calculations presented so far, five size-groups are used for each fluid to accommodate the droplets according to their size. This subsection explores the

---

¶ The **absolute** values are, of course, smaller, but this has been hidden by the normalisation.



• *Figure F6.33: Inlet size-distribution with 8 size-groups • (evaporating spray)*



• *Figure F6.34: SMD evolution with 5 and 8 size-groups • (evaporating spray)*

effect of considering a finer size-discretisation, such as the one shown in figure F6.33 (8 groups).

The SMD is bound to be, for obvious reasons, the quantity in which the effect of this increase may be more noticeable. Figure F6.34 shows that very similar evolutions are obtained for 5 and 8 size-groups, thus indicating that 5 groups suffice to convey the distribution information.

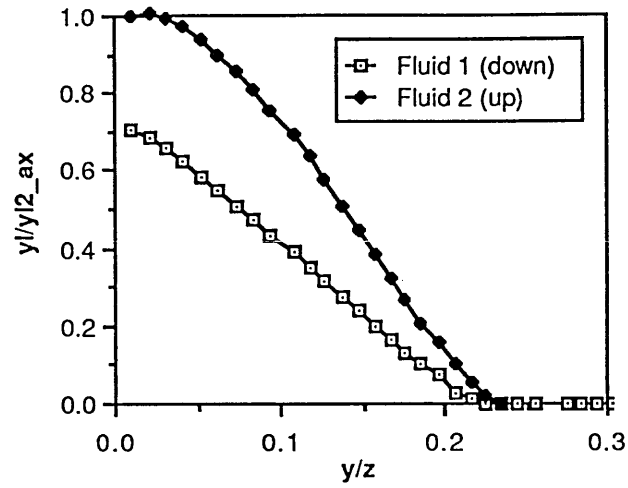
6.6.6 Density differences between both fluids

A direct consequence of the definition of both fluids as in- and out-moving is the different concentration of liquid in them. Fluid 1 (the in-moving fluid) is drawn from the surroundings with no liquid. As the parcels travel towards the axis, diffusive and convective interphase-exchange with fluid 2 (the out-moving fluid) increases the liquid content of the parcel. This interphase exchange is brought about by the terms $f_{ji}(m_j^k - m_i^k)$ ("diffusive" term) and $[\![m_{ji}]\!](m_j^k - m_i^k)$ ("convective" term) in equation E5.5.

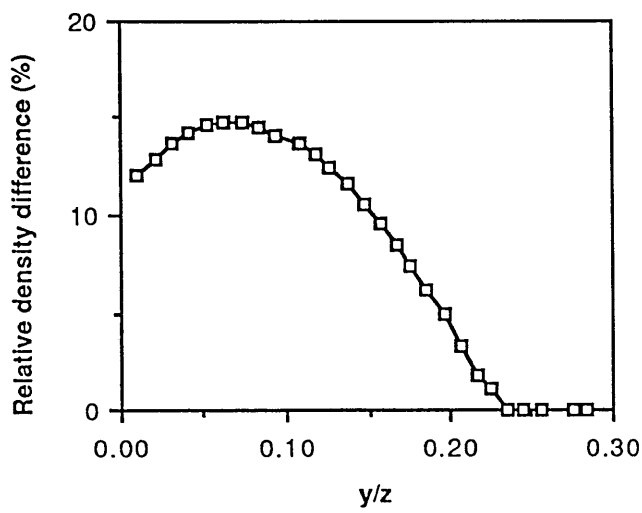
The radial distribution of liquid volume-fraction is shown in figure F6.35. As it should be expected from the process outlined above, the liquid content is higher for fluid 2 (out-moving) than for fluid 1 (in-moving). The difference in liquid concentration has, obviously, a direct effect on the density of the fluids: the out-moving fluid is denser than the in-moving one. The radial profile of density difference is shown in figure F7.36 (difference in % of the local average-density).

6.6.7 Effect of the interphase-transfer constants

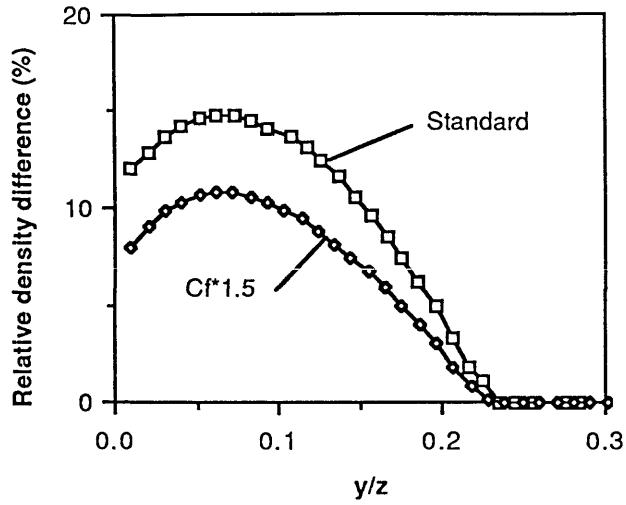
The role of m_{ji} and f_{ji} in the density difference has been outlined in the preceding section. Figure F6.37 reveals the consequences of an increase in f_{ji} through an



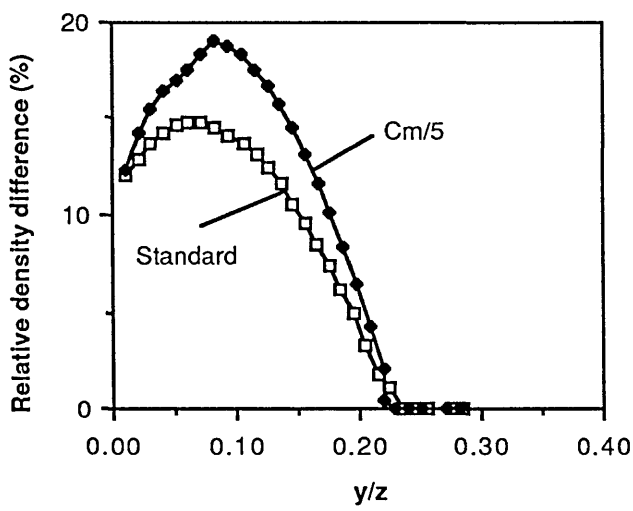
• *Figure F6.35: Radial profile of liquid volume-fraction in each fluid (normalised with the axial value for fluid 2)*



• *Figure F6.36: Radial profile of density difference (in % of the local average)*



• ***Figure F6.37: Effect of C_f on density difference*** •



• ***Figure F6.38: Effect of C_m on density difference*** •

increase of its multiplicative constant C_f: the density difference is smaller because of the enhanced interphase diffusion.

A decrease of C_m (the constant affecting m_{ji}) would be expected to have an opposite effect. This is confirmed by figure F6.38, showing the greater density-difference as a consequence of the reduced exchange of liquid through mass transfer.

6.7 Closure

The two-fluid model for sprays developed in Chapter 5 has been, in this chapter, applied to the simulation of cold and evaporating sprays.

The model results are, in general, adequate, and comparable to those yielded by SSF models. The results have been found to be better for the evaporating spray than for the cold spray, a fact that has been attributed in this research to:-

(a) The decreasing presence of droplets;

(b) The quantity used for the comparison (liquid flux in the cold spray, but concentration in the evaporating one), combined with the fact that the present model cannot yield liquid velocity as a separate quantity.

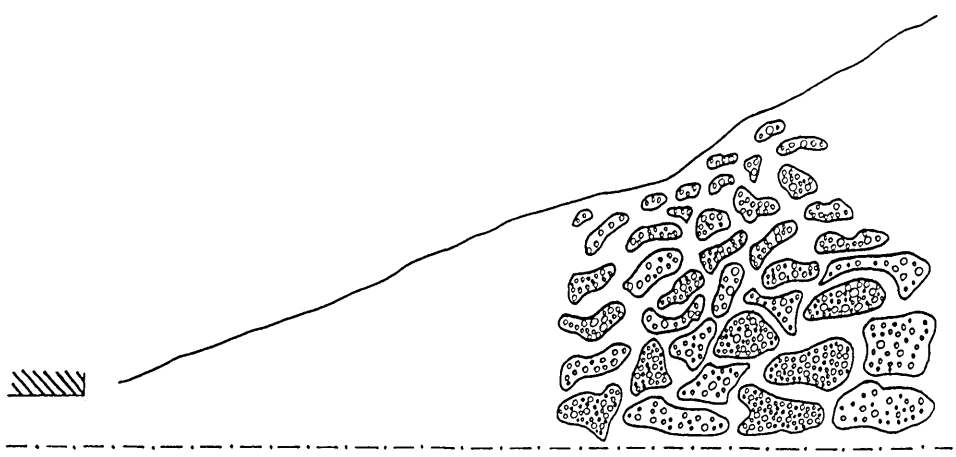
The interesting finding which concerns the fragment size l for single-phase jets has also been found in sprays. Namely, the fragment size is, after a region of jet development, proportional to the Prandtl mixing length l_p. With the constants employed in the present model, the ratio l/l_p is, approximately, 0.5.

In the evaporating spray, both the computed and the experimental axial evolution of the SMD increase initially with the axial coordinate. It has been shown that size

redistribution caused by the vaporisation law contributes to this increase as much as the turbulent diffusion of droplets.

A direct consequence of the mathematical formulation of the two-fluid model is the different density of both fluids. The in-moving fluid parcels are drawn from the surrounding air without liquid, and the liquid contents increase as they travel inwards through interphase exchange with the richer out-moving parcels. Figure F6.39 is a "qualitative" representation of these results. "Rich" parcels of droplets intermingle in the spray with "lean" ones; and the size of the parcels increases as we move towards the centreline. (This was represented quantitatively for the single-phase jet in figure F4.9.)

This different liquid content of the parcels of both fluids is bound to have some significance in combusting sprays. An example of this is shown in the next chapter, where a demonstrative run with combustion will be studied.



• *Figure F6.39: Qualitative representation of results* •

Chapter 7

Further studies: combustion

7.1 Introduction

7.1.1 The purpose of this chapter

In preceding chapters, a two-fluid model of turbulence has been developed for, and applied to, single-phase jets (Chapter 4) and cold and evaporating sprays (Chapters 5 and 6). This chapter will extend the model to study the case in which the liquid injected is a fuel, which subsequently evaporates and burns. The combustion scheme employed is the so-called Simple Chemically-Reacting System (Spalding, 1979), also known as the Shvab-Zeldovich formulation (Williams, 1965; Bilger, 1980). An extension of this scheme for two-fluid models is presented in this chapter.

The conclusions that can be expected from this chapter are, it should be noted now, essentially qualitative in nature; for, unlike preceding chapters, the present one does not include a comparison with experimental data. Its aim is, rather, to demonstrate the implications of the two-fluid idea in combusting flows.

7.1.2 Layout of the chapter

The present introductory section is followed by Section 7.2, which summarises the SCRS scheme for single-phase flows and proposes an extension for two-fluid models. Section 7.3 supplies the remainder of the mathematical model for the combusting spray. Then, Section 7.4 checks the correctness of the SCRS extension

through a simple numerical test. Section 7.5 follows with the presentation and analysis of the model results, and Section 7.6 closes the chapter with a summary.

7.2 The Simple Chemically-Reacting System (SCRS)

Single-phase, combusting flows are frequently modelled using the SCRS scheme (Spalding, 1979), also known as the Shvab-Zeldovich formulation. Subsequent sections will show that the SCRS cannot be used, in general, for systems involving two miscible phases, and will set out the circumstances in which an extension for two-fluid models can be applied.

Although well known and widely used, a brief description of the SCRS principles is in order, since it will pose the problem for the two-fluid extension proposed in this work.

7.2.1 The SCRS for single-phase flows

The SCRS considers a simple, one-step chemical reaction in which fuel (F) and oxidant (O) combine to give products (P):

$$F + s\,O \longrightarrow (1+s)\,P + \text{Heat},$$

where s is the stoichiometric ratio.

The transport equations for fuel and oxidant can be written as:-

$$\frac{\partial(\rho y^f)}{\partial t} + \nabla(\rho \mathbf{V} y^f) - \nabla(\Gamma_f \nabla y^f) = -R' \qquad \text{[E7.1]};$$

$$\frac{\partial(\rho y^o)}{\partial t} + \nabla(\rho \mathbf{V} y^o) - \nabla(\Gamma_o \nabla y^o) = -sR' \qquad \text{[E7.2]},$$

where R' is the reaction rate, normally a function of y^f, y^o, and the temperature.

On the assumption that $\Gamma_f=\Gamma_o=\Gamma$, both equations can be combined by substracting, from E7.1, E7.2 divided by s. This yields:

$$\mathbf{LHS}\ (y^f-y^o/s)=0 \qquad [E7.3],$$

where **LHS** represents the linear operator

$$\mathbf{LHS}\ (\zeta) = \frac{\partial(\rho\zeta)}{\partial t} + \nabla(\rho \mathbf{V}\zeta) - \nabla(\Gamma \nabla\zeta) \qquad [E7.4].$$

The variable $f=y^f-y^o/s$, obeying the homogeneous differential equation E7.3, is called a **conserved property** (sometimes "passive scalar"). Some other conserved properties (Spalding, 1979) are:-

- $y^f+y^p/(1+s)$;
- $y^o/s+y^p/(1+s)$;
- any dilutant;
- any inert species.

Furthermore, if the specific heats of all the species are the same (say C), and the Lewis number $Le=\lambda/\Gamma C$ is one, then it can be shown that the following definition of enthalpy is also a conserved property:

$$h = CT + y^f H \qquad [E7.5].$$

(H is the heat of combustion.)

When the fluid emanates from only two streams (say A and B), it can be easily proved that any two conserved properties f and g verifying **LHS**(f)=0 and **LHS**(g)=0 are related by a linear relationship of the form:

$$g = a f + b \qquad \text{[E7.6].}$$

The proof can be considered as having two parts, namely:-

(1) The linear relationship E7.6 satisfies the equation for g, **LHS** (g)=0; and

(2) The linear relationship E7.6 satisfies the boundary conditions for g.

If (1) and (2) are fulfilled, and the solution of the equation for g is unique, then E7.6 is **the** solution.

(1) is proved by simple substitution of E7.6 in the differential equation for g:

LHS (g) = **LHS** (a f + b) = a **LHS** (f) = 0.

(2) is proved, if the fluid emanates only from two streams, as follows:

At stream A: $g_A = a f_A + b$ [E7.7a];

At stream B: $g_B = a f_B + b$ [E7.7b],

from which the values of a and b can be found. The resulting linear relationship is:

$$\frac{f - f_A}{f_B - f_A} = \frac{g - g_A}{g_B - g_A} \qquad \text{[E7.8].}$$

The existence of a relationship such as E7.8 means that only one of these conserved properties (also called passive scalars) has to be solved for. The calculation of the combustion-related variables under an SCRS proceeds therefore as follows:-

1. An equation is solved for the fuel mass-fraction, y^f, in which a source term accounts for the consumption of fuel.

2. A further equation is set up and solved for a conserved scalar. In this work, this scalar will be taken as

$$f = y^f + y^p/(1+s) \qquad \text{[E7.9]},$$

where y^p is the mass fraction of products. The variable f, as defined by E7.9, can be regarded as the mass fraction of material arising from the fuel, whether burned or not.

3. The amount of oxidant is calculated from y^f and f as

$$y^o = 1 - y^f - (1+s)\ (f-y^f) \qquad \text{[E7.10]}.$$

4. The mass fraction of products is obtained as

$$y^p = 1- y^f- y^o \qquad \text{[E7.11]}.$$

5. Since the enthalpy defined as in E7.5 is a conserved property, it can be obtained from the passive scalar f using E7.8.

6. Although no inert species has been considered thus far, they can be easily accommodated within the scheme: since they are conserved properties as a matter of definition, then they can be obtained from f using also E7.8.

7.2.2 An SCRS for two-fluid models (SCRS2)

The main assumption upon which the SCRS scheme rests is the fact that the properties f and g related by E7.8 are conserved.

For two-phase flows of miscible fluids (such as those arising from two-fluid models), fuel and oxidant verify equations having the form:

$$\frac{\partial(r_i\rho_i y_i^f)}{\partial t} + \nabla(r_i\rho_i \mathbf{V}_i y_i^f) - \nabla(r_i\Gamma_f\nabla y_i^f) = I_{ji}(y_j^f-y_i^f) - r_i R_i' \qquad \text{[E7.12a]};$$

$$\frac{\partial(r_i\rho_i y_i^o)}{\partial t} + \nabla(r_i\rho_i \mathbf{V}_i y_i^o) - \nabla(r_i\Gamma_o \nabla y_i^o) = I_{ji}(y_j^o - y_i^o) - r_i\, sR_i' \qquad \text{[E7.12b]},$$

where I_{ji} represents the interphase transfer.

If the assumption $\Gamma_f=\Gamma_o=\Gamma$ is made, and E7.12a and F7.12b are combined as for the single-phase case (E7.3), the following equation is obtained:

$$\mathbf{LHS2_i}\ (f_i) = I_{ji}[f_j - f_i] \qquad \text{[E7.13]},$$

where $f_i=y_i^f - y_i^o/s$ and $\mathbf{LHS2_i}$ is the two-phase counterpart of the operator **LHS**.

Clearly, f_i is not conserved, and a result such as E7.8 cannot be, for this reason, generally granted for two-phase flows if $I_{ji}\neq 0$. The remainder of this section sets out the conditions in which the SCRS is applicable to two-fluid models. The discussion is parallel to that for the single-phase case above, and involves the following steps:-

1. Let us consider two properties f and g verifying the two-phase, transport equations:

   $$\mathbf{LHS2_i}\ (f_1) = I_{21}(f_2 - f_1) \qquad \text{[E7.14a]};$$
   $$\mathbf{LHS2_i}\ (f_2) = I_{12}(f_1 - f_2) \qquad \text{[E7.14b]}.$$

   And similarly for g:

   $$\mathbf{LHS2_i}\ (g_1) = I_{21}(g_2 - g_1) \qquad \text{[E7.14c]};$$
   $$\mathbf{LHS2_i}\ (g_2) = I_{12}(g_1 - g_2) \qquad \text{[E7.14d]}.$$

2. Let us postulate, as for the single-phase case, that **there is** a linear relationship between g_i and f_i of the kind:

$g_i = a_i f_i + b_i$ with i=1, 2 [E7.15].

3. Substitution of E7.15 into the equation for g_1 (E7.14c) yields:

$a_1 \mathbf{LHS2_i}(f_1) = I_{21}[(a_2 f_2 - a_1 f_1) + (b_2 - b_1)]$ [E7.16].

Since f_1 satisfies equation E7.14a, E7.16 is satisfied if $a_1=a_2$ (=a, say) a and $b_1=b_2$ (=b, say). The same results hold for g_2 and its equation.

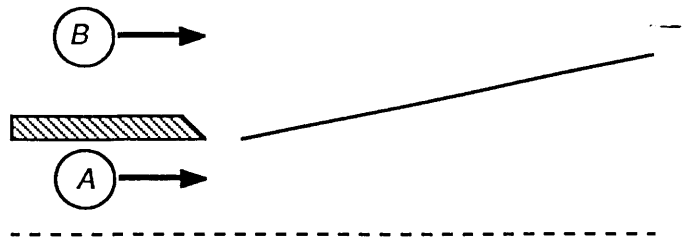
5. Therefore, the expressions

$g_i = a f_i + b$ (i=1, 2) [E7.17]

satisfy the differential equations for g_i (i=1, 2) for any values of a and b. If they satisfy the boundary conditions, and assuming that the solution is unique, then $g_i = a f_i + b$ is **the** solution.

6. If a two-stream system is considered, such as that sketched in figure F7.1, boundary conditions must be provided at A and B for g_i and f_i (i=1,2). The boundary conditions must of course fulfil the postulated linear relationships E7.17. Thus:

$g_{1A} = a f_{1A} + b$ [E7.18a];
$g_{1B} = a f_{1B} + b$ [E7.18b];
$g_{2A} = a f_{2A} + b$ [E7.18c];
$g_{2B} = a f_{2B} + b$ [E7.18d].



• ***Figure F7.1: Two-stream system*** •

7. The system E7.18x has four equations and only two unknowns; some additional constraints must therefore be imposed upon the boundary values of f and g.

8. Let us assume that

   (a) Only fluid 2 is injected through A;

   (b) Both fluids have at B the same value of their properties.

   (NB both (a) and (b) are true in the two-fluid models proposed in preceding chapters.)

   Assumption (b) implies that $g_{1B}=g_{2B}$, and $f_{1B}=f_{2B}$; The equations E7.18b and E7.18d are reduced to one: $g_B = a\, f_B + b$.

   Assumption (a) implies that E7.18a is not needed, since no property f_1 or g_1 is injected through the outlet A.

9. The resulting system for the two-fluid model is, therefore:

   $g_B = a\, f_B + b$ [E7.19a];

   $g_{2A} = a\, f_{2A} + b$ [E7.19b],

   from where a and b can be found.

Substitution of these values for a and b into the postulated linear relationship E7.17 yields:-

$$\frac{f_1 - f_{2A}}{f_B - f_{2A}} = \frac{g_1 - g_{2A}}{g_B - g_{2A}} \qquad \text{[E7.20a];}$$

$$\frac{f_2 - f_{2A}}{f_B - f_{2A}} = \frac{g_2 - g_{2A}}{g_B - g_{2A}} \qquad \text{[E7.20b].}$$

10. The equations E7.20x allow the computation of all quasi-conserved properties in an SCRS2 from a single one, using linear relationships formally identical to that for the single-phase SCRS (E7.8). Under these conditions, paragraphs (1) to (6) in the preceding section are still valid.

11. A more general conclusion can be drawn for the foregoing discussion: it is contended that the SCRS is applicable to two-phase flows of the kind described above if and only if the boundary conditions are such that render E7.18x a compatible system of equations. (This is, eg, the case when only one fluid emanates from A while only the other does from B.)

The next section describes the modifications which have to be made to the vaporising-spray model of preceding chapters to accommodate the SCRS2.

7.3 The mathematical model

The new situation considered (Section 7.1.1) shares many features with the evaporating spray of Chapters 5 and 6. Only modifications and additions to the mathematical model will be listed in this section; the complete set of equations may be found in Appendix B.

The consequences of considering combustion in the evaporating-spray model are essentially three:

1. The consumption of vapour and oxidant;
2. The release of products of the chemical reaction;
3. The release of heat in the process.

Although the presence of two fluids, rather than only one, does not entail any significant departure from the single-phase SCRS scheme, as shown in the preceding section, the inclusion of a liquid phase within each fluid requires some thinking. The task is tackled in the next subsections.

7.3.1 Droplets, vapour and total fuel

The vaporising-spray model of Chapters 5 and 6 provides differential equations for the droplet-group mass-fraction (E5.5) and for the mass-fraction of vapour (E5.7).

However, the SCRS2 requires an equation for the **global** fuel mass-fraction of each phase (y_i^f), as discussed in Section 7.2.1. These equations are E7.12a:

$$\nabla (r_i \rho_i \mathbf{V}_i y_i^f) - \nabla (r_i \Gamma \nabla y_i^f) = (f_{ji} + [\![m_{ji}]\!])(y_j^f - y_i^f) - r_i R_i' \qquad \text{[E7.12a].}$$

Since equations must still be solved for the droplet-group mass-fraction (E5.5), the mass fraction of vapour can now be calculated by substracting the amount of fuel in liquid state from the total amount of fuel:

$$y_i^v = y_i^f - y_i^l \qquad \text{[E7.21].}$$

In E7.21, y_i^l, the mass fraction of fuel in liquid state, can be found from the droplet-group mass-fractions m_i^k as in the evaporating spray (E5.7).

It should be noted that the SCRS2 formulation requires the equality of the diffusion coefficients of droplets, vapour and other species.

7.3.2 The quasi-conserved-scalar equation

The quasi-conserved scalar is taken, for each phase i, as (Section 7.2.1):

$$f_i = y_i^f + y_i^p /(1+s) \qquad \text{[E7.22]},$$

which can be regarded as the total mass-fraction of fuel, whether liquid or gas, burned or unburned. The equation for f_i is:

$$\nabla (r_i \rho_i \mathbf{V}_i f_i) - \nabla (r_i \Gamma \nabla f_i) = I_{ji}(f_j - f_i) \qquad \text{[E7.23]}.$$

7.3.3 Mass fractions of oxidant and product

As shown in Section 7.2.2, y_i^o and y_i^p can be calculated in an SCRS2 from f_i and y_i^f using similar formulae to those for the SCRS. Thus:

$$y_i^o = 1 - y_i^f - (1+s)(f_i - y_i^f) \qquad \text{[E7.24]};$$

$$y_i^p = 1 - y_i^o - y_i^f \qquad \text{[E7.25]}.$$

7.3.4 Gas and droplet temperature, and droplet-vaporisation rate

Droplet vaporisation will be supposed to proceed, as in the evaporating-spray model, according to equilibrium-vaporisation laws. The droplet temperature remains constant in these circumstances, and the vaporisation rate is:

$$s_i' = \frac{\lambda_v}{C_v \rho_l} \ln \left(1 + \frac{C_v (T_i - T_d)}{L}\right) \qquad \text{[E7.26]}.$$

However, the gas temperature T_i is likely to vary significantly in the combusting spray, and the influence of these variations on the vaporisation rate cannot be neglected. The remainder of this subsection details how T_i is calculated.

To do so, enthalpy is defined using the droplet temperature as reference:-

$$h_i = \Sigma\ y_i^j\ C_j\ (T_i - T_d) + y_i^f\ H \qquad \text{[E7.27]},$$

where j indicates species.

The presence of droplets having different temperature (T_d) from that of the gas (T_i) requires additional assumptions for E7.27 to be a quasi-conserved property. Namely, the diffusion term in the equation for h_i must be

$$-\ \nabla\ (r_i \Gamma \nabla h_i),$$

with Γ being the species diffusion-coefficient. (Otherwise, h_i could be computed from a differential equation having the appropriate diffusion term.)

With that assumption, h_i can be found from the quasi-conserved property f using E7.20. And T_i, which intervines in the vaporisation rate, can be found from E7.27 as

$$T_i = \frac{h_i - y_i^f\ H}{\Sigma\ y_i^j\ C_j} + T_d \qquad \text{[E7.28]}.$$

7.3.5 Reaction rate

An Arrhenius law is considered for the reaction rate, having the form:

$$R_i' = -\ a\ y_i^o\ y_i^v\ e^{-b/T_i} \qquad \text{[E7.29]},$$

where a and b are constants.

7.3.6 Boundary conditions and other data

As in preceding chapters, a mixture of droplets and oxidant is injected through the nozzle, at a velocity of 10m/s. The mass fraction of fuel in the injected mixture is $y_2^f=y_2^l=f_2=0.45$, and this is distributed in 5 droplet-groups yielding a size distribution identical to that of the vaporising spray of Chapter 6. In the inlet mixture, the droplet temperature is supposed to be 100 ºC, and the gas temperature is 300 ºC. Only oxidant is present in the surroundings, also at a temperature of 300 ºC. The additional boundary conditions for the differential equations are summarised in table T7.1. (The boundary-condition nomenclature is that of figure F4.2.)

• ***Table T7.1: Additional boundary conditions for the combusting spray*** •

Boundary	w_1	w_2	v_1	v_2	y_1^f	y_2^f	f_1	f_2
Inlet		10.0		0.0		0.45		0.45
Inlet plane	0.0	0.0	0.0	0.0	0.0	0.0	0.0	0.0
Free stream	0.0	0.0	0.0	0.0	0.0	0.0	0.0	0.0
Axis	No flux							
Downstream	Not required since parabolic							

The numerical data of table T7.2 complement those used in the evaporating-spray model.

• ***Table T7.2: Additional numerical data*** •

s (Stoichiometric ratio)	2.6
a (in the reaction rate, E7.29)	10^8 Kg/s•m^3
b (in the reaction rate, E7.29)	10,000 K
H (Heat of reaction)	$6.2 \cdot 10^6$ J/Kg
M_o (Molecular weight of oxidant)	32
M_v (Molecular weight of vapour)	12
M_p (Molecular weight of products)	44

7.4 Checking the SCRS2 formulation

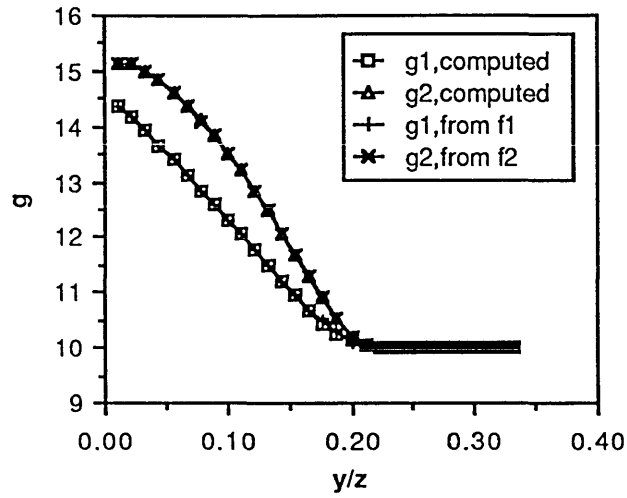
The correctness of the ideas put forward in Section 7.2 about the applicability of the SCRS scheme to two-phase (miscible) flows can be easily checked by setting up an equation for a dummy quasi-conserved variable (say g). The computed results of g_1 and g_2 can be then compared with those obtained from the passive scalar f_i through the SCRS2 relationship (E7.20).

Thus, if :

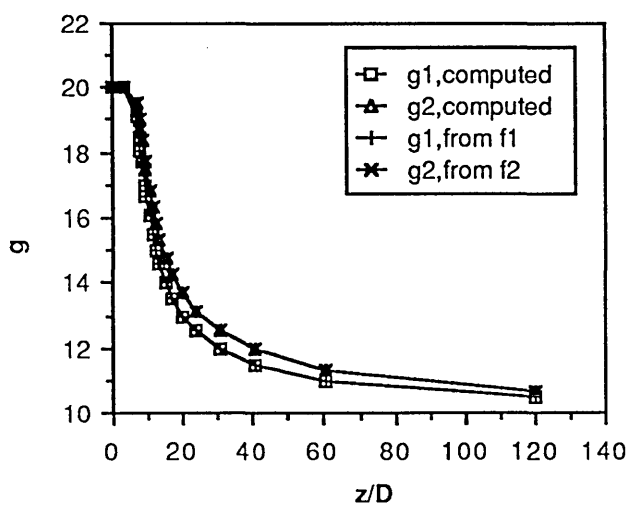
- the values of f_2 and g_2 in the stream A (figure F7.1) are f_{2A}=0.45 and g_{2A}=20.0;
- the values of f_1 and f_2 in the stream B are f_B=0.0;
- and the values of g_1 and g_2 in the stream B are g_B=10.0,

then g_i can be related to f_i by:

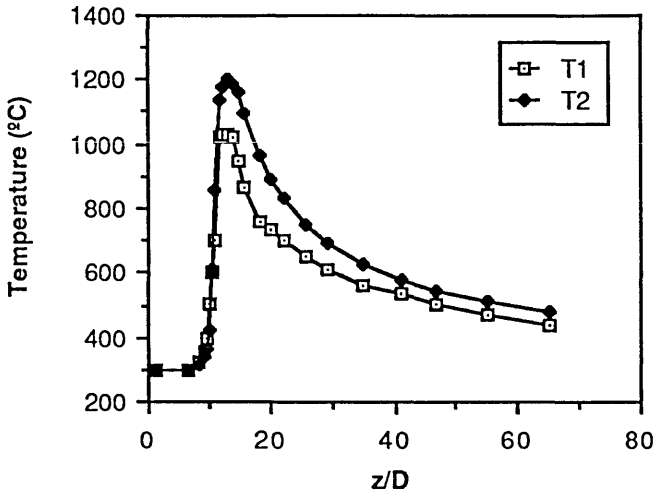
$$g_i = \frac{g_{2A}-g_B}{f_{2A}-f_B} f_i + g_B = (10/0.45)\ f_i + 10 \qquad \text{[E7.30].}$$



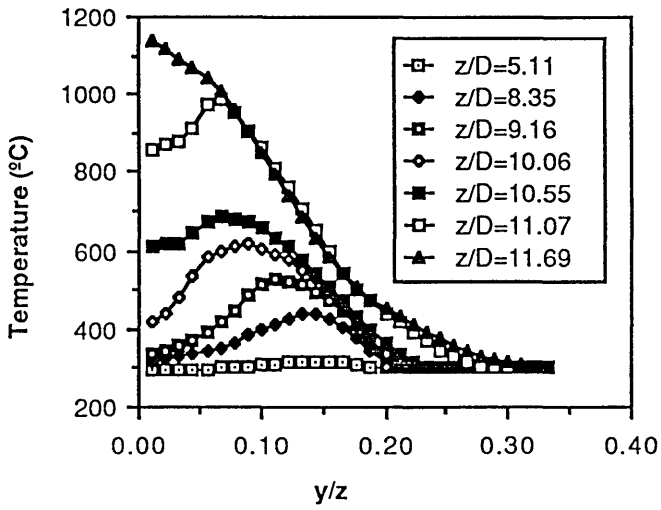
• *Figure F7.2: SCRS2 check -- Radial profiles* •



• *Figure F7.3: SCRS2 check -- Axial profiles* •



• *Figure F7.4: Axial evolution of temperatures* •



• *Figure F7.5: Radial profiles of temperature (T_2)* •

These arrangements were implemented in the model described in the preceding section, and the results obtained are presented now. Figure F7.2 shows the radial evolution of g_1 and g_2, both the value computed from their differential equations and the value obtained from E7.30. The corresponding axial evolution is that of figure F7.3. The difference between both sets of values was found to be always under 0.001%.

7.5 Results: presentation and discussion

This section analyses the results obtained by applying the model proposed above to the combusting spray, focusing particularly on the implications of the use of a two-fluid model.

(a) Axial profiles of temperature

Figure F7.4 represents the axial evolution of the fluid temperature at the centreline.

The steep gradient in the profile indicates the break-out of the reaction. The fuel is injected in the computational domain as a liquid, and has therefore to evaporate before this break-out takes place. Once it starts, the heat released promotes, by increasing the gas temperature, the vaporisation of the droplets, and therefore the reaction and heat release. This feedback process is the reason behind the sudden break-out.

The higher temperature of the second (out-moving) fluid is an interesting consequence of the ability of two-fluid models to represent the fragmentariness of the flow. It will be recalled that, in Chapter 6, it was shown how the two-fluid model yielded a higher concentration of liquid in the out-moving fluid. The higher

concentration of fuel in the combustion spray brings about a higher temperature when the reaction breaks out, and this is what figure F7.4 shows.

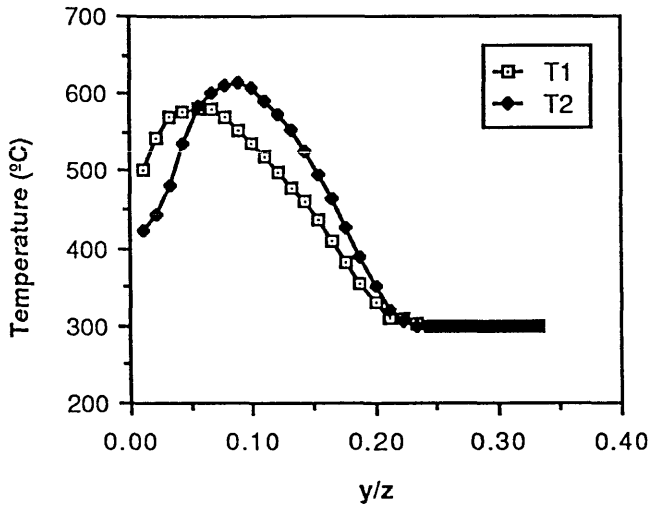
(b) Radial profiles of temperature

The lightoff process can also be traced in the radial profiles of temperature (see figure F7.5).

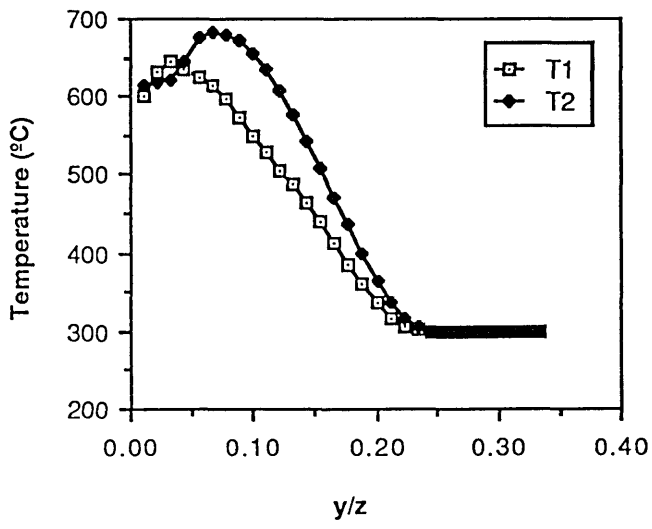
At z/D=5.11, the reaction rate is still low, and the temperature is close to 300 ºC (which is the temperature of both the inlet and the surrounding air). At z/D=8.35, the temperature starts to rise in the middle zone of the spray. The temperature in that area increases rapidly as the spray evolves downstream. The reason why the reaction breaks out in the central region is clear: owing to the cooling caused by droplet vaporisation, the temperature **increases** towards the edge of the spray, while the fuel concentration **decreases** in that direction. Therefore, the product of both (which is a factor in the reaction-rate expression, E7.29) is maximum in the middle.

As the sprays evolves downstream, the reaction peak moves towards the spray axis, as a consequence of the higher concentrations of fuel in that area.

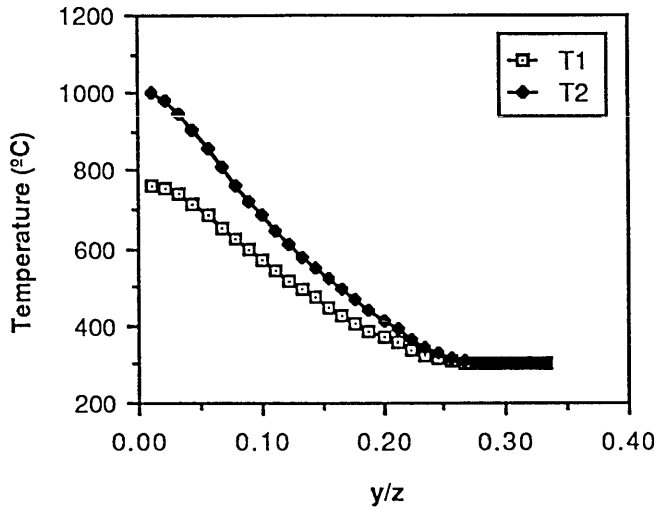
A comparison of the radial profiles of temperature of both fluids is provided in figures F7.6 to F7.8. Figure F7.6 (z/D=10.05) shows how the fluid-1 parcels have a higher temperature in a region close to the axis. This is due to the reaction rate being slower for fluid 2, which, because of its higher liquid content, was cooler than fluid 1. Figure F7.7 (z/D=10.55) shows how fluid 2 is catching up with fluid 1 as the reaction proceeds; and figure F7.8 (z/D=17.4) indicates that, because of their higher fuel content, fluid-2 fragments become hotter when the reaction is fully developed.



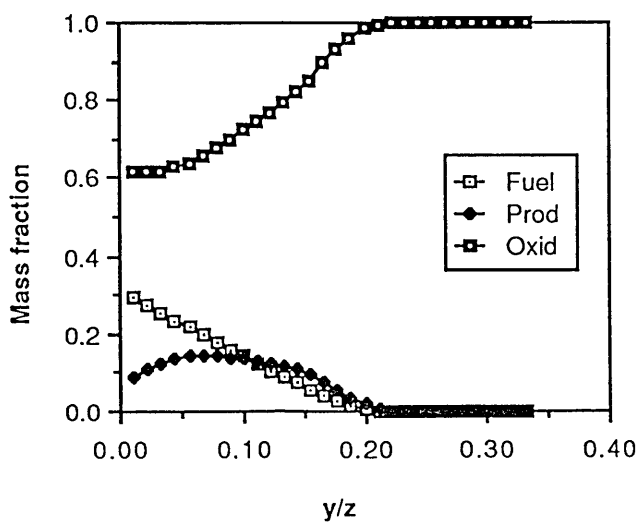
• *Figure F7.6: Radial profiles of temperature (z/D=10.05)* •



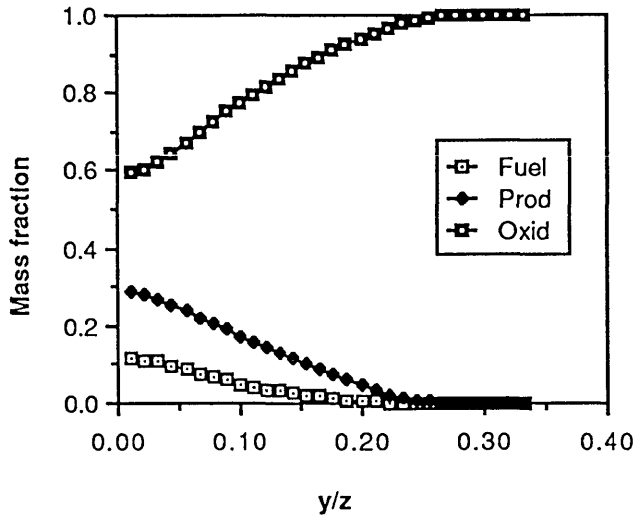
• *Figure F7.7: Radial profiles of temperature (z/D=10.55)* •



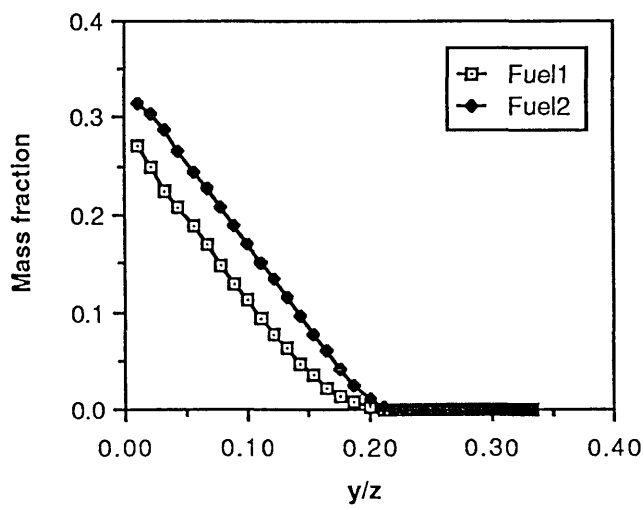
• *Figure F7.8: Radial profiles of temperature • (z/D=17.40)*



• *Figure F7.9: Radial profiles of average mixture-fraction • (z/D=10.05)*



• *Figure F7.10: Radial profiles of average mixture-fraction • (z/D=17.40)*



• *Figure F7.11: Radial profiles of fuel mass-fraction • (z/D=10.05)*

(c) Radial profiles of mixture fraction

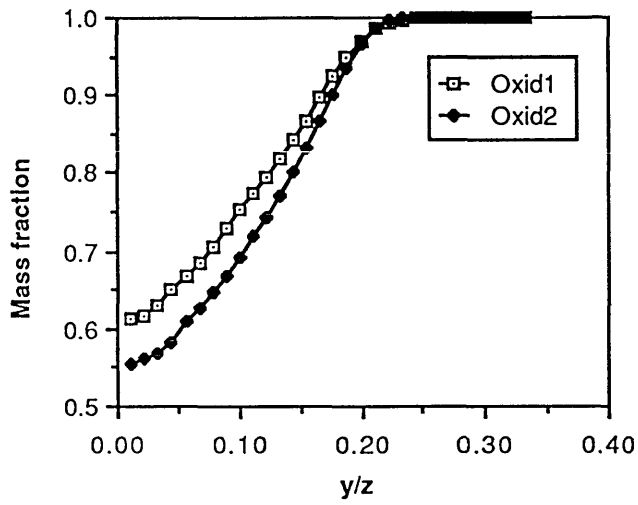
Figures F7.9 and F7.10 display two typical radial profiles of mixture fractions. F7.9, with the average concentrations at z/D=10.05, shows how the concentration of oxidant increases, as it should, towards the edge of the spray (the surrounding gas is assumed to be 100% oxidant as a boundary condition). The average concentration of products exhibits a maximum in the central region, which is where the highest rate of combustion is to be found (see figure F7.6).

A downstream profile is shown in figure F7.10 (z/D=17.4). The maximum chemical activity is now at the centreline (F7.8), and the concentration of products is maximum there.

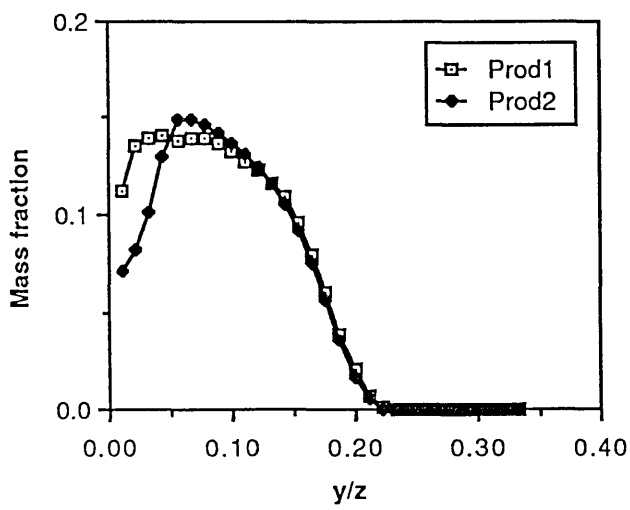
Figure F7.11 represents the radial profile of fuel concentration at z/D=10.05. It confirms the higher concentration in fluid 2, a result which was also found and discussed in the non-combusting sprays of Chapter 6, and which has been assumed in the preceding explanations.

Figure F7.12 conveys similar information for the mass fractions of oxidant. The concentration is higher for fluid 1, since the mass fraction of fuel is smaller for that fluid.

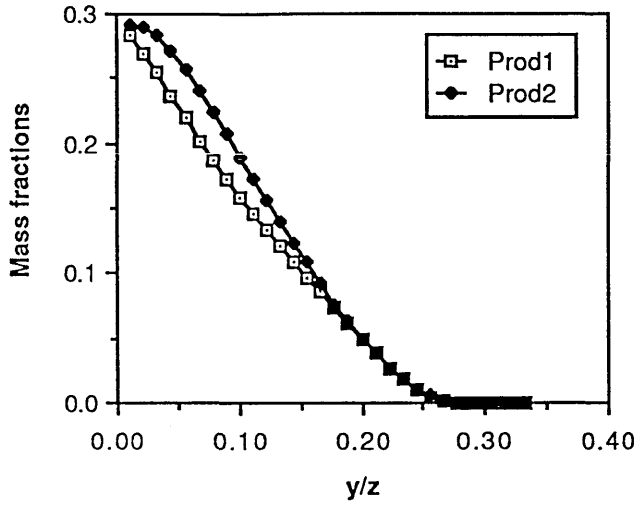
Figures F7.13 and F.14 represent two radial profiles of product concentration. The former shows how during the development of the lightoff the product concentration is higher where the temperature is higher (F7.6). Figure F7.14 represents the same profile when the lightoff is fully developed, and shows how the higher concentration of fuel in fluid 2 has now been transformed in a higher concentration of product.



• *Figure F7.12: Radial profiles of oxidant mass-fraction • (z/D=10.55)*



• *Figure F7.13: Radial profiles of product mass-fraction • (z/D=10.55)*



• *Figure F7.14: Radial profiles of product mass-fraction • (z/D=17.40)*

7.6 Closure

The chapter now closing has proposed a two-fluid model of spray combustion. The model has been built by supplementing the spray model of Chapters 5 and 6 with an extension of the SCRS (or Shvab-Zeldovich) formulation for combusting systems. The need for the extension (here called SCRS2) has been shown to arise from the non-homogeneity of the equation for the passive scalars in a two-fluid model, which is in turn brought about by the interphase-transport terms. The conditions in which the extension can be used have been set out, and it has been shown that they are fulfilled by the kind of two-fluid models proposed in this work.

The correctness of the SCRS2 scheme has been checked through a test computation in which a variable was both computed from differential equations and calculated through the scheme. The difference between both set of values was found to be below 0.001%.

The model shows how the different liquid content of the fragments of both fluids (first shown in Chapter 6) is transformed, when the reaction breaks out, in a difference in temperature. Hotter fluid-2 fragments intermingle then with cooler fluid-1 fragments, in what can be regarded as a hotter/cooler kind of intermittency.

Chapter 8

Summary

8.1 Purpose and layout of this chapter

This chapter closes the present work with:-

(a) A survey of the main ideas put forward in this thesis, and of its main achievements;

(b) Some proposals for the continuation of the work.

The first item is the subject tackled in the next section (8.1.2), while the second is addressed in Section 8.3.

In this chapter, cross-references to sections, equations and figures in preceding chapters will be superscripted and enclosed in a box (such as [S8.1]).

8.2 Summary of achievements

8.2.1 The two-fluid model

This thesis has further developed a new kind of turbulence models, the so-called "two-fluid models"[S2.4] of Spalding (1984b). It has been shown [S2.3.1] that these re-formulate many of Prandtl's original ideas on turbulence, such as the fragmentariness of turbulence (the existence of "parcels of fluid") and the role, in shear flows, of the cross-stream velocity in turbulence mixing.

The kind of model employed represents turbulence, in single-phase flows, as the interaction of structures (here called fragments) belonging to two different fluids which fill up the physical space. This interaction results [S2..4] in the exchange of mass, momentum and other properties through the fragment boundaries. The present version includes a source of cross-stream momentum [S2.6.3] which acts, in the presence of shear, as the driving force of $|v_1-v_2|$ (the "mixing" transverse velocity of Prandtl's theory [S2.3.1]).

8.2.2 Application to the single-phase, axi-symmetrical jet

The two-fluid model has been firstly applied to the prediction of single-phase, axi-symmetrical, jets [S4.3]. As a new feature, the fragment size has been modelled through differential equations [S4.4] which account for fragment growth by entrainment and agglomeration, and fragment break-up by shear.

The results provided by the model have been compared with documented experiments [S4.6], and the agreement has been found to be satisfactory. Furthermore, the results have been shown to be, as they should, self-similar, grid-independent and valid over a wide range of inlet conditions [S4.6.3].

The results have been further examined [S4.6.2] to show the implications of the two-fluid idea. Explanations have been provided for the behaviour and the role in the model of:-

(a) The cross-stream-velocity difference;

(b) The turbulent viscosity;

(c) The shear source;

(d) The departures of the volume fraction from its equilibrium value ($r_1=r_2=0.5$).

A parametric study has been also carried out [S.4.6.4] to find the sensibility of the model to changes in the model constants.

The axial evolution of the fragment size [F4.10] has yielded a most interesting result: when differential equations are used for its modelling, the fragment size turns out to be, after a development region, proportional to Prandtl's mixing-length. This agrees with Prandtl's intuition of "the magnitude of l ... [being] of the same order of magnitude as the diameter of the fluid fragments themselves" [S2.3.1].

8.2.3 Application to cold and evaporating sprays

The same two-fluid model has been then applied to the prediction of two-phase flows, namely cold and evaporating sprays [S5.3]. To achieve this, the model has been conveniently extended to accommodate a droplet size-distribution within each fluid [S5.3.2]. Equations have been proposed for the group mass-fraction [E5.5] and, in the evaporating spray, for the liquid-vapour mass-fraction [E5.7].

Apart from these additions, the remainder of the model has not been changed in the shift from single to two-phase simulations. (This includes the model constants [T4.3], the interphase-exchange terms [T4.1] and the fragment-size model [E4.9].)

The model results have been compared [S6.3&6.4] both with experimental data and with the results provided by two alternative models (one Eulerian - LHF- and other other Lagrangian - SSF). It may be concluded that the model results are, in general, superior to those yielded by the LHF model, and comparable to those provided by the SSF model.

The study has also shown [S6.6.3&6.6.4] that the initial increase in the axial evolution of the SMD, which is documented in the experimental references, is not exclusively the effect of the turbulent diffusion of small droplets: the D^2-law for

the vaporisation process implies a re-shaping F6.29-F6.32 of the droplet distribution which results in this initial increase.

A much sought-for result is that concerning the density difference between the fragments of both fluids S6.6.6: it shows that the two-fluid formulation yields, as a natural outcome, the "richer-leaner" fragmentariness of turbulent mixing.

8.2.4 Combustion studies

The present work has also tackled the task of incorporating a combustion sub-model into the two-fluid model, and of working out the consequences of the two-fluid idea in this situation.

The formulation of the submodel has entailed the extension, for two-phase (miscible) flows, of the Shvab-Zeldovich (or SCRS) scheme S7.3.2. The extension, called here SCRS2, is needed because, owing to the interphase-exchange terms, the "conserved scalars" of the single-phase formulation S7.3.1 are no longer conserved when each fluid is considered separately.

The conditions in which the extension (SCRS2) may be used have been related to the existence of a compatible set of boundary conditions, represented by a system of algebraic equations E7.18x; and the validity of the new approach has been shown in a test computation.

The model results, purely "demonstrative" in intention, show how the "richer-leaner" fragmentariness of the non-combusting spray results, when combustion breaks up, in a "hotter-colder" fragmentariness S7.5.

8.3 Suggestions for future work

As it is usually the case, the present thesis must be regarded only as a step forward in the study of the two-fluid character of turbulence; and, as such, it starts from existing works and will prompt, hopefully, new ideas resulting in its further development. The link to the past was provided in Chapter 2; and this section suggests some directions in which this further development could take place.

The section has been divided in two parts; the first deals with "immediate" development, and the second with "long-term" suggestions involving "serious surgery" in the model.

8.3.1 Immediate development

1. **Model testing in other configurations.** The present model was developed for, and applied to, single-phase jets and sprays. The model does not, however, pose any intrinsic limitation to its application to other single-phase flows (eg plane and wall jets) and two-phase, dispersed flows (eg particle-laden jets). A great deal of the merit (and the usefulness) of a turbulence model is related to its ability to represent different configurations with minimal (if any) changes.

   Some work in this direction has been carried out in the past with two-fluid models [S2.7]; its continuation with the present model (and, particularly, with the fragment-size submodel) has to be, necessarily, a priority.

2. **Turbulent-diffusion laws for the droplets.** In the present model, turbulent diffusion has been considered to have the same effect in small and large droplets [T5.1] (however, this hypothesis has been removed in some exploratory runs, and the consequences of its removal have been shown

S6.6.3). The modification of the diffusion laws to account for droplet inertia (ie droplet size) is worth to be investigated. (It should be nevertheless noted that the combustion scheme, SCRS2, requires that all droplet groups and vapour share a common diffusion coefficient.)

3. **Vaporisation rate.** The present **evaporating-spray model** features a "DD'=constant" law E5.15, which has provided results of a reasonable accuracy. In the **combusting spray,** the gas temperature has been allowed to modify the vaporisation rate E7.26, still within a D^2-law.

   The two-fluid model, however, places no restriction on the choice of vaporisation-rate law, and more sophisticated laws can be proposed to account for:-

   (a) The effect of the interphase slip ($|V_1-V_2|$) in enhancing the vaporisation process;

   (b) The reduction of the vaporisation rate by the saturation of the air with liquid vapour (ie, the inclusion of y_i^v in the formulation).

   Although the present model has been developed under the hypothesis that s' does not depend on s (the droplet size) S5.3.2f, laws other than the D^2 type can be used by either

   (a) re-defining the droplet size (s) so that s' continues to be independent from s; or

   (b) modifying the source/sink terms in the droplet-group equations Sa.2&Sa.3.

4. **Enthalpy modelling.** The use of more sophisticated laws for droplet vaporisation may require the modelling of gas (and possibly also droplet)

temperature. Some work along these lines has been done for the combusting spray [S7.3.4], but this is liable to further generalisation.

5. **Droplet coalescence and break-up.** Both effects can be incorporated into the model as additional source/sink terms in the droplet-group equations [E5.5]. It must be pointed out that, in the present model, the collision of droplets belonging to the same fluid is prevented by the no-slip hypothesis, which implies that such droplets have the same velocity; however droplet-to-droplet effects **can** be considered when fragments of different fluids (which **do** possess a relative velocity) collide.

8.3.2 Long-term development

The main limitation of the present model is, undoubtedly, the no-slip assumption. While slip might not be the dominant effect in sprays in the open if the droplet size is not large, there are many practical circumstances in which the relative velocity **is** significant. (Eg, the injection of the spray into swirling air in Diesel-engine cylinders.)

An approach for the introduction of a droplet velocity is the development of "four-fluid" models, in which

- Two fluids represent, as in the present model, the continuous phase;
- Each "continuous-phase fluid" has an associated "disperse-phase fluid", with a velocity different to that of the continuous phase in the fluid.

The interphase transfer between liquid and gas "fluids" would, in these circumstances, represent a real change of phase; and the interphase transfer

between droplet phases and between gas phases would retain its current meaning of fragment-to-fragment exchange.

This four-fluid model would, additionally, facilitate a more flexible modelling of droplet and gas temperature, something which is probably crucial in combusting-spray modelling.

8.4 Closure

Finally, it will not be contended that the kind of model proposed in this thesis is, in any way, superior to existing models. It is however hoped that the novel approach to the modelling of turbulence will be found to provide an alternative formulation in which the salient features of turbulence (fragmentariness, intermittency) can be suitably accommodated, and their effects predicted.

It is also hoped that the ideas proposed in this work, and their consequences, will stimulate further research.

Appendix A

The size-distribution equations

a.1 Introduction

A differential equation for m_i was proposed in Chapter 5. $m_i(x, y, z, t, s)\,ds$ is the **mass fraction** of droplets whose sizes are between s and s+ds per unit volume of phase i and per unit increment of s, and it is linked to the **number** of droplets fulfilling these conditions by a simple relationship (E5.2).

The equation for m_i, E5.3, brought a new **independent** variable into the mathematical model (namely s, the droplet size). A way around this new, undesired dimension was proposed as consisting in the break-up of the s-domain into a finite number (say n_s) of intervals $[s_1, s_2]$, $[s_2, s_3]$, ..., $[s_{ns}, s_{ns+1}]$, and integrating the equation for m_i in each interval.

The result was announced to be n_s differential equations (with s removed as independent variable) for the mass fraction of droplets belonging to a size group k, m_i^k. Only the final form of these equations was provided in Chapter 5; the full derivation is the subject of this appendix.

The starting point is therefore E5.2, which runs:

$$\frac{\partial(r_i\rho_i m_i)}{\partial t} + \nabla(r_i\rho_i m_i \mathbf{V}_i) - \nabla(r_i\Gamma_{m\,i}\nabla m_i) = -\,M(s)\,\frac{\partial}{\partial s}\left(\frac{r_i\rho_i m_i s'}{M(s)}\right) +$$

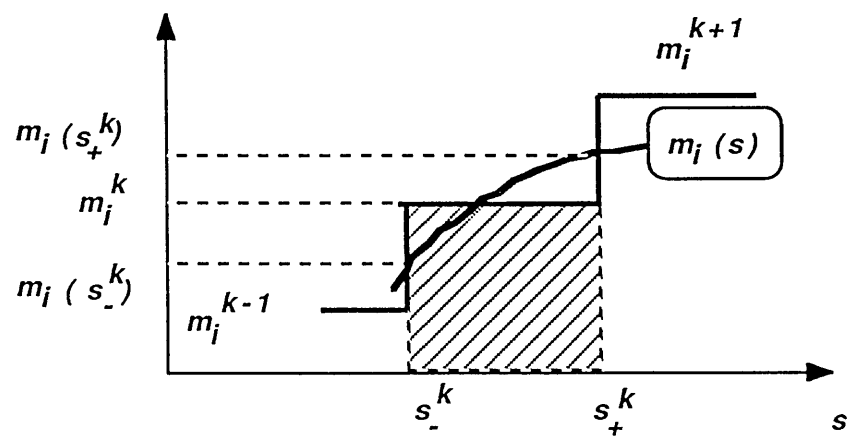
$$+\,(f_{ji}^{*} + [\![m_{ji}^{*}]\!])\,(\rho_j m_j - \rho_i m_i) \qquad \text{[Ea.1]},$$

where the factor M(s) appearing on the LHS of E5.3 has been transferred to the RHS.

A slightly different approach will be used depending on whether the interval to be treated is or not the first one (k=1), which starts at s=0; the case k≠1 will be dealt with first.

a.2 The transport equation for m_i^k, k≠1

Ea.1 will be integrated over the interval $[s_k, s_{k+1}]$, where k≠1 (figure Fa.1). For sake of simplicity, the interval limits will be referred to as s_- and s_+.



• *Figure Fa.1: The k^{th} interval and m_i^k* •

On the LHS of Ea.1, the derivative and integral operators can be interchanged, giving, for the transient term:

$$\int_{s_-}^{s_+} \frac{\partial (r_i \rho_i m_i)}{\partial t} ds = \frac{\partial}{\partial t} (r_i \rho_i \int_{s_-}^{s_+} m_i \, ds) = (s_+ - s_-) \frac{\partial (r_i \rho_i m_i^k)}{\partial t} \qquad \text{[Ea.2]},$$

where the definition of m_i^k (E5.4) has been used.

Since the procedure is similar for the convective and diffusive terms, the manipulation of these will be omitted here; and the handling of the second term of the RHS of Ea.1 (interphase exchange) is also straightforward, since the rates f_{ji}^* and m_{ji}^* are not a function of s.

This leaves only the first term on the RHS of Ea.1 to be treated; for this term, integration yields:

$$\int_{s_-}^{s_+} -M(s) \frac{\partial}{\partial t} \left(\frac{r_i \rho_i m_i s'}{M(s)} \right) ds = -[r_i \rho_i m_i s']_{s_-}^{s_+} + \int_{s_-}^{s_+} \left(\frac{r_i \rho_i m_i s'}{M(s)} \right) dM \qquad \text{[Ea.3]}.$$

Assuming that:

i• s' does not depend on s (which is true under D^2-law assumptions);

ii• M(s) (the mass of a droplet of size s) is proportional to s^ξ (eg, $\xi=3/2$ if $s=D^2$);

then the RHS of Ea.3 can be written as:

$$-r_i \rho_i s' \left[(m_i^+ - m_i^-) - \xi \int_{s_-}^{s_+} \left(\frac{m_i}{s} \right) ds \right] \qquad \text{[Ea.4]},$$

where $m_i^+ = m_i(s_+)$ and $m_i^- = m_i(s_-)$ are the values of the m-function at the interval limits.

The choice of m_i^+ and m_i^-, and the approximation of the integral term are now the two final issues to be tackled.

i. The choice of m_i^- and m_i^+

m_i^- and m_i^+ are the values of the m-function at the limits of the s-interval. However, the actual m(s)-profile has been lost during the discretisation, and now only the top-hat profile of m_i^k's remains (only at very particular locations in the domain, such as the inlet boundary, the original m(s)-profile is known and can be made available).

From figure Fa.1, the choice

$$m_i^- = m_i^{k-1};$$
$$m_i^+ = m_i^{k+1}$$

seems an obvious one.

However, if $m_i^- = m_i^{k-1}$ is chosen and $s'<0$ (ie vaporisation is considered), then m_i^{k-1} appears in the source term of the m_i^k-equation (of which Ea.4 is a source term). Since the droplets are vaporising, any influence of the number of droplets in group k (ie m_i^k) of groups of smaller size (ie m_i^{k-1}) is undeniably unrealistic. A similar situation occurs if $s'>0$ (condensation) and $m_i^+ = m_i^{k+1}$.

The practice recommended by Spalding (1985) will be adopted here; namely, if $s'<0$, then $m_i^+ = m_i^{k+1}$ but $m_i^- = m_i^k$. This can be regarded as being analogous to the upwind scheme in the formulation of the convective term of the finite-difference equations.

ii. The integral term

As for the integral term in Ea.4, the following approximation will be applied:

$$\int_{s_-}^{s_+} \left(\frac{m_i}{s} \right) ds = m_i^k \ln \left(\frac{s_+}{s_-} \right) \qquad \text{[Ea.5].}$$

Finally, gathering together all these results (Ea.2, Ea.3, Ea.4), equation Ea.1 becomes:-

$$\frac{\partial (r_i \rho_i m_i^k)}{\partial t} + \nabla (r_i \rho_i m_i^k \mathbf{V}_i) - \nabla (r_i \Gamma_{m_{ik}} \nabla m_i^k) =$$

$$= r_i \rho_i |s'| \frac{1}{s_+ - s_-} \{ m_i^{k+1} - [1 + \xi \ln (\frac{s_+}{s_-})] \, m_i^k \} +$$

$$+ (f_{ji} + [\![m_{ji}]\!]) \, (m_j^k - m_i^k) \qquad \text{[Ea.6],}$$

which is the transport equation for m_i^k when $k \neq 1$.

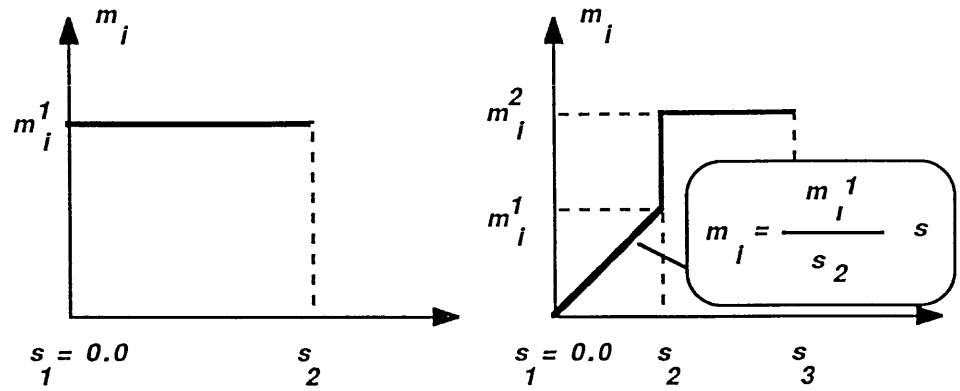
(In the interphase-exchange term, the factor $(\rho_j m_j^k - \rho_i m_i^k)$ has been approximated by $\rho(m_j^k - m_i^k)$, where $\rho = r_1\rho_1 + r_2\rho_2$ is the average density. This approximation allows the use of the conventional exchange rates f_{ji} and m_{ji} as given by E4.6 and E4.7, since $f_{ji} = \rho \, f_{ji}^*$ and likewise for m_{ji}^*).

a.3 Transport equation for m_i^1

a.3.1 The problem

When k=1, the s-interval is likely to start at $s_-=0$; and then the logarithm in Ea.5 is not finite, and any other approximation of the integral term would be a coarse one.

This problem might arise from the fact that a top-hat profile for m_i^1 would physically imply the existence of a finite number of droplets of size 0, as shown in figure Fa.2a.



(a) Flat profile *(b) Linear profile*

• ***Figure Fa.2: Top-hat and linear profiles for the first interval*** •

a.3.2 The solution

A linear profile for this interval (as shown in figure Fa.2b) would both avoid this hindrance and provide a closer resemblance of the discretised profile to experimental size-distributions.

Thus, the equation for the first interval will now be written in terms of m_i^1, which is the value at $s=s_2$ rather than the average of m over the interval.

o Ea.2 for the first interval is then expressed, using $m_i=m_i^1 s/s_2$, as:

$$\int_{s_-}^{s_+} \frac{\partial(r_i\rho_i m_i)}{\partial t} ds = \frac{\partial}{\partial t}(r_i\rho_i \int_0^{s_2} \frac{m_i^1 s}{s_2} ds) = \frac{s_2}{2} \frac{\partial(r_i\rho_i m_i^1)}{\partial t} \qquad \text{[Ea.7]},$$

and similarly for the diffusive and convective terms.

o In Ea.4, the "upwind" practice of Section a.2.i implies, for s'<0 :

$$m_i^+ = m_i^2 \text{ and } m_i^- = 0;$$

and the integral term of Ea.7 finally becomes:

$$\int_0^{s_2} \frac{m_i}{s} ds = \int_0^{s_2} \frac{m_i^1}{s_2} ds = m_i^1 \qquad \text{[Ea.8].}$$

When all these results are collected, the final equation for m_i^1 is:

$$\frac{\partial (r_i \rho_i m_i^1)}{\partial t} + \nabla (r_i \rho_i m_i^1 \mathbf{V}_i) - \nabla (r_i \Gamma_{m_{i1}} \nabla m_i^1) =$$

$$= r_i \rho_i |s'| \frac{1}{s_2} \{m_i^2 - \xi \; m_i^1]\} + (f_{ji} + [\![m_{ji}]\!]) \; (m_j^1 - m_i^1) \qquad \text{[Ea.9].}$$

(The comments made in Section a.2 for the interphase terms in Ea.6 also apply here.)

Appendix B

The complete equations

b.1 Single-phase jet

Closure

$$r_1 + r_2 = 1$$

Volume fraction

$$\nabla(\rho_i r_i \mathbf{V}_i) = m_{ji}$$

v-momentum

$$\nabla(\rho_i r_i \mathbf{V}_i v_i) - \nabla(r_i \mu \nabla v_i) = (f_{ji} + [\![m_{ji}]\!])(v_j - v_i) - r_i \frac{\partial p}{\partial y} + (-1)^i S_v$$

w-momentum

$$\nabla(\rho_i r_i \mathbf{V}_i w_i) - \nabla(r_i \mu \nabla w_i) = (f_{ji} + [\![m_{ji}]\!])(w_j - w_i) - r_i \frac{\partial p}{\partial z}$$

Phase-fragment size (model b only)

$$\frac{D l_i}{Dt} = C_a |\mathbf{V}_1 - \mathbf{V}_2| - C_b l_i \left| \frac{\partial w_i}{\partial y} \right|$$

Fragment size

$l = 0.01794 * z$ (Model **a** only) $\qquad l = \min(l_1, l_2)$ (Model **b** only)

Turbulent viscosity

$$\mu_t = C_\mu \rho r_1 r_2 |v_1 - v_2| l$$

Interphase mass-transfer

$$m_{ji} = C_m \rho r_1 r_2 (0.5 - r_i) |\mathbf{V}_1 - \mathbf{V}_2| / l$$

Interphase friction

$$f_{ji} = C_f \rho r_1 r_2 |\mathbf{V}_1 - \mathbf{V}_2| / l$$

Shear source

$$S_v = C_v \frac{l_p}{l} \rho |\mathbf{V}_1 - \mathbf{V}_2| \left| \frac{\partial w}{\partial y} \right|$$

Density

$$\rho_1 = \rho_2 = \rho = 1$$

b.2 Non-evaporating spray

Closure

$$r_1 + r_2 = 1$$

Volume fraction

$$\nabla(\rho_i r_i V_i) = m_{ji}$$

v-momentum

$$\nabla(\rho_i r_i V_i v_i) - \nabla(r_i \mu \nabla v_i) = (f_{ji} + [\![m_{ji}]\!])(v_j - v_i) - r_i \frac{\partial p}{\partial y} + (-1)^i S_v$$

w-momentum

$$\nabla(\rho_i r_i V_i w_i) - \nabla(r_i \mu \nabla w_i) = (f_{ji} + [\![m_{ji}]\!])(w_j - w_i) - r_i \frac{\partial p}{\partial z} + r_i g (\rho_i - \rho_g)$$

Phase-fragment size

$$\frac{D l_i}{Dt} = C_a |V_1 - V_2| - C_b l_i \left| \frac{\partial w_i}{\partial y} \right|$$

Droplet-group mass-fraction

$$\nabla(r_i \rho_i m_i^k V_i) - \nabla(r_i \Gamma_{m_{ik}} \nabla m_i^k) = (f_{ji} + [\![m_{ji}]\!])(m_j^k - m_i^k)$$

Liquid mass-fraction

$$y_i^l = \frac{s_2 m_i^1}{2} + \sum_{k=2} m_i^k (s_+ - s_-)$$

Gas mass-fraction

$$y_i^g = 1 - y_i^l$$

Fragment size

$$l = \min(l_1, l_2)$$

Turbulent viscosity

$$\mu_t = C_\mu \rho r_1 r_2 |v_1 - v_2| l$$

Turbulent diffusion of droplets

$$\Gamma_{m_{ik}} = C_{m_{ik}} \rho r_1 r_2 |v_1 - v_1| l$$

Interphase mass-transfer

$$m_{ji} = C_m \rho r_1 r_2 (0.5 - r_i) |V_1 - V_2| / l$$

Interphase friction

$$f_{ji} = C_f \rho r_1 r_2 |V_1 - V_2| / l$$

Shear source

$$S_v = C_v \frac{l_p}{l} \rho |V_1 - V_2| \left| \frac{\partial w}{\partial y} \right|$$

Phase density

$$\frac{1}{\rho_i} = \frac{y_i^l}{\rho_l} + \frac{y_i^g}{\rho_g}$$

Average density

$$\rho = r_1 \rho_1 + r_2 \rho_2$$

b.3 Evaporating spray

Closure

$$r_1 + r_2 = 1$$

Volume fraction

$$\nabla(\rho_i r_i \mathbf{V}_i) = m_{ji}$$

v-momentum

$$\nabla(\rho_i r_i \mathbf{V}_i v_i) - \nabla(r_i \mu \nabla v_i) = (f_{ji} + [\![m_{ji}]\!])(v_j - v_i) - r_i \frac{\partial p}{\partial y} + (-1)^i S_v$$

w-momentum

$$\nabla(\rho_i r_i \mathbf{V}_i w_i) - \nabla(r_i \mu \nabla w_i) = (f_{ji} + [\![m_{ji}]\!])(w_j - w_i) - r_i \frac{\partial p}{\partial z} + r_i g (\rho_i - \rho_g)$$

Phase-fragment size

$$\frac{D l_i}{Dt} = C_a |V_1 - V_2| - C_b l_i \left| \frac{\partial w_i}{\partial y} \right|$$

Droplet-group mass-fraction

$$\nabla(r_i \rho_i m_i^k \mathbf{V}_i) - \nabla(r_i \Gamma_{m_{ik}} \nabla m_i^k) = \Pi_i^k + (f_{ji} + [\![m_{ji}]\!])(m_j^k - m_i^k)$$

$$\text{with } \Pi_i^k = \begin{cases} r_i \rho_i |s'| \frac{1}{s_2} [m_i^2 - \xi m_i^1] & \text{if } k = 1 \\ r_i \rho_i |s'| \frac{1}{s_+ - s_-} \{m_i^{k+1} - [1 + \xi \ln(\frac{s_+}{s_-})] m_i^k\} & \text{if } k > 1 \end{cases}$$

Vapour mass-fraction

$$\nabla(\rho_i r_i \mathbf{V}_i y_i^v) - \nabla(r_i \Gamma_{y_{iv}} \nabla y_i^v) = r_i \frac{3}{2} \rho_i |s'| \left[m_i^1 + \sum_{k=2} m_i^k \ln\left(\frac{s_+}{s_-}\right) \right] + (f_{ji} + [\![m_{ji}]\!])(y_j^v - y_i^v)$$

Liquid mass-fraction

$$y_i^l = \frac{s_2 m_i^1}{2} + \sum_{k=2} m_i^k (s_+ - s_-)$$

Air mass-fraction

$$y_i^g = 1 - y_i^l - y_i^v$$

Turbulent viscosity

$$\mu_t = C_\mu \rho r_1 r_2 |v_1 - v_2| l$$

Turbulent diffusion of droplets

$$\Gamma_{m_{ik}} = C_{m_{ik}} \rho r_1 r_2 |v_1 - v_1| l$$

Turbulent diffusion of vapour

$$\Gamma_{y_{iv}} = C_{y_{iv}} \rho r_1 r_2 |v_1 - v_2| l$$

Vaporisation rate

$$s' = \frac{\lambda_v}{C_v \rho_l} \ln \left(1 + \frac{Cp_v (T_g - T_{bp})}{L}\right)$$

Interphase mass-transfer

$$m_{ji} = C_m \rho r_1 r_2 (0.5 - r_i) |V_1 - V_2| / l$$

Interphase friction

$$f_{ji} = C_f \rho r_1 r_2 |V_1 - V_2| / l$$

Shear source

$$S_v = C_v \frac{l_p}{l} \rho |V_1 - V_2| \left| \frac{\partial w}{\partial y} \right|$$

Phase density

$$\frac{1}{\rho_i} = \frac{y_i^l}{\rho_l} + \frac{y_i^g}{\rho_g} + \frac{y_i^v}{\rho_v}$$

Average density

$$\rho = r_1 \rho_1 + r_2 \rho_2$$

b.4 Combusting spray

Closure

$$r_1 + r_2 = 1$$

Volume fraction

$$\nabla (\rho_i r_i V_i) = m_{ji}$$

v-momentum

$$\nabla (\rho_i r_i V_i v_i) - \nabla (r_i \mu \nabla v_i) = (f_{ji} + [\![m_{ji}]\!]) (v_j - v_i) - r_i \frac{\partial p}{\partial y} + (-1)^i S_v$$

w-momentum

$$\nabla(\rho_i r_i \mathbf{V}_i w_i) - \nabla(r_i \mu \nabla w_i) = (f_{ji}+[\![m_{ji}]\!])\ (w_j - w_i) - r_i \frac{\partial p}{\partial z} + r_i\, g\, (\rho_i - \rho_g)$$

Phase-fragment size

$$\frac{D l_i}{Dt} = C_a\, |\mathbf{V}_1 - \mathbf{V}_2| - C_b\, l_i\, \left| \frac{\partial w_i}{\partial y} \right|$$

Droplet-group mass-fraction

$$\nabla(r_i \rho_i m_i^k \mathbf{V}_i) - \nabla(r_i \Gamma \nabla m_i^k) = \Pi_i^k + (f_{ji}+[\![m_{ji}]\!])\ (m_j^k - m_i^k)$$

with $$\Pi_i^k = \begin{cases} r_i\, \rho_i\, |s'|\, \dfrac{1}{s_2}\, [\, m_i^2 - \xi\ m_i^1\,] & \text{if } k = 1 \\[2ex] r_i\, \rho_i\, |s'|\, \dfrac{1}{s_+ - s_-}\, \{ m_i^{k+1} - [\, 1 + \xi\, \ln(\dfrac{s_+}{s_-})\,]\ m_i^k \} & \text{if } k > 1 \end{cases}$$

Fuel mass-fraction

$$\nabla(\rho_i r_i \mathbf{V}_i y_i^f) - \nabla(r_i \Gamma \nabla y_i^f) = - r_i\, R'_i + (f_{ji}+[\![m_{ji}]\!])\ (y_j^f - y_i^f)$$

Passive scalar

Definition: $f_i = y_i^f + y_i^p / (1+s)$

Equation: $\nabla(\rho_i r_i \mathbf{V}_i f_i) - \nabla(r_i \Gamma \nabla f_i) = (f_{ji}+[\![m_{ji}]\!])\ (f_j - f_i)$

Liquid mass-fraction

$$y_i^l = \frac{s_2\, m_i^1}{2} + \sum_{k=2} m_i^k\, (s_+ - s_-)$$

Vapour mass-fraction

$$y_i^v = y_i^f - y_i^l$$

Oxidant mass-fraction

$$y_i^o = 1 - y_i^f - (1+s)(f_i - y_i^f)$$

Product mass-fraction

$$y_i^p = 1 - y_i^o - y_i^f$$

Enthalpy

$$\frac{h_i - h_{2A}}{h_B - h_{2A}} = \frac{f_i - f_{2A}}{f_B - f_{2A}}$$

Temperature

$$T_i = \frac{h_i - y_i^f\, H}{\Sigma\ y_i^j\, C_j} + T_d$$

Vaporisation rate

$$s' = \frac{\lambda_v}{C_v \rho_l} \ln\left(1 + \frac{C_v (T_i - T_d)}{L}\right)$$

Reaction rate

$$R'_i = - a\, y_i^o\, y_i^v\, e^{-b/T_i}$$

Turbulent viscosity

$$\mu_t = C_\mu\ \rho\ r_1\ r_2\ |v_1 - v_2|\ l$$

Turbulent-diffusion coefficient

$$\Gamma = C\ \rho\ r_1\ r_2\ |v_1 - v_1|\ l$$

Interphase mass-transfer

$$m_{ji} = C_m\ \rho\ r_1 r_2 (0.5 - r_i) |V_1 - V_2| / l$$

Interphase friction

$$f_{ji} = C_f\ \rho\ r_1\ r_2\ |V_1 - V_2| / l$$

Shear source

$$S_v = C_v \frac{l_p}{l} \rho\ |V_1 - V_2|\ \left|\frac{\partial w}{\partial y}\right|$$

Phase density

$$\frac{1}{\rho_i} = \frac{y_i^l}{\rho_l} + \frac{R\ T_i}{p}\left[\frac{y_i^o}{M_o} + \frac{y_i^v}{M_v} + \frac{y_i^p}{M_p}\right]$$

Average density

$$\rho = r_1\ \rho_1\ + r_2 \rho_2$$

Appendix C

Q1 files

c.1 Introduction

Problem specification in PHOENICS is effected, to a great extent, through a data file (the so-called Q1 file). Data settings in this file are written in a special "CFD language", the PIL. (PIL stands for PHOENICS Input Language.)

The reminder of this Appendix C presents the Q1 files corresponding to the four main cases presented in this thesis. These are, namely:-

- The single-phase jet (Section c.2);
- The cold spray (Section c.3);
- The evaporating spray (Section c.4); and
- The combusting spray using the SCRS2 model (Section c.5).

These files, used in conjuction with the FORTRAN coding provided in Appendix D, would enable any PHOENICS user to repeat, exactly, the calculations presented. If the reader is not, on the other hand, a PHOENICS user, then the data settings that follow will need some additional explanations to be properly understood. These explanations can be found in Rosten and Spalding (1987).

c.2 Q1 file for single-phase jet

```
TALK=F;RUN(1,3);VDU=ACW
    ************************************************************
    **  Two-fluid model of turbulence applied to 2-phase flows **
    **               Single-phase-jet calculations              **
    **                         File: S1PQ1                      **
    **    NB current settings are for Model (b) (Size eqns)     **
    **        Norberto Fueyo, CFDU, IC, London, 02.02.88        **
    ************************************************************
    *
    * ------------------------------------------------------------
    * GROUP 1. Run title and other preliminaries
    * ------------------------------------------------------------
TEXT( Two-fluid model for s/phase jet )
    *.........Variable declaration
REAL(W1IN,W2IN,DENSIN,FACTOR,R1IN,R2IN,COEFP,RESIDU)
REAL(RLXCNT,INISIZ)
INTEGER(NINLET)
    *.........Inlet conditions (self-explanatory)
W1IN=30.0;W2IN=30.0;RG(15)=W2IN
R1IN=0.0;R2IN=1.0-R1IN
INISIZ=4.5E-6
    *
    * ------------------------------------------------------------
    * GROUP 2. Transience; time-step specification
    * ------------------------------------------------------------
    * ------------------------------------------------------------
    * GROUP 3. X-direction grid specification
    * ------------------------------------------------------------
CARTES=F
    * ------------------------------------------------------------
    * GROUP 4. Y-direction grid specification
    * ------------------------------------------------------------
    *  RG(16) is the nozzle diameter
RG(16)=0.025
GRDPWR(Y,20,RG(16),1.0)
NINLET=NY/2
    *  Linear expansion: AZYV=1 for linear growth
    *                    ZWADD=YVLAST(inlet)/tg(alpha)
AZYV=1.0
ZWADD=YVLAST/0.252
    * ------------------------------------------------------------
    * GROUP 5. Z-direction grid specification
    * ------------------------------------------------------------
PARAB=T
NZ=130
    *  DZ = RG(14) * WIDTH_1%
AZDZ=GRND;RG(14)=0.20
    * ------------------------------------------------------------
    * GROUP 6. Body-fitted coordinates or grid distortion
    * ------------------------------------------------------------
    * ------------------------------------------------------------
    * GROUP 7. Variables stored, solved & named
```

```
    * ------------------------------------------------------------
    * Two-phase option activated
ONEPHS=F
    * C1: average velocity w, w = w1 r1 + w2 r2
NAME(C1)=AVEL
    * C3 & C4: Fragment size when SOLVEd
NAME(C3)=1SIZ;NAME(C4)=2SIZ
    * Multi-purpose, auxiliary storage
STORE (C2,C5)
    *
NAME(R1)=1R;NAME(R2)=2R
NAME(W1)=1W;NAME(W2)=2W
NAME(V1)=1V;NAME(V2)=2V
    *
SOLVE(P1,1R,2R,1V,2V,1W,2W)
SOLVE(1SIZ,2SIZ)
STORE(ENUT,EL1,CFIPS,CMDOT,AVEL)
    *
    * ------------------------------------------------------------
    * GROUP 8. Terms (in differential equations) & devices
    * ------------------------------------------------------------
    *
    * No interphase exchange and diffusion for sizes
TERMS(1SIZ,P,P,N,P,P,N);TERMS(2SIZ,P,P,N,P,P,N)
    * ------------------------------------------------------------
    * GROUP 9. Properties of the medium (or media)
    * ------------------------------------------------------------
    * - - - - - - - - - - RHO - - - - - - - - - - - - - - - - - -
DENSIN=1.0;RHO1=DENSIN;RHO2=DENSIN;RG(20)=DENSIN
    * - - - - - - - - - - EL - - - - - - - - - - - - - - - - - -
    * Model (a): Algebraic model for l --> EL1 = EL1B * z
EL1=GRND3;EL1B=0.01794
    * Model (b): l from differential eq --> l=min(l1, l2)
EL1=GRND
    * - - - - - - - - - - ENUT - - - - - - - - - - - - - - - - -
    * 2-fluid formula
    * ENUT = GRND4 => Two-fluid model formula supplied in GREX2
ENUT=GRND4;ENUTA=15.0
    * ------------------------------------------------------------
    * GROUP 10. Inter-phase-transfer processes and properties
    * ------------------------------------------------------------
    * - - - - - - - - - - CFIPS - - - - - - - - - - - - - - - - -
CFIPS=GRND4;CFIPA=0.0;CFIPB=1.0;CFIPD=-1.0;CFIPC=0.0375
    * - - - - - - - - - - CMDOT - - - - - - - - - - - - - - - - -
    * Symmetric mass-transfer
CMDOT=GRND1;CMDTA=10./CFIPC;CMDTB=0.5;CMDTC=0.0
    * ------------------------------------------------------------
    * GROUP 11. Initialization of variable or porosity fields
    * ------------------------------------------------------------
FIINIT(1R)=0.5;FIINIT(2R)=0.5
FIINIT(1W)=0.0;FIINIT(2W)=0.0;FIINIT(1V)=0.0;FIINIT(2V)=0.0
FIINIT(1SIZ)=INISIZ;FIINIT(2SIZ)=INISIZ
    * ------------------------------------------------------------
    * GROUP 12. Convection and diffusion adjustments
    * ------------------------------------------------------------
    * ------------------------------------------------------------
    * GROUP 13. Boundary conditions and special sources
```

```
    * ------------------------------------------------------------

              ^   y
              |                    frest
              -------------------------------
              |                               |
              | top                           |bottom
              |                               |
         --> inlet (--->)                     |
         -->   _.-._.-._.-._.-._.-._.-._.-._.-._.-._.-._.-._.-._.|  --> z

    * --- Inlet (= jet exit) -----------------------------------
    * Location
PATCH(--->,LOW,1,1,1,NINLET,1,1,1,1000)
    * Phase 2
COVAL(--->,P2,FIXFLU, DENSIN*W2IN*R2IN)
COVAL(--->,2W,ONLYMS,W2IN)
COVAL(--->,2SIZ,ONLYMS,INISIZ)
    * Phase 1
COVAL(--->,P1,FIXFLU,DENSIN*W1IN*R1IN)
COVAL(--->,1W,ONLYMS,W1IN)
COVAL(--->,1SIZ,ONLYMS,INISIZ)

   * --- Fragment size: growth and diminuition ----------------
   * Growth by entrainment and agglomeration
PATCH(E+A,VOLUME,1,NX,1,NY,1,NZ,1,1000)
COVAL(E+A,1SIZ,FIXFLU,GRND2);COVAL(E+A,2SIZ,FIXFLU,GRND2)
RG(23)=0.03
   * Diminuition by shear
PATCH(TEAR,VOLUME,1,NX,1,NY,1,NZ,1,1000)
COVAL(TEAR,1SIZ,GRND3,0.0);COVAL(TEAR,2SIZ,GRND3,0.0)
RG(24)=0.01

   * --- Shear source -----------------------------------------
PATCH(SHSO,CELL,1,NX,1,NY,15,NZ,1,1000)
COVAL(SHSO,1V,FIXFLU,GRND5);COVAL(SHSO,2V,FIXFLU,GRND5)
   * Model a
RSG10=0.250
   * Model b
RSG10=0.175
   * --- Free-stream boundary conditions ------------------
   *  Coefficient for fixed-pressure boundary-conditions
COEFP=1.0
   * --- Top
PATCH(TOP,CELL,1,1,NINLET+1,NY,1,1,1,1000)
COVAL(TOP,P1,FIXP,0.0);COVAL(TOP,P2,FIXP,0.0)
   * --- Free stream
PATCH(FREST,CELL,1,1,NY,NY,1,NZ,1,1000)
COVAL(FREST,P1,COEFP,0.0);COVAL(FREST,P2,COEFP,0.0)
    * ------------------------------------------------------------
    * GROUP 14. Downstream pressure for PARAB=.TRUE.
    * ------------------------------------------------------------
IPARAB=1
    * ------------------------------------------------------------
    * GROUP 15. Termination of sweeps
    * ------------------------------------------------------------
LITHYD=40
```

```
RESIDU=1.0E-10;RESREF(P1)=RESIDU
RESREF(1R)=RESIDU;RESREF(2R)=RESIDU
RESREF(1W)=RESIDU;RESREF(2W)=RESIDU
RESREF(1V)=RESIDU;RESREF(2V)=RESIDU
RESREF(1SIZ)=1.0E-15;RESREF(2SIZ)=1.0E-15
    * ------------------------------------------------------------
    * GROUP 16. Termination of iterations
    * ------------------------------------------------------------
    * ------------------------------------------------------------
    * GROUP 17. Under-relaxation devices
    * ------------------------------------------------------------
RLXCNT=1.0E-2
RELAX(P1,LINRLX,0.5)
RELAX(1V,FALSDT,RLXCNT);RELAX(2V,FALSDT,RLXCNT)
RELAX(1W,FALSDT,RLXCNT);RELAX(2W,FALSDT,RLXCNT)
RELAX(1R,LINRLX,0.5);RELAX(2R,LINRLX,0.5)
    * ------------------------------------------------------------
    * GROUP 18. Limits on variables or increments to them
    * ------------------------------------------------------------
VARMIN(1SIZ)=0.0;VARMIN(2SIZ)=0.0
VARMAX(1SIZ)=0.1;VARMAX(2SIZ)=0.1
VARMIN(1V)=-5.0;VARMIN(2V)=-5.0
VARMAX(1V)=5.0;VARMAX(2V)=5.0
    * ------------------------------------------------------------
    * GROUP 19. Data communicated by satellite to GROUND
    * ------------------------------------------------------------
DWDY=T
    * Debug print-out
LG(1)=F
    * Minimum z/d_inlet for least sq adjustment of jet boundary
RG(17)=50.0
    * Printout of least sq adj error
LG(3)=T
    * AVEL normalised ?
LG(6)=T
    * Computation of jet spread-rate, etc
LG(5)=T
    * Print-out of MYPLOT
LG(7)=T
    * SHSO multiplied by l_prndtl/l
LG(8)=T
    * Fixing EL1 at IZ=1 (<0 => no intervention)
RG(26)=INISIZ
    * CMDOT=0.0 if IZ<IG(4)
IG(4)=0
    * ------------------------------------------------------------
    * GROUP 20. Preliminary print-out
    * ------------------------------------------------------------
ECHO=T
    * ------------------------------------------------------------
    * GROUP 21. Print-out of variables
    * ------------------------------------------------------------
OUTPUT(P1,N,Y,N,Y,N,N);OUTPUT(CFIP,N,Y,N,Y,N,N)
OUTPUT(1R,N,Y,N,Y,N,N)
    * ------------------------------------------------------------
    * GROUP 22. Spot-value print-out
    * ------------------------------------------------------------
```

```
TSTSWP=5;NPLT=1
    * ------------------------------------------------------------
    * GROUP 23. Field print-out and plot control
    * ------------------------------------------------------------
NZPRIN=20;IZPRF=80;IPROF=3;ORSIZ=0.4;ITABL=1;IPROF=1

PATCH(AIR1,PROFIL,1,1,1,NY,1,NZ,1,1000)
PLOT(AIR1,1SIZ,-1.0,-1.0);PLOT(AIR1,2SIZ,-1.0,-1.0)

PATCH(AIR2,PROFIL,1,1,1,NY,1,NZ,1,1000)
PLOT(AIR2,1v,-1.0,-1.0);PLOT(AIR2,2v,-1.0,-1.0)
PLOT(AIR2,C2,0.0,0.0);PLOT(AIR2,AVEL,0.0,0.0)
PLOT(AIR2,ENUT,0.0,0.0)

PATCH(AIR3,PROFIL,1,1,1,NY,1,NZ,1,1000)
PLOT(AIR3,AVEL,0.0,0.0)

PATCH(AIR,PROFIL,1,1,1,NY,1,NZ,1,1000)
PLOT(AIR,1W,0.0,W1IN);PLOT(AIR,2W,0.0,W2IN)
PLOT(AIR,AVEL,0.0,1.0)
PLOT(AIR,2R,0.0,1.0)

NAME(2R)=IN2R
    *
    * ------------------------------------------------------------
    * GROUP 24. Dumps for restarts
    * ------------------------------------------------------------
NSAVE=RPHI
STOP
```

c.3 Q1 file for the cold spray

```
 TALK=F;RUN(1,1);VDU=3

    ************************************************************
    **  Two-fluid model of turbulence applied to 2-phase flows **
    **                    Cold-spray simulation                 **
    **                         File: S2PQ1                      **
    **        Norberto Fueyo, CFDU, IC, London, 12.08.88        **
    ************************************************************
    *
    * ------------------------------------------------------------
    * GROUP 1. Run title and other preliminaries
    * ------------------------------------------------------------
TEXT(Cold spray)
    *
    *.........Variables
    *
REAL(W1IN,W2IN,DENSIN,FACTOR,R1IN,R2IN,COEFP,RESIDU)
REAL(RLXCNT,PRD,INISIZ,RSIZ)
INTEGER(NINLET)
    *.........Properties
    * Liquid and gas densities
RG(12)=878.0;RG(20)=1.0
    *.........Inlet conditions (self-explanatory)
W1IN=43.4;W2IN=43.4;RG(15)=W2IN
R1IN=0.0001;R2IN=1.0-R1IN
DENSIN=29.7656
INISIZ=4.5E-6
    *
FACTOR=4.849381E5*RG(12)/(DENSIN*r2in);RG(30)=FACTOR
    *.........Satellit ---> Earth
    *
    * Number of size categories
IG(1)=5
    * Diameters. Use RG(1) to RG(11)  ONLY for diameters.

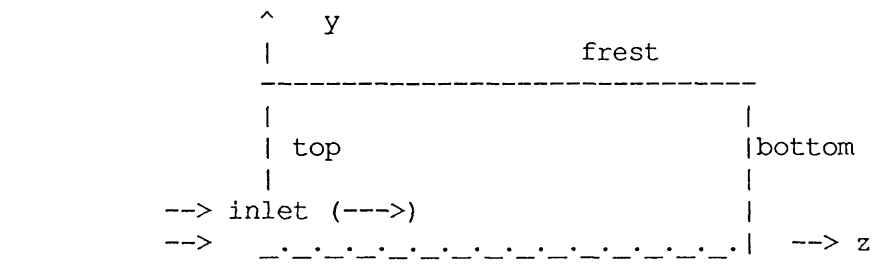
        size n           size 3   size 2   size 1
      |--------|--...--|--------|--------|--------|---------> Size
  diam n+1  diam n   diam 4   diam 3   diam 2   diam 1

RG(6)=0.0;RG(5)=25.0E-6
RG(4)=45.0E-6;RG(3)=75.0E-6;RG(2)=100.0E-6;RG(1)=150.0E-6
    *          Form factor:  Volume=const*size**form_factor
    *          Ex: 3/2 if size=diameter**2
RG(18)=3.0/2.0
    *
    * ------------------------------------------------------------
    * GROUP 2. Transience; time-step specification
    * ------------------------------------------------------------
    * ------------------------------------------------------------
    * GROUP 3. X-direction grid specification
```

```
    * ------------------------------------------------------------
CARTES=F
    * ------------------------------------------------------------
    * GROUP 4. Y-direction grid specification
    * ------------------------------------------------------------
    *  RG(16) is the inlet diameter
RG(16)=1.194E-3
GRDPWR(Y,20,RG(16),1.0)
NINLET=NY/2
    *  Linear expansion: AZYV=1 for linear growth
    *                    ZWADD=YVLAST(inlet)/tg(alpha)
AZYV=1.0
    * alpha=15 deg;tg(15)=0.2679
ZWADD=YVLAST/0.3
    * ------------------------------------------------------------
    * GROUP 5. Z-direction grid specification
    * ------------------------------------------------------------
PARAB=T
NZ=160
    *  DZ = RG(14) * WIDTH_1%
AZDZ=GRND;RG(14)=0.20
    * ------------------------------------------------------------
    * GROUP 6. Body-fitted coordinates or grid distortion
    * ------------------------------------------------------------
    * ------------------------------------------------------------
    * GROUP 7. Variables stored, solved & named
    * ------------------------------------------------------------
ONEPHS=F
    * LIQi is the volume occupied by the liquid.
NAME(27)=LIQ1;NAME(26)=LIQ2
    * Variables 31 to 50 reserved for size groups.
NAME(30)=1D;NAME(32)=2D;NAME(34)=3D;NAME(36)=4D;NAME(38)=5D
NAME(31)=1U;NAME(33)=2U;NAME(35)=3U;NAME(37)=4U;NAME(39)=5U
    *
    * C1: average velocity w, w = w1 r1 + w2 r2
NAME(C1)=AVEL
    * C3 & C4: Fragment size
NAME(C3)=1SIZ;NAME(C4)=2SIZ
    * Multi-purpose, auxiliary storage
STORE (C2, C5)
    *
NAME(R1)=1R;NAME(R2)=2R
NAME(W1)=1W;NAME(W2)=2W
NAME(V1)=1V;NAME(V2)=2V
    *
SOLVE(P1,1R,2R,1V,2V,1W,2W,1SIZ,2SIZ)
SOLVE(1U,2U,3U,4U,5U);SOLVE(1D,2D,3D,4D,5D)
STORE(LIQ1,LIQ2,RHO1,RHO2)
STORE(ENUT,EL1,CFIPS,CMDOT,AVEL)
    *
    * ------------------------------------------------------------
    * GROUP 8. Terms (in differential equations) & devices
    * ------------------------------------------------------------
    * No interphase exchange and diffusion for sizes
TERMS(1SIZ,P,P,N,P,P,N);TERMS(2SIZ,P,P,N,P,P,N)

    * ------------------------------------------------------------
```

```
    * GROUP 9. Properties of the medium (or media)
    * -------------------------------------------------------
    * - - - - - - - - - - RHO - - - - - - - - - - - - - - - - -
RHO1=GRND;RHO2=GRND
    * - - - - - - - - - - EL - - - - - - - - - - - - - - - - - -
EL1=GRND
    * - - - - - - - - - - ENUT - - - - - - - - - - - - - - - - -
    * 2-fluid formula
    * ENUT = GRND4 => Two-fluid model formula supplied in GREX2
ENUT=GRND4;ENUTA=15.0
    * - - - - - - - - - - PRT's - - - - - - - - - - - - - - - - -
PRD=0.5
PRT(1U)=PRD;PRT(2U)=PRD;PRT(3U)=PRD;PRT(4U)=PRD;PRT(5U)=PRD
PRT(1D)=PRD;PRT(2D)=PRD;PRT(3D)=PRD;PRT(4D)=PRD;PRT(5D)=PRD
    * -------------------------------------------------------
    * GROUP 10. Inter-phase-transfer processes and properties
    * -------------------------------------------------------
    * - - - - - - - - - - CFIPS - - - - - - - - - - - - - - - -
CFIPS=GRND4;CFIPA=0.0;CFIPB=1.0;CFIPD=-1.0;CFIPC=0.0375
    * - - - - - - - - - - CMDOT - - - - - - - - - - - - - - - -
CMDOT=GRND1;CMDTA=10.0/CFIPC;CMDTB=0.5;CMDTC=0.0
    * -------------------------------------------------------
    * GROUP 11. Initialization of variable or porosity fields
    * -------------------------------------------------------
FIINIT(1R)=1.0;FIINIT(2R)=0.0
FIINIT(1W)=0.0;FIINIT(2W)=0.0;FIINIT(1V)=0.0;FIINIT(2V)=0.0
FIINIT(1U)=0.0;FIINIT(2U)=0.0;FIINIT(3U)=0.0;FIINIT(4U)=0.0
FIINIT(5U)=0.0
FIINIT(1D)=0.0;FIINIT(2D)=0.0;FIINIT(3D)=0.0;FIINIT(4D)=0.0
FIINIT(5D)=0.0
FIINIT(RHO2)=1.0;FIINIT(RHO1)=1.0
FIINIT(1SIZ)=INISIZ;FIINIT(2SIZ)=INISIZ
    * -------------------------------------------------------
    * GROUP 12. Convection and diffusion adjustments
    * -------------------------------------------------------
    * -------------------------------------------------------
    * GROUP 13. Boundary conditions and special sources
    * -------------------------------------------------------
```




```
    * --- Inlet (= jet exit) ----------------------------------

PATCH(--->,LOW,1,1,1,NINLET,1,1,1,1000)

COVAL(--->,P2,FIXFLU, DENSIN*W2IN*R2IN)
COVAL(--->,2W,ONLYMS,W2IN);COVAL(--->,2SIZ,ONLYMS,INISIZ)

COVAL(--->,P1,FIXFLU,DENSIN*W1IN*R1IN)
COVAL(--->,1W,ONLYMS,W1IN);COVAL(--->,1SIZ,ONLYMS,INISIZ)
```

```
COVAL(--->,1U,ONLYMS,1.0);COVAL(--->,2U,ONLYMS,3.0)
COVAL(--->,3U,ONLYMS,7.0);COVAL(--->,4U,ONLYMS,10.0)
COVAL(--->,5U,ONLYMS,9.0)

COVAL(--->,1D,ONLYMS,1.0);COVAL(--->,2D,ONLYMS,3.0)
COVAL(--->,3D,ONLYMS,7.0);COVAL(--->,4D,ONLYMS,10.0)
COVAL(--->,5D,ONLYMS,9.0)

   * --- Fragment size: growth and diminuition ------------------

PATCH(E+A,VOLUME,1,NX,1,NY,1,NZ,1,1000)
COVAL(E+A,1SIZ,FIXFLU,GRND2);COVAL(E+A,2SIZ,FIXFLU,GRND2)
RG(23)=0.03

PATCH(TEAR,VOLUME,1,NX,1,NY,1,NZ,1,1000)
COVAL(TEAR,1SIZ,GRND3,0.0);COVAL(TEAR,2SIZ,GRND3,0.0)
RG(24)=0.01

   * --- Shear source -------------------------------------------
PATCH(SHSO,CELL,1,NX,1,NY,15,NZ,1,1000)
COVAL(SHSO,1V,FIXFLU,GRND5);COVAL(SHSO,2V,FIXFLU,GRND5)
RSG10=0.175

   * --- Gravity ------------------------------------------------
PATCH(GSOM,VOLUME,1,NX,1,NY,1,NZ,1,1000)
COVAL(GSOM,1W,FIXFLU,GRND3)
COVAL(GSOM,2W,FIXFLU,GRND3)
    * --- Free-stream/wall boundary conditions -------------------
    *  Coefficient for fixed-pressure boundary-conditions
COEFP=1.0
    * --- Top
PATCH(TOP,CELL,1,1,NINLET+1,NY,1,1,1000)
COVAL(TOP,P1,FIXP,0.0);COVAL(TOP,P2,FIXP,0.0)
    * --- Free stream
PATCH(FREST,CELL,1,1,NY,NY,1,NZ,1,1000)
COVAL(FREST,P1,COEFP,0.0);COVAL(FREST,P2,COEFP,0.0)
    * ------------------------------------------------------------
    * GROUP 14. Downstream pressure for PARAB=.TRUE.
    * ------------------------------------------------------------
IPARAB=1
    * ------------------------------------------------------------
    * GROUP 15. Termination of sweeps
    * ------------------------------------------------------------
LITHYD=30
RESIDU=1.0E-10;RESREF(P1)=RESIDU
RESREF(1R)=RESIDU;RESREF(2R)=RESIDU
RESREF(1W)=RESIDU;RESREF(2W)=RESIDU
RESREF(1V)=RESIDU;RESREF(2V)=RESIDU
RESREF(1SIZ)=1.0E-15;RESREF(2SIZ)=1.0E-15
RSIZ=1.0E-12
RESREF(1U)=RSIZ;RESREF(2U)=RSIZ;RESREF(3U)=RSIZ
RESREF(4U)=RSIZ;RESREF(5U)=RSIZ
RESREF(1D)=RSIZ;RESREF(2D)=RSIZ;RESREF(3D)=RSIZ
RESREF(4D)=RSIZ;RESREF(5D)=RSIZ
    * ------------------------------------------------------------
```

```
    * GROUP 16. Termination of iterations
    * ----------------------------------------------------------
    * ----------------------------------------------------------
    * GROUP 17. Under-relaxation devices
    * ----------------------------------------------------------
RLXCNT=1.0E-2;RELAX(P1,LINRLX,0.2)
RELAX(1V,FALSDT,RLXCNT);RELAX(2V,FALSDT,RLXCNT)
RELAX(1W,FALSDT,RLXCNT);RELAX(2W,FALSDT,RLXCNT)
RELAX(1R,LINRLX,0.1);RELAX(2R,LINRLX,0.1)
RELAX(DEN1,LINRLX,0.2);RELAX(DEN2,LINRLX,0.2)
    * ----------------------------------------------------------
    * GROUP 18. Limits on variables or increments to them
    * ----------------------------------------------------------
VARMAX(1U)=1.0E20;VARMAX(2U)=1.0E20;VARMAX(3U)=1.0E20
VARMAX(4U)=1.0E20;VARMAX(5U)=1.0E20
VARMAX(1D)=1.0E20;VARMAX(2D)=1.0E20;VARMAX(3D)=1.0E20
VARMAX(4D)=1.0E20;VARMAX(5D)=1.0E20

VARMAX(1V)=10.0;VARMAX(2V)=10.0
VARMIN(1V)=-10.0;VARMIN(2V)=-10.0
VARMIN(1SIZ)=1.0E-10;VARMIN(2SIZ)=1.0E-10
VARMAX(1SIZ)=0.1;VARMAX(2SIZ)=0.1
    * ----------------------------------------------------------
    * GROUP 19. Data communicated by satellite to GROUND
    * ----------------------------------------------------------
DWDY=T
    * Debug print-out
LG(1)=F
    * AVEL normalised ?
LG(6)=T
    * r (if F) or r-density (if T) average
LG(4)=T
    * SHSO multiplied by l_prndtl/l
LG(8)=T
    * Fixing EL1 at IZ=1 (<0 => no intervention)
RG(26)=INISIZ
    * cmdot=0 if iz<ig(4)
IG(4)=4
    * cfips*rg(27) if iz<ig(5)
IG(5)=0;RG(27)=500.0
    *
    * ----------------------------------------------------------
    * GROUP 20. Preliminary print-out
    * ----------------------------------------------------------
ECHO=T
    * ----------------------------------------------------------
    * GROUP 21. Print-out of variables
    * ----------------------------------------------------------
OUTPUT(MAS1,N,N,N,N,N,N);OUTPUT(MAS2,N,N,N,N,N,N)
OUTPUT(SDOT,N,N,N,N,N,N)
    * ----------------------------------------------------------
    * GROUP 22. Spot-value print-out
    * ----------------------------------------------------------
TSTSWP=5
    * ----------------------------------------------------------
    * GROUP 23. Field print-out and plot control
    * ----------------------------------------------------------
```

```
NZPRIN=10;IPROF=3;ORSIZ=0.4;ITABL=0;IPROF=1

PATCH(AIR,PROFIL,1,1,1,NY,1,NZ,1,1000)
PLOT(AIR,1W,0.0,W1IN);PLOT(AIR,2W,0.0,W2IN)
PLOT(AIR,AVEL,0.0,1.0);PLOT(AIR,2R,0.0,1.0)

PATCH(U's,PROFIL,1,1,1,NY,1,NZ,1,1000)
PLOT(U's,1U,0.0,0.0);PLOT(U's,2U,0.0,0.0)
PLOT(U's,3U,0.0,0.0);PLOT(U's,4U,0.0,0.0)

NAME(2R)=IN2R
    *
    * ----------------------------------------------------------------
    * GROUP 24. Dumps for restarts
    * ----------------------------------------------------------------
NSAVE=RPHI
STOP
```

C.4 Q1 file for the evaporating spray

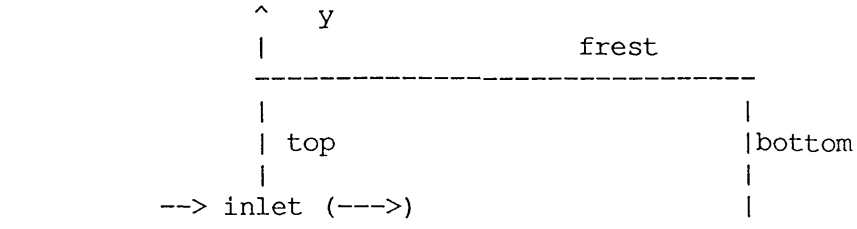
```
 TALK=F;RUN(1,1);VDU=3
    ************************************************************
    **  Two-fluid model of turbulence applied to 2-phase flows **
    **                      Evaporating spray                   **
    **                         File: S2VQ1                      **
    **        Norberto Fueyo, CFDU, IC, London, 13.10.88        **
    ************************************************************
    *
    * ----------------------------------------------------------
    * GROUP 1. Run title and other preliminaries
    * ----------------------------------------------------------
TEXT(Evaporating spray)
    *
    *.........Variables
    *
REAL(W1IN,W2IN,DENSIN,FACTOR,R1IN,R2IN,COEFP,RESIDU)
REAL(RLXCNT,PRD,INISIZ,RSIZ)
INTEGER(NINLET)
    *.........Properties
    * Liquid, gas and vapour densities
RG(12)=1494.0;RG(20)=1.0;RG(13)=5.86
    * Vapour diffusivity (Gammavap)
RG(29)=1.0E-5
    * Sdot (>0 => constant; <0 => to be computed)
RG(21)=1.0E-7
    *.........Inlet conditions (self-explanatory)
W1IN=29.64;W2IN=29.64;RG(15)=W2IN
R1IN=0.0001;R2IN=1.0-R1IN
DENSIN=58.03259
INISIZ=4.5E-6
    *
FACTOR=1.201305E6*RG(12)/(DENSIN*R2IN);RG(30)=FACTOR
    *
    *.........Satellit ---> Earth
    *
    * Number of size categories
IG(1)=5
    * Diameters. Use RG(1) to RG(11)  ONLY for diameters.

        size n            size 3   size 2   size 1
      |--------|--...--|--------|--------|--------|---------> Size
  diam n+1  diam n   diam 4   diam 3   diam 2   diam 1

RG(6)=0.0;RG(5)=15.0E-6
RG(4)=30.0E-6;RG(3)=50.0E-6;RG(2)=70.0E-6;RG(1)=95.0E-6
    *          Form factor:  Volume=const*size**form_factor
    *          Ex: 3/2 if size=diameter**2
RG(18)=3.0/2.0
    *
```

```
    * ------------------------------------------------------------
    * GROUP 2. Transience; time-step specification
    * ------------------------------------------------------------
    * ------------------------------------------------------------
    * GROUP 3. X-direction grid specification
    * ------------------------------------------------------------
CARTES=F
    * ------------------------------------------------------------
    * GROUP 4. Y-direction grid specification
    * ------------------------------------------------------------
RG(16)=1.194E-3
GRDPWR(Y,20,RG(16),1.0)
    *  RG(16) is the inlet diameter
NINLET=NY/2
    *  Linear expansion: AZYV=1 for linear growth
    *                    ZWADD=YVLAST(inlet)/tg(alpha)
AZYV=1.0
    * tg(15)=0.2679
ZWADD=YVLAST/0.3
    * ------------------------------------------------------------
    * GROUP 5. Z-direction grid specification
    * ------------------------------------------------------------
PARAB=T
NZ=300
    *  DZ = RG(14) * WIDTH_1%
AZDZ=GRND;RG(14)=.20
    * ------------------------------------------------------------
    * GROUP 6. Body-fitted coordinates or grid distortion
    * ------------------------------------------------------------
    * ------------------------------------------------------------
    * GROUP 7. Variables stored, solved & named
    * ------------------------------------------------------------
ONEPHS=F
    * SDOT is Sdot.
NAME(C6)=SDOT
    * MASi is mass of liquid transferred to gas
NAME(C9)=MAS2;NAME(C10)=MAS1
    * LIQi is the volume occupied by the liquid.
NAME(27)=LIQ1;NAME(26)=LIQ2
NAME(C7)=DVAP;NAME(C8)=UVAP
    * Variables 31 to 50 reserved for size groups.
NAME(30)=1D;NAME(32)=2D;NAME(34)=3D;NAME(36)=4D;NAME(38)=5D
NAME(31)=1U;NAME(33)=2U;NAME(35)=3U;NAME(37)=4U;NAME(39)=5U
    * C1: average velocity w, w = w1 r1 + w2 r2
NAME(C1)=AVEL
    * C3 & C4: Fragment size when SOLVEd
NAME(C3)=1SIZ;NAME(C4)=2SIZ
    * Multi-purpose, auxiliary storage
STORE (C2,C5)
    *
NAME(R1)=1R;NAME(R2)=2R;NAME(W1)=1W;NAME(W2)=2W
NAME(V1)=1V;NAME(V2)=2V
    *
SOLVE(P1,1R,2R,1V,2V,1W,2W,1SIZ,2SIZ,DVAP,UVAP)
SOLVE(1U,2U,3U,4U,5U);SOLVE(1D,2D,3D,4D,5D)
STORE(MAS1,MAS2,LIQ1,LIQ2,SDOT,RHO1,RHO2,ENUT,EL1)
STORE(CFIPS,CMDOT,AVEL)
```

```
    *
    * ------------------------------------------------------------
    * GROUP 8. Terms (in differential equations) & devices
    * ------------------------------------------------------------
    * No interphase transport of size
TERMS(1SIZ,P,P,N,P,P,N);TERMS(2SIZ,P,P,N,P,P,N)
    *
    * ------------------------------------------------------------
    * GROUP 9. Properties of the medium (or media)
    * ------------------------------------------------------------
    * - - - - - - - - - - RHO - - - - - - - - - - - - - - - - - -
RHO1=GRND;RHO2=GRND
    * - - - - - - - - - - EL - - - - - - - - - - - - - - - - - -
EL1=GRND
    * - - - - - - - - - - ENUT - - - - - - - - - - - - - - - - -
    * 2-fluid formula
    * ENUT = GRND4 => Two-fluid model formula supplied in GREX2
ENUT=GRND4;ENUTA=15.0
    * - - - - - - - - - - PRT's - - - - - - - - - - - - - - - - -
PRD=0.5
PRT(1U)=PRD;PRT(2U)=PRD;PRT(3U)=PRD;PRT(4U)=PRD;PRT(5U)=PRD
PRT(1D)=PRD;PRT(2D)=PRD;PRT(3D)=PRD;PRT(4D)=PRD;PRT(5D)=PRD
    *
    * ------------------------------------------------------------
    * GROUP 10. Inter-phase-transfer processes and properties
    * ------------------------------------------------------------
    * - - - - - - - - - - CFIPS - - - - - - - - - - - - - - - - -
CFIPS=GRND4;CFIPA=0.0;CFIPB=1.0;CFIPD=-1.0;CFIPC=0.0375
    * - - - - - - - - - - CMDOT - - - - - - - - - - - - - - - - -
    * Symmetry is considered
CMDOT=GRND1;CMDTA=10.0/CFIPC;CMDTB=0.5;CMDTC=0.0
    * - - - - - - - - - - CINTs - - - - - - - - - - - - - - - - -
    * ------------------------------------------------------------
    * GROUP 11. Initialization of variable or porosity fields
    * ------------------------------------------------------------
FIINIT(1R)=1.0;FIINIT(2R)=0.0
FIINIT(1W)=0.0;FIINIT(2W)=0.0;FIINIT(1V)=0.0;FIINIT(2V)=0.0
FIINIT(1U)=0.0;FIINIT(2U)=0.0;FIINIT(3U)=0.0;FIINIT(4U)=0.0
FIINIT(5U)=0.0
FIINIT(1D)=0.0;FIINIT(2D)=0.0;FIINIT(3D)=0.0;FIINIT(4D)=0.0
FIINIT(5D)=0.0
FIINIT(RHO2)=1.0;FIINIT(RHO1)=1.0
FIINIT(1SIZ)=INISIZ;FIINIT(2SIZ)=INISIZ
    * ------------------------------------------------------------
    * GROUP 12. Convection and diffusion adjustments
    * ------------------------------------------------------------
    * ------------------------------------------------------------
    * GROUP 13. Boundary conditions and special sources
    * ------------------------------------------------------------
```



```
        -->   _·_·_·_
```

```
COVAL(TOP,P1,FIXP,0.0);COVAL(TOP,P2,FIXP,0.0)
    * --- Free stream
PATCH(FREST,CELL,1,1,NY,NY,1,NZ,1,1000)
COVAL(FREST,P1,COEFP,0.0);COVAL(FREST,P2,COEFP,0.0)
    * ------------------------------------------------------------
    * GROUP 14. Downstream pressure for PARAB=.TRUE.
    * ------------------------------------------------------------
IPARAB=1
    * ------------------------------------------------------------
    * GROUP 15. Termination of sweeps
    * ------------------------------------------------------------
LITHYD=20;RESIDU=1.0E-10
RESREF(1R)=RESIDU;RESREF(2R)=RESIDU
RESREF(1W)=RESIDU;RESREF(2W)=RESIDU
RESREF(1V)=RESIDU;RESREF(2V)=RESIDU
RESREF(UVAP)=RESIDU;RESREF(DVAP)=RESIDU
RESREF(P1)=RESIDU
RESREF(1SIZ)=1.0E-15;RESREF(2SIZ)=1.0E-15
RSIZ=1.0E-12
RESREF(1U)=RSIZ;RESREF(2U)=RSIZ;RESREF(3U)=RSIZ
RESREF(4U)=RSIZ;RESREF(5U)=RSIZ
RESREF(1D)=RSIZ;RESREF(2D)=RSIZ;RESREF(3D)=RSIZ
RESREF(4D)=RSIZ;RESREF(5D)=RSIZ
    * ------------------------------------------------------------
    * GROUP 16. Termination of iterations
    * ------------------------------------------------------------
    * ------------------------------------------------------------
    * GROUP 17. Under-relaxation devices
    * ------------------------------------------------------------
RLXCNT=1.0E-2
RELAX(P1,LINRLX,0.2)
RELAX(1V,FALSDT,RLXCNT);RELAX(2V,FALSDT,RLXCNT)
RELAX(1W,FALSDT,RLXCNT);RELAX(2W,FALSDT,RLXCNT)
RELAX(1R,LINRLX,0.1);RELAX(2R,LINRLX,0.1)
RELAX(DEN1,LINRLX,0.2);RELAX(DEN2,LINRLX,0.2)
    * ------------------------------------------------------------
    * GROUP 18. Limits on variables or increments to them
    * ------------------------------------------------------------
VARMAX(1U)=1.0E20;VARMAX(2U)=1.0E20;VARMAX(3U)=1.0E20
VARMAX(4U)=1.0E20;VARMAX(5U)=1.0E20
VARMAX(1D)=1.0E20;VARMAX(2D)=1.0E20;VARMAX(3D)=1.0E20
VARMAX(4D)=1.0E20;VARMAX(5D)=1.0E20

VARMAX(1V)=10.0;VARMAX(2V)=10.0
VARMIN(1V)=-10.0;VARMIN(2V)=-10.0
VARMIN(1SIZ)=1.0E-10;VARMIN(2SIZ)=1.0E-10
VARMAX(1SIZ)=0.1;VARMAX(2SIZ)=0.1

VARMIN(UVAP)=0.0;VARMIN(DVAP)=0.0
    * ------------------------------------------------------------
    * GROUP 19. Data communicated by satellite to GROUND
    * ------------------------------------------------------------
DWDY=T
    * Debug print-out
LG(1)=F
    * AVEL normalised ?
LG(6)=T
```

```
    * r (if F) or r-d (if T) average
LG(4)=T
    * Sdot=0 if IZ<=IG(3)
IG(3)=0
    * SHSO multiplied by l_prndtl/l
LG(8)=T
    * Fixing EL1 at IZ=1 (<0 => no intervention)
RG(26)=INISIZ
    * cmdot=0 if iz<ig(4)
IG(4)=4
    * cfips*rg(27) if iz<ig(5)
IG(5)=0;RG(27)=500.0
    * ----------------------------------------------------------
    * GROUP 20. Preliminary print-out
    * ----------------------------------------------------------
ECHO=T
    * ----------------------------------------------------------
    * GROUP 21. Print-out of variables
    * ----------------------------------------------------------
    * ----------------------------------------------------------
    * GROUP 22. Spot-value print-out
    * ----------------------------------------------------------
TSTSWP=5;NPLT=1
    * ----------------------------------------------------------
    * GROUP 23. Field print-out and plot control
    * ----------------------------------------------------------
NZPRIN=10;IPROF=3;ORSIZ=0.4;ITABL=1;IPROF=3

PATCH(AX1,PROFIL,1,1,1,1,1,100,1,1000)
PLOT(AX1,1U,0.0,0.0);PLOT(AX1,2U,0.0,0.0)
PLOT(AX1,3U,0.0,0.0);PLOT(AX1,4U,0.0,0.0);PLOT(AX1,5U,0.0,0.0)

NAME(2R)=IN2R
    *
    * ----------------------------------------------------------
    * GROUP 24. Dumps for restarts
    * ----------------------------------------------------------
NSAVE=RPHI
STOP
```

c.5 Q1 file for the combusting spray

```
TALK=F;RUN(1,1);VDU=3
    ************************************************************
    **  Two-fluid model of turbulence applied to 2-phase flows **
    **             Demonstrative run with combustion            **
    **                          File: S2MQ1                     **
    **        Norberto Fueyo, CFDU, IC, London, 06.02.89        **
    ************************************************************
    *
    * ------------------------------------------------------------
    * GROUP 1. Run title and other preliminaries
    * ------------------------------------------------------------
TEXT(Demonstrative run with combustion)
    *.........Local variables
REAL(W1IN,W2IN,DENSIN,FACTOR,R1IN,R2IN,RESIDU)
REAL(RLXCNT,PRD,INISIZ,RSIZ,TDROP,TAIR,CPA,HLV,THCOND,YAIN,YFIN)
INTEGER(NINLET)
    *.........Properties
    * Liquid, gas and vapour densities
RG(12)=1494.0;RG(20)=1.0;RG(13)=5.86
    * Vapour diffusivity (Gammavap)
RG(29)=1.0E-5
    * Latent heat, Thermal cond of vap, Heat of comb
HLV=1.804E5;THCOND=0.0026;RG(41)=6.2e6
RG(37)=HLV;RG(38)=THCOND
    * Reaction_rate=-a*Yox*Yfu*e**(-b/T);a=RG(39);b=RG(40)
RG(39)=1.0E8;RG(40)=8000.0
    * Stoichiometric ratio
RG(35)=2.6
    * Sdot (>0 => constant; <0 => to be computed)
    * -2 activates option 2
RG(21)=-2.0
    *.........Inlet conditions (self-explanatory)
W1IN=10.0;W2IN=10.0;RG(15)=W2IN;INISIZ=4.5E-6
R1IN=0.0001;R2IN=1.0-R1IN
TDROP=100.0;TAIR=300.0;RG(34)=TDROP
    *
YFIN=0.45;YAIN=1.0-YFIN
DENSIN=1.0/(YAIN/0.6087+YFIN/RG(12))
FACTOR=YFIN/31798.75E-12;RG(30)=FACTOR
    *.........Satellit ---> Earth
    * Number of size categories
IG(1)=5
    * Diameters. Use RG(1) to RG(11)  ONLY for diameters.

        size n           size 3   size 2   size 1
      |--------|--...--|--------|--------|--------|---------> Size
  diam n+1  diam n   diam 4   diam 3   diam 2   diam 1

RG(6)=0.0;RG(5)=15.0E-6
```

```
RG(4)=30.0E-6;RG(3)=50.0E-6;RG(2)=70.0E-6;RG(1)=95.0E-6
    * Form factor:  Volume=const*size**form_factor
    * Example: 3/2 if size=diameter**2
RG(18)=3.0/2.0
    *.........End of data definition
    *
    * ---------------------------------------------------------
    * GROUP 2. Transience; time-step specification
    * ---------------------------------------------------------
    * ---------------------------------------------------------
    * GROUP 3. X-direction grid specification
    * ---------------------------------------------------------
CARTES=F
    * ---------------------------------------------------------
    * GROUP 4. Y-direction grid specification
    * ---------------------------------------------------------
    *  RG(16) is the inlet diameter
RG(16)=0.002
GRDPWR(Y,30,RG(16),1.0)
NINLET=NY/2
    *  Linear expansion: AZYV=1 for linear growth
    *                    ZWADD=YVLAST(inlet)/tg(alpha)
AZYV=1.0
    * According to Salomon et al, the spray angle is 30 deg at
    * alpha=15.0;tg(15)=0.2679
ZWADD=YVLAST/0.3
    * ---------------------------------------------------------
    * GROUP 5. Z-direction grid specification
    * ---------------------------------------------------------
PARAB=T
NZ=150
    *  DZ = RG(14) * WIDTH_1%
AZDZ=GRND;RG(14)=0.20
    * ---------------------------------------------------------
    * GROUP 6. Body-fitted coordinates or grid distortion
    * ---------------------------------------------------------
    * ---------------------------------------------------------
    * GROUP 7. Variables stored, solved & named
    * ---------------------------------------------------------
ONEPHS=F
    * SDTi is Sdot;
    * MASi is mass of liquid transferred to gas;
    * LIQi is the volume occupied by the liquid.
NAME(C6)=SDT1;NAME(KE)=SDT2;NAME(C9)=MAS2;NAME(C10)=MAS1
NAME(27)=LIQ1;NAME(26)=LIQ2;NAME(C7)=1VAP;NAME(C8)=2VAP
NAME(46)=1AIR;NAME(47)=2AIR;NAME(48)=1PRD;NAME(49)=2PRD
NAME(40)=1FUE;NAME(41)=2FUE;NAME(42)=1MFR;NAME(43)=2MFR
    * Variables 31 to 50 reserved for size groups.
NAME(30)=1D;NAME(32)=2D;NAME(34)=3D;NAME(36)=4D;NAME(38)=5D
NAME(31)=1U;NAME(33)=2U;NAME(35)=3U;NAME(37)=4U;NAME(39)=5U
    * C1: average velocity w, w = w1 r1 + w2 r2
NAME(C1)=AVEL
    * C3 & C4: Fragment size when SOLVEd
NAME(C3)=1SIZ;NAME(C4)=2SIZ
    *
NAME(R1)=1R;NAME(R2)=2R;NAME(W1)=1W;NAME(W2)=2W
NAME(V1)=1V;NAME(V2)=2V
```

```
    *
SOLVE(P1,1R,2R,1V,2V,1W,2W,1SIZ,2SIZ,1MFR,2MFR,1FUE,2FUE)
SOLVE(1U,2U,3U,4U,5U);SOLVE(1D,2D,3D,4D,5D)
STORE(1VAP,2VAP,1PRD,2PRD,1AIR,2AIR,H1,H2,EL1,AVEL,TMP1,TMP2)
STORE(MAS1,MAS2,LIQ1,LIQ2,SDT1,SDT2,RHO1,RHO2)
    *
    * ------------------------------------------------------------
    * GROUP 8. Terms (in differential equations) & devices
    * ------------------------------------------------------------
    * No interphase transfer of fragment size
TERMS(1SIZ,P,P,N,P,P,N);TERMS(2SIZ,P,P,N,P,P,N)
    * ------------------------------------------------------------
    * GROUP 9. Properties of the medium (or media)
    * ------------------------------------------------------------
    * - - - - - - - - - - TMP - - - - - - - - - - - - - - - - - -
TMP1=GRND;TMP2=GRND
    * Specific heats of
      Air        Vap           Prod
TMP1A=1000.0;TMP1B=1000.0;TMP1C=1000.0
CPA=TMP1A
    * - - - - - - - - - - RHO - - - - - - - - - - - - - - - - - -
RHO1=GRND;RHO2=GRND
    * Molecular weights of
      Air        Vap        Prod
RHO1A=32.0;RHO1B=12.0;RHO1C=44.0
TEMP0=-273.0;PRESS0=100000.0
    * - - - - - - - - - - EL1 - - - - - - - - - - - - - - - - - -
EL1=GRND
    * - - - - - - - - - - ENUT - - - - - - - - - - - - - - - - - -
    * 2-fluid formula
      ENUT = GRND4 => Two-fluid model formula supplied in GREX2
ENUT=GRND4;ENUTA=15.0
    * - - - - - - - - - - PRT's - - - - - - - - - - - - - - - - -
    * NB: PRT are used for mass diffusion, rather than Cd
PRT(1R)=ENUTA/0.3;PRT(2R)=PRT(1R)
PRD=0.5
PRT(1U)=PRD;PRT(2U)=PRD;PRT(3U)=PRD;PRT(4U)=PRD;PRT(5U)=PRD
PRT(1D)=PRD;PRT(2D)=PRD;PRT(3D)=PRD;PRT(4D)=PRD;PRT(5D)=PRD
PRT(H1)=PRD;PRT(H2)=PRD
PRT(2MFR)=PRD;PRT(1MFR)=PRD;PRT(2FUE)=PRD;PRT(1FUE)=PRD
    * ------------------------------------------------------------
    * GROUP 10. Inter-phase-transfer processes and properties
    * ------------------------------------------------------------
    * - - - - - - - - - - CFIPS - - - - - - - - - - - - - - - - -
CFIPS=GRND4;CFIPA=0.0;CFIPB=1.0;CFIPD=-1.0;CFIPC=0.0375
    * - - - - - - - - - - CMDOT - - - - - - - - - - - - - - - - -
    * Symmetry is considered
CMDOT=GRND1;CMDTA=10.0/CFIPC;CMDTB=0.5;CMDTC=0.0
    * ------------------------------------------------------------
    * GROUP 11. Initialization of variable or porosity fields
    * ------------------------------------------------------------
FIINIT(1R)=1.0;FIINIT(2R)=0.0
FIINIT(1W)=0.0;FIINIT(2W)=0.0;FIINIT(1V)=0.0;FIINIT(2V)=0.0
FIINIT(1U)=0.0;FIINIT(2U)=0.0;FIINIT(3U)=0.0;FIINIT(4U)=0.0
FIINIT(5U)=0.0
FIINIT(1D)=0.0;FIINIT(2D)=0.0;FIINIT(3D)=0.0;FIINIT(4D)=0.0
FIINIT(5D)=0.0
```

```
FIINIT(RHO2)=1.0;FIINIT(RHO1)=1.0
FIINIT(LIQ2)=0.0;FIINIT(LIQ1)=0.0
FIINIT(H1)=CPA*TAIR;FIINIT(H2)=CPA*TAIR
FIINIT(1AIR)=0.0;FIINIT(2AIR)=0.0
FIINIT(1MFR)=YFIN;FIINIT(2MFR)=YFIN
FIINIT(1FUE)=YFIN;FIINIT(2FUE)=YFIN

FIINIT(TMP1)=TAIR;FIINIT(TMP2)=TAIR
FIINIT(1SIZ)=INISIZ;FIINIT(2SIZ)=INISIZ
    * ------------------------------------------------------------
    * GROUP 12. Convection and diffusion adjustments
    * ------------------------------------------------------------
    * ------------------------------------------------------------
    * GROUP 13. Boundary conditions and special sources
    * ------------------------------------------------------------

            ^   y
            |                    frest
            -------------------------------
            |                              |
            | top                          |bottom
            |                              |
        --> inlet (--->)                   |
        -->   _.-._.-._.-._.-._.-._.-._.-._.-._.-._.-._.-._.|  --> z

    * --- Inlet (jet exit) ----------------------------------

PATCH(--->,LOW,1,1,1,NINLET,1,1,1,1000)

COVAL(--->,P2,FIXFLU,DENSIN*W2IN*R2IN)
COVAL(--->,2W,ONLYMS,W2IN);COVAL(--->,2SIZ,ONLYMS,INISIZ)
COVAL(--->,2MFR,ONLYMS,YFIN);COVAL(--->,2FUEL,ONLYMS,YFIN)
RG(43)=CPA*YAIN*(TAIR-TDROP)+YFIN*RG(41)
RG(44)=YFIN

COVAL(--->,P1,FIXFLU,DENSIN*W1IN*R1IN)
COVAL(--->,1W,ONLYMS,W1IN);COVAL(--->,1SIZ,ONLYMS,INISIZ)
COVAL(--->,1MFR,ONLYMS,YFIN);COVAL(--->,1FUEL,ONLYMS,YFIN)

COVAL(--->,1U,ONLYMS,1.38);COVAL(--->,2U,ONLYMS,3.0)
COVAL(--->,3U,ONLYMS,7.0);COVAL(--->,4U,ONLYMS,10.0)
COVAL(--->,5U,ONLYMS,8.5)

COVAL(--->,1D,ONLYMS,1.38);COVAL(--->,2D,ONLYMS,3.0)
COVAL(--->,3D,ONLYMS,7.0);COVAL(--->,4D,ONLYMS,10.0)
COVAL(--->,5D,ONLYMS,8.5)

    * --- Free-stream boundary conditions -------------------
    * --- Top
PATCH(TOP,CELL,1,1,NINLET+1,NY,1,1,1,1000)
COVAL(TOP,P1,FIXP,0.0);COVAL(TOP,P2,FIXP,0.0)
COVAL(TOP,1AIR,ONLYMS,1.0);COVAL(TOP,2AIR,ONLYMS,1.0)
RG(42)=CPA*(TAIR-TDROP)
    * --- Free stream
PATCH(FREST,CELL,1,1,NY,NY,1,NZ,1,1000)
COVAL(FREST,P1,FIXP,0.0);COVAL(FREST,P2,FIXP,0.0)
COVAL(FREST,1AIR,ONLYMS,1.0);COVAL(FREST,2AIR,ONLYMS,1.0)
```

```
    * --- Vapour sources ----------------------------------------
PATCH(VAPSOS,VOLUME,1,1,1,NY,1,NZ,1,1000)
COVAL(VAPSOS,2VAP,FIXFLU,GRND4);COVAL(VAPSOS,1VAP,FIXFLU,GRND4)

    * --- Droplet-number sources and sinks ---------------------
PATCH(DOM,VOLUME,1,1,1,NY,1,NZ,1,1000)
COVAL(DOM,1U,GRND,GRND1);COVAL(DOM,2U,GRND,GRND1)
COVAL(DOM,3U,GRND,GRND1);COVAL(DOM,4U,GRND,GRND1)
COVAL(DOM,1D,GRND,GRND1);COVAL(DOM,2D,GRND,GRND1)
COVAL(DOM,5U,GRND,GRND1)
COVAL(DOM,3D,GRND,GRND1);COVAL(DOM,4D,GRND,GRND1)
COVAL(DOM,5D,GRND,GRND1)

   * --- Fragment size: growth and diminuition ------------------
PATCH(E+A,VOLUME,1,NX,1,NY,1,NZ,1,1000)
COVAL(E+A,1SIZ,FIXFLU,GRND2);COVAL(E+A,2SIZ,FIXFLU,GRND2)
RG(23)=0.03

PATCH(TEAR,VOLUME,1,NX,1,NY,1,NZ,1,1000)
COVAL(TEAR,1SIZ,GRND3,0.0);COVAL(TEAR,2SIZ,GRND3,0.0)
RG(24)=0.01

   * --- Shear source -----------------------------------------
PATCH(SHSO,CELL,1,NX,1,NY,10,NZ,1,1000)
COVAL(SHSO,1V,FIXFLU,GRND5);COVAL(SHSO,2V,FIXFLU,GRND5)
RSG10=0.175

   * --- Combustion -------------------------------------------
PATCH(COMBUS,VOLUME,1,NX,1,NY,15,NZ,1,1000)
COVAL(COMBUS,1FUE,FIXFLU,GRND7);COVAL(COMBUS,2FUE,FIXFLU,GRND7)

    * ------------------------------------------------------------
    * GROUP 14. Downstream pressure for PARAB=.TRUE.
    * ------------------------------------------------------------
IPARAB=1
    * ------------------------------------------------------------
    * GROUP 15. Termination of sweeps
    * ------------------------------------------------------------
LITHYD=20
RESIDU=1.0E-14;RESREF(P1)=RESIDU
RESREF(1R)=RESIDU;RESREF(2R)=RESIDU
RESREF(1W)=RESIDU;RESREF(2W)=RESIDU
RESREF(1V)=RESIDU;RESREF(2V)=RESIDU
RESREF(2MFR)=RESIDU;RESREF(1MFR)=RESIDU
RESREF(2FUE)=RESIDU;RESREF(1FUE)=RESIDU
RESREF(1SIZ)=1.0E-15;RESREF(2SIZ)=1.0E-15
    *
RSIZ=1.0E-12
RESREF(1U)=RSIZ;RESREF(2U)=RSIZ;RESREF(3U)=RSIZ
RESREF(4U)=RSIZ;RESREF(5U)=RSIZ
RESREF(1D)=RSIZ;RESREF(2D)=RSIZ;RESREF(3D)=RSIZ
RESREF(4D)=RSIZ;RESREF(5D)=RSIZ
    * ------------------------------------------------------------
    * GROUP 16. Termination of iterations
    * ------------------------------------------------------------
    * ------------------------------------------------------------
```

```
    * GROUP 17. Under-relaxation devices
    * ------------------------------------------------------------
RLXCNT=1.0E-2
RELAX(P1,LINRLX,0.2)
RELAX(1V,FALSDT,RLXCNT/10.0);RELAX(2V,FALSDT,RLXCNT/10.0)
RELAX(TMP1,LINRLX,0.1);RELAX(TMP2,LINRLX,0.1)
RELAX(1R,LINRLX,0.1);RELAX(2R,LINRLX,0.1)
RELAX(DEN1,LINRLX,0.2);RELAX(DEN2,LINRLX,0.2)
    * ------------------------------------------------------------
    * GROUP 18. Limits on variables or increments to them
    * ------------------------------------------------------------
VARMAX(1V)=10.0;VARMAX(2V)=10.0
VARMIN(1V)=-10.0;VARMIN(2V)=-10.0
VARMIN(1SIZ)=1.0E-10;VARMIN(2SIZ)=1.0E-10
VARMAX(1SIZ)=0.1;VARMAX(2SIZ)=0.1

VARMIN(2VAP)=0.0;VARMIN(1VAP)=0.0
VARMIN(2AIR)=0.0;VARMIN(1AIR)=0.0
VARMIN(TMP1)=TDROP+1.0;VARMIN(TMP2)=TDROP+1.0
VARMIN(2PRD)=0.0;VARMIN(1PRD)=0.0
VARMIN(2FUE)=0.0;VARMIN(1FUE)=0.0
    * ------------------------------------------------------------
    * GROUP 19. Data communicated by satellite to GROUND
    * ------------------------------------------------------------
DWDY=T
    * Debug print-out
LG(1)=F
    * AVEL normalised ?
LG(6)=T
    * r (if F) or r-d (if T) average
LG(4)=T
    * Sdot=0 if IZ<=IG(3)
IG(3)=1
    * SHSO multiplied by l_prndtl/l
LG(8)=T
    * Fixing EL1 at IZ=1 (<0 => no intervention)
RG(26)=INISIZ
LG(9)=T
    * cmdot=0 if iz<ig(4)
IG(4)=4
    * cfips*rg(27) if iz<ig(5)
IG(5)=0;RG(27)=500.0
    * LG(9)=T selects SCRS2
LG(9)=T
    *
    * ------------------------------------------------------------
    * GROUP 20. Preliminary print-out
    * ------------------------------------------------------------
ECHO=T
    * ------------------------------------------------------------
    * GROUP 21. Print-out of variables
    * ------------------------------------------------------------
OUTPUT(1R,N,Y,N,Y,N,N)

OUTPUT(1D,N,N,N,N,N,N);OUTPUT(2D,N,N,N,N,N,N)
OUTPUT(3D,N,N,N,N,N,N);OUTPUT(4D,N,N,N,N,N,N)
OUTPUT(5D,N,N,N,N,N,N)
```

```
OUTPUT(1U,N,N,N,N,N,N);OUTPUT(2U,N,N,N,N,N,N)
OUTPUT(3U,N,N,N,N,N,N);OUTPUT(4U,N,N,N,N,N,N)
OUTPUT(5U,N,N,N,N,N,N)

OUTPUT(MAS1,N,N,N,N,N,N);OUTPUT(MAS2,N,N,N,N,N,N)
OUTPUT(1SIZ,N,N,N,N,N,N);OUTPUT(2SIZ,N,N,N,N,N,N)

OUTPUT(C2,N,N,N,N,N,N);OUTPUT(C5,N,N,N,N,N,N)
    * ------------------------------------------------------------
    * GROUP 22. Spot-value print-out
    * ------------------------------------------------------------
IYMON=1;TSTSWP=5;NPLT=1
    * ------------------------------------------------------------
    * GROUP 23. Field print-out and plot control
    * ------------------------------------------------------------
NZPRIN=2;IZPRF=20;IZPRL=100;IPROF=1;ORSIZ=0.4;ITABL=0

PATCH(CROS1,PROFIL,1,1,1,NY,1,NZ,1,1000)
PATCH(CROS2,PROFIL,1,1,1,NY,1,NZ,1,1000)
PLOT(CROS1,TMP1,-1.0,-1.0)
PLOT(CROS2,TMP2,-1.0,-1.0)
PLOT(CROS2,2VAP,-5.0,-5.0)
PLOT(CROS1,1VAP,-5.0,-5.0)
PLOT(CROS2,2PRD,-5.0,-5.0)
PLOT(CROS1,1PRD,-5.0,-5.0)
PLOT(CROS2,2FUE,-5.0,-5.0)
PLOT(CROS1,1FUE,-5.0,-5.0)
PLOT(CROS2,2AIR,-5.0,-5.0)
PLOT(CROS1,1AIR,-5.0,-5.0)


NAME(2R)=IN2R

PATCH(AX2,PROFIL,1,1,1,1,1,100,1,1000)
PLOT(AX2,TMP2,-4.0,-4.0)

PLOT(AX2,TMP1,-4.0,-4.0)

    * ------------------------------------------------------------
    * GROUP 24. Dumps for restarts
    * ------------------------------------------------------------
NSAVE=RPHI
NAME(LIQ1)=A.L1;NAME(LIQ2)=B.L2
NAME(SDT1)=C.S1;NAME(SDT2)=E.S2
NAME(TMP1)=1.T1;NAME(TMP2)=2.T2
NAME(1PRD)=PRD1;NAME(2PRD)=PRD2
NAME(1FUE)=FUE1;NAME(2FUE)=FUE2
NAME(1MFR)=N.M1;NAME(2MFR)=O.M2
NAME(2AIR)=OXI2;NAME(1AIR)=OXI1
NAME(2VAP)=VAP2;NAME(1VAP)=VAP1
STOP
```

Appendix D

FORTRAN coding

d.1 Introduction

GROUND is the FORTRAN subroutine of PHOENICS in which the user can insert his/her own coding to supplement or replace built-in features.

In the present work, coding was inserted in GROUND for, among others, the following purposes:-

- The computation of the forward step in the parabolic calculation;
- The computation of the source/sink terms in the equations for the fragment size;
- The set-up of the droplet-mass-fraction equations;
- The computation of the droplet-vaporisation rate, s'.
- The calculation of the fluid density, taking into account the mixture composition and the temperature;
- The coding of the combustion model, SCRS2;

The listing of the GROUND subroutine follows below. For the sake of compactness, all the auxilary coding (ie the coding which is not essential for the computations) has been withdrawn.

d.2 GROUND subroutine

```
C***************************************************************
C$DIR**GROUND
      SUBROUTINE GROUND
      INCLUDE '$.public.SATEAR'
      INCLUDE '$.public.GRDLOC'
      INCLUDE '$.public.GRDEAR'
      EQUIVALENCE (IZ,IZSTEP)
CXXXXXXXXXXXXXXXXXXXXXXXXXXXXXXXXXXXXXXXXX USER SECTION STARTS:
C
C 1   Set dimensions of data-for-GROUND arrays here. WARNING: the
C     corresponding arrays in the MAIN program of the satellite
C     and EARTH must have the same dimensions.
      COMMON/LGRND/LG(20)/IGRND/IG(20)/RGRND/RG(100)/CGRND/CG(10)
      LOGICAL LG
      CHARACTER*4 CG
C
C 2   User dimensions own arrays here, for example:
C     DIMENSION UUH(10,10),UUC(10,10),UUX(10,10),UUZ(10)
C
      DIMENSION WARR(200),ZNARR(200),ZARR(200),YARR(200)
      DIMENSION AVELO (100,1)
      DIMENSION CONAY(200),CONAW(200),ZOVD(200)
      DIMENSION DISTRI(10), DIAMET(11)
      DIMENSION SPS(10), SMS(10), COEFIC (10), ALS (10)
      LOGICAL FLUID1, QEQ, SCRS2
      INTEGER WHEREG, WHICHG
C
C 3   User places his data statements here, for example:
C     DATA NXDIM,NYDIM/10,10/
C
C 4   Insert own coding below as desired, guided by GREX examples.
C     Note that the satellite-to-GREX special data in the labelled
C     COMMONs /RSG/, /ISG/, /LSG/ and /CSG/ can be included and
C     used below but the user must check GREX for any conflicting
C     uses. The same comment applies to the EARTH-spare working
C     arrays EASP1, EASP2,....EASP10. If the call to GREX has been
C     deactivated then they can all be used without reservation.
C
C.....Functions to deal with the storage of size groups:
C
C     WHEREG (IPHASE, IGROUP) gives the INDVAR for group number
C            IGROUP of phase number IPHASE (1 or 2)
C     WHICHG (IPHASE, INDVAR) gives the group number of the group
C            stored in INDVAR
C
      WHEREG (IPHASE, IGROUP) = 29+IPHASE+2*(IGROUP-1)
      WHICHG (IPHASE, INDEXV) = (INDEXV-29-IPHASE)/2 + 1
C
      IXL=IABS(IXL)
C
          IF(IGR.EQ.13) GO TO 13
          IF(IGR.EQ.19) GO TO 19
       GO TO (1,2,3,4,5,6,7,8,9,10,11,12,13,14,15,16,17,18,19,20,21,
     122,23,24),IGR
```

```
 999 CONTINUE
     RETURN
C*****************************************************************
C
C--- GROUP 1. Run title and other preliminaries
C
    1 GO TO (1001,1002),ISC
 1001 CONTINUE
C
C..... The following provisions cater for all models, and
C      therefore some of them may not be useful (but otherwise
C      harmless) for particular cases
C
C.....Sub-section A: Provision of storage .....................
C
C.....EASP2 is used as a work space on an 'always-available' basis;
C     EASP3 and EASP4 are used as temporary storage in the print-out
C     section
C
      CALL MAKE (EASP2)
      CALL MAKE (EASP3)
      CALL MAKE (EASP4)
C
C.....LGEN1 is used in GREX2 to compute SHSO.
C
      CALL MAKE (LGEN1)
C
C.....DYG2D used to compute d(quantity)/dy
C
      CALL MAKE (DYG2D)
C
C.....YG2D used to compute jet width
C
      CALL MAKE (YG2D)
C
C.....LGEN2 stored if (dw2/dy)**2 is to be computed.
C
      CALL MAKE (LGEN2)
C
C.....EASP8, EASP9, and EASP10 stored for use in GXGENK + GXSQUR:-
C
      CALL MAKE (EASP8)
      CALL MAKE (EASP9)
      CALL MAKE (EASP10)
C
C.....Sub-section B: Data from Satellite .....................
C
C.....Limits of droplet size-groups
C
      NSIZ=IG(1)
      DO III=1, NSIZ+1
        DIAMET(III)=RG(III)
      END DO
C
C.....Other quantities
C
      SR    =RG(21)
```

```
      DENLIQ=RG(12)
      DENGAS=RG(20)
      DENVAP=RG(13)
      TDROP =RG(34)
      CPA   =TMP1A
      CPV   =TMP1B
      CPP   =TMP1C
      HLV   =RG(37)
      THCOND=RG(38)
      HCOMB =RG(41)
      STOICH=RG(35)
      HAIR  =RG(42)
      HIN   =RG(43)
      AMIXIN=RG(44)
      FORMF =RG(18)
      DEBU  =LG(1)
      FACTOR=RG(30)
      WIN   =RG(15)
      DIN   =RG(16)
      RATMIN=RG(17)
      SCRS2 =LG(9)
C
C.....Sub-section C: internal settings and initialisations .......
C
C     Integer indices for some STOREd variables:
C     ------------------------------------------------------------
C     ILIQi  ... Liquid mass-fraction of phase i
C     IVAPi  ... Vapour mass-fraction of phase i
C     IAIRi  ... Air/Oxidant mass-fraction of phase i
C     IPRODi ... Prod mass-fraction of phase i (only for comb spray)
C     IMFRi  ... Mixture fraction of phase i (only if SCRS2)
C     IFUEi  ... Fuel mass-fraction of phase i
C     IMASSi ... Mass from drops to gas owing to vaporisation
C     ISDOTi ... Sdot for phase i
C
      ILIQ1 = 27
      ILIQ2 = 26
      IVAP1 = 22
      IVAP2 = 23
      IAIR1 = 46
      IAIR2 = 47
      IPRD1 = 48
      IPRD2 = 49
      IMASS1= 25
      IMASS2= 24
      ISDOT1= 21
      ISDOT2= 12
      IMFR1 = 42
      IMFR2 = 43
      IFUE1 = 40
      IFUE2 = 41
C
C.....FSTOIC
C
      FSTOIC=1.0/(1.0+STOICH)
C
C.....Some coefficients for the m-equations are assembled here
```

```
C     (not for the smallest size group, ie, NSIZ)
C
      DO 1004, JJJ=1, NSIZ-1
        SPS (JJJ) = DIAMET (JJJ)**2+DIAMET(JJJ+1)**2
        SMS (JJJ) = DIAMET (JJJ)**2-DIAMET(JJJ+1)**2
        SPS (JJJ) = 1.0 / SPS(JJJ)
        SMS (JJJ) = 1.0 / SMS (JJJ)
        IF (DIAMET (JJJ+1).LE.0.0) THEN
          STOP ' Droplet diameter <= 0 !'
        ELSE
          ALS (JJJ) = 2.0*ALOG (DIAMET(JJJ)/DIAMET(JJJ+1))
        END IF
        COEFIC (JJJ) = SMS (JJJ) * (1.0 + ALS(JJJ)*FORMF)
 1004 CONTINUE
C     Smallest group practices ...
      COEFIC (NSIZ) = 2.0*FORMF/(DIAMET(NSIZ)**2)
C
C.....This is to avoid the (possible) dangers of width=0.0
C
      IF (YVLAST.EQ.0.0) THEN
        STOP ' !!!! YVLAST = 0.0 in GROUND !'
      ELSE
        WID=YVLAST/2.0
        WIDHAF=YVLAST/2.0
      END IF
C
C.....Initialisations for LSQA02-INC
C
      SXW   =0.0
      SX2W  =0.0
      SYW   =0.0
      SXYW  =0.0
      SXY   =0.0
      SX2Y  =0.0
      SYY   =0.0
      SXYY  =0.0
      NDATA =0
C
      RETURN
 1002 CONTINUE
      RETURN
C*****************************************************************
C
C--- GROUP 2. Transience; time-step specification
C
    2 CONTINUE
      RETURN
C*****************************************************************
C
C--- GROUP 3. X-direction grid specification
C
    3 CONTINUE
      RETURN
C*****************************************************************
C
C--- GROUP 4. Y-direction grid specification
C
```

```
    4 CONTINUE
      RETURN
C*****************************************************************
C
C--- GROUP 5. Z-direction grid specification
C
    5 CONTINUE
C
C.....Include-file name: STEP08-INC ..... Start
C     Insertion in:      Group 5
C     Date:              01.03.88/07.03.88
C     Purpose:           Computation of z-step in a PARABolic computa-
C                        tion as a fraction of jet width
C
C.....Width of z-step = fraction of  jet width
C
      IF ((.NOT.PARAB).OR.(.NOT.LG(5)))   RETURN
      IF (AZDZ.EQ.GRND) DZ=RG(14)*WID
C
C.....End of STEP08-INC ..... End
C
      IF (DEBU) WRITE (6, *) 'G5: DZ set to ', DZ
C
      RETURN
C*****************************************************************
C
C--- GROUP 6. Body-fitted coordinates or grid distortion
C
    6 CONTINUE
      RETURN
C*****************************************************************
C
C--- GROUP 7. Variables stored, solved & named
    7 CONTINUE
      RETURN
C*****************************************************************
C
C--- GROUP 8. Terms (in differential equations) & devices
C
    8 GO TO (81,82,83,84,85,86,87,88,89,810,811,812,813,814,815)
     1,ISC
   81 CONTINUE
C   * -------------------- SECTION  1 --------------------------
C    For U1AD.LE.GRND--- phase 1 additional velocity (VELAD).
      RETURN
   82 CONTINUE
C   * -------------------- SECTION  2 --------------------------
C    For U2AD.LE.GRND--- phase 2 additional velocity (VELAD).
      RETURN
   83 CONTINUE
C   * -------------------- SECTION  3 --------------------------
C    For V1AD.LE.GRND--- phase 1 additional velocity (VELAD).
      RETURN
   84 CONTINUE
C   * -------------------- SECTION  4 --------------------------
C    For V2AD.LE.GRND--- phase 2 additional velocity (VELAD).
      RETURN
```

```
   85 CONTINUE
C    * ------------------- SECTION  5 --------------------------
C     For W1AD.LE.GRND--- phase 1 additional velocity (VELAD).
      RETURN
   86 CONTINUE
C    * ------------------- SECTION  6 --------------------------
C     For W2AD.LE.GRND--- phase 2 additional velocity (VELAD).
      RETURN
   87 CONTINUE
C    * ------------------- SECTION 7 ---- VOLUMETRIC SOURCE FOR GALA
      RETURN
   88 CONTINUE
C    * ------------------- SECTION 8 --- CONVECTION FLUXES
      RETURN
   89 CONTINUE
C    * ------------------- SECTION 9 --- DIFFUSION COEFFICIENTS
      RETURN
  810 CONTINUE
C    * ------------------- SECTION 10 --- CONVECTION NEIGHBOURS
      RETURN
  811 CONTINUE
C    * ------------------- SECTION 11 --- DIFFUSION NEIGHBOURS
      RETURN
  812 CONTINUE
C    * ------------------- SECTION 12 --- LINEARISED SOURCES
      RETURN
  813 CONTINUE
C    * ------------------- SECTION 13 --- CORRECTION COEFFICIENTS
      RETURN
  814 CONTINUE
C    * ------------------- SECTION 14 --- USER'S SOLVER
      RETURN
  815 CONTINUE
C    * ------------------- SECTION 15 --- CHANGE SOLUTION
      RETURN
C    * Make all other group-8 changes in group 19.
C*****************************************************************
C
C--- GROUP 9. Properties of the medium (or media)
C
C    The sections in this group are arranged sequentially in their
C    order of calling from EARTH. Thus, as can be seen from below,
C    the temperature sections (10 and 11) precede the density
C    sections (1 and 3); so, density formulae can refer to
C    temperature stores already set.
    9 GO TO (91,92,93,94,95,96,97,98,99,900,901,902,903),ISC
C*****************************************************************
  900 CONTINUE
C    * ------------------- SECTION 10 --------------------------
C     For TMP1.LE.GRND--------- phase-1 temperature Index AUX(TEMP1)
C
C.....This is to compute, in the combusting spray,  the temperature
C     of the mixture as:
C              T=Tr+(h-yf*HCOMB)/(yv*Cpv+yg*Cpg+yp*Cpp)
C     where Tr=ref temperature=droplet temperature
C
C     Note that the temperature of both phases is computed here; the
```

```
C     adequate variables are chosen according to the value of ISC.
C
      IF (TMP1.NE.GRND) RETURN
  901 CONTINUE
      IF (TMP2.NE.GRND) RETURN
      IF (DEBU) WRITE (6, *) ' G9S10: Entering compu of temp '
      L0E=L0F(EASP2)
      IF (ISC.EQ.10) THEN
        L0T=L0F(AUX(TEMP1))
        L0V=L0F(IVAP1)
        L0A=L0F(IAIR1)
        L0P=L0F(IPRD1)
        L0H=L0F(H1)
        L0FU=L0F(IFUE1)
        L0M=L0F(IMFR1)
        IPHASE=1
      ELSE
        L0T=L0F(AUX(TEMP2))
        L0V=L0F(IVAP2)
        L0A=L0F(IAIR2)
        L0P=L0F(IPRD2)
        L0H=L0F(H2)
        L0FU=L0F(IFUE2)
        L0M=L0F(IMFR2)
        IPHASE=2
      END IF
C
C.....The following lines are to compute the liquid mass-fraction
C
      CALL FN1  (EASP2, 0.0)
C     NB: The smallest size group is excluded from the next loop
      DO  IGROUP=1, NSIZ-1
        INDEXG = WHEREG (IPHASE, IGROUP)
        CALL FN34 (EASP2, INDEXG, 1.0/SMS(IGROUP))
      END DO
C     Special practices for the smallest size group
      CALL FN34 (EASP2, WHEREG(IPHASE,NSIZ), 0.5*DIAMET(NSIZ)**2)
C     Mutiplication for the scaling factor for m
      CALL FN25 (EASP2, FACTOR)
C
C.....EASP2 has now the liquid mass-fraction
C
C.....Products, air and vapour mass-fractions and the temperature are
C     set below depending on whether SCRS2.
C
      IF (.NOT.SCRS2) THEN
        DO II=1, NX*NY
          IF (SOLVE(IAIR1)) THEN
            F(L0P+II)=1.0-F(L0V+II)-F(L0E+II)-F(L0A+II)
            F(L0P+II)=MAX(0.0, F(L0P+II))
          ELSE
            F(L0A+II)=1.0-F(L0V+II)-F(L0E+II)-F(L0P+II)
            F(L0A+II)=MAX(0.0, F(L0A+II))
          END IF
          F(L0T+II)=F(L0H+II)/(F(L0V+II)*CPV
     >              +F(L0A+II)*CPA+CPP*F(L0P+II))+TDROP
        END DO
```

```
      ELSE
        IF (.NOT.SOLVE(H1)) THEN
C         The enthalpy is set here as a funct of the scalar
          DO II=1, NX*NY
            F(L0H+II)=HAIR+F(L0M+II)*(HIN-HAIR)/AMIXIN
          END DO
        END IF
        DO II=1, NX*NY
          F(L0V+II)=F(L0FU+II)-F(L0E+II)
          F(L0A+II)=1.0+F(L0FU+II)*(1./FSTOIC-1.)-F(L0M+II)/FSTOIC
          IF (DEBU) WRITE (6, *) ' II, AIR FU MF ',
     >                  II,F(L0A+II),F(L0FU+II),F(L0M+II)
          F(L0P+II)=1.0-F(L0A+II)-F(L0FU+II)
          IF (DEBU) WRITE (6, *) ' II, AIR VAP PROD ',
     >                  II,F(L0A+II),F(L0V+II),F(L0P+II)
          F(L0T+II)=F(L0H+II)-F(L0FU+II)*HCOMB
          F(L0T+II)=F(L0T+II)/(F(L0V+II)*CPV
     >              +F(L0A+II)*CPA+CPP*F(L0P+II))+TDROP
        END DO
      END IF
C
      IF (DEBU) WRITE (6, *) ' G9S10: Tmp set. Phase: ',IPHASE
      RETURN
C
C 901 CONTINUE
C   * ------------------- SECTION 11 ----------------------------
C    For TMP2.LE.GRND--------- phase-2 temperature Index AUX(TEMP2)
C
C     RETURN
  902 CONTINUE
C   * ------------------- SECTION 12 ----------------------------
C    For EL1.LE.GRND--------- phase-1 length scale Index AUX(LEN1)
C
C.....Include-file name: SIZE18-INC ........................... Start
C     Insertion in:      Group 9 Section 12
C     Date:              25.03.88/12.04.88
C     Purpose:           Computation of fragment size as MIN (C3,C4)
C
      IF (EL1.EQ.GRND) THEN
        IF ((IZ.EQ.1).AND.(RG(26).GE.0.0)) THEN
          WRITE (2, *) ' RG(26) @ IZ=1 ... ', RG(26)
          CALL FN1 (AUX(LEN1),RG(26))
        ELSE
          L0C3=L0F(C3)
          L0C4=L0F(C4)
          L0L1=L0F(AUX(LEN1))
          DO II=1, NX*NY
            F(L0L1+II)=MIN(F(L0C3+II),F(L0C4+II))
          END DO
        END IF
      END IF
C
C.....End of SIZE18-INC ....................................... End
C
      RETURN
  903 CONTINUE
C   * ------------------- SECTION 13 ----------------------------
```

```
C     For EL2.LE.GRND--------- phase-2 length scale Index AUX(LEN2)
C
      RETURN
   91 CONTINUE
C    * -------------------- SECTION  1 --------------------------
C     For RHO1.LE.GRND--- density for phase 1 Index AUX(DEN1).
C
C     NB: Both RHO1 and RHO2 are computed here, since the 93 flag
C         has  been moved to this section. ISC decides on which
C         variables (phase 1 or 2) are employed
C
      IF (RHO1.NE.GRND) RETURN
   93 CONTINUE
      IF (RHO2.NE.GRND) RETURN
      IF (ISC.EQ.1) THEN
        IPHASE=1
        ILIQ  =ILIQ1
        IVAP  =IVAP1
        IAXDEN=AUX(DEN1)
        IF (TEMP0.LT.0.0) THEN
          L0D=L0F(AUX(DEN1))
          L02=L0F(EASP2)
          L0T=L0F(TEMP1)
          L0V=L0F(IVAP1)
          L0A=L0F(IAIR1)
          L0PR=L0F(IPRD1)
          L0L=L0F(ILIQ1)
          L0P=L0F(P1)
          IF (SCRS2) THEN
            L0FU=L0F(IFUE1)
            L0M =L0F(IMFR1)
          END IF
        END IF
      ELSE
        IPHASE=2
        ILIQ  =ILIQ2
        IVAP  =IVAP2
        IAXDEN=AUX(DEN2)
        IF (TEMP0.LT.0.0) THEN
          L0D=L0F(AUX(DEN2))
          L02=L0F(EASP2)
          L0T=L0F(TEMP2)
          L0V=L0F(IVAP2)
          L0A=L0F(IAIR2)
          L0PR=L0F(IPRD2)
          L0L=L0F(ILIQ2)
          L0P=L0F(P1)
          IF (SCRS2) THEN
            L0FU=L0F(IFUE2)
            L0M =L0F(IMFR2)
          END IF
        END IF
      END IF
C
C.....The following lines are to compute the liquid mass-fraction
C
```

```
      CALL FN1  (ILIQ, 0.0)
C     NB: The smallest size group-is excluded from the next loop
      DO  IGROUP=1, NSIZ-1
        INDEXG = WHEREG (IPHASE, IGROUP)
        CALL FN34 (ILIQ, INDEXG, 1.0/SMS(IGROUP))
      END DO
C     Special practices for the smallest size group
      CALL FN34 (ILIQ, WHEREG(IPHASE,NSIZ), 0.5*DIAMET(NSIZ)**2)
C     Mutiplication for the scaling factor for m
      CALL FN25 (ILIQ, FACTOR)
C
C.....LVOL has now the liquid mass-fraction
C
C
C.....Case A: Cold spray.....................................
C
      IF (SR.EQ.0.0) THEN
        CALL FN6  (IAXDEN, ILIQ, 1.0, DENGAS-DENLIQ)
        CALL FN25 (IAXDEN, DENGAS)
      END IF
C
C.....End of Case A: cold spray .............................
C
      IF (SR.NE.0.0) THEN
        CALL FN10 (EASP2, IVAP, ILIQ, 1.0, -1.0, -1.0)
C
C.......TEMP0<0 is the flag to activate the computation of gas
C       and vapour densities from ideal-gas laws.
C
        IF (TEMP0.GE.0.0) THEN
C
C.....Case B: evaporating spray .............................
C
          CALL FN12 (EASP3, ILIQ, IVAP, EASP2, 0.0,
     >               1.0/DENLIQ, 1.0/DENVAP, 1.0/DENGAS)
          CALL FN28 (IAXDEN, EASP3, 1.0)
C
C.....End of Case B: evaporating spray ......................
C
        ELSE
C
C..... Case C: combusting spray .............................
C
C.......Products, air and vapour mass-fractions are set below
C       depending on whether SCRS2.
C
          IF (.NOT.SCRS2) THEN
            DO II=1, NX*NY
              IF (SOLVE(IAIR1)) THEN
                F(L0PR+II)=1.0-F(L0V+II)-F(L0L+II)-F(L0A+II)
              ELSE
                F(L0A+II)=1.0-F(L0V+II)-F(L0L+II)-F(L0PR+II)
              END IF
            END DO
          ELSE
            DO II=1, NX*NY
              F(L0V+II)=F(L0FU+II)-F(L0L+II)
              F(L0A+II)=1.0+F(L0FU+II)*(1./FSTOIC-1.)-F(L0M+II)/FSTOIC
```

```
              F(L0PR+II)=1.0-F(L0A+II)-F(L0FU+II)
            END DO
          END IF
          DO II=1, NX*NY
            DENSIT=F(L0L+II)/DENLIQ
            DENSIT=DENSIT+8314.3*(F(L0T+II)+ABS(TEMP0))
     >             *(1.0/(F(L0P+II)+PRESS0))*
     >              (F(L0A+II)/RHO1A+F(L0V+II)/RHO1B+F(L0PR+II)/RHO1C)
            F(L0D+II)=1.0/DENSIT
          END DO
        END IF
C
C.....End of Case C: combusting spray ..............................
C
      END IF
C
      IF (DEBU) WRITE(6,*) 'G9S3: DENS computed; IPHASE: ',IPHASE
C
      RETURN
   92 CONTINUE

C   * -------------------- SECTION  2 ----------------------------
C    For DRH1DP.LE.GRND--- D(LN(DEN))/DP for phase 1 (D1DP).
      RETURN
C   93 CONTINUE
C   * -------------------- SECTION  3 ----------------------------
C    For RHO2.LE.GRND--- density for phase 2 Index AUX(DEN2).
C
C      RETURN
   94 CONTINUE
C   * -------------------- SECTION  4 ----------------------------
C    For DRH2DP.LE.GRND--- D(LN(DEN))/DP for phase 2 (D2DP).
      RETURN
   95 CONTINUE
C   * -------------------- SECTION  5 ----------------------------
C    For ENUT.LE.GRND--- reference turbulent kinematic viscosity.
C
C
C.....Include-file name: ENUT05-INC ............................. Start
C     Insertion in:      Group 9 Section 5
C     Date:              29.02.88
C     Purpose:           Choice of:-
C                     1. Absolute value of ENUT as computed in GXENUT
C                        when ENUT=GRND4
C                     2. Prandtl mixing-length model based upon r- or
C                        r*density-averaged W
C     Activation:     1. ENUT=GRND4
C                     2. ENUT=GRND
C
C
C.....Use of 2-f model viscosity with non-up_&_down models
C
      IF (ENUT.EQ.GRND4) CALL FN40 (AUX(VIST))
C
      IF (ENUT.NE.GRND) RETURN
C
C......Prandtl mixing-length for 2-f models
```

```
C
C       Y=A+B*X1*X : Y         X1         X2     A     B
        CALL FN21 (AUX(VIST),AUX(LEN1),AUX(LEN1),0.0,ENUTA)
C
C       Average
C       CALL FNAV (AUX(VIST),EASP2,'NORTH')
C
        IF (LG(4)) THEN
          CALL FNDRAV (EASP2,R1,DEN1,W1,R2,DEN2,W2)
        ELSE
C         Y=A*X1*X2+B*X3*X4      Y   X1  X2  X3  X4   A    B
          CALL FN48          (EASP2, R1, W1, R2, W2, 1.0, 1.0)
        END IF
C
C       Y=X(J+1)-X(J)   Y       X   DIR
        CALL FN103     (EASP2, EASP2, 1)
C
C       EASP2 (ny) = EASP2 (ny-1)
        L0SP2=L0F(EASP2)
        F(L0SP2+NY+(IX-1)*NY)=F(L0SP2+NY-1+(IX-1)*NY)
C
C       Y=A*X1*X2/X3         Y    X1         X2    X3    A
        CALL FN56     (AUX(VIST),EASP2,AUX(VIST),DYG2D,1.0)
C
C       Y=ABS(Y)
        CALL FN40 (AUX(VIST))
C
C......End of ENUT05-INC ..................................... End
C
C
      RETURN
   96 CONTINUE
C    * -------------------- SECTION  6 --------------------------
C     For ENUL.LE.GRND--- reference laminar kinematic viscosity.
      RETURN
   97 CONTINUE
C    * -------------------- SECTION  7 --------------------------
C     For PRNDTL( ).LE.GRND--- laminar PRANDTL nos., or diffusivity.
      RETURN
   98 CONTINUE
C    * -------------------- SECTION  8 --------------------------
C     For PHINT( ).LE.GRND--- interface value of first phase(FII1).
      RETURN
   99 CONTINUE
C    * -------------------- SECTION  9 --------------------------
C     For PHINT( ).LE.GRND--- interface value of second phase(FII2)
      RETURN
C*****************************************************************
C
C--- GROUP 10. Inter-phase-transfer processes and properties
C
   10 GO TO (101,102,103,104),ISC
  101 CONTINUE
C    * -------------------- SECTION  1 --------------------------
C     For CFIPS.LE.GRND--- inter-phase friction coeff. AUX(INTFRC).
C
C.....Special pratices for IZ<=IG(5)
```

```
C
      IF (IZ.LE.IG(5)) CALL FN25 (AUX(INTFRC), RG(27))
C
      RETURN
  102 CONTINUE
C   * -------------------- SECTION  2 --------------------------
C    For CMDOT.EQ.GRND- inter-phase mass transfer Index AUX(INTMDT)
C
C.....Mass transfer cut off if IZ<=IG(4)
C
      IF (IZ.LE.IG(4)) CALL FN1 (AUX(INTMDT),0.0)
C
      RETURN
  103 CONTINUE
C   * -------------------- SECTION  3 --------------------------
C    For CINT( ).EQ.GRND--- phase1-to-interface transfer
C                                              coefficients (COI1)
      RETURN
  104 CONTINUE
C   * -------------------- SECTION  4 --------------------------
C    For CINT( ).EQ.GRND--- phase2-to-interface transfer
C                                             coefficients (COI2)
      RETURN
C*********************************************************************
C
C--- GROUP 11. Initialization of variable or porosity fields
C
   11 CONTINUE
      RETURN
C*********************************************************************
C
C--- GROUP 12. Convection and diffusion adjustments
C
   12 CONTINUE
      RETURN
C*********************************************************************
C
C--- GROUP 13. Boundary conditions and special sources
C
   13 CONTINUE
      GO TO (130,131,132,133,134,135,136,137,138,139,1310,
     11311,1312,1313,1314,1315,1316,1317,1318,1319,1320,1321),ISC
  130 CONTINUE
C------------------- SECTION  1 ------------- coefficient = GRND
C
C.....This is to compute the coefficient in the source-term of
C     the m-equation (NB: Vaporisation is assumed).
C     The coding is common for both phases; the appropriate
C     indices are selected below.
C
      IF (FLUID1(INDVAR)) THEN
        IPHASE=1
        INDR=R1
        INDDEN=AUX(DEN1)
        ISDOT=ISDOT1
      ELSE
        IPHASE=2
```

```
        INDR=R2
        INDDEN=AUX(DEN2)
        ISDOT=ISDOT2
      END IF
C
      IF (SR.EQ.0.0) THEN
C       Avoids complications ...
        CALL FN1 (CO, 0.0)
        RETURN
      END IF
C
      IGROUP=WHICHG (IPHASE,INDVAR)
C     Y = A X1 X2 X3 :   Y     X1    X2     X3    ----- A -----
      CALL FN55         (CO, ISDOT, INDDEN, INDR, COEFIC(IGROUP))
C
      RETURN
  131 CONTINUE
C------------------- SECTION  2 ------------- coefficient = GRND1
C
      RETURN
  132 CONTINUE
C------------------- SECTION  3 ------------- coefficient = GRND2
C
      RETURN
  133 CONTINUE
C------------------- SECTION  4 ------------- coefficient = GRND3
C
C.....Include-file name: FDIM16-INC ........................... Start
C     Insertion in:      Group 13 Section 4
C     Date:              24.03.88/21.07.88
C     Purpose:           Source term due to shear in the
C                        fragment-size equations
C     Activation:        From Q1 when NPATCH='TEAR' and coeff=GRND3
C
      IF (NPATCH.EQ.'TEAR') THEN
        IF (INDVAR.EQ.C3) THEN
          INDR=R1
          INDL=LGEN1
          IPH=1
          INDD=DEN1
        ELSE IF (INDVAR.EQ.C4) THEN
          INDR=R2
          INDL=LGEN2
          IPH=2
          INDD=DEN2
        END IF
      END IF
      INDL=EASP2
      CALL GXSQUR (IPH-1, PARAB, NX, NY, NZ, INDL)
C     Y = Y**A      Y     A
      CALL FN51    (INDL, 0.5)
C     Y=A*X1*X2*X3   Y    X1    X2    X3     A
      CALL FN55     (CO, INDR, INDL, INDD, RG(24))
C
C.....End of FDIM16-INC ....................................... End
C
      RETURN
```

```
  134 CONTINUE
C------------------- SECTION  5 ------------- coefficient = GRND4
C
C.....This is to compute the source of vapour owing to droplet
C     vaporisation. It is computed as a source per unit volume of
C         (0.0+mass)(1.0-phi), where mass is given by the variables
C     IMASS1 and IMASS2 (MAS1 and MAS2 in Q1)
C
      IF (NPATCH.EQ.'VAPSOS') THEN
        IF (FLUID1(INDVAR)) THEN
          INDMAS=IMASS1
        ELSE
          INDMAS=IMASS2
        END IF
        CALL FN0 (CO, INDMAS)
      END IF
C
      RETURN
  135 CONTINUE
C------------------- SECTION  6 ------------- coefficient = GRND5
      RETURN
  136 CONTINUE
C------------------- SECTION  7 ------------- coefficient = GRND6
      RETURN
  137 CONTINUE
C------------------- SECTION  8 ------------- coefficient = GRND7
C
C.....Provisions for combustion processes: sink of fuel
C
      IF (NPATCH.EQ.'COMBUS') THEN
        IF (FLUID1(INDVAR)) THEN
          INDVAP=IVAP1
          INDAIR=IAIR1
          INDTEM=TEMP1
          INDR=  R1
        ELSE
          INDVAP=IVAP2
          INDAIR=IAIR2
          INDTEM=TEMP2
          INDR=  R2
        END IF
C
C.......The exponential part of the reaction rate is assembled
C       here, and will be multiplied by the adequate mass-fraction
C       depending on the variable
C
        CALL FN1  (CO, RG(39))
        CALL FN32 (CO, INDTEM, -RG(40), ABS(TEMP0))
C
        IF ((INDVAR.EQ.IVAP1).OR.(INDVAR.EQ.IVAP2)) THEN
C         Reaction_rate/Yvap to CO
          CALL FN26 (CO, INDAIR)
        END IF
        IF ((INDVAR.EQ.IAIR1).OR.(INDVAR.EQ.IAIR2)) THEN
C         Reaction_rate/Yair to CO
          CALL FN26 (CO, INDVAP)
C         Multiplication by the stoichiometric ratio
```

```
          CALL FN25 (CO, STOICH)
        END IF
        CALL FN26 (CO, INDR)
      END IF
C
      RETURN
  138 CONTINUE
C------------------- SECTION  9 ------------- coefficient = GRND8
      RETURN
  139 CONTINUE
C------------------- SECTION 10 ------------- coefficient = GRND9
      RETURN
 1310 CONTINUE
C------------------- SECTION 11 ------------- coefficient = GRND10
      RETURN
 1311 CONTINUE
C------------------- SECTION 12 --------------------- value = GRND
C
      RETURN
 1312 CONTINUE
C------------------- SECTION 13 --------------------- value = GRND1
C
C.....This is to compute the values in the source-terms of the
C     m-equations (NB: Vaporisation is assumed); and also the
C     mass transferred to the gas phase (IMASS1 and IMASS2). The
C     latter is computed first.
C     The coding is common for both phases; the appropriate indices
C     in each case are chosen now
C
      IF (FLUID1(INDVAR)) THEN
        IPHASE=1
        INDMAS=IMASS1
        INDR  =R1
        INDDEN=DEN1
        ISDOT =ISDOT1
      ELSE
        IPHASE=2
        INDMAS=IMASS2
        INDR  =R2
        INDDEN=DEN2
        ISDOT =ISDOT2
      END IF
C
C.....Time-saving practices for Sdot=0.0, 11.03.88
C
      CALL FN65 (INDMAS, VAL, 0.0)
      IF (SR.EQ.0.0) RETURN
C
C.....NB: The smallest size group is excluded from the next loop
C
      DO  IGROUP=1, NSIZ-1
        INDEXG=WHEREG(IPHASE,IGROUP)
        CALL FN34 (INDMAS, INDEXG, 3.0*ALS (IGROUP)/2.0)
      END DO
C
C.....Special practices for the smallest size group
C
```

```
      CALL FN34 (INDMAS, WHEREG(IPHASE,NSIZ), 3.0/2.0)
C
      CALL FN55 (INDMAS, INDMAS, ISDOT, INDDEN, FACTOR)
      CALL FN26 (INDMAS, INDR)
C
C.....So far for INDMAS. Now the value of the source term
C
      IGROUP=WHICHG(IPHASE,INDVAR)
C
C.... The VALue is 0.0 for the largest size (ie IGROUP=1)
C
      IF (IGROUP.NE.1) THEN
        IF (IGROUP.EQ.NSIZ) THEN
C         Special practices for the smallest size group:
          CALL FN1 (VAL, 1.0/FORMF)
        ELSE
          CALL FN1  (VAL, SMS (IGROUP) / COEFIC (IGROUP))
        END IF
        CALL FN26 (VAL, INDVAR-1)
      END IF
C
      RETURN
 1313 CONTINUE
C------------------- SECTION 14 -------------------- value = GRND2
C.....Include-file name: FGRO15-INC ........................... Start
C     Insertion in:      Group 13 Section 14
C     Date:              24.03.88/25.07.88
C     Purpose:           Source term due to entrainment and agglome-
C                        ration in the fragment-size equations
C     Activation:        From Q1 when NPATCH='E+A' and value=GRND2
C
      IF (NPATCH.EQ.'E+A') THEN
        IF (INDVAR.EQ.C3) THEN
          INDR=R1
          INDD=DEN1
        ELSE IF (INDVAR.EQ.C4) THEN
          INDR=R2
          INDD=DEN2
        END IF
C
        L0R=L0F(INDR)
        L0D=L0F(INDD)
        L0W1=L0F(W1)
        L0W2=L0F(W2)
        L0V1=L0F(V1)
        L0V2=L0F(V2)
        L0VAL=L0F(VAL)
        DO II=1, NY
          F(L0VAL+II)=SQRT((F(L0V1+II)-F(L0V2+II))**2
     >               +     (F(L0W1+II)-F(L0W2+II))**2)
     >               *      F(L0D+II)*F(L0R+II)*RG(23)
        END DO
      END IF
C
C.....End of FGRO15-INC ....................................... End
C
      RETURN
```

```
 1314 CONTINUE
C---------------------- SECTION 15 -------------------- value = GRND3
C
C.....Source of momentum owing to gravity
C
      IF (NPATCH.EQ.'GSOM') THEN
        IF (INDVAR.EQ.W1) THEN
          INDDEN=DEN1
        ELSE
          INDDEN=DEN2
        END IF
        CALL FN2 (VAL, INDDEN, -DENGAS*9.8,9.8)
      END IF
C
      RETURN
 1315 CONTINUE
C-------------------- SECTION 16 -------------------- value = GRND4
C
C.....Source of vapour mass-fraction as FIXFLU of INDMAS
C
      IF (NPATCH.EQ.'VAPSOS') THEN
        IF (FLUID1(INDVAR)) THEN
          INDMAS=IMASS1
        ELSE
          INDMAS=IMASS2
        END IF
C
        CALL FN0 (VAL, INDMAS)
C
      END IF
C
      RETURN
 1316 CONTINUE
C-------------------- SECTION 17 -------------------- value = GRND5
C
C.....Include-file name: MYSH04-INC ........................... Start
C     Insertion in:      Group 13 Section 17
C     Date:              29.02.88/20.07.88
C     Purpose:        1. Change of sign of built-in SHSO (GXSHSO) and
C                     2. Duplication of the coding here (research
C                        purposes).
C                     3. 1 multiplied by l_prndtl/l
C
C     Activation:        1 active if the patch name is SHSO;
C                        2 active if the patch name is MYSHSO;
C                        3 active if 1 active and LG(8)=T.
C
C.....This is to change the sign of the shear source provided
C     in GXSHSO. Fluid=2 => source > 0.
C
      IF (NPATCH.EQ.'SHSO') THEN
C       Y=A*Y       Y     A
        CALL FN25 (VAL, -1.0)
        IF (LG(8)) THEN
          CALL FN25 (VAL, EL1B*ZW)
C         Y=Y/X       Y       X
          CALL FN27 (VAL, AUX(LEN1))
```

```
        END IF
        L0VAL=L0F(VAL)
        F(L0VAL+NY)=0.0
      ELSE IF (NPATCH.EQ.'MYSHSO') THEN
C
C....This is to compute the source, taking into account the
C    volume fractions r1, r2.
C
C       Y=A+B*X1*X : Y        X1         X2      A  B
        CALL FN21 (EASP2,AUX(INTFRC),AUX(LEN1),0.0,1.0)
C
C       Average
        CALL FNAV (VAL,EASP2,'NORTH')
C
        IF (LG(4)) THEN
          CALL FNDRAV (EASP2,R1,DEN1,W1,R2,DEN2,W2)
        ELSE
C         Y=A*X1*X2+B*X3*X4      Y   X1  X2  X3  X4   A    B
          CALL FN48          (EASP2, R1, W1, R2, W2, 1.0, 1.0)
        END IF
C
C       Y=X(J+1)-X(J)    Y        X   DIR
        CALL FN103     (EASP2, EASP2, 1)
C
C       Y=A*X1*X2/X3  Y    X1   X2   X3     A
        CALL FN56     (VAL,EASP2,VAL,DYG2D,RSG10)
C
C       Y=ABS(Y)
        CALL FN40 (VAL)
C
        IF (INDVAR.EQ.V1) CALL FN25 (VAL, -1.0)
      END IF
C
C.....End of MYSH04-INC ..................................... End
C
      RETURN
 1317 CONTINUE
C------------------- SECTION 18 -------------------- value = GRND6
      RETURN
 1318 CONTINUE
C------------------- SECTION 19 -------------------- value = GRND7
C
C.....Provisions for combustion processes
C
      IF (NPATCH.EQ.'COMBUS') THEN
        IF (FLUID1(INDVAR)) THEN
          INDVAP=IVAP1
          INDAIR=IAIR1
          INDTEM=TEMP1
          INDR=  R1
        ELSE
          INDVAP=IVAP2
          INDAIR=IAIR2
          INDTEM=TEMP2
          INDR=  R2
        END IF
        IF (DEBU) WRITE (6, *) ' COMBUS for INDVAR= ',INDVAR
```

```
C       Reaction rate to EASP2
        CALL FN21 (EASP2, INDVAP,INDAIR, 0.0, -RG(39))
        CALL FN32 (EASP2, INDTEM, -RG(40), ABS(TEMP0))
C
C.......Heat of reaction
C
        IF ((INDVAR.EQ.H1).OR.(INDVAR.EQ.H2)) THEN
          CALL FN2 (VAL, EASP2, 0.0, -HCOMB)
C          CALL FN0 (EP, VAL)
        END IF
C
C.......Source of products (as an alternative to sink of air)
C
        IF ((INDVAR.EQ.IPRD1).OR.(INDVAR.EQ.IPRD2)) THEN
          CALL FN2 (VAL, EASP2, 0.0, -(1.0+STOICH))
        END IF
C
C.......Sink of fuel in SCRS2
C
        IF ((INDVAR.EQ.IFUE1).OR.(INDVAR.EQ.IFUE2)) THEN
          CALL FN0 (VAL, EASP2)
        END IF
C
        IF (DEBU) THEN
          NFPR=0
          L0V=L0F(VAL)
          DO II=1, NX*NY
            IF (F(L0V+II).LT.0.0) NFPR=1
          END DO
          IF (NFPR.EQ.1) THEN
            CALL WRIT2I ('INDVAR  ',INDVAR,'ITHYD   ',ITHYD)
            CALL PRN ('ESP2', EASP2 )
            CALL PRN ('VAL ', VAL   )
            CALL PRN ('IAIR', INDAIR)
            CALL PRN ('1AIR', IAIR1)
            CALL PRN ('2AIR', IAIR2)
            CALL PRN ('VAP ', INDVAP)
            CALL PRN ('TEMP', INDTEM)
          END IF
        END IF
        CALL FN26 (VAL, INDR)
C     End if for NPATCH
      END IF
C
      RETURN
 1319 CONTINUE
C------------------- SECTION 20 -------------------- value = GRND8
      RETURN
 1320 CONTINUE
C------------------- SECTION 21 -------------------- value = GRND9
      RETURN
 1321 CONTINUE
C------------------- SECTION 22 -------------------- value = GRND10
      RETURN
C*****************************************************************
C
C--- GROUP 14. Downstream pressure for PARAB=.TRUE.
```

```
C
   14 CONTINUE
      RETURN
C*****************************************************************
C
C--- GROUP 15. Termination of sweeps
C
   15 CONTINUE
C    * Make changes for this group only in group 19.
      RETURN
C*****************************************************************
C
C--- GROUP 16. Termination of iterations
C
   16 CONTINUE
C    * Make changes for this group only in group 19.
      RETURN
C*****************************************************************
C
C--- GROUP 17. Under-relaxation devices
C
   17 CONTINUE
C    * Make changes for this group only in group 19.
      RETURN
C*****************************************************************
C
C--- GROUP 18. Limits on variables or increments to them
C
   18 CONTINUE
C    * Make changes for this group only in group 19.
      RETURN
C*****************************************************************
C
C--- GROUP 19. Special calls to GROUND from EARTH
C
   19 GO TO (191,192,193,194,195,196,197,198),ISC
  191 CONTINUE
C    * ------------------- SECTION 1 ---- START OF TIME STEP.
      RETURN
  192 CONTINUE
C    * ------------------- SECTION 2 ---- START OF SWEEP.
      RETURN
  193 CONTINUE
C    * ------------------- SECTION 3 ---- START OF IZ SLAB.
C
C....SR to ISDOT if positive
C
      IF (SR.GE.0.0) THEN
        IF (IZ.GT.IG(3)) THEN
          CALL FN65 (ISDOT1, ISDOT2, SR)
        ELSE
          CALL FN65 (ISDOT1,ISDOT2, 0.0)
        END IF
      END IF
C
      RETURN
  194 CONTINUE
```

```
C   * ------------------- SECTION 4 ---- START OF ITERATION.
C
C....Sdot computed and stored in C6 if SR<0. Options:
C    SR    Option
C    ------------------------------------------------------------------
C    -1.0  Driving force=(mvap,0 - mvap,inf)/(1-mvap,0)
C          mvap,0 = RG(28); vapour-mass diffusivity = RG(29)
C    -2.0  Driving force=Cpvap*(T-Tdrop)/hlv
C
      IF (SR.LT.0.0) THEN
        DO IPHASE=1, 2
          IF (IPHASE.EQ.1) THEN
            ISDOT =ISDOT1
            INDVAP=IVAP1
            ITEMP =TEMP1
          ELSE
            ISDOT =ISDOT2
            INDVAP=IVAP2
            ITEMP =TEMP2
          END IF
          IF (QEQ(SR,-1.0)) THEN
            IF (IZ.GT.IG(3)) THEN
              L0VAP=L0F(INDVAP)
              L0SDO=L0F(ISDOT)
              DO II=1, NX*NY
                IIV=II+L0VAP
                IIS=II+L0SDO
                F(IIS)=(RG(28)-F(IIV))/(1.0-RG(28))
                F(IIS)=8.0*RG(29)*ALOG(1.0+F(IIS))/DENLIQ
              END DO
            ELSE
              CALL FN1 (ISDOT, 0.0)
            END IF
          END IF
          IF (QEQ(SR,-2.0)) THEN
            IF (IZ.GT.IG(3)) THEN
              L0T=L0F(ITEMP)
              L0SDO=L0F(ISDOT)
              DO II=1, NX*NY
                AAA=CPV*(F(L0T+II)-TDROP)/HLV
                IF (AAA.LE.0.0) THEN
                  WRITE(6, *) ' !!!! Tgas= ', F(L0T+II),
     >                        ' Tdrop= ',TDROP
                END IF
                F(L0SDO+II)=8.0*THCOND*ALOG(1.0+AAA)/(CPV*DENLIQ)
              END DO
            ELSE
              CALL FN1 (ISDOT, 0.0)
            END IF
          END IF
        END DO
      END IF
C
      RETURN
  195 CONTINUE
C   * ------------------- SECTION 5 ---- FINISH OF ITERATION.
C
```

```
C
C.....Include-file name: AVEL03-INC .....................Start
C     Insertion in:      Group 19, Section 5
C     Date:              29.02.88/04.03.88/29.03.88
C     Purpose:           Computation of average axial velocity and
C                        jet widths (Width_1% & Width_0.5)
C     Activation:        r-average if LG(4)=F, r*density otherwise
C                        jet widths computed if LG(5)=T
C     Notes:             Only y-direction widths at IX=1 are considered
C                        (these are, of course, the only ones in 2-D
C                        cases).
C
C.....r- or r*density- average of axial velocity is stored in C1
C
      IF (LG(4)) THEN
         CALL FNDRAV       (C1,R1,DEN1,W1,R2,DEN2,W2)
      ELSE
C        Y=A*X1*X2+B*X3*X4: Y  X1 X2 X3 X4  A   B
         CALL FN48         (C1,R1,W1,R2,W2,1.0,1.0)
      END IF
C
      L0C1  =L0F(C1)
      AXVEL =F(L0C1+1)
      W1PC  =0.01*AXVEL
      W50PC =0.5 *AXVEL
      WID   =-1.0
      WIDHAF=-1.0
C
C.....LG(5)=T => Jet widths and jet spread to be computed
C
      IF (LG(5)) THEN
        DO IQ=1, NY
          LQ=IQ+L0C1
          IF ((WIDHAF.LT.0.0).AND.(F(LQ).LT.W50PC)) THEN
            WID1=VARONE(YG2D,IQ-1,1)
            WID2=VARONE(YG2D,IQ,  1)
            VEL1=F(LQ-1)
            VEL2=F(LQ)
C           Interpolation
            WIDHAF=(WID2-WID1)*(W50PC-VEL1)/(VEL2-VEL1)+WID1
          END IF
          IF ((WID.LT.0.0).AND.(F(LQ).LT.W1PC)) THEN
            WID1=VARONE(YG2D,IQ-1,1)
            WID2=VARONE(YG2D,IQ,  1)
            VEL1=F(LQ-1)
            VEL2=F(LQ)
C           Interpolation
            WID=(WID2-WID1)*(W1PC-VEL1)/(VEL2-VEL1)+WID1
            GOTO 1961
          END IF
        END DO
      END IF
C
 1961 CONTINUE
      IF(WID.EQ.-1.0) WID=YVLAST
      IF (LG(6)) CALL FN25 (C1, 1.0/AXVEL)
C
```

```
C.....End of AVEL03-INC ..................................... End
C
      RETURN
  196 CONTINUE
C   * ------------------- SECTION 6 ---- FINISH OF IZ SLAB.
C
      L0T1=L0F(TEMP1)
      L0T2=L0F(TEMP2)
      TMAX=0.0
      DO II=1, NX*NY
        TMAX = MAX (TMAX, F(L0T1+II))
        TMAX = MAX (TMAX, F(L0T2+II))
      END DO
C
C     WRITE (11, *) ZW, ZW*0.01794, F(L0F(AUX(LEN1))+1), WID, AXVEL
      WRITE (11, *) IZ, ZW/DIN, VARONE(TEMP1,1,1),VARONE(TEMP2,1,1),
     >              TMAX, WIDHAF,  WID
      WRITE (6, *) ' ------------------------------CL TMP1 TMP2 '
      WRITE (6, *)  VARONE(TEMP1,1,1), VARONE (TEMP2, 1, 1)
      WRITE (6, *) ' -------------------------------------------'
C
C.....Include-file name: LSQA02-INC .........................Start
C     Insertion in:      Group 19 Section 6
C     Date:              29.02.88/04.03.88/16.03.88/25.03.88
C     Purpose:           Computation of jet spread-rate & axial-
C                        velocity decay rate. Least square adj.
C     Activation:        LG(5)=T for whole section
C                        z/D > RG(17) for least sq adj
C                        LG(3)=T for computation and print-out of
C                          adjustment error
C
C.....ONLY if LG(5).EQ.T
C
      IF (LG(5)) THEN
C
C.....Print-out of variables
C
      CALL WRIT40('---------------------------------------')
      CALL WRIT3R ( 'Zslab   ', IZ*1.0,
     &              'ZW/Din  ', ZW/DIN,
     &              'ZW      ', ZW     )
      CALL WRIT3R ( 'VELax   ', AXVEL,
     &              'Wid 1%  ', WID,
     &              'Wid50%  ', WIDHAF)
      WRITE (6,*)   ' ---------------------------------------'
      WRITE (6, *)  '  Zslab   ', IZ,
     &              '  ZW/Din  ', ZW/DIN,
     &              '  ZW      ', ZW
      WRITE (6, *)  '  VELax   ', AXVEL,
     &              '  Wid 1%  ', WID,
     &              '  Wid50%  ', WIDHAF
C
C.....Least-square adjust of:-
C          * widhaf vs zw
C          * w_inlet/w_axis vs zw/D_inlet
C
C     NB: only if zw/D_inlet >= ratmin = rg(17).
```

```
C
      IF ((ZW/DIN).GE.RATMIN) THEN
C
        NDATA=NDATA + 1
        IF (NDATA.GT.200) THEN
          CALL WRIT40(' !!!! NDATA > 200: I am recycling ')
          NDATA=1
        END IF
C
        WARR(NDATA)=WIN/AXVEL
        ZNARR(NDATA)=ZW/DIN
        ZARR(NDATA)=ZW
        YARR(NDATA)=WIDHAF
C
        SXW=SXW+ZW/DIN
        SX2W=SX2W+(ZW/DIN)**2
        SYW=SYW+WIN/AXVEL
        SXYW=SXYW+(ZW/DIN)*(WIN/AXVEL)
C
        SXY=SXY+ZW
        SX2Y=SX2Y+ZW**2
        SYY=SYY+WIDHAF
        SXYY=SXYY+ZW*WIDHAF
C
C
C.......Assembling the coefficients & print-out
C
        IF ((IZ/NZPRIN).EQ.INT(IZ/NZPRIN).AND.(NDATA.GT.2)) THEN
          AW=(NDATA*SXYW-SXW*SYW)/(NDATA*SX2W-SXW*SXW)
          BW=(SX2W*SYW-SXW*SXYW)/(NDATA*SX2W-SXW*SXW)
          AY=(NDATA*SXYY-SXY*SYY)/(NDATA*SX2Y-SXY*SXY)
          BY=(SX2Y*SYY-SXY*SXYY)/(NDATA*SX2Y-SXY*SXY)
C
          CALL WRIT1I ('  NDATA  ',NDATA)
          CALL WRIT2R ('   AW    ',AW,'   BW    ',BW)
          CALL WRIT2R ('   AY    ',AY,'   BY    ',BY)
          WRITE (6, *) '   AW    ',AW,'   BW    ',BW
          WRITE (6, *) '   AY    ',AY,'   BY    ',BY
C
C........Computation and print-out of the adjustment error
C
          IF (LG(3)) THEN
            ERRW=0.0
            ERRY=0.0
            DO II=1, NDATA
              ERRW=ERRW+ABS(AW*ZNARR(II)+BW-WARR(II))
              ERRY=ERRY+ABS(AY*ZARR(II)+BY-YARR(II))
            END DO
            ERRW=ERRW/NDATA
            ERRY=ERRY/NDATA
            CALL WRIT2R ('  ERRW   ',ERRW,'  ERRY   ',ERRY)
          END IF
        END IF
      END IF
      END IF
C
C.........Conventional calculation (NOT valid for 1st point) & p-o
```

```
C
      IF (LG(3)) THEN
        IF ((IZ.GE.2).AND.(IZ.LE.200)) THEN
          CONAY(IZ)=(WIDHAF-YYOLD)/(ZW-XYOLD)
          CONAW(IZ)=(WIN/AXVEL-YWOLD)/(ZW/DIN-XWOLD)
          ZOVD(IZ) =ZW/DIN
          CALL WRIT2R ('CONV AY ',CONAY(IZ), 'CONV AW ',CONAW(IZ))
          WRITE (6, *) 'CONV AY ',CONAY(IZ), 'CONV AW ',CONAW(IZ)
          NPRAT=NPRAT+1
        ELSE IF (IZ.GT.200) THEN
          CALL WRIT40 ('!!!! IZ>200 in convention cal of rates')
        ELSE IF (IZ.EQ.1) THEN
          NPRAT=0.0
          IDRAT=0
        END IF
        XYOLD=ZW
        XWOLD=ZW/DIN
        YYOLD=WIDHAF
        YWOLD=WIN/AXVEL
      END IF
      WRITE (6,*)    ' ----------------------------------------'
C
C.....End of LSQA02-INC .....................................End
C
C
      RETURN
  197 CONTINUE
C   * ------------------- SECTION 7 ---- FINISH OF SWEEP.
      RETURN
  198 CONTINUE
C   * ------------------- SECTION 8 ---- FINISH OF TIME STEP.
      RETURN
C*****************************************************************
C
C--- GROUP 20. Preliminary print-out
C
   20 CONTINUE
      RETURN
C*****************************************************************
C
C--- GROUP 21. Print-out of variables
C
   21 CONTINUE
C   * Make changes for this group only in group 19.
      RETURN
C*****************************************************************
C
C--- GROUP 22. Spot-value print-out
   22 CONTINUE
C   * Make changes for this group only in group 19.
      RETURN
C*****************************************************************
C
C--- GROUP 23. Field print-out and plot control
   23 CONTINUE
      RETURN
C*****************************************************************
```

```
C
C--- GROUP 24. Dumps for restarts
C
   24 CONTINUE
      RETURN
      END
```

A. *Latin symbols*

Symbol	Meaning	Eq/Sectn
a	constant in Rosin-Rammler distribution	E5.16
a	coefficient in the SCRS2 linear-relationship	E7.6
a	constant in the reaction-rate expression	E7.29
b	constant in Rosin-Rammler distribution	E5.16
b	coefficient in the SCRS2 linear-relationship	E7.6
b	constant in the reaction-rate expression	E7.29
C_a	constant in the fragment-size equation	E4.9
C_b	constant in the fragment-size equation	E4.9
C_f	interphase-friction constant	E4.7
C_m	interphase-mass-transfer constant	E4.6
$C_{m_{ik}}$	constant in the diffusion law for m_i^k	E5.6
$C_{y_{iv}}$	constant in the diffusion law for y_i^v	E5.8
C_v	shear-source constant	E4.8
C_v	specific heat of vapour	E5.15
C_μ	turbulent-viscosity constant	E4.5
d	jet decay-rate	S4.6.1
D	droplet diameter	S5.3.1
D	inlet (nozzle) diameter	-
D'	rate of change of droplet diameter	S6.2.3
D_{32}	Sauter Mean Diameter	E5.17

Symbol	Meaning	Eq/Sectn
f	mixture fraction	S1.2.2
f	passive scalar	S7.2.1
f_{ji}	interphase friction	E4.7
f_{ji}^*	f_{ji}/ρ	E5.1
fc	Freon concentration	E6.2
g	variance of f	E1.2
g	gravitational acceleration	5.11
h	enthalpy	S7.2
H	heat of combustion	E7.5
I_{ji}	$= [\![m_{ji}]\!] + f_{ji}$	S7.2.1
g	passive scalar	S7.2.1
l	fragment size	S2.4.2
l_p	Prandtl mixing-length	S4.4.1
L	latent heat of vaporisation	E5.15
lf	liquid flux	E6.1
m_i	mass-fraction distribution of droplets	E5.2
m_i^k	average of m_i in the k^{th} size-interval	E5.4
m_{ji}	interphase mass-transfer	E4.6
m_{ji}^*	m_{ji}/ρ	E5.1
m_i^-	value of m_i at s_-	Ea.4
m_i^+	value of m_i at s_+	Ea.4
M	molecular weight	S7.3.6
n	droplet-number density	S5.3.1
p	pressure	-
r_i	volume fraction of phase i	S2.4.1
R	droplet radius	E5.9
R'	rate of change of R	E5.9
R'	reaction rate	S7.2.1

Symbol	Meaning	Eq/Sectn
s	stoichiometric ratio	S7.2.1
s	jet spread-rate	S4.6.1
s	droplet size ($s=D^2$ in this work)	S5.3.2a
s_-^k	lower limit of the k^{th} size-interval	E5.4
s_-	same as s_-^k	-
s_+	upper limit of the k^{th} size-interval	E5.4
s_+^k	same as s_+^k	-
s'	rate of change of droplet size (eg, vaporisation rate)	E5.1
$S_{\phi i}$	generic source of ϕ_i	E2.4
S_v	shear-induced source of momentum	E2.9
t	time	-
T_g	gas temperature	E5.15
Ti	gas temperature	S7.3.4
T_{bp}	liquid boiling-point	E5.15
T_d	droplet temperature	E7.26
v_i	velocity component of phase i in the y direction	-
$\mathbf{V}_i$	velocity vector of phase i	-
w_i	velocity component of phase i in the z direction	-
w_{in}	inlet velocity	F4.1
w_{ax}	w at the axis	-
x	spatial coordinate (normally circumferential)	-
y	spatial coordinate (normally radial)	-
y	mass fraction	-
$y_{1\%}$	jet width at which $w=0.01w_{ax}$	-
$y_{0.5}$	jet width at which $w=0.5w_{ax}$	-
z	spatial coordinate (normally axial)	-

B. Greek symbols

Symbol	Meaning	Eq/Sectn
α	constant in Rosin-Rammler distribution	E5.16
β	constant in Rosin-Rammler distribution	E5.16
Γ	diffusion-exchange coefficient	E2.4
Γ	Gamma function	E5.17
λ_v	vapour thermal-conductivity	E5.15
μ	dynamic viscosity	E4.2
μ_l	laminar dynamic viscosity	E4.2
μ_t	turbulent dynamic viscosity	E4.2
ξ	geometrical factor	E5.5
ρ	average density: $\rho = r_1\rho_1+r_2\rho_2$	-
ρ_i	density of phase i	-
ρ_g	gas (air or oxidant) density	E5.12
ρ_l	liquid density	E5.12
ρ_v	vapour density	E5.12
ϕ	average of ϕ_1 and ϕ_2: $\phi=(r_1\rho_1\phi_1+r_2\rho_2\phi_2)/(r_1\rho_1+r_2\rho_2)$	-
ϕ_i	generic property of phase i	S2.4.1

C. *Subindexes/Superindexes*

Symbol	Meaning	Eq/Sectn
1	fluid 1	-
2	fluid 2	-
A	condition at A in the SCRS	S7.2.1
B	condition at B in the SCRS	S7.2.1
f	fuel (both liquid and vapour)	-
g	gas	-
i	fluid (phase) index	-
j	fluid (phase) index	-
k	droplet size-group	-
l	liquid	-
o	oxidant	-
p	products	-
v	vapour	-

D. Acronyms

Acronym	Meaning	Section
CDF	Computational Fluid Dynamics	-
DDM	Discret Droplet Model	1.2.7
DSF	Deterministically separated flow	1.2.7
IPSA	Interphase-slip algorithm	3.4
LHF	Locally homogeneous flow	1.2.2
LHS	Left-hand side (of an equation)	-
NSC	No-slip cloud	1.2.3
pdf	Probability density-function	1.2.2
PEA	Partial-elimination algorithm	3.4.2
PHOENICS	Parabolic, Hiperbolic or Elliptic Numerical Integration Code Series	3.6
PSI-Cell	Particle-source-in cell	1.2.6
RHS	Right-hand side (of an equation)	-
SCRS	Simple chemically-reacting system	7.2.1
SCRS2	SCRS for 2-phase flows	7.2.2
SMD	Sauter Mean Diameter	5.6
SIC	Several interpenetrating continua	1.2.4
SIMPLE	Semi-implicit method for pressure-linked equations	-
SSF	Stochastically separated flow	1.2.7

References

1. Aggarwal SK, Tong AY, Sirignano WA (1984):
A comparison of vaporization models in spray calculations,
AIAA Journal, vol 22, num 10, p1448 (1984).

2. Al Tawel AM and Landau J (1977):
Turbulence modulation in two-phase jets.
International Journal of Multiphase Flows, vol 3, p341 (1977).

3. Andrews MJ (1986):
Turbulent mixing by Rayleigh-Taylor instability.
PhD Thesis, Imperial College, University of London, March 1986.

4. Beshay KR (1985):
Computer modelling of diesel spray dispersion and evaporation.
PhD Thesis, Imperial College, University of London, April 1985.

5. Bilger RW (1980):
Turbulent flows with nonpremixed reactants.
In *"Turbulent Reacting Flows"*, PA Libby and FA Williams (Ed), Springer-Verlag (1980).

6. Boyson F and Swithenbank J (1979):
Spray evaporation in recirculating flows.
Seventeenth Symposium (International) on Combustion, pp443-453,
The Combustion Institute, Pittsburgh (1979).

7. Brown DJ and Hutchinson P (1979):
The interaction of solid or liquid particles and turbulent flow fields — A numerical simulation.
Journal of Fluids in Engineering, vol 101, pp265-269 (1979).

8. Chigier N (1976):
The atomization and burning of liquid sprays.
Progress in Energy and Combustion Science, vol 2 pp94-114, (1976).

9. Chin JS, Freeman WG, Lefebvre AH (1985):
Evaporation histories of fuel sprays injected across a flowing air stream.
ASME paper 85-IGT-49 (1985).

10. Crowe CT and Pratt DT (1972):
Two-dimensional gas-particle flows.
Proceedings of the 1972 Heat Transfer and Fluid Mechanics Institute, pp387-399,
Stanford University Press, 1972.

11. Crowe CT, Sharma MP, Stock DE (1977):
The Particle-Source-In Cell (PSI-Cell) model for gas-droplet flows.
Journal of Fluid Mechanics, vol 99, p325 (1977).

12. Dodge LG and Schwalb JA (1989):
Fuel spray evolution: comparison of experiment and CFD simulation of non-evaporating spray.
Journal of Engineering for Gas Turbines and Power, vol 111, pp15-23 (1989).

13. Dopazo C (1977):
On conditional averages for intermittent turbulent flows.
Journal of Fluid Mechanics, vol 81, part 3, pp433-438.

14. Dopazo C and O'Brian EE (1980):
Intermittency in free turbulent shear flows.
Proceedings of the First Symposium on Turbulent Shear Flows,
Pennsylvania State University.
F Durst, BE Launder, FW Schmidt, JH Whitelaw (Editors),
Springer-Verlag.

15. Dukowicz JK (1980):
A particle-fluid numerical model for liquid sprays.
Journal of Computational Physics, vol 35, num 2, pp229-253 (1980).

16. Faeth GM (1983):
Evaporation and combustion of sprays.
Progress in Energy and Combustion Science, vol 9, pp1-76 (1983).

17. Faeth GM (1987):
Mixing, transport and combustion in sprays.
Progress in Energy and Combustion Science, vol 13, pp293-345 (1987).

18. Gauvin WH, Katta S, Knelman FH (1975):
Drop trajectories predictions and their importance in the design of spray dryers.
International Journal of Multiphase Flows, vol 1, p793 (1975).

19. Gertz T, Schumann U and Elghobashi E (1989):
Direct numerical simulation of stratified homogeneous turbulent shear flows.
Journal of Fluid Mechanics, vol 200, pp563-594 (1989).

20. Gosman AD and Ioannides E (1981):
Aspects of computer simulation of liquid-fuelled combustors.
AIAA Paper num 81-0323 (1981).

21. Gosman AD and Johns RJR (1980):
Computer analysis of fuel-air mixing in direct-injection engines.
SAE Paper num 800091 (1980).

22. Gosman AD, Lockwood FC, Salooja AP (1979):
The prediction of cylindrical furnaces gaseous fueled with premixed and diffusion burners.
17th Symposium (International) on Combustion, pp747-760,
The Combustion Institute, Pittsburgh (1979).

23. Harlow FH and Amsden AA (1975a): Numerical computation of multiphase flows.
Journal of Computational Physics, vol 17, pp19-52 (1975).

24. Harlow FH and Amsden AA (1975b):
Flow of interpenetrating material phases.
Journal of Computational Physics, vol 18, p440 (1975).

25. Harlow FH and Welch JE (1965):
Numerical calculation of time-dependent viscous incompressible flow of fluid with free surface.
The Physics of Fluids, vol 8, p2182 (1965).

26. Hiroyasu H (1987):
Measurements of spray characteristics and fuel vapour concentration in a diesel spray.
ICHMT Conference on Heat and Mass Transfer in Gasoline and Diesel Engines, Dubrovnik, Yugoslavia, 24-28 August 1987.

27. Hunt JCR (1988):
Studying turbulence using direct numerical simulation: 1987 Center for Turbulence Research NASA Ames/Stanford Summer Programme.
Journal of Fluid Mechanics, vol 190, pp375-392 (1988).

28. Hutchinson P, Hewitt GF, Dukler AE (1971):
Deposition of liquid or solid dispersions from turbulent gas streams: a stochastic model.
Chemical Engineering Science, vol 26, p419 (1971).

29. Ilegbusi JO and Spalding DB (1987a):
A two-fluid model of turbulence and its application to near-wall flows.
International Journal of PhysicoChemical Hydrodynamics,
vol 9, num 1/2, pp127-160 (1987).

30. Ilegbusi JO and Spalding DB (1987b):
Application of a two-fluid model of turbulence to turbulent flows in conduits and shear layers.
International Journal of PhysicoChemical Hydrodynamics,
vol 9, num 1/2, pp161-181 (1987).

31. Khalil EE, Hutchinson P, Whitelaw JH (1981):
The calculation of the flow and heat-transfer characteristics of gas-fired furnaces.
18th Symposium (International) on Combustion, p1927,
The Combustion Institute, Pittsburgh (1981).

32. Khalil EE and Whitelaw JH (1976):
Aerodynamic and Thermodynamic characteristics of kerosene-spray flames.
16th Symposium (International) on Combustion, pp569-576.
The Combustion Institute, Pittsburgh, 1976.

33. Kollmann W (1984):
Prediction of the intermittency factor for turbulent shear flows.
AIAA Journal, vol 22, num 4, pp486-492 (1984).

34. Kuo KK (1986):
"*Principles of Combustion* ".
John Wiley and Sons (1986).

35. LaRue JC and Libby PA (1977):
Measurements in the turbulent boundary layer with slot injection of helium.
The Physics of Fluids, vol 20, pp192-202, February 1977.

36. Launder BE and Spalding DB (1972):
"Lectures in Mathematical Models of Turbulence".
Academic Press, 1972.

37. Law CK (1982):
Recent advances in droplet vaporisation and combustion.
Progress in Energy and Combustion Science, vol 8, pp171-201 (1982).

38. Libby PA (1975):
On the prediction of intermittent turbulent flows.
Journal of Fluid Mechanics, vol 68, part 2, pp273-295 (1975).

39. Libby PA (1976):
Prediction of the intermittent turbulent wake of a heated cylinder.
The Physics of Fluids, vol 19, num 4, pp494-501, April 1976.

40. Libby PA and Bray KNC (1981):
Countergradient diffussion in premixed turbulent flames.
AIAA Journal, vol 19, num 2, p205, February 1981.

41. Lockwood FC and Naguib AS (1975):
The prediction of the fluctuations in the properties of free, round-jet, turbulent, diffusion flames.
Combustion and Flame, vol 24, pp109-124 (1975).

42. Malin MR (1986):
Turbulence modelling for flow and heat transfer in jets, wakes and plumes.
PhD Thesis, Imperial College, University of London, October 1986.

43. Mao C-P, Wakamatsu Y and Faeth GM (1981):
A simplified model of high pressure spray combustion.
Eighteenth Symposium (International) on Combustion, pp337-347, The Combustion Institute, Pittsburgh (1981).

44. Moss JB (1980):
Simultaneous measurements of concentration and velocity in an open premixed turbulent flame.
Combustion Science and Technology, vol 22, pp119 (1980).

45. Mostafa AA and Elgobashi SE (1985):
A two-equation turbulence model of jet flows laden with vaporizing droplets.
International Journal of Multiphase Flow, vol 11, num 4, pp515-533 (1985).

46. Mostafa AA and Mongia HC (1987):
On the modeling of turbulent evaporating sprays: Eulerian versus Lagrangian approach.
International Journal of Heat and Mass Transfer, vol 30, num 12, pp2583-2593 (1987).

47. Mostafa AA, Mongia HC, MacDonell VG, Samuleson GS (1989):
Evolution of particle-laden jet flows: a theoretical and experimental study.
AIAA Journal, vol 27, num 2, pp167-183, February 1989.

48. Nukizama S and Tanasawa Y (1940):
Transactions of SME Japan, Vol 6, pp5-7 (1940).
(Quoted by Kuo 1986, p524.)

49. O'Rourke PJ (1981):
Collective drop effects in vaporizing liquid sprays.
PhD Thesis, Princeton University and Los Alamos Scientific Laboratory, March 1981.

50. O'Rourke PJ and Bracco FV (1980):
Modelling of drop interactions in thick sprays and a comparison with experiments.
Stratified Charge Automotive Engines Conference,
IMechE paper C404/80, London, November 1980.

51. Patankar SV (1980):
"Numerical Heat Transfer and Fluid Flow",
Hemisphere Publishing Corporation (1980).

52. Patankar SV (1981):
A calculation procedure for two-dimensional elliptic problems.
Numerical Heat Transfer, vol 4, pp409-426, 1981.

53. Patankar SV and Spalding DB (1972):
A calculation procedure for heat, mass and momentum transfer in three-dimensional parabolic flows.
International Journal of Heat and Mass Transfer, vol 15, pp1787-1806 (1972).

54. Pope SB (1984):
Calculations of a plane turbulent jet.
AIAA Journal, vol 22, num 7, pp896-904 (1984).

55. Pope SB (1985):
Pdf methods for turbulent reactive flows.
Progress in Energy and Combustion Science,
vol 11, num 2, pp119-192 (1985)

56. Prandtl L (1925):
Bericht über Untersuchungen zur ausgebildeten Turbulenz.
Zeitschrift für angewandten Mathematik und Mechanik,
vol 5, num 2, pp136-139, April 1925.

57. Reynolds O (1874):
On the extent and action of the heating surface of steam boilers.
Proceedings of the Literary and Philosophical Society of Manchester, Session 1874-1875, 14th volume.
Reprinted as "Pioneering Paper" in International Journal of Heat and Mass Transfer, vol 3, pp163-166 (1961).

58. Rizk MA and Elghobashi SE (1989):
A two-equation turbulence model for dispersed dilute confined two-phase flows.
International Journal of Multiphase Flow, vol 15, num 1, pp119-133 (1989).

59. Rodi W (1972):
The prediction of turbulent boundary layers by the use of a two-equation model of turbulence.
PhD Thesis, Imperial College, University of London, December 1972.

60. Rosin P and Rammler E (1933):
The laws governing the fineness of powdered coal.
Journal of the Institute of Fuel, vol 7, pp26-36, October 1933.

61. Rosten HI and Spalding DB (1987):
PHOENICS Reference Manual.
CHAM Report TR200 (1987).

62. Shearer AJ, Tamura H and Faeth GM (1979):
Evaluation of a locally homogeneous flow model of spray evaporation.
Journal of Energy, vol 3, num 5, p271 (1979).

63. Shepherd IL and Moss B (1981):
Measurements of conditioned velocities in a turbulent, pre-mixed flame.
Paper number 81-0181,
AIAA 19th Aerospace Science Meeting,
St Louis, Louisiana, 1981.

64. Shirakawa S, Ohsawa K, Aoyama T (1987):
Simulation of spray combustion in an axisymmetric small direct injection

diesel engine.
IMechE International Symposium on Computers in Engine Technology, Paper C01/87, Cambridge, 1987.

65. Shuen J-S, Solomon ASP, Zhang Q-F, Faeth GM (1983):
A theoretical and experimental study of particle laden jets.
NASA Report number CR-168293, 1983.

66. Shuen J-S, Solomon ASP, Zhang Q-F, Faeth GM (1985):
Structure of particle laden jets: measurements and predictions.
AIAA Journal, vol 23, num 3, p396 (1985).

67. Sirignano, WA (1986):
The formulation of spray combustion models: resolution compared to droplet spacing.
Journal of Heat Transfer, vol 108, pp633-639, August 1986.

68. Solomon ASP, Shuen JS, Zhang Q-F and Faeth GM (1985a):
Structure of nonevaporating sprays.
AIAA Journal, vol 23, num 10, p1548 (1985).

69. Solomon ASP, Shuen JS, Zhang Q-F and Faeth GM (1985b):
Measurements and predictions of the structure of evaporating sprays.
Journal of Heat Transfer, vol 107, pp 679-686, August 1985.

70. Spalding DB (1971):
Concentration fluctuations in a round, turbulent, free jet.
Chemical Engineering Science, vol 26, p95 (1971).

71. Spalding DB (1972):
A novel finite-difference formulation for differential expressions involving both first and second derivatives.
International Journal of Numerical Methods in Engineering, vol 4, p551 (1972).

72. Spalding DB (1976a):
Development of the eddy-break-up model of turbulent combustion.

Sixteenth Symposium (International) on Combustion, pp1657-1663,
The Combustion Institute, Pittsburgh (1976).

73. Spalding DB (1976b):
The ESCIMO theory of turbulent combustion.
Imperial College Mec Engg Dpt Report Number HTS/76/13 (1976).

74. Spalding DB (1976c):
The calculation of free convection phenomena in gas-liquid mixtures.
ICHMT Seminar, Dubrovnik 1976,
in *"Turbulent Buoyant Convection"*,
N Afgan and DB Spalding (Editors), Hemisphere Pub, Washington (1977).

75. Spalding DB (1976d):
Mathematical models of turbulent flames: a review.
Combustion Science and Technology, vol 13, p3 (1976).

76. Spalding DB (1979):
"Combustion and Mass Transfer".
Pergamon Press (1979).

77. Spalding DB (1980a):
Mathematical modelling of fluid-mechanics, heat-transfer and chemical-reaction processes: A lecture course.
Imperial College CFDU Report Number HTS/80/1, January 1980.

78. Spalding DB (1980b):
Numerical computation of multiphase fluid flow and heat transfer.
In *"Recent Advances in Numerical Methods in Fluids"*,
C Taylor and K Morgan (Editors).

79. Spalding DB (1981):
IPSA 1981: New developments and computed results.
Imperial College CFDU Report HTS/81/2 (1981).

80. Spalding DB (1982a):
Chemical reactions in turbulent fluids.

4th PhysicoChemical Hydrodynamics Conference,
New York, June 1982.

81. Spalding DB (1982b):
Turbulence models: a lecture course.
Imperial College CFDU report number CFD/82/4, January 1983.

82. Spalding DB (1982c):
Four lectures on the PHOENICS computer code.
Imperial College CFDU Report CFD/82/5, November 1982.

83. Spalding DB (1982d):
The SHADOW method of particle-size calculation in 2-phase combustion.
Nineteenth Symposium (International) on Combustion, pp941-951,
The Combustion Institute, Pittsburg (1982).

84. Spalding DB (1983):
Towards a two-fluid model of turbulent combustion in gases, with special reference to the spark-ignition engine.
IMechE Conference in Combustion in Engineering, Oxford, April 1983,
Volume 1, paper number C53/83, pp135-142.

85. Spalding DB (1984a):
Two-fluid models of turbulence.
NASA Langley workshop on theoretical approaches to turbulence,
Hampton, Virgina, 10-12 October 1984.

86. Spalding DB (1984b):
A turbulence model for buoyant and combusting flows.
4th International Conference on Numerical methods in Thermal Problems,
Swansea, 15-18 July 1984.
Also as Imperial College CFDU report CFD/86/4.

87. Spalding DB (1985):
The numerical calculation of particle-size distributions in 2D jets and boundary layers.
Imperial College CFDU Report Number CFD/85/6,
April 1985.

88. Spalding DB (1987):
A two-fluid model of turbulent combustion in the reciprocating engine.
ICHMT Advanced Course on Computer Simulation of Fluid Flow, Heat and Mass Transfer and Combustion in Reciprocating Engines,
31 August - 4 September 1987, Dubrovnik, Yugoslavia.

89. Spalding DB (1988):
Computer simulation of turbulent combustion in reciprocating engines.
IMechE International Conference on Combustion in Engines,
London, 10-12 May 1988.

90. Spiegel EA (1972):
Qualitative model for turbulent intermittency.
The Physics of Fluids, vol 15, num 8 (August 1972).

91. Tanasawa Y and Tesima T (1958):
On the theory of combustion rate of liquid fuel spray.
Bulletin of the JSME, vol 1, num 1, pp36-41, (1958).

92. Watkins AP, Khaleghi H (1987):
Three-dimensional diesel engine spray modelling.
IMechE International Symposium on Computers in Engine Technology,
Paper C12/87, Cambridge, 1987.

93. Weast RC (Editor) (1984):
"Handbook of Chemistry and Physics".
64th Editon, CRC Press Inc, Boca Raton, Florida (1983-1984).

94. Williams FA (1965):
"*Combustion Theory*".
Addison-Wesley Publising Company, Inc (1965).
(2nd edition from The Benjamin/Cummings Publishing Company, Inc, 1985).

95. Williams FA (1985):
Some theoretical aspects of spray combustion.
ASME paper 85-WA/HT-44 (1985).

96. Wu JZY (1984):
The two-fluid model of turbulence applied to an idealised, one-dimensional, unsteady, confined, pre-mixed flame.
Imperial College CFDU Report number PDR/CFDU IC/21, August 1984.

97. Wu JZY (1987):
The application of the two-fluid model of turbulence to ducted flames.
Imperial College CFDU Report, June 1987.

98. Xi ST (1986):
Transient turbulent jets of miscible and inmiscible fluids.
PhD Thesis, Imperial College, University of London (1986).

99. Youngs DL (1988):
Modelling of turbulent mixing by Rayleigh-Taylor instability.
Paper at "Advances in Fluid Turbulence" Conference, 16-20 May 1988, Los Alamos.